**Terms and Conditions of Use of Digitised Theses from Trinity College Library Dublin**

**Copyright statement**

All material supplied by Trinity College Library is protected by copyright (under the Copyright and Related Rights Act, 2000 as amended) and other relevant Intellectual Property Rights. By accessing and using a Digitised Thesis from Trinity College Library you acknowledge that all Intellectual Property Rights in any Works supplied are the sole and exclusive property of the copyright and/or other IPR holder. Specific copyright holders may not be explicitly identified. Use of materials from other sources within a thesis should not be construed as a claim over them.

A non-exclusive, non-transferable licence is hereby granted to those using or reproducing, in whole or in part, the material for valid purposes, providing the copyright owners are acknowledged using the normal conventions. Where specific permission to use material is required, this is identified and such permission must be sought from the copyright holder or agency cited.

**Liability statement**

By using a Digitised Thesis, I accept that Trinity College Dublin bears no legal responsibility for the accuracy, legality or comprehensiveness of materials contained within the thesis, and that Trinity College Dublin accepts no liability for indirect, consequential, or incidental, damages or losses arising from use of the thesis for whatever reason. Information located in a thesis may be subject to specific use constraints, details of which may not be explicitly described. It is the responsibility of potential and actual users to be aware of such constraints and to abide by them. By making use of material from a digitised thesis, you accept these copyright and disclaimer provisions. Where it is brought to the attention of Trinity College Library that there may be a breach of copyright or other restraint, it is the policy to withdraw or take down access to a thesis while the issue is being resolved.

**Access Agreement**

By using a Digitised Thesis from Trinity College Library you are bound by the following Terms & Conditions. Please read them carefully.

I have read and I understand the following statement: All material supplied via a Digitised Thesis from Trinity College Library is protected by copyright and other intellectual property rights, and duplication or sale of all or part of any of a thesis is not permitted, except that material may be duplicated by you for your research use or for educational purposes in electronic or print form providing the copyright owners are acknowledged using the normal conventions. You must obtain permission for any other use. Electronic or print copies may not be offered, whether for sale or otherwise to anyone. This copy has been supplied on the understanding that it is copyright material and that no quotation from the thesis may be published without proper acknowledgement.

# The role of the lysosomal system in beta amyloid$_{1-40}$-mediated neurodegeneration in cultured cortical neurons

By

**Róisín Maureen McCormack**

Thesis submitted for the degree of Doctor of Philosophy at the University of Dublin, Trinity College

Thesis submitted February 2007

**Trinity College Institute of Neuroscience and**
**Department of Physiology**
**Trinity College**
**Dublin 2**

## Declaration

This thesis is submitted by the understated for the degree of Doctor of Philosophy at the University of Dublin, Trinity College and has not been submitted to any other university as an exercise for a degree. I declare that this thesis is entirely my own work and I give permission to the library to lend or copy this thesis upon request

Róisín M. McCormack.

Róisín Maureen McCormack, BA mod Physiology

## Summary

β-amyloid ($A\beta_{1-40}$) is a component of the senile plaques found in Alzheimer's disease (AD). There is evidence that Aβ mediates its apoptotic effect through release of lysosomal proteases to the cytosol with subsequent apoptosis. The aim of this study was to investigate the mechanisms of Aβ-mediated regulation of the lysosomal system. Primary cultured rat cortical neurons were treated with fibrillar $A\beta_{1-40}$ peptide (2μM). To assess the role of p53 in mediating the modulatory effects of $A\beta_{1-40}$, cells were pretreated with the p53 inhibitor, pifithrin-α (50nM). $A\beta_{1-40}$ significantly increased phospho-$p53^{ser15}$ expression and its transcriptional target, Bax, in a p53-dependent manner. In Aβ-treated cells, there was increased localisation of phospho-$p53^{ser15}$at the lysosome and this was attenuated by pifithrin-α. The increased association of p53 with lysosomes correlated with a destablisation of the lysosomal membrane, as demonstrated by a relocalisation of acridine orange from the lysosomes to cytosol and pifithrin-α reversed the Aβ-induced disruption of lysosomal stability. Aβ evoked a significant reduction in expression of the lysosome associated membrane protein (LAMP-1) as assessed by fluorescence microscopy and western immunoblot, however this was not dependent on p53. Overall, these results provide evidence that $A\beta_{1-40}$ impacts on p53 leading to destablisation of the lysosomal membrane.

Western immunoblot analysis revealed that Aβ evoked a significant increase in expression of the spleen tyrosine kinase (Syk). Expression of Syk was also investigated using fluorescence microscopy, similarly, Aβ increased expression of Syk and mediated increased localisation of phospho-Syk at the lysosome, this was not p53 dependent. The $A\beta_{1-40}$-mediated increased in caspase-3 activity and DNA fragmentation was attenuated by the Syk inhibitor. These findings suggest that Syk modulates the apooptotic effect of Aβ in cultured cortical neurons. Furthermore, Syk mediates the Aβ-induced release of cathepsin-L from the lysosome to the cytosol, and regulates lysosomal membrane integrity, as indicated by the acridine orange relocation assay, reflective of a role for Syk in modulation of the lysosomal system. To deliniate some of the signalling pathways of Syk in cortical neurons, the effect

of Syk on Aβ-induced c-Jun N-terminal kinase (JNK) and extracellular regulated kinase (ERK) was investigated. The results demonstrate that Aβ modulates JNK 2/3 at differential timepoints and Aβ mediates an increase in ERK activity at relatively late timepoints. Finally, the association of phospho-p53$^{ser15}$ at the lysosome was dependent on Syk signaling. These data indicate that Syk may play an important role in signal transdution in neuronal cells, which may be pertinent in the lysosomal branch of the apoptotic cascade.

# Table of Contents

**Chapter 2 Methods**

# List of Figures

## III List of Tables

## Acknowledgements

A PhD takes a lot of time, commitment and an infinite amount of help and support, so although my name is on the cover there are many people I need to sincerely thank for their assistance. To my supervisor, Dr. Veronica Campbell, thank you for giving me the opportunity to work in your lab and observe your enthusiasm and love for science. You have imparted on me the wisdom to know that you can always give and do more than you think.

I would like to thank all my lab buddies past and present for all the craic we had, especially back in Physiology in 'Veronica's closet'. The cramped conditions were obviously conducive to banter and gossip. Thanks to Marie who steered me in the right direction in the early days and expecially to Eric Downer and Eric Farrell, who took such good care of me at every RAMI! I know both of you will be very successful in your respective scientific careers. I wish the best to Aoife and Manoj in the rest of their PhDs and hope they will be comfortable in their less plush surrondings of their new office!

As I'm sure I would leave someone out I will just acknowledge the friendship of my colleagues in the other labs by naming the groups, MAL, Connor and Kelly groups. In my five years in Physiology I've come to realise the people who make up the Physiology Dept. have to be the friendliest, most helpful and warm people in the college,so thank you all. Finally, I would like extend my gratitude to Prof. Christopher Bell, Prof. Marina Lynch and Dr. Alan Tuffery.

I can't write an acknowledgements without mentioning all the love, support and friendship from Amy, Ceire and Rachael. Not forgetting the blackie connors, Joan and Noreen. Girls, I could have never survived this 3 years without you all. From coffee's and lunches (or drinks if things got really serious), gossiping, scheming, whatever made things easier, I am enormously grateful and will never forget the fun we had and the pleasure of coming into work everyday to a room of generally loud boisterous girls. I hope you all will find what makes you happy and content in life. Thanks to Tony for graciously accepting the joys of having a poor student girlfriend and looking after me so well.

Finally, I would like to dedicate this thesis to my parents. Although they might never read this thesis, I could not have done it without them. Thank you both.

## List of Abbreviations

| | |
|---|---|
| Ab | antibody |
| AD | Alzheimer's disease |
| ADDL | Aβ-derived diffusible ligands |
| AFC | 7-amino-4-(trifluoromethyl) coumarin |
| AIF | apoptosis-inducing factor |
| APAF | apoptosis activating factor |
| ALS | Amyotropic lateral sclerosis |
| ANOVA | analysis of variances |
| ANT | adenine nucleotide translocator |
| ApoE | apolipoprotein allelle type E |
| APP | amyloid precursor protein |
| $APP_{s-\alpha}$ | soluble APP fragment cleaved by α-secretase |
| $APP_{s-\beta}$ | soluble APP fragment cleaved by β-secretase |
| APS | ammonium persulphate |
| ARA-C | cytosine-arabino-furanoside |
| ATP | adenosine 5' -triphosphate |
| $A\beta_{1-40}$ | beta-amyloid fragment containing 1-40 amino acids |
| $A\beta_{1-42}$ | beta-amyloid fragment containing 1-42 amino acids |
| $A\beta_{25-35}$ | beta-amyloid fragment containing 25-35 amino acids |
| BACE | Beta site AP cleaving enzyme |
| BSA | bovine serum albumin |
| $Ca^{2+}$ | calcium ion |
| cDNA | copy deoxyribonucleic acid |
| CFT | Carboxy terminal fragment |
| CED | cell death domain |
| CNS | central nervous system |
| -COOH | carboxy terminus |
| CPP32 | cysteine protease of 32 kilo Daltons (caspase-3) |
| CREB | cAMP-responsive element binding protein |
| DAB | diaminobenzidine |
| DED | death effector domains |

| | |
|---|---|
| DEPC | diethylpyrocarbonate |
| DEVD | aspartie-glutamic-valine-aspartic residue |
| DMSO | dimethyl sulphoxide |
| DNA | deoxyribonucleic acid |
| dNTP | deoxynucleotidetriphosphate |
| DNAse | deoxyribonucleic acid |
| DTT | dithiothreitol |
| EGTA | ethylenediamin-tetracetic acid |
| EDTA | ethylene glycol bis (β-aminoethyether) N,N 'tetraacetic acid |
| ELISA | enzyme-linked immunosorbent assay |
| EtOH | ethanol |
| FAD | familial Alzheimer's disease |
| FDA | food and drug administration |
| FITC | flourescein isothiocyanate |
| GAPDH | glyceraldehyde-3-phosphate dehydrogenase |
| G-protein | GTD-binding protein |
| GTP | guanosine 5'-diphosphate |
| HBSS | Hank's balanced salt solution |
| HD | Huntingtons's disease |
| HEPA | high efficiency particle air |
| HEPES | (N-[2-Hydroxyethyl]piperazine-N'-[2-ethane-sulphonic acid]) |
| $H_2O_2$ | hydrogen peroxide |
| hr | hour |
| HRP | horseradish peroxidase |
| HSP | heat shock protein |
| HVA | high voltage activated |
| IgG | immunoglobulin G |
| INCL | infantile neuronal ceroid lipofuscinosis |
| ITAM | immunoreceptor tyrosine-based activating motif |
| JIP | JNK interacting proteins |
| JNCL | juvenile form of neuronal ceroid lipofuscinosis |
| JNK | c-jun-N-terminal kinases |

| | |
|---|---|
| KCL | potassium chloride |
| kDa | kilo Dalton |
| LAMP | lysosomal associated membrane protein |
| LIMP | lysosomal integral membrane protein |
| LAP | lysosomal acid phosphatase |
| LPS | lipopolysaccharide |
| LSD | lysosomal storage disease |
| LTP | long term potentiation |
| LVA | low voltage activated |
| mA | milliamp |
| MAPK | mitogen activated protein kinase |
| MAPKK | MAPK kinase |
| MAPKKK | MAPK kinase kinase |
| MAP-2 | microtubule-associated protein 2 |
| mg | milligram |
| $MgCl_2$ | magnesium chloride |
| $MgSO_4$ | magnesium sulphate |
| min | minute |
| mM | millimolar |
| MMP | mitochondrial membrane permeabilisation |
| Mn | manganese |
| MPR | mannose-6-phosphate receptors |
| mRNA | message ribonucleic acid |
| μM | micromolar |
| μm | micrometer |
| NBM | neurobasal medium |
| NFT | neurofibrillary tangles |
| ng | nanogram |
| $-NH_2$ | amino terminal |
| nm | nanometer |
| NMDA | N-methyl-D-aspartate |
| NTR | neurotrophin receptor |
| p53AIP1 | p53-regulated apoptosis-inducing protein-1 |

| | |
|---|---|
| PBS | phosphate buffered saline |
| PCD | programmed cell death |
| PCR | polymerase chain reaction |
| PD | Parkinson's disease |
| PIG | P53-inducible gene |
| PKA | protein kinase A |
| PKC | protein kinase C |
| PMSF | phenylmethylsulphonyl fluoride |
| PPT | palmotoyl protein thioesterase 1 |
| PS | phosphatidylserine |
| PS1 | presenilin-1 |
| PS2 | presenilin-2 |
| PTK | protein tyrosine kinases |
| PTP | permeability transition pore |
| RAGE | receptor for advanced glycation end products |
| RNA | ribonucleic acid |
| RNAse | ribonuclease |
| RT | room temperature |
| ROS | reactive oxygen species |
| SAPK | stress-activated protein kinase |
| SDS | sodium dodecyl sulphate |
| SDS-PAGE | SDS-polyacrylamide gel electrophoresis |
| SEM | standard error of the mean |
| Se | serine |
| Smase | sphingomyelinase |
| Syk | spleen tyrosine kinase |
| TBE | tris borate edta |
| TBS | tris buffered saline |
| TBS-T | tbs-tween |
| Tdt | terminal deoxynucleotidyl transferase |
| TEMED | N,N,N,-N-tetramethylenediamine |
| Thr | threonine |
| TNF | tumour necrosis factor |
| TRAIL | TNF-related apoptosis-inducing ligand |

| | |
|---|---|
| TUNEL | TdT-mediated-UTP-end nick labelling |
| U | unit |
| UV | ultraviolet |
| VDAC | voltage-dependent anion channel |
| VDCC | voltage dependent $Ca^{2+}$ channel |
| ZAP-70 | zeta-activated protein of 70kDa |

To Mammy and Daddy

*Chapter 1*

# Introduction

## 1.1 AD

AD is a multifactorial disease that involves progressive synaptic loss and neuronal death. Clinically characterised by an irreversible loss of cognitive function, it is associated with impairment in activities of daily living, mental and physical deterioration with progressive behavioural disturbances, and ultimately by death (Goldman, 1991). AD is the most prominent cause of senile dementia accounting for over 60% of all dementia cases, with over 20 million people affected worldwide. It is estimated that 50% of people over the age of 85 years old are suffering from AD. The average length of time from diagnosis to death is 4 to 8 years, although it can take 20 years or more for the disease to run its course. Due to increasing human life expectancy in the developed world, the incidence of this disease is expected to escalate along with the subsequent emotional, physical and financial stresses among caregiving families and health care resources. Therefore, there is urgent need to decipher the underlying cause of this disease and to develop new strategies for its treatment.

The factors contributing to the evolution of AD remain largely obscure. Biomedical researchers have devised psychological screening tests to try to identify people in the early stages of AD. Apart from memory loss, there are nine other warning signs - among them difficulty performing familiar tasks, problems with language, such as remembering words, disorientation in time and space, and changes in personality (St George-Hyslop, 2000a). For the most part, diagnosis has been a process of elimination. Early and careful examination is important because many conditions can cause dementia, some of which are treatable. Potential reversible conditions include depression, adverse drug reactions, metabolic changes, and nutritional deficiencies (St George-Hyslop, 2000b). A comprehensive patient evaluation includes a complete health history, physical examination, neurological and mental status assessments, and other tests including analysis of blood and urine, electrocardiogram and an imaging exam, such as Computerised Axial Tomography scan (CT) scan or Magnetic Resonance Imaging (MRI). While this type of evaluation may provide a diagnosis of possible or probable AD, confirmation requires examination of brain tissue at autopsy.

Although no cure for AD is yet available, medical and social management of the disease can ease the burdens on the patient, and his or her caregiver and family. A number of pharmacological treatments for AD have been demonstrated to have some beneficial effects on cognitive, functional, and behavioural symptoms of AD. To date, there are four FDA-approved drugs for the treatment of AD - tacrine (Cognex), donepezil (Aricept), rivastigmine (Exelon) and galantamine (Reminyl). These are mainly acetylcholinesterase inhibitors which compensate for cholinerigic deficits which occur in AD (Hirai, 2000). Although many neurotransmitter systems are affected in AD, degeneration in the cholinergic system occurs earlier and more consistently then in other systems (Katzman *et al.,* 1986) and these changes are closely correlated with the presence of plaques and NFT. Both choline acetyltralnsferase and acetylcholinesterase, responsible for the synthesis and breakdown of acetylcholine (ACh) are decreased in the brains of persons with AD (Davies & Maloney, 1976). The loss of cholinergice markers is particularly prominent in the cortex and hippocampus, areas of the brain involved in cognition and memory. The resultant decrease in ACh-dependent neurotransmission is thought to lead to the functional deficits of AD. These inhibitors prevent the break down of acetylcholine and prolong cholinergic transmission at synapses. In addition, inhibitors of β- and γ-secretases are used to prevent the generation of Aβ from the amyloid precursor protein (APP; Schenk *et al.,* 2001). Increased cholesterol can be a risk factor and studies of patients taking statins have shown a lower incidence of the disease (Simons *et al.,* 2002). Zinc and copper have been found to enhance aggregation of Aβ, therefore chelating agents maybe beneficial to administer to susceptible groups (Rosenberg, 2003).

### 1.1.2 AD Pathology

Almost a century ago the first case of AD was diagnosed by the Bavarian psychiatrist, Alois Alzheimer (1907), when he identified 'dense bundles' of neurofibrils and the 'deposition of a peculiar substance in the cerebral cortex and hippocampus' of the autopsy brain of a 51 year old women. Today AD pathology is associated with synaptic dysfunction and

neurodegeneration of neurons in limbic (hippocampus, amygdala, septum) structures and associated regions of the cerebral cortex, areas essential for intellectual function (see Figure 1.1). Microscopic views have revealed a loss of nerve cells in certain regions of the brain, such as the hippocampus, a center for memory, and the cerebral cortex, whish is involved in reasoning, memory, language and other important thought processes (St George-Hyslop, 2000c). The more directly observable hallmarks of AD are clusters of proteins that accumulate in the brain. These accumulations ususally occur in two forms: those found inside nerve cells (intracellular tangles) and those found between nerve cells (extracellular plaques of Aβ peptide). The clusters of neurofibrillary tangles (NFTs) resemble pairs of threads wound around each other in a form of a helix (see Figure 1.2). These tangles consist of a protein called tau (Anderton *et al.*, 2001). Tau can bind to tubulin, which in turn forms structures known as microtubules, which are crucial for the structural

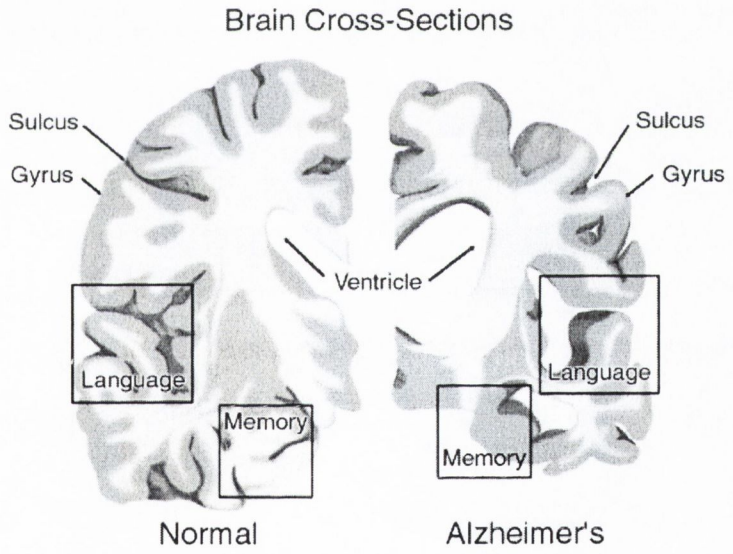


**Figure 1.1** Neurodegeneration of limbic and cerebral cortical regions in AD brain (http://abdellab.sunderland.ac.uk).

framework of living cells (Selkoe, 1995). However, abnormal phosphoryation of tau leads to a destabilisation of the abnormal phosphorylated tau (Hashiguchi *et al.*, 2000). Senile plaques are roughly spherical complex extracellular deposits within the neuropil, composed of a core containing Aβ

protein surrounded by activated microglia, astrocytes, dystrophic neurites and cellular debris. Neurons near these plaques appear swollen and deformed, however, it is unclear whether these neurons function normally.

A great deal of debate has focused on which of the hallmarks of AD, the senile plaques or neurofibrillary tangles appear first in the disease. Some groups have proposed that hyperphosphorylation of tau precedes plaque formation in the AD brain (Su *et al.*, 1994) and the appearance of neurofibrillary tangles have been demonstrated to correlate spatially and temporally with Alzheimer's disease severity (Braak & Braak, 1991). The formation of neurofibrillary tangles, containing tau protein is proposed to result from an imbalance between Aβ production and Aβ clearance (Hardy & Selkoe, 2002). Evidence that Aβ deposition precedes neurofibrillary tangle formation in AD is provided by the following observations. Mutations in the gene encoding tau protein cause frontotemporal dementia with parkinsonism (Hardy *et al.*, 1998). This disease is characterised by severe deposition of tau in neurofibrillary tangles in the brain, but no deposition of amyloid. This demonstrated that profound neurofibrillary tangle formation leading to neurodegeneration is not sufficient to induce formation of the amyloid plaques characteristic of AD, providing evidence that the neuofibrillary tangles of wild-type tau seen in AD brains are likely to be deposited after changes in Aβ metabolism and plaque formation rather than before (Hardy *et al.*, 1998).

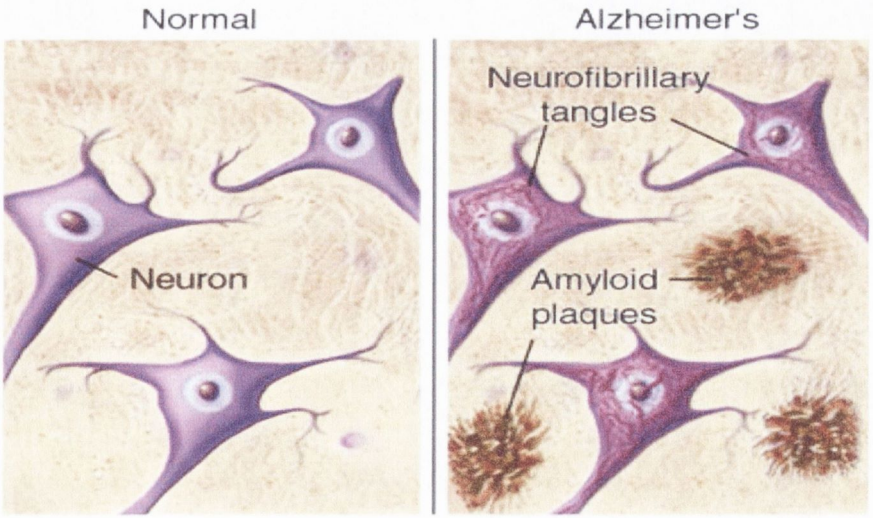


**Figure 1.2** Schematic respresentative images of amyloid plaques and neurofibrillary tangles. (www.ahaf.org/alzdis/about/AmyloidPlaques.htm).

In addition, transgenic mice overexpressing both mutant human APP and mutant human tau undergo increased formation of tangles as opposed to mice overexpressing tau alone, whereas the structure of amyloid plaques remained unaltered (Lewis *et al.*, 2001). This finding indicates that altered processing of APP protein precedes alterations in tau in the patholgical cascade of AD. Development of amyloid deposits in the AD brain can be categorised into three stages. Amyloid deposition initially develops in poorly myelinated areas of the basal neocortex, spreading to the adjoining areas of the hippocampus, neocortex archicarical areas and amygdala, until finally populating the entire cortex (Braak & Braak, 1997).

### 1.1.3 Mutations in AD

The proximal cause of neurodegeneration in AD is an actively debated issue that has become focused on several proteins implicated by genetics. A central role for Aβ protein is supported by the effects of genetic mutations that cause familial AD (Selkoe, 1994), all of which predispose to amyloid deposition and by the observation that Aβ can be neurotoxic *in vitro* and *in vivo* (Yankner, 1996). The toxicity of abnormal structural forms of Aβ provides a unifying theme with other age related neurodegenerative disorders characterised by the appearance of pathological protein structures, such as Parkinson's disease (PD), Huntington's disease (HD), Frontotemporal dementia and Amyotropic Lateral Sclerosis (ALS). AD can be divided into two subgroups based on inheritance (see Figure 1.3). The majority of AD cases are non-inherited and have a late mean age of onset, and are thereby classified as sporadic late-onset AD. The second form of AD is inherited and has an early mean age of onset, and is classified as familial early-onset AD (FAD). FAD is rare, being responsible for less than 10% of all cases of AD (Gandy & Petanceska, 2000). FAD is associated with specific mutations of 3 particular genes. Early studies demonstrated significant linkage of early onset FAD to chromosome 21. The gene encoding the amyloid precursor protein in found on chromosome 21 and so this made APP a candidate gene for AD mutations. To date, 11 different pathogenic mutations have been identified in APP all of which are missense mutations lying within or close to the domain

encoding the Aβ peptide (Tanzi & Bertram, 2001). All APP mutations lead to increased production of either total Aβ or a specific Aβ isoform (Selkoe, 1994). Down's syndrome sufferers who inherit an extra copy of chromosome 21, and therefore an extra copy of the APP gene, develop AD pathology if they live past 40, providing further evidence for the role of APP in early develoment of AD (Armstrong, 1994).

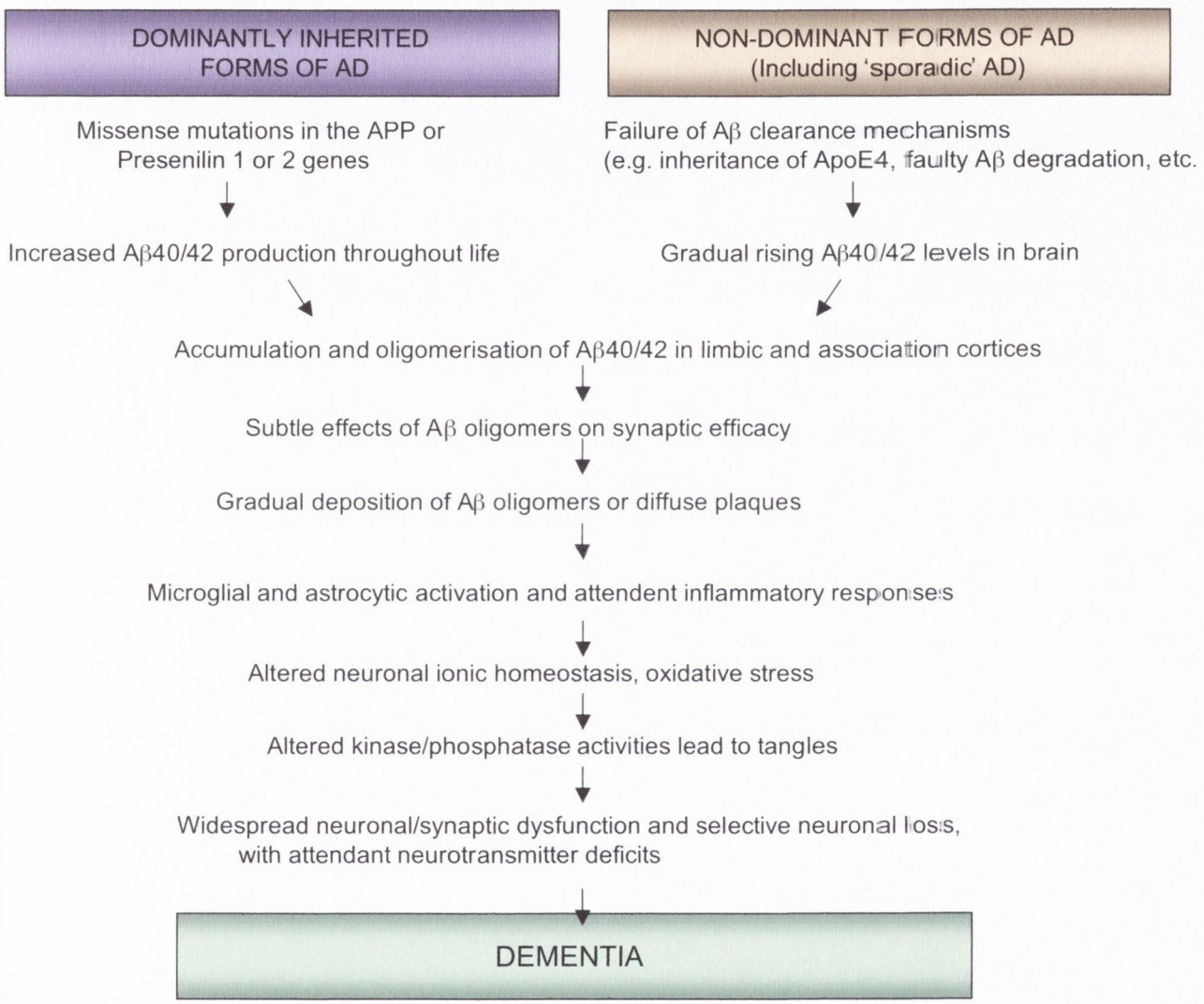


**Figure 1.3** Amyloid cascade hypothesis (Edited, Selkoe, D. 2005 Alzheimer research forum).

The next two AD genes identified were *presenilin1 (PS1)* and *presenilin2 (PS2)* found on chromosome 14 and 1, respectively. These genes encode for highly homologous, multitransmembrane proteins which are

predominantly localised within the endoplasmic reticulum, and to a lesser extent in the Golgi compartment (Walter *et al.*, 1996). The precise function of presenilins within the cell is unknown but it is suggested that they play a role in neurite outgrowth and increase activity of γ-secretase (Dowjat *et al.*, 1999). Together mutations in these two genes account for about 30% of all FAD cases but only 2-3% of all sporadic AD cases.

The majority of AD cases are late onset sporadic AD, not related to any single gene mutation. The etiology of sporadic AD is complex due to interactions between environmental conditions and genetic features of the individual. Individuals containing one or two E4 alleles of the *apoE* gene are predisposed to late onset AD (Dekroom, 2001). Apolipoprotein E4 (ApoE4) is a major serum lipoprotein that plays a key role in cholesterol metabolism in the body by binding to lipoproteins and mediating transport of lipids to and from the bloodstream. It has been shown to be critical in deposition of Aβ peptide in transgenic mice overproducing APP (Raber, 1998). It is believed that the inheritance of apoE4 may lead to a rise in the steady-state levels of Aβ in the brain by decreasing its clearance from the brains extracellular space or by enhancing the fibrillogenic potential of Aβ (Schmechel *et al.*, 1993). Despite its established association, the apoE4 allele is neither necessary nor sufficient to cause AD, but instead operates as a genetic risk modifier by decreasing the age of onset in a dose-dependent manner (Blacker, 1997).

### 1.1.4 AD and causative factors

It is a widely held belief that multiple environmental and genetic determinants interacting throughout life are likely to create susceptibility to sporadic late onset AD. Several environmental risk factors have been implicated in development of late onset AD including head injury, increased concentration of aluminium in drinking water, alcohol abuse, early or late parental age and vascular factors such as high cholesterol (Richard & Amouyel, 2001). Several protective factors have also been associated with decreased AD development including high education level, antioxidants such as vitamin C, E and B12, hormone replacement therapy in women,

polyunsaturated fatty acids, moderate wine consumption and use of anti-inflammatory drugs (Nourhashemi *et al.*, 2000).

## 1.2 Structure of Aβ

Aβ, the 40-42 amino acid peptide which is the major constituent of the senile plaques associated with AD (Selkoe, 1991) is formed during constitutive proteolytic processing of its precursor protein, APP, that is encoded by a gene on human chromosome 21 (Kang *et al.*, 1987). Amyloid precursor proteins are a family of type 1 integral membrane proteins (Haass *et al.*, 1993). It has been shown that in the brain a proportion of APP is present on the cell surface, and although the exact function of APP is still unknown it is proposed that this cell surface APP mediates the transduction of extracellular signals into the cell (Perez *et al.*, 1997). In addition, there is a considerable amount of evidence to indicate a role for APP in promoting neuronal survival. Exogenously added APP has been demonstrated to protect primary neuronal cultures and cell lines from a range of toxic insults including hypoglycemia, glutamate excitotoxicity or Aβ toxicity (Mattson *et al.*, 1993a; Schubert & Behl, 1993; Goodman & Mattson, 1994). The protective effect of APP is thought to occur by lowering intracellular $[Ca^{2+}]_i$ levels (Mattson *et al.*, 1993b). The amino-terminus of the Aβ peptide is located 99 residues proximal to the carboxy-terminus of APP and extends into the membrane-spanning domain. Thus, proteolytic cleavage occurs at both the amino- and carboxy-termini of the Aβ domain within APP to yield the Aβ peptide, an amphipathic molecule (see Figure1.4).

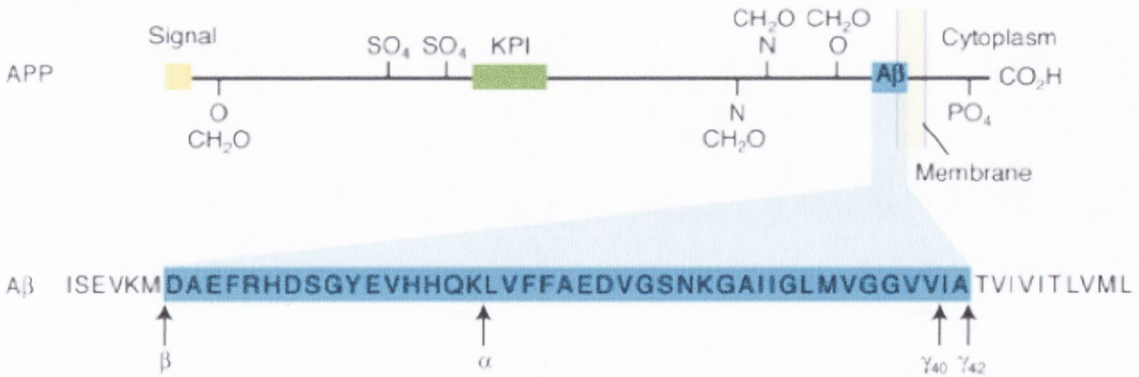


**Figure 1.4** Structure of Amyloid Precursor Protein
(Chen & Schubert, 2002. Expert Reviews in Molecular Medicine)

The three key APP processing steps are mediated by enzymes referred to as, α, β, γ-secretases (Tischer & Cordell, 1996). APP is cleaved by α and β secretases, thereby shedding the large ectodomain and producing membrane anchored 83- and 99- amino acid carboxy terminal fragments (CTF83 and CTF99) with release of soluble derivatives of the protein termed α-APPs and β-APPs (Selkoe, 1994). α-APPs are known to be neuroprotective and have been demonstrated to protect against ischemic brain injury (Smith-Swintosky *et al.*, 1994) and to protect hippocampal neurons from oxidative injury (Goodman & Mattson, 1994). The generated CTF83 and CTF99 fragments can serve as substrates for γ-secretases, which cleaves within the transmembrane domain of the APP, to form the 40-42 amino acid Aβ peptide from CTF99 and an amino-terminal truncated non-pathological fragment of Aβ, p3, from CTF83 (Haass *et al.*, 1995). Aβ peptides are normal products of cellular metabolism with roughly 90% of Aβ being the 1-40 form of the peptide and 10% being the 1-42 variant. While $A\beta_{1-42}$ is less soluble and more amyloidogenic than the $A\beta_{1-40}$ form of the peptide, neuritic plaques contain both forms of the peptide (Selkoe, 2001).

### 1.2.1 Aβ as a Neurotoxic substance

Increasing evidence favours the hypothesis that a primary cause of AD is neuron dysfunction and death triggered by assembled forms of Aβ (Klein *et al.*, 2001). The amyloid cascade hypothesis, formulated in 1992 took the insoluble amyloid fibrils as the primary molecular pathogens of AD. There are a variety of forms of the Aβ peptide. The soluble forms include mononers, dimers and oligomers and the insoluble forms include diffuse 'non-fibril' plaques and mature compound 'fibril' plaques. While it has been known for many years that Aβ monomers assemble into large neurotoxic amyloid fibrils, recent studies show that non-fibrillar Aβ-derived toxins also exist. These toxic soluble oligomer species comprise Aβ-derived diffusible ligands (ADDLs). With this in mind, the amyloid cascade hypothesis was modified to include additional pathogenic Aβ assembles, which are quite different in structure from amyloid fibrils. Unlike the large and conspicuous fibril deposits, oligomers would be undetected in typical pathology assays.

It is generally accepted that AD is associated with various gene defects, leading to altered APP expression or proteolytic processing, and to changes in Aβ stability or aggregation. These in turn result in a chronic imbalance between Aβ production and clearance. Aβ is released extra- and intracellularly, and can also be accumulated extra- or intracellularly. The gradual accumulation of aggregated Aβ may initiate a complex, multistep cascade that includes gliosis, inflammatory changes, neurite/synaptic changes, the formation of neurofibrillary tangles and transmitter loss (Selkoe, 2001). The aggregation of physiologically secreted soluble Aβ to oligomers and large Aβ fibrils is currently considered to be a crucial event in AD. Fibril formation is a multistep process (see Figure 1.5), comprising an initial nucleation step, which is rate limiting, and results in small oligomers (dimers, trimers to dodekamers) followed by rapid fibril elongation stage to protofibrils and fibrils.

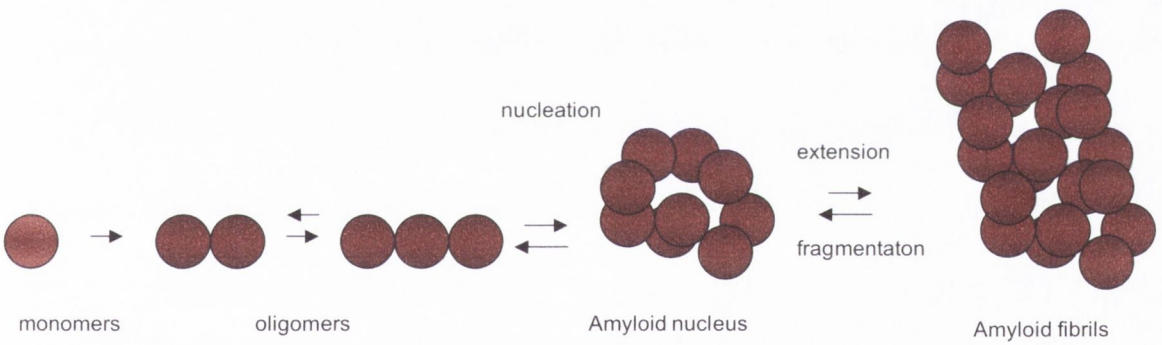


**Figure 1.5** Aggregation of Aβ is a multistep process (Adapted, Verdier *et al.*, 2004. J.Peptide Science, **10**:229-248)

Fibril elongation initially occurs via the formation of small intermediate species that are toxic to cultured neurons (Walsh *et al.*, 1999). The mechanism of its neurotoxicity and its precise cellular locus of action are unsettled, but it has been shown that Aβ can induce oxidative stress and elevate intracellular calcium concentration (Behl *et al.*, 1994). Aβ oligomers and protofibrils have been implicated in neurotoxicity through their direct action on neuronal cells. However, neurotoxicity can also be induced indirectly

by glial cells, since fibrillar Aβ (fAβ) has been shown to produce toxic mediators, leading to the progressive neurodegeneration associated with AD. The binding of Aβ to the plasma membrane is a potential point of intervention in the events leading to the development of AD, although the view is now emerging that a toxic intracellular Aβ accumulation can be detected in neurons before extracellular Aβ deposits (Talaga & Quere, 2002). However, this is still under debate.

By virtue of its structure, Aβ is able to bind a variety of lipids. Soluble Aβ can bind to normal human plasma high-density lipoproteins (HDLs) including apolipoprotein A (ApoA) and ApoE (Kuo *et al.*, 1998). ApoE binds Aβ peptides and is believed to promote fibrillisation of soluble Aβ, affecting amyloid clearance from the brain (Fagan & Holtzman, 2000). ApoE-4, a cholesterol transport protein has been proposed to be a risk factor for late-onset development of AD (Chalmers *et al.*, 2003), but its role in the disease is poorly understood. Aβ is known to interact with the cell membrane and also with the membranes of subcellular organelles (lysosomes, Golgi and ER). In consequence of its lipophilicity, Aβ can interact strongly with the lipid bilayer (Terzi *et al.*, 1997), leading to an increase in Aβ fibrillogenesis and modifications of bilayer properties. Aβ fibrillogenesis has been proposed to take place in lipid rafts of the membrane containing cholesterol, as Aβ displays a specific affinity to cholesterol (Kakio *et al.*, 2002). This fibrillogenesis perturbs the membrane and causes damage. A subset of membrane proteins can bind Aβ, inducing various proteins on neurons (See Figure 1.6). These include the insulin receptor (Xie *et al.*, 2002), the receptor for advanced glycation end products (RAGE; Yan *et al.*, 1996), which can mediate free-radical production, APP which can also induce neuronal death (Lorenzo *et al.*, 2000), scavenger receptor CD36 (Coraci *et al.*, 2002), heat shock protein (HSP; Giulian *et al.*, 1998), NMDA-receptor (Bi *et al.*, 2002), α 7 nicotinic acetylcholine receptor (α7nAChR; Liu *et al.*, 2001), serpin-enzyme complex receptor (SEC-R; Boland *et al.*, 1996) and p75 neurotrophin receptor (NTR) which can induce neuronal cell death (Yaar *et al.*, 1997).

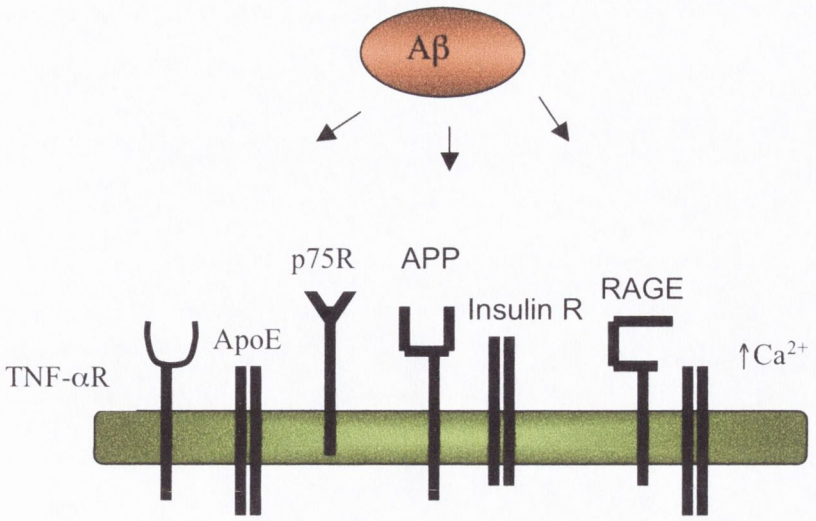


**Figure 1.6** Receptor 'targets' for Aβ.

Debate continues over the normal physiological function of Aβ. An upregulation of the APP molecule after brain injury is thought to serve a neuroprotective role in cells by maintaining $[Ca^{2+}]_i$ and protecting neurons against excitotoxicity insults (Mattson *et al.*, 1993a). A trophic effect of low-dose monomers of Aβ has been reported (Cotman & Anderson, 2000), this is probably due to the proteins ability to capture redox metal ions ($Cu^{2+}$, $Fe^{2+}$) and also Zn, thereby preventing them from participating in redox cycling with other ligands. Indeed, previous results from this laboratory have demonstrated that Aβ targets L and P-type calcium channels (MacManus *et al.*, 2000). Although no specific cellular function appears to rely on the presence of Aβ, the termination of clinical trials using a vaccine designed to remove Aβ from the AD brain, has been met by reports suggesting trace amount of Aβ provide antioxidant effects and regulate membrane lipid dynamics (Kontush, 2001; Koudinov, 2001). Whether Aβ is a mediator of AD neurondegeneration or is produced in response to an underlying etiology, sufficient evidence now exists to confirm its contribution to AD pathology when over produced.

## 1.3 Apoptosis

PCD is a complex genetic and biochemical pathway. This process leads to the specific loss of some cell populations at precise stages in embryonic development. Contrary to necrosis, PCD is an active mechanism and often requires de novo gene expression (Ellis *et al.*, 1991; Nykjaer *et al.*, 1998). Three types of PCD have been distinguished, depending on the nuclear morphology (Schweichel & Merker, 1973; Clarke, 1990). Type I PCD is classical apoptosis, it is characterised by a progressive retraction of chromatin and cytoplasm, followed by DNA internucleosomal fragmentation (Kerr *et al.*, 1972). Type II PCD, or autophagic cell death, is defined by accumulation of autophagic vacuoles. Type III PCD, caspase or cytoplasmic cell death, leads to lysosome-independent degradation of cell material and is much less frequently observed than the other two types of PCD.

The term 'apoptosis' is derived from the Greek word which translates as 'falling leaves'. The apoptosis theory which was first proposed by Kerr and colleagues (1972), has challenged conceptual thinking in all aspects of cell biology. During normal embryonic development and adult development, cells that are unnecessary or deleterious undergo apoptosis (Raffray & Cohen, 1997). Apoptosis occurs in both vertebrates and invertebrates and is distinguished by unique morphological alterations such as blebbing of the plasma membrane, cell shrinkage without membrane rupture, chromatin condensation and migration to the nuclear membrane, packaging of cellular contents into membrane bound bodies for deletion, presentation of epitopes identifying the cell as a phagocytic target and specific DNA cleavage into oligonucleosomal fragments (Behl, 2000). Apoptosis is an active process with organised and regulated biochemical events, including intracellular signal transduction, ordered enzyme cascades and gene transcription (Kerr, 1991). Multiple inducers of apoptosis have been identified including ionising radiation, oxidative stress, sustained increase in calcium, addition or withdrawal of steroid hormones, cytokines and chemotherapeutic drugs (Gerschenson & Rotello, 1992; Raff, 1998).

In mammalian cells, two major molecular pathways can lead to this process; the death-receptor pathway and the mitochondrial pathway

(Herngartner, 2000; see figure 1.7). The former is triggered by members of the deatth-receptor superfamily such as Fas and tumour necrosis factor receptor-1 (TNFF-R1). Binding of a death-ligand (such as CD95 ligand or TNF-α) to its cognate death-receptor induces receptor clustering and activation of the caspase cascade. The second pathway is activated by stimuli such as heat, UV rradiaion or growth factor starvation (Liu *et al.*, 1996; Jiang & Wang, 2000). These stimuli involve mitochondrial membrane permeabilisation (MMP) and then release of pro-apoptotic mitochondrial proteins into the cytosol (Haldestrap *et al.*, 2000), leading to cytochrome *c* release and caspase activation. Apoptosis generally results in activation of certain key players, which include a family of cysteine proteases termed caspases, adaptor proteins such as APAF-1 (required for the activation of caspases), and a family of mitochondrial-associated proteins termed the Bcl-2 family (Yuan & Yankner, 2000). Typically, the apoptotic cell death process has a very rapid time course and is complete within a few hours.

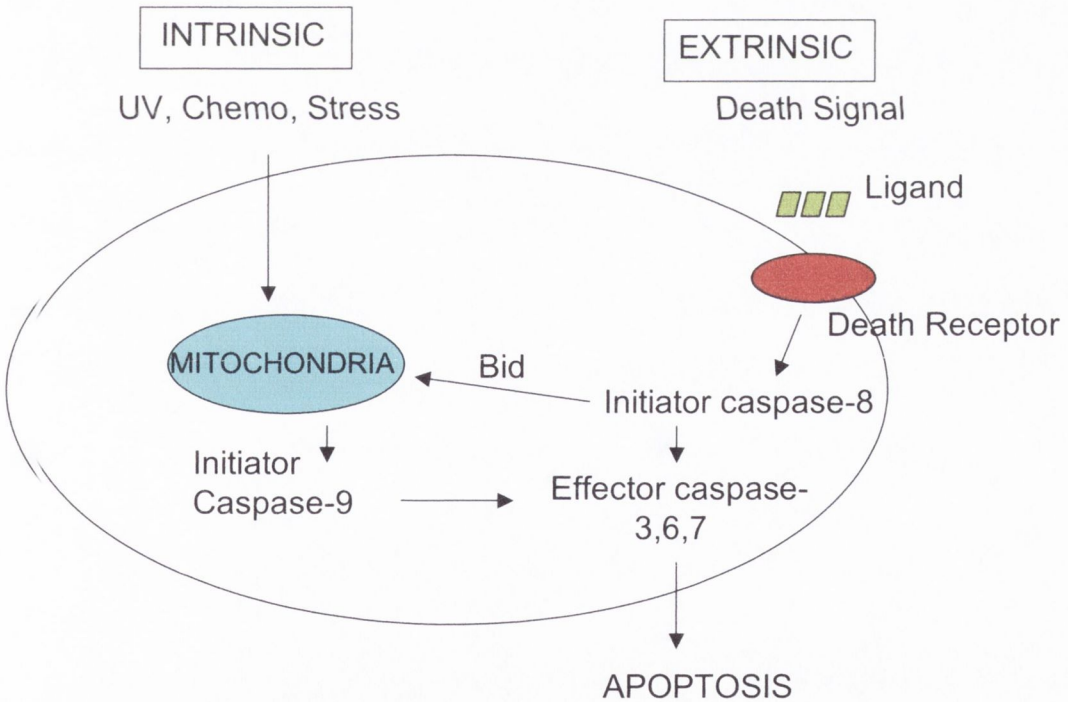


**Figure 1.7** Two distinct pathways of apoptosis. Death receptor pathway and mitochondrial pathway use distinct initiator caspases but common effector caspases. Death receptor and mitochondrial pathways are linked via the Bcl-2 protein Bid.

For more than a century the term necrosis has been used in English, French, and German to describe the "mortification of tissue" until its use became more specific during the 1980s to refer to one of the cell death pathways (Graeber & Moran, 2002). Generally necrosis is defined as caspase-independent cell death that occurs under certain normal physiological and pathological conditions. In contrast, to apoptosis, the necrotic cell death process has an extended duration with a time course of days or even weeks similar to other cell death phenotypes.

There is growing acceptance that the strict adherence to the dichotomous view of cell death does not adequately accommodate the diverse range of morphologies observed in degenerating neurons. As a result, novel descriptive terms have been devised to more accurately describe the various cell death types which occur in neurodegenerative disorders, such as aposklesis (a slow type of cell death occuring over many weeks, the nucleus and nucleoluus remain intact, with no significant chromatin condensation or DNA fragmentation; Ellis & Horvitz, 1986), paraptosis (absence of chromatin condensation or nuclear fragmenation, however cytoplasmic vacuolation from ER and membrane blebbing with apoptotic body formation; Sperandio et al., 2000), abortosis (elevated upstream caspases 8/9 but not effector caspases 3/7, absence of chromatin condensation and apoptotic bodies; Raina et al., 2001) and the autophagia (endocytosis and blebbing of plasma membrane, abundant autophagic vacuoles; Roth, 2001). The existance of several forms of cell death rather than a single one may guarantee elimination of unwanted cells even in the presence of alterations of one particular death pathway. An obvious example is oxidative stress, which when applied in low doses may induce cell proliferation, while higher doses induce apoptosis and overwhelming the cell leads to necrosis (Dypbukt *et al.*, 1994).

### 1.3.2 Cytochrome c

The electron transport protein, cytochrome c, resides in the space between the outer and inner membranes of mitochondria where it participates in electron transport (Reed, 1997). The intermembrane space also contains apoptosis-inducing factor (AIF) caspase 2, 3 and 9. Two theories on the

mechanism of cytochrome c release from the mitochondria have been suggested. First, the opening of pores called the permeability transition pore (PTP) (Eskes *et al.*, 1998). This consists of the adenine nucleotide translocator (ANT) and the voltage-dependent anion channel (VDAC) located in the inner and outer mitochondrial membranes. An alternative model predicts that cytochome c is regulated by a specific channel located in the outer mitochondrial membrane (Reed, 1997). Potential effects may be the Bcl-2 family members of mitochondria-associated membrane proteins.

### 1.3.3 Bcl-2 protein family

As implied by its name the bcl-2 gene was first discovered in human β-cell leukaemias/lymphomas, by various biochemical, genetic and molecular techniques. Homologues of Bcl-2 have been identified forming a Bcl-2 family of proteins. This family of mitochondria-associated proteins modulate cell death by controlling the integrity of the outer mitochondrial membrane (Korsmeyer, 1995). To date, 15 members have been identified (Adams & Cory, 1998) all of which have conserved regions known as Bcl-2 homology (BH) domains, which allows interaction between family members (Oltvai *et al.*, 1993). The Bcl-2 family consists of two subfamilies (See figure 1.8) that regulate apoptosis; anti-apoptotic family members prevent cytochrome *c* translocation from the mitochondria while pro-apoptotic members induce the release of cytochrome *c* from the mitochondria. While the anti-apoptotic members contain four conserved (BH1-4) BH domains, the pro-apoptotic members are divided into two groups, those that possess BH1, BH2 and BH3 domains (Bax, BAK, BOK/MTD, Bcl-$X_s$) and those that possess only BH3 short domain (BID, Bad, BIK/NBK, BLK, Hrk, BIM/BOD). The BH3 domain is presumed as a critical death domain in the pro-apoptotic members. This concept is supported by 'BH3-domain only' members who show sequence homology only within the BH3 domain and to date are all apoptotic. The Bcl-2 family can form homodimers and heterodimers through BH domain interaction, enabling these proteins to function either independently or together in the regulation of apoptosis. The BH1, BH2 and BH3 regions can form a hydrophobic pocket that can bind a BH3 region of another family

member (Korsmeyer, 1995). The interaction of Bcl-2 with Bax was first reported in lymphokine-dependent hemopoietic cells, those studies indicated that Bax antogonises Bcl-2 function abrogating the ability of Bcl-2 to prolong cell survival (Oltvai *et al.*, 1993). The ratio of pro-apoptotic to anti-apoptotic proteins in the Bcl-2 family is involved in determination of cellular fate. Protection from apoptosis occurs when there is an overexpression of anti-apoptotic members (Choi *et al.*, 2001), similarly overexpression of pro-apoptotic members results in the demise of the cell (Gross *et al.*, 1998). Several studies suggest the involvement of Bcl-2 proteins in the formation of specific channels in the mitochondrial membrane. The structure of Bcl-xl and Bid have been found to be similar to the pore forming domains of some bacterial toxins (Muchmore *et al.*, 1996) and when added to synthetic membranes, Bcl-2, Bcl-X and Bax were able to form ion channels (Minn *et al.*, 1997).

The intracellular location of Bcl-2 family members vary depending on the type of Bcl-2 protein and the condition of the cell. In the absence of a death signal, pro- and anti-apoptotic Bcl-2 proteins are localised to distinct intracellular compartments, providing important functions. Anti-apoptotic members are initially integral membrane proteins found especially in the mitochondria, endoplasmic reticulum, and nuclear membranes. The large majority of the pro-apoptotic proteins are localised to the cytosol but following a death signal it appears that they undergo a conformational change that enables them to target and integrate into the mitochondria outer membrane and to function as pro-apoptotic proteins. The regulation of Bcl-2 family members seems to occur at the transcriptional level, by protein degradation and phosphorylation. Bcl-2 protein levels have been shown to be enhanced in cancer tissues (Krajewski *et al.*, 1997), and downregulated in neurons subsequent to cerebral ischemia. Bax is transcriptionally silent in healthy cells, responsive to p53 induction and death stimuli. The BH3 only molecule, Bad, is regulated by rapid changes in phosphorylation that modulate its protein-protein interactions.

| Anti-apoptotic | Pro-apoptotic | BH3-only |
|---|---|---|
| Bcl-2 | Bax | Bid |
| Bcl-$X_L$ | Bak | Bad |
| Bcl-W | Bok/MTD | Bik/NBK |
| MCL-1 | Bcl-$X_S$ | Blk |
| | | Bim/Bod |

**Figure 1.8** Summary of anti-apoptotic and pro-apoptotic Bcl-2 members.

Bax is a soluble monomeric cytosolic protein that translocates to the mitochondria during apoptosis, where it becomes an integral membrane protein. The exact molecular mechanisms involved remain unclear (Wolter *et al.*, 1997; Gross *et al.*, 1998). The Bax translocation process seems to involve its dimerisation, however, it is unknown whether dimerisation is a cause or consequence of its insertion into the membrane. In addition, upon induction of apoptosis a conformation change in Bax, resulting in the exposure of its C- and N-termini enables Bax insertion into the mitochondria (Nechushtan *et al.*, 1999). The BH3-domain-only proteins such as Bid have the ability to induce structural changes in Bax enhancing its apoptotic actions (Desagher *et al.*, 1999). Cleavage of Bax at its N-terminus by the non-lysosomal cysteine protease, calpain is also possible (Gao & Dou, 2000; Choi *et al.*, 2001). The pro-apoptotic activity of Bax, however, can be counteracted by co-expression with pro-survival factors Bcl-2 and Bcl-XI, which can block Bax transloction to mitochondria during apoptosis (Gross *et al.*, 1998). *In vitro* studies have shown that the insertion of Bax causes the release of cytochrome c from mitochondria (Jurgensmeier *et al.*, 1998). Although the exact mechanism has yet to be elucidated, several candidate pathways have been suggested. Some reports indicate that the release of cytochrome c is associated with Bax interaction with ANT or VDAC, both of which are putative members of the mitochondrial permeability transition pore. However, cytochrome c release

can occur in the absence of permeability transition and collapse of mitochondria membrane potential.

Physiologically, Bax plays an important role in neuronal development and spermatogenesis. Animals that are deficient in Bax have increased numbers of neurons and males are known to be sterile (Knudson *et al.*, 1995). Under pathological conditions such as cerebral ischemia, upregulation of Bax has been reported in the afflicted area of the tissues, implicating tha participation of this protein in the promotion of neuronal and cardiomyoctic cell death (Krajewski *et al.*, 1997). Changes in levels of expression of Bcl-2 family members including Bax, have been reported in Aβ-mediated apoptosis (Zhang *et al.*, 2002). Indeed, Bax protein levels have been shown to increase in AD (MacGibbon *et al.*, 1997).

### 1.3.4 Caspase-3

Caspases, a family of cysteine-aspartate proteases (Namura *et al.*, 1998) that include at least 14 members divided into threee groups (I, II and III), are essential players in apoptotic death (Martin & Green, 1995). The role of caspases in apoptosis first became evident when a cell death-related gene, *ced-3*, which is essential for apoptosis in *Caenorhabditis elegans,* was found to be homologous to the mammalian caspases (Yuan *et al.*, 1993). Caspases specifically cleave their substrate after an aspartate residue. Caspases which have long prodomains are believed to be the up-stream initiator caspases. Among them, caspase-8 and caspase-10 contain two tandem repeats of the 'death effector domains' (DEDs). By contrast, caspases with short prodomains, including caspase-3 and caspase-7, are believed to be downstream effector caspases that depend on the upstream initiator caspase for activation. Various apoptotic stimuli, such as oxidative stess, ultraviolet light and chemotherapeutic drugs, activate early phase initiator caspases which procedes to activate the executioner caspases (Hoffman, 1999).

Caspases reside in the cell as inactive proforms, which are proteolytically converted into their active forms by autoprocessing or by other caspases (Raff, 1998). Active caspases then cleave specific substrates that need to be activated or inactivated during the process of apoptosis. In the case of caspase-3 (CPP32/Yama/Apopain), the most commonly activated

executioner caspase, this involves the cleavage and processing of an inactive pro-enzyme (32kDa) in the cytoplasm to a 17kDa-12kDa heterodimer (Slee *et al.*, 1999). Activation of caspase-3 is considered to be a reliable marker of apoptotic cell death (Green, 1998). Regulation of caspase-3 occurs by several mechanisms, see Figure 1.9. Engagement of death receptors activate caspase-8 as a result of its interaction with Fas-associated death domain (FADD), which can then cleave pro-caspase-3 to its active form (Wang & Lenardo, 2000). The accumulation of cytochrome *c* in the cytoplasm also plays a pivotal role in the activation of caspase-3. The formation of the complex containing cytochrome c, Apaf-1, and caspase-9 results in the activation of caspase-9. Active caspase-9 further proteolytically activates downstream effector caspase, such as caspase-3 by direct cleavage by the serine protease, granzyme B, or the lysosomal protease, cathepsin-L (Ishisaka *et al.*, 1999). Increased expression of caspase-3 has been detected in AD brain (Nixon et al., 1994). Aβ has been previously found to induce caspase-3 activation (Jordan *et al.,* 1997, Boland & Campbell, 2004) and has the proclivity to cleave PARP (Lazebnik, 1994). Allthough several reports have dismissed the involvement of caspase-3 in Aβ-mediated neuronal cell death (Suzuki, 1997) it seems likely that the role of caspase-3 in Aβ-mediated neurodegeneration is brain region specific (Selnick et al., 1999). It remains a possibility that other members of the caspase family contribute to the residual Aβ-induced cortical apoptosis. Taken together, these reports suggest that caspase-3 is pertinent in the neuronal cell loss that is associated with AD. Once activated, caspase-3 is capable of autocatalysis as well as cleaving and activating other members of the caspase family, resulting in rapid and irreversible apoptosis (Zou *et al.*, 1997).

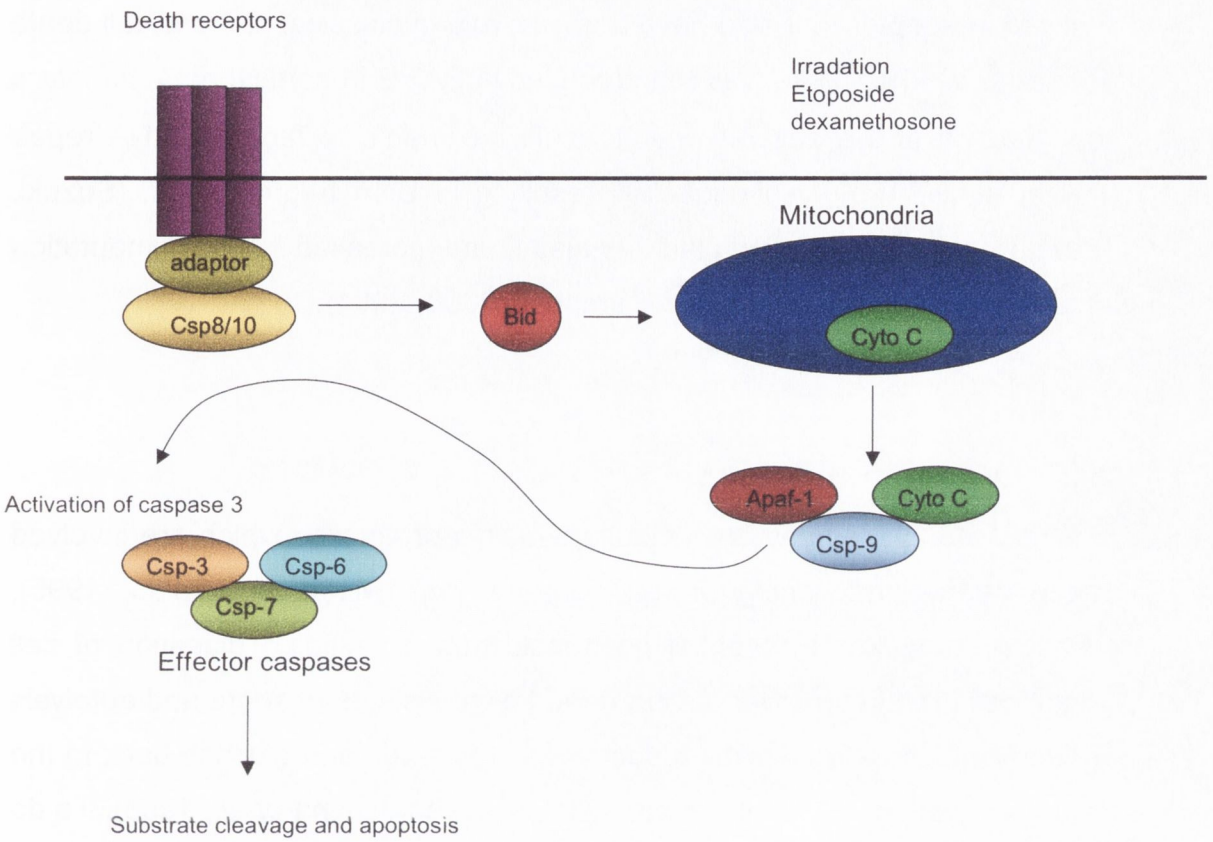


**Figure 1.9** Caspase-dependent apoptosis

Capases operate by cleaving cytoskeletal and nuclear proteins critical for maintenance of cell structure, such as β-actin, lamin B and α-fodrin (Blatt & Glick, 2001). In addition, caspase-3 also cleaves enzymes involved in metabolism, Protein Kinase C (PKC) and the repair enzyme, Poly-(ADP-ribose) polymerase (PARP). Several observations also report that caspases can regulate the mitochondrial-associated proteins, Bcl-2 and Bax and its endogenous inhibitor, inhibitor of caspase activated deoxyribonuclease (ICAD).

### 1.3.5 Poly(ADP-ribose) polymerase

An early target of caspase-3 is the DNA repair enzyme, Poly-(ADP-ribose) polymerase (PARP; (Kaufmann *et al.*, 1993). Following a death stimulus the PARP polypeptide (113kDa) is cleaved by apoptotic proteases

such as caspase-3 to 89kDa and 24kDa PARP fragments, that are considered to be apoptotic markers (Nicotera *et al.*, 1999). DNA strand breaks activate nuclear PARP to participate in DNA repair. Although PARP is centrally involved in apoptosis, it also have a pivotal role in classical necrotic cell death (Pieper *et al.*, 1999). Aβ was found to cleave PARP in cortical neurons into a configuration of the enzyme which would be unable to facilitate DNA repair (Pieper et al., 1999), subsequently resulting in DNA fragmentation (Suzuki, 1997). Results from our own lab has also found increased DNA fragmentation in cells exposed to Aβ (Boland & Campbell, 2003, 2004).

## 1.4 Lysosomal System

Lysosomes are ubiquitous acidic organelles which are involved in the normal functioning of the neuronal cell (Nixon & Cataldo, 1995). Lysosomes carry out essential household duties including digestion of cell waste, cell protein turnover, tissue remodeling, lysis of invaders and autolysis of dead cells, thus replenishing pools of amino acids and glucose back to the cell to be used for *de novo* protein synthesis (Yamashima *et al.*, 1998). To do this more than 80 hydrolytic enzymes are found in lysosomes (Ditaranto-Desimone, 2003). These hydrolytic enzymes function in break down of damaged macromolecules into smaller subunits. All these substrates originate both from endocytosis and autophagy. The acidic pH of the lysosome is maintained by H-ATPase pump in the lysosomal membrane. These pumps function via ATP-dependent active transport of $H^+$ ions through the concentration gradient from cytosol to lysosomal lumen (Geisow, 1982). In this way the physiological pH of the cytosol is maintained. Lysosomes also function as intracellular $Ca^{2+}$ regulators helping to maintain cellular calcium homeostasis (He *et al.,* 2002).

Lysosomal enzymes are synthesised as latent proenzymes (glycoproteins) in the rough endoplasmic recticulum, see Figure 1.10. At this early stage they are inactive. They are then co-translationally glycosylated in the rough ER on some asparagine residues by addition of N-linked oligosaccharides from a lipid dolichol intermediate. They are transferred to the

cis-Golgi through the ER. In the Golgi compartment, they acquire a mannose-6-phosphate (M6-P) ligand, owing to the sequential action of two enzymes, a phosphotransferase (Reitman & Kornfeld, 1981; Waheed *et al.*, 1981) and a diesterase (Varki & Kornfeld, 1981). These receptor-ligand complexes are transported to the endolysosomal compartments where the acidic pH leads to the dissociation of lysosomal enzymes from the mannose-6-phosphate receptors (MPRs). While the receptors then recycle back to the Golgi apparatus, the major part of enzymes that borrows this targeting pathway reaches lysosomes. However, a small proportion of phosphorylated lysosomal polypeptides are released from cells. These secreted enzymes can interact with MPRs present on the plasma membrane and can therefore be internalised and targeted to lysosomes (McHugh *et al.*, 2004).

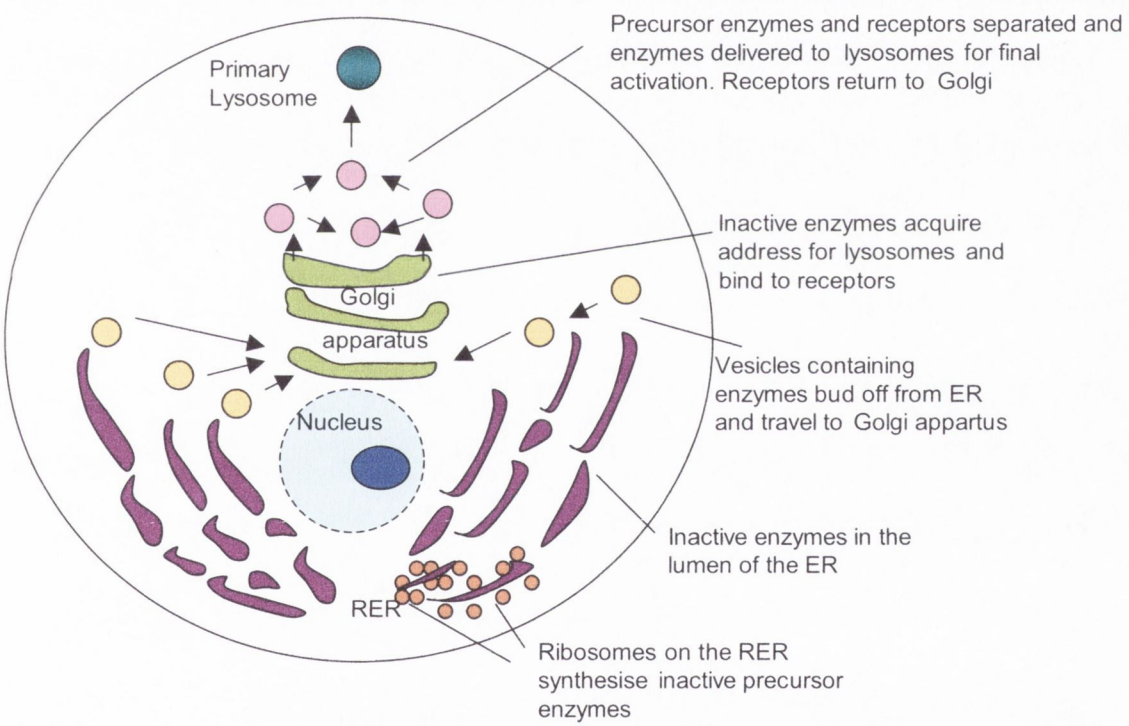


**Figure 1.10** Synthesis of lysosomal enzymes

Different processes lead to degradation by lysosomes, endocytosis and autophagy (see Figure 1.11). Endocytosis provides lysosomes with extracellular material for digestion. It comprises three distinct processes (i) phagocytosis, that results in the digestion of particular material such as bacteria and occurs only in certain specialised cells like neutrophils and

macroghages, (ii) pinocytosis, that allows for internalisation of soluble material, and (iii) receptor-mediated endocytosis, in which the recognition of a molecule by its cognate membrane receptor is required to lead to its engulfment. The autophagic process is implicated in the degradation of cytoplasmic constituents, it is used to recycle damaged or worn out organelles, such as mitochondria and is generally activated in response to stress conditions. Three types of autophagy can be distinguished: (i) macroautophagy, which involves the formation of a double membrane vesicle that fuses with the lysosomal compartment, (ii), microautophagy, which consists of the sequestration of cytosolic components directly at the surface of the degradative organelle and (iii), chaperone-mediated autophagy that targets to the lysosomal membrane substrate proteins having a peptide motif related to KFERQ which is recognised by a cytosolic molecular chaperone. Binding to the LAMP2 protein is then followed by translocation of the substrate protein to the lysosomal lumen.

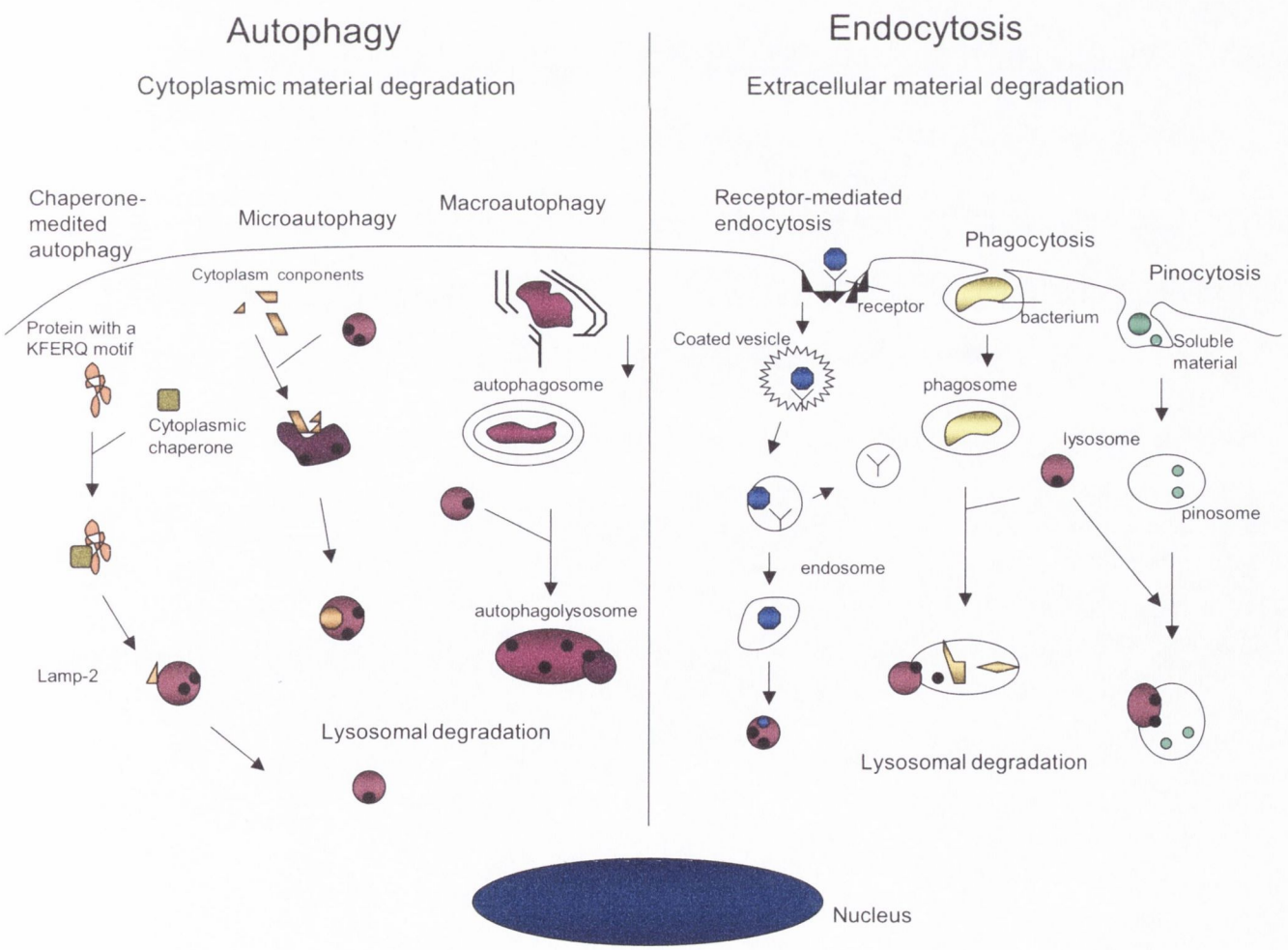

### 1.4.1 Lysosomal membrane proteins

The lysosomal membrane is composed of a phospholipid bilayer which allows passage of uncharged molecules. The proteins in the lysosomal membrane are extensively glycosylated. Based on their amino acid sequence five different membrane proteins have been identified, LAMP 1 and 2, LIMP I and II and Lysosomal acid phosphatase (LAP). These membrane proteins have multiple functions such as sequestration of numerous acid hydrolases, maintenance of an acidic environment and transport of degenerative products and some as yet unknown functions. The collective abundance of LAMP 1 and 2 has been estimated to be high enough to form a nearly continuous carbohydrate coat on the inner surface of the lysosome, thereby protecting them from the highly acidic lumenal region. Lysosomal membrane disruption, with resultant leakage of lysosomal hydrolases to the cytosol, has a potential for killing cells and lysosomal leakage had been implicated in apoptosis (Brunk *et al.*, 2001).

### 1.4.2 Lysosomal Enzymes

A number of enzymes are contained in the lysosome including amylases, lipases and proteases (Adler, 1989). Amongst the proteases found in lysosomes, the cathepsin family are the most prevalent, however before I discuss the cathepsins I would like to briefly mention other types of lysosomal enzymes.

The lysosome contains hydrolases which can generate two sphingolipids, ceramide and sphingosine, believed to mediate the pro-apoptotic effect of various agents. These hydrolases are the acid sphingomyelinase (SMase) and ceramidase and both are active at acidic pH. Lysosomal SMase cleaves sphingomyelin, a main lipid in plasma membranes of mammalian cells, releasing phosphocholine and ceramide and acid ceramidase hydrolases ceramide to sphingosine. These enzymes are activated in response to TNF and other cytokines. Therefore, it is not surprising that SMase has been suggested to play a role in cell death. Lymphoblasts from patients affected with Niemann-Pick disease, an inherited

deficiency of acid SMase activity, were found to be more resistant to ionising radiation-induced apoptosis than normal cells (Santana *et al.*, 1996). In addition, SMase-deficient lymphoblasts were described to resist ionising radiation, ultraviolet (Zhang *et al.*, 2001), and hydrogen peroxide- (Komatsu *et al.*, 2001), Fas- (Cifone *et al.*, 1995), and lipopolysaccharide (LPS)- (Haimovitz-Frienman et al., 1997) induced apoptosis. Palmotoyl protein thioesterase 1 (PPT1) is a lysosomal enzyme targeted to the lysosome in a M6P-dependent manner (Hellsten *et al.*, 1996). The deficiency in PPT1 activity is responsible for a human lysosomal storage disorder called infantile neuronal ceroid lipofuscinosis (INCL) and is characterised clinically by early visual loss and massive neuronal death by apoptosis (Riikonen *et al.*, 2000). Mutations in the CLN2 gene encoding battenin, a transmembrane protein with unknown function, results in the juvenile form of neuronal ceroid lipofuscinosis (JNCL). Preliminary data also suggest that the CLN3 protein might behave as an anti-apoptotic protein that could regulate the production of the pro-apoptotic sphingolipid ceramide (Puranam *et al.*, 1999).

### 1.4.3 Cathepsins

The term "cathepsin" was introduced in 1920 and stands for "lysosomal proteolytic enzyme", regardless of the enzyme class (Chwieralski et al., 2006,Turk *et al.*, 2000), see Figure 1.12. Two classes of lysosomal proteolytic enzymes seem to be the most active in the lysosome; aspartyl proteases (cathepsin D) and cysteine proteases, including cathepsin B, C, H, K, and L proteases. Cathepsin B, D and L are ubiquitously expressed and the most abundant in mammalian cells (Turk *et al.*, 1993). Cathepsins are synthesised as inactive preproenzymes and directed torwards the lysosomal compartment using cellular mannos-6-phosphate receptors. The processing of the proenzymes into the catalytically active form usually occurs within the lysosome (Ishidoh & Kominami, 2002). Any enzymes escaping from the lysosome are in their active, monomeric form and generally do not require any other conformational change.

Cathepsin-L is a broad-spectrum cysteine protease, potent in degrading extracellular proteins such as laminins and fibronectin, serum proteins, cytoplasmic proteins, such as caspase-3 and nuclear proteins (Barrett & Kirschke, 1981). It is responsible for most of the intralysosomal breakdown of normal cells and is synthesised as an inactive proenzyme (31kDa) preventing its premature activity. Conversion to the active enzyme (27kDa) occurs intracellular in the lysosomes at pH 3-3.5 by autocatalytic removal of the prosegment and extracellularly at pH 5.5-6 (Turk *et al.*, 1993).

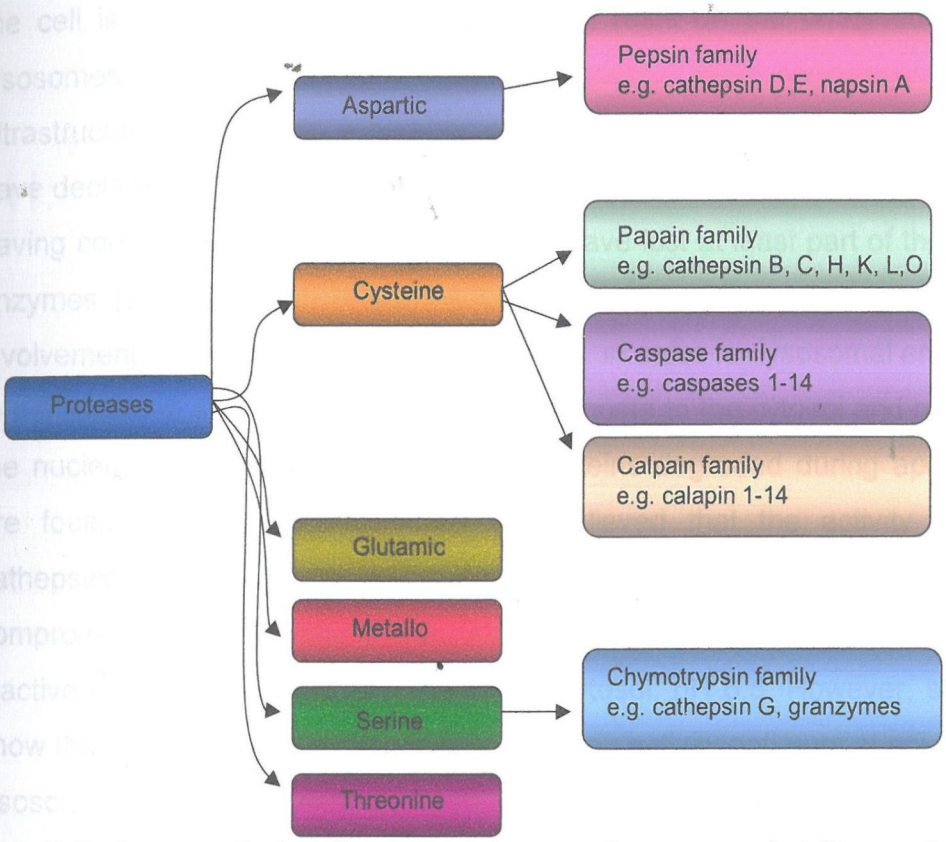


Its activity is normally localised to endosomes/lysosomes but it can also be found in the nucleus.

**Figure 1.12** Classification of proteolytic enzymes

Besides their role in protein degradation, cathepsins also have other physiological functions in the cells. Cathepsin B has been involved in processing and release of other proteins (Turk *et al.*, 2000). Both cathepsin L and S play an important role in antigen processing and presenting (Chapman *et al.*, 1997). Cathepsin K contributes to bone remodelling (Chapman *et al.*, 1997) and cathepsin D is known to participate in protein targeting (Cantor &

Kornfeld, 1992). The implication that cathepsins are involved in the initiation of cell death is addressed in the next section.

### 1.4.4 Lysosomal system and cell death

During the last few years scattered reports have raised the heretical concept that lysosomes might be involved not only in necrosis, as they are well known to be, but in apoptosis as well (Brunk *et al.*, 2001). Reports observe that the lysosomal system can contribute to cell death in a number of ways, including excess autophagy, accumulation of residual bodies or rupture of the lysosome releasing lysosomal enzymes (Yamashima *et al.*, 1998). The old assumption that lysosomes are sturdy organelles that do not break until the cell is already in the proccess of dying rests on the observation that lysosomes, even in severly damaged cells, look suprisingly intact ultrastructurally and thus, a number of accomplished electron microscopists have declared them normal. It has, however long been known that lysosomes having completely normal morphology may have lost at least part of their lytic enzymes (Brunk & Brun, 1972). Another controversial issue regarding the involvement of lysosomes in apoptosis is that, in order for lysosomal enzymes to participate in apoptosis they need to translocate to the cytosol and possibly the nucleus, where most of the cellular proteins degraded during apoptosis are found. However, for years it was believed that the activity of the cathepsins was pH specific and that even if the lysosomal membrane was compromised and cathepsins were released into the cytosol, they would be inactive in the relatively neutral pH of the cytosol, pH 6.5. However, studies show that although lysosomal enzymes have an activity optimum at acidic pH, lysosomal cysteine proteases are stable and active at neutral pH for a time that ranges from a few minutes to an hour or more, confirming their destructive potential in cellular compartments (Turk *et al.*, 1993).

Recently it has emerged that there is an upregulation of the lysosomal system in the brains of patients with AD (Nixon & Cataldo, 1995). Also reports have observed a massive increase in cathepsin B and D levels as well as an increase in the number of lysosomes in the vulnerable neurons of the CA1 region (Nixon *et al.*, 2000). Previous findings from this laboratory has shown increased cathepsin-L activity induced by Aβ (Boland & Campbell, 2004). The mechanism underlying Aβ-mediated release of cathepsin-L from the lysosomal compartment are unclear. However, there is evidence for a $Ca^{2+}$-

dependent mechanism of lysosomal cathepsin release (Gardella et al., 2001), and this may be pertinent given that Aβ has been shown to disrupt $Ca^{2+}$ homeostasis in cortical neurons (MacManus et al., 2000). Similar to Aβ, lysosomal dysfunction has been proposed to play a role in other neurodegenerative diseases such as PD and HD. These findings prompted research into the role of lysosomes and lysosomal proteases in neurodegeneration and apoptosis.

The participation of lysosomal cathepsins B, L and D in apoptosis have been reported (Isahara *et al.*, 1999). For instance, cathepsins have been implicated in CNS apoptosis following ischemia and during neurodegenerative processes (Yamashima *et al.*, 1998). Cathepsin B, which is one of the most stable proteases at physiological pH, is essential in different models of apoptosis, including bile acid-induced hepatocyte apoptosis (Roberts *et al.*, 1997), after brain ischemia (Yamashima *et al.*, 1998), in liver injury in cholestasis (Canbay *et al.*, 2003), in TNF-α-mediated apoptosis of murine hepatocytes (Guicciardi *et al.*, 2000), tumor cells (Foghsgaard *et al.*, 2001), and embryonic fibroblasts. Cathepsin D has also been implicated in apoptosis induced by staurosporane (Bidere *et al.*, 2003) and kainate (Hetman *et al.*, 1995). Finally Cathepsin L, the least stable of the lysosomal cysteine proteases at neutral pH, is an important regulator of ultraviolet-induced apoptosis of keratinocytes (Tobin *et al.*, 2002).

Firestone and co-workers (1979) induced selective lysosomal rupture of a variety of cells by the use of lysomotropic detergents. They descibed the morphology of the dying cell in terms that today would signify classical apoptosis. Release of lysosomal enzymes into the cytosol can lead to variety of consequences. However, it should be noted that in the cytosol there is some protection from the lysosomal proteases that may leak out. Endogenous inhibitors of proteases "cystatins" are located in the cytosol, however this cytosolic insurance is limited and can become overwhelmed.

### 1.4.5 Mechanisms of lysosomal permeabilisation and cell death

Given that cathepsins can translocate and are active in the cytosol, two new questions arise. First, what mechanism leads to the destabilisation of the lysosomal membrane and selective release of cathepsins without a complete breakdown of the organelle and the induction of a necrotic process? Second, exactly what role do cathepsins play in initiating apoptosis. A number of mechanisms have been suggested, see Figure 1.13. Sphingosine a known inducer of apoptosis (Hung *et al.*, 1999) has detergent as well as lysosomotropic properties. Moderate doses were found to induce apoptosis associated with the initial rupture of a limited number of lysosomes (Brunk, 2000; Kagedal *et al.*, 2001). Cells exposed to higher concentrations of sphingosine exhibited early massive and rapid lysosomal rupture and became necrotic. The reason that overwhelming lysosomal rupture caused by agents such as *O*-methyl-L-serine dodecylamide hydrochloride (MSDH) and sphingosine eventuates in necrosis rather than apoptosis may be that the abundant lysosomal enzymes released into the cytosol quickly kill not only the cell but also proteolytically destroy the caspases, thereby disabling the cascade of reactions needed for orderly apoptotic cell death *(*Li *et al. 2000).* Furthermore, Vancompernolle and co-workers (1998) found that atractyloside (a diterpenoid glycoside which causes renal and hepatic necrosis in mammals) induced leakage not only of cytochrome c from mitochondria but also of cathepsin B from lysosomes. In addition, the Bcl-2 family, are known to induce pores in the outer mitochondrial membrane allowing release of cytochrome c from the mitochondria, with subsequent apoptosis (Narita *et al.*, 1998). It is conceivable that Bcl-2 members could also translocate to the lysosomal membrane where they would induce the formation of pores with a similar mechanism. Generation of reactive oxygen species by TNF-$\alpha$ (Manna *et al.*, 1998), LPS (Wang *et al.*, 1997), or increases in intracellular calcium (Smolen *et al.*, 1986) has been shown to cause leakage of the lysosome, possibly as a result of intralysosonmal iron-catalysed oxidative processes

(Antunes *et al.*, 2001). The stress-inducible heat shock protein Hsp70 is an integral part of the lysosomal membrane and it has important anti-apoptotic functions. Depletion of Hsp70 induces the release of lysosomal enzymes in to the cytosol, and apoptosis, which is caspase-independent. Hsp70 increases the volume of the acidic compartments and the resistence against chemical and physical membrane destabilisation (Nylandsted *et al.*, 2002). The 'calpain-cathepsin' hypothesis whereby lysosome rupture is mediated by activation of the calpain protease also has been implicated.

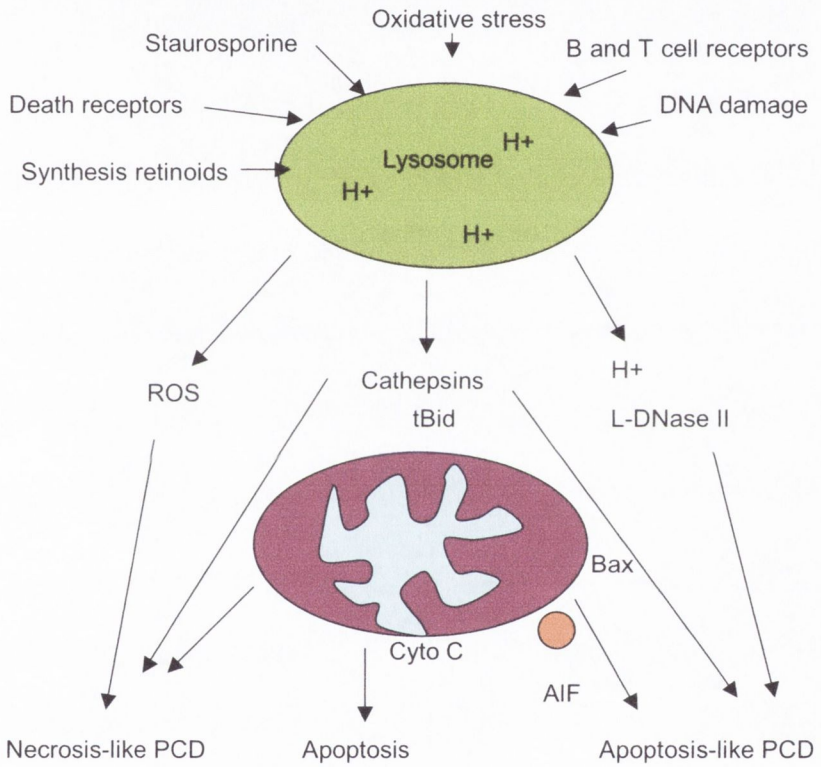


**Figure 1.13** Lysosomal control of PCD

The mechanism by which lysosomes direct apoptosis and the possible cross talk with other known apoptotic pathways remain largely unclear. Lysosomal permeabilisation appears to be an early event in the apoptotic cascade, preceeding other hallmarks of apoptosis like destabilisation of the mitochondria and caspase activation (Bidere *et al.*, 2003). Work by Scholte and colleagues (1998) indicated translocation of cathepsin B from the lysosome to cytosol resulted in cleavage of procaspase 1 and 11 with

subsequent cell death (Katunuma *et al.*, 2001). Although many of the studies so far have addressed cleavage of pro-caspases by lysosomal proteases other substrates of lysosomal enzymes have been suggested. Evidence indicates that lysosomal proteases promote apoptosis by acting on mitochondrial dysfunction, associated with release of proapoptogenic factors (Bidere *et al.*, 2003). Bid, is a cytosolic member of the Bcl family, cleavage of it leads to activation, which goes on to trigger cytochrome c release from the mitochondria, with subsequent caspase activation and apoptosis (Stoka *et al.*, 2001). It appears that lysosomal proteases trigger apoptosis not via a single specific pathway, but rather multiple molecular pathways, which often integrate with the ones controlled by traditional mediators of apoptosis, like caspases and Bcl-2 family proteins.

It is important to note that the lysosomal pathway of apoptosis does not appear to contribute to developmental or physiologic apoptosis of the central nervous system (CNS), heart, liver and limbs. It has been identified primarily in pathological situations and during normal ageing (Bi *et al.*, 2000). Generally knockout mice for single cathepsins develop normally and so do not have any manifest phenotype at the time of birth that distinguish them from their wildtype littermates. This may be due to the redundancy of the cathepsin pathways in the lysosomes and their functional overlap, which ensures that the proper intralysosomal protein degradation and protein turnover during embryonic development occur even in the absence of one protease. However, these mice can develop abnormalities later in life. Cathepsin D knockout mice manifest a normal phenotype at birth, but die at postnatal day 26 ± 1 (Saftig *et al.*, 1995). Cathepsin L knockout mice do not show any difference from their wildtype littermates, except for a slightly higher mortility rate upon weaning. However, they start to lose their fur at postnatal day 21 (Reinheckel *et al.*, 2001). Combined deficiency of cathepsins B and L in mice is lethal during the second to fourth week of life, due to massive apoptosis of select neurons in the cerebral cortex, the cerebellar Purkinje and granule cell layers, resulting in severe brain atrophy (Felbor *et al.*, 2002). It is not clear whether the increased neuronal apoptosis is directly caused by the absence of the two proteases, but, considering their proapoptotic role in other models, it is an area that warrants further research.

### 1.4.6 Lysosomal disorders

Briefly, lysosomal storage disorders (LSDs) represent a class of inborn metabolic diseases related to abnormal functions of the acidic compartments, endosomes and lysosomes (Tardy *et al.*, 2004, for a review). They comprise about 50 different entities and are due to abnormalities in the break-down of all classes of molecules expect nucleic acids. Thus, LSDs include lipidoses, mucopolysaccharidoses, oligosaccharidoses and disorders of protein catabolism. The primary defect underlying LSDs is a more or less severe loss of function of an acid endosomal/lysosomal protein. Hence, a substrate will accumulate in the acidic organelles wither because its transport or its catabolism is impaired. These disorders are not simply a consequence of pure storage, but result from pertubation of complex signalling mechanisms.

## 1.5 Mitogen-activated protein kinases

The mitogen-activated protein kinases (MAPK) represent a group of enzymes that are activated by phosphorylation on serine/threonine amino acid residues and in turn activate other kinases giving rise to a signaling cascade (Derkinderen *et al.*, 1999). The function of these kinases is to convert extracellular stimuli to intracellular signals that, in turn, control the expression of genes that are essential for many cellular responses, including cell growth and death (Marshall, 1995). MAPK have been strongly conserved through evolution demonstrating their importance in intracellular signalling (Sugden & Clerk, 1997). Three structurally related MAPK subfamilies have been identified in mammalian cells; the p42 and p44 kinases ERKs, JNKs/stress activated protein kinases (SAPKs) and the p38 MAPK family.

### 1.5.1 JNK

JNK signalling has been demonstrated in a variety of cellular responses, including proliferation, differentiation, and cellular stress-induced apoptosis (Herr & Debatin, 2001). Several pathways leading to JNK activation have been described, which, although stimulus-dependent, display common features, including the small G-proteins Cdc42 and Rac1 (Coso *et al.*, 1995;

Minden *et al.*, 1995) and phosphotidylinositol 3 kinase (PI3K; Timokhina *et al.*, 1998; Ishizuka *et al.*, 1999). Three JNK isoforms have been identified, JNK1, JNK2 and JNK3, and these are encoded by independent genes, *jnk1, jnk2* and *jnk3*. The product of each gene reveal isoforms with approximate molecular weights of 46 (JNK1), 54 (JNK2) and 57 (JNK3), all of which are found in the mammalian brain (Gupta *et al.*, 1996). Studies of mice deficient in JNK1, JNK2, and JNK3 provide evidence for the functional diversity of isoforms, with mice deficient in JNK1 and JNK2 being embryonically lethal (Kuan, 1999).

JNK proteins are anchored and retained in the cytoplasm by proteins known as JNK interacting proteins (JIPs). These proteins act as a scaffold and mediate signal transduction through upstream kinases leading to final activation of JNK. Following dissociation from this anchor complex JNK can translocate to the nucleus where it can associate with its substrates (Gupta *et al.,* 1995). JNK substrates include c-Jun, activating transcription factor and Elk-1.

JNK has been proposed as a mediator of cell death in response to a variety of stimuli such as excitotoxicity (Yang *et al.*, 1997), oxidative stress (Yoshizumi *et al.*, 2002), irradiation (Timokhina *et al.*, 1998), heat shock (Kyriakis *et al.*, 1994), LPS (Lynch *et al.,* 2004) and cytokines (Minogue *et al.,* 2003). It has been reported that JNK promotes cell death by promoting cytochrome *c* release from the mitochondria (Tournier *et al.*, 2000). In the nervous system, the proapoptotic mitochondrial-associated protein, Bax, acts downstream of JNK in regulating the translocation of mitochondrial cytochrome *c* into the cytosol (Kang *et al.*, 1998), and several studies have demonstrated an interaction between JNK and Bax in the cell death cascade (Lei *et al.*, 2002). Furthermore, increases in JNK are found in association with apoptotic neurons that are detected in the AD brain (Anderson *et al.*, 1994; de la Monte *et al.*, 1997), suggesting that activation of the JNK signalling cascade may mediate Aβ-induced neuronal cell death. However, JNK is also linked to neuroprotection (Herdegen *et al.,* 1997). Therefore its function appears to be cell type and environment specific.

### 1.5.2 ERK

The ERK signalling pathway was the first MAP kinase cascade to be characterised. The ERK family consists of three isoforms denoted ERK1 (p44), ERK2 (p42) and ERK3 (p62). ERK 1 and ERK2 are highly expressed in the brain (Marshall, 1995). Activation of ERK occurs after phosphorylation at threonine and tyrosine residues by MAPK/ERK kinases (MEKs) which, in turn, are activated by MEK kinases (MEKKs). Once activated, ERK phosphorylates and activates other protein kinases, among the substrates of ERK is the family of p90 ribosomal S6 kinases (p90rsk), and cAMP-regulatory element binding (CREB) protein (Wiggin *et al.*, 2002). Brain-derived neurotrophic factor (BDNF) and growth factors including nerve growth factor (NGF) induce ERK signaling in the CNS (York *et al.,* 1998). In addition, activation of NMDA receptors or voltage gated calcium channels increases intracellular $Ca^{2+}$ and stimulate ERK1/2 in neuronal cells (Ely *et al.,* 1990).

ERK activation can lead to contrasting physiological responses in the same cellular type, either transient stimulation of the ERK cascade leading to proliferation in PC12 cells, whereas sustained stimulation leads to differentiation (Marshall, 1995). The ERK2 MAPK cascade is known to play a critical role in hippocampus synaptic plasticity and learning (English & Sweatt, 1997). Activation of ERK2 is required for contextual and spatial memory formation in mammals (Atkins *et al.*, 1998). In the CA1 area of the rodent hippocampus ERK2 is necessary for the expression of a late phase of LTP and is an important pathway through which neurotransmitters modulate LTP induction (Watabe *et al.*, 2000). Studies using a variety of cell cultures point to a possible linkage between Aβ and ERK activation (McDonald *et al.*, 1998; Combs *et al.*, 1999).

## 1.6 p53

The p53 tumour suppressor protein plays an important role in the regulation of stress-mediated G1 cell-cycle arrest to enable DNA repair, or if this is not possible, promoting cell deletion by apoptosis (Levine, 1997). The cell type and environmental conditions (Zornig *et al.*, 2001) are two of a variety of factors that determine the course of the cell. The ability of p53 to induce growth arrest depends on its activity as a sequence-specific transcriptional activator of the $p21^{waf1/cip-1}$ protein, which inhibits cell proliferation by regulating cyclin-dependent kinases (Zornig *et al.*, 2001). However, as most neurons are in a post-mitotic state (Miller *et al.*, 2000), the cell cycle regulatory function of p53 is absent in these cells. In post-mitotic neurons in which DNA fragmentation is occuring following a toxic insult, the regulation of p53 expression is associated with mechanisms underlying cellular apoptosis rather than recovery from the insult (Enokido *et al.*, 1996; Jordan *et al.*, 1997). Mounting evidence now suggests that p53 is involved in neuronal apoptosis (Xiang *et al.*, 1996; Jordan *et al.*, 1997; Napieralski *et al.*, 1999).

While the primary stimulus for inducing p53 activation are DNA single strand breaks (Blatt & Glick, 2001), various other stimuli such as cytotoxic drugs, metabolite deprivation and heat shock can also activate it. Although it is still largely unknown how p53 regulates apoptosis, it appears that transcription-dependent and -independent pathways are involved (Attardi *et al.*, 1996). At the gene level, p53 has been shown to upregulate Bax transcription and repress Bcl-2 transcription, favouring mitochondrial-dependent apoptosis (Miyashita & Reed, 1995). In addition, p53 transcriptionally induces the TNF-related apoptosis-inducing ligand (TRAIL) receptor DR5 and the Fas receptor (CD95), priming the cell for apoptosis (Bennett *et al.*,1998). Other apoptotic genes which p53 targets include, c-fos (Elkeles *et al.*, 1999), MCG10 (Zhu & Chen, 2000), and p53AIP1 (p53-regulated apoptosis-inducing protein-1). P53-inducible gene 3 (PIG3), a p53 inducible gene, produces ROS also resulting in apoptosis (Johnson *et al.*, 1997). Transcriptionally-independent mechanisms of p53-induced apoptotic death included increased surface expression of the CD95 (Bennett *et*

*al.*,1998) death receptor and direct signalling at the mitochondria (Bonini *et al.*, 2004) promoting cytochrome c translocation and procaspase-3 activation.

Cellular p53 concentrations are low due to its short half-life (20 minutes) and metabolic instability when inactivated (Evan & Littlewood, 1998). Studies demonstrate that phosphorylation modulates the biological activities of p53 following p53 DNA damage or cellular stress (Herr & Debatin, 2001). Numerous phosphorylation sites have been mapped on p53, the location of phosphorylation depends on the phosphorylating kinase and the stress-inducing stimulus involved. In response to cellular stress, studies have shown that p53 becomes phosphorylated on a critical serine-15 residue at the p53 N-terminus (Appella & Anderson, 2001). Phosphorylation at this site disrupts the association of p53 with its negative regulator, the oncoprotein, Mdm2, preventing ubiquitin-mediated proteolysis (Shieh *et al.*, 1997). Once phosphorylated the stability of the p53 protein is increased, allowing it to act as a transcription factor to enhance and repress genes involved in the apoptotic process (Herr & Debatin, 2001). Interestingly Mdm2 is a p53-inducible gene, and Mdm2 levels increase following p53 activation (Levine, 1997). Mdm2 in turn inactivates p53 thus forming a negative feedback loop. The phosphorylation state of p53 is controlled by a large number of proteins including JNK, ERKs, caesin kinases and PKC (Blatt & Glick, 2001). Additionally, p53 activation may also involve a change in subcellular localisation, whereas latent p53 may often be cytoplasmic, at least during part of the cell cycle, exposure to stress results in its accumulation in the nucleus, where it is expected to exert its biochemical effects (Shaulsky *et al.*, 1990).

Accumulation of p53 has been linked to the neuronal apoptosis characteristically seen in AD in a number of studies (de la Monte *et al.*, 1997; Culmsee *et al.*, 2001). Previous work from this laboratory has shown a $A\beta_{1-40}$-induced increase in total p53 in cortical neurons. Furthermore, assessment of DNA fragmentation, PARP cleavage and caspase-3 activation were all found to be p53-dependent. The exact intracellular mechanisms have yet to be elucidated.

## 1.7 Calpains

Calpains are a family of calcium-activated intracellular cysteine proteases that carry out proteolytic cleavage on a diverse range of substrates in all eukaryotic cells. Of the 14 members, μ calpain is the form most widely expressed in neurons (Hamakubo, 1986). Calpains reside in the cytosol in an inactive form and become activated when calcium concentration in the cell is elevated (Wang, 2000). Calpains are activated by various stimuli, such as irradiation, etoposide, neurotoxins and ionophores, that increase $[Ca2+]_i$ (Leist & Jaattela, 2001a). Calpain activity is regulated by calpastatin, a natural inhibitor that can be inactivated by calpain- or caspase-mediated cleavage. Calpain plays a role in normal synaptic function (Geinisman, 1991) and is involved in cell death. A sustained influx of $[Ca2+]_i$ ions, such as those seen in neurotoxicity (Siman, 1988) and ischemia (Tolnai and Korecky, 1986), are believed to activate calpain to an extent that is detrimental to the cell. Cathepsin proteases are liberated in the cytoplasm after active calpains compromise the integrity of lysosomal membranes. In AD, a chronic persistent level of μ calpain activation develops at an early stage in the disease, well before neuronal death occurs. In line with this, an *in vitro* study carried out in this laboratory reported Aβ-mediated increase in calpain activation (Boland & Campbell, 2003). The abnormally high level of calpain activation in individuals with familial AD, in conjunction with other findings, suggest that this activity is contributing to the neurodegenerative process and not simply a consequence of it (Nixon, 2003).

## 1.8 Syk

Syk is an enigmatic protein tyrosine kinase functional in a number of diverse cellular processes. Syk was first recognised as a 40 kDa proteolytic fragment derived from a p72 tyrosine kinase present in spleen thymus and lung (Zioncheck *et al.*, 1988). It is best known as a non receptor protein kinase involved in signal transduction in cells of hematopoietic origin and plays a crucial role in signalling in most of these cells (Sada *et al.*, 2001). Originally cloned from porcine spleen (Taniguchi *et al.*, 1991) Syk has been

almost exclusively studied in hematopoietic cells such as B and T lymphocytes, natural killer cells, mast cells, macrophages and platelets (Sada *et al.*, 2001). Recently, it has been found in tissues outside of the hematopoietic lineage and it now appears Syk has fundamental cellular functions that are receptor and immunoreceptor tyrosine-based activating motif (ITAM)-independent indicating that Syk is a key molecule controlling multiple physiological functions in non-hematopoietic cells. One interesting non-traditional role of Syk is that of a potential tumour suppressor in breast cancer. Absence of Syk protein in primary breast tumors is correlated with poor outcomes (Coopman *et al.*, 2000).

Syk and zeta activating protein (ZAP)-70 are members of the Syk subfamily which belongs to the protein tyrosine kinases (PTKs). Other members include the Src family and the Tec family (Turner *et al.*, 2000). Activation of Syk occurs through binding of tandem SH2 domains to ITAM. Syk is analogous to JNK as it activates certain pathways by phosphorylation. Activated Syk is critical for tyrosine phosphorylation of multiple proteins which regulate important pathways leading from the receptor, such as calcium mobilisation and MAPK cascades (Coopman & Mueller, 2006).

## 1.9 Aims

The main aims of this thesis were

- to delinate the biochemical pathways induced by $A\beta_{1-40}$ in cortical neurons which results in the demise of neurons
- to examine the role of p53 and Bax in the $A\beta_{1-40}$-signalling cascade in cultured cortical neurons
- to establish whether $A\beta_{1-40}$ impacts on the lysosomal system and if so to elucidate the underlying mechanisms, specifically to examine the expression of lysosomal membrane proteins
- to examine the involvement of Syk in $A\beta_{1-40}$ signalling in cortical cells
- to ascertain whether Syk mediates the $A\beta_{1-40}$–induced destabilisation of the lysosomal membrane

*Chapter 2*

# Methods

## 2.1 Cell culture

### 2.1.1 Aseptic technique

Tissue culture requires the use of sterile techniques to prevent both bacterial and fungal infection. An aseptic technique is required to maintain the sterility of any areas that the cultured cells are exposed to, including the internal areas of culture flasks, bottles, plastics and dissection instruments. The following aseptic technique procedures were adhered to for all cell culture procedures.

### 2.1.2 Sterilisation of glassware, plastics and dissection instruments

All glassware, pipette tips, dissection instruments, deionised $H_2O$ and microfuge tubes (Sarstedt, Leicester, UK) were wrapped in aluminum foil, sealed with autoclave tape (Sigma-Aldrich, Dorset, UK) and autoclaved at 121°C for 30 min (Priorcalve Ltd., Model # EH150, London, UK). To ensure sterility, all equipment used in the dissection procedure was oven baked overnight at 200°C (Sanyo-Gallenkamp Hotbox Oven, Model # OHG050, Loughborough, UK) prior to use.

### 2.1.3 Sterility of work environment

All cell work was carried out in a laminar flow hood (Astec-Microflow laminar flow workstation, Florida, USA). In the laminar flow workstation air passes through high efficiency particle air (HEPA) filters at the top of the flowhood and flows downwards. The airflow creates a downward barrier in front of the open portion of the hood preventing the entry of external airborne contaminants into the laminar flow hood. Before using the laminar flow hood, the interior was sterilized by wiping down all accessable surfaces with 70% ethanol (EtOH), followed by a 15 min exposure to ultraviolet (UV) light. Disposable latex gloves (sprayed with 70% EtOH) were worn at all times when cell manipulations were being performed in the hood. Gloves were changed regularly to avoid contamination.

### 2.1.4 Reagents

Solutions such as phosphate buffered saline (PBS; 100mM NaCl, 80 mM $Na_2HPO_4$, 20mM $NaH_2PO_4$, pH 7.4) were hand filtered into autoclaved glass bottles or sterile 15/50 ml plastic tubes (BD Biosciences, Pharmingen, San Diego, USA) using a 0.2 μm cellulose acetate membrane syringe filter (Pall Corporation, Michigan, USA) attached to a 10 ml sterile syringe (B.Braun Medical Ltd., Melsungen, Germany). Neurobasal medium (NBM: Invitrogen, Paisley, UK) supplemented with heat inactivated horse serum (10%), penicillin (100U/ml), streptomycin (100 U/ml) and glutamax (2mM; Invitrogen, Paisley, UK) was filtered through a 0.2 μm cellulose acetate membrane (Millipore Ireland B.V, Cork, Ireland) in a Millipore Sterifil unit (Sigma-Aldrich, St. Louis, USA) connected to a vacuum pump. Care was taken to ensure that the side and tip of a pipette did not contact anything except the sterile racks (Bell-Art Products, New Jersey, USA) between use and were regularly wiped down with 70% EtOH.

### 2.1.5 Disposal

All used plastic ware was discarded in autoclavable plastic bags (BibbySterlin Ltd., Staffordshire, UK) and autoclaved.

## 2.2 Primary culture of cortical neurons

The culturing of primary cortical neurons is an *in vitro* technique involving dissection of the brain, removal of the cortex and dissociation of the cortical tissue to obtain a population of neurons, which can be maintained for up to two weeks in culture. Primary neuronal cell cultures are superior to cell line models as they represent non-transformed unaltered phenotypes.

### 2.2.1 Preparation of sterile coverslips

13mm diameter glass coverslips (Chance Propper, West Midlands, UK) were sterilised by soaking in 70% EtOH for 24 hr, followed by an overnight exposure to UV light in the laminar flow hood. Sterile coverslips were then coated with poly-L-lysine (60μg/ml in sterile $H_2O$) in a final volume of 25 ml for 1 hr at 37°C to provide a suitable surface to which dissociated neurons would adhere. Coated coverslips were then air-dried in the laminar flow workstation, placed in sterile 24-well plates (Greiner Bio One Gmbh, Kremsmuendter, Austria) and stored at 4°C until required for use (maximum 2 week storage).

### 2.2.2 Animals

Postnatal 1-day old Wistar rats were born at the BioResourses Unit (Trinity College, Dublin 2, Ireland). Animals were maintained under a 12 hr light/dark cycle at an ambient temperature of 22-23°C. On the day of birth, animals were removed from the litter cage and placed in a ventilated box containing suitable cotton wool bedding for transportation to the culture room.

### 2.2.3 Dissection

Primary cortical neurons were established from postnatal 1-day old Wistar rats. Dissection of one brain yielded a preparation of cells which would require 2 individual 24-well plates. Working in a laminar flow hood, rats were decapitated using a large sterile scissors. The skull was exposed by cutting the skin with a smaller sterile scissors close to the inside of the skull. A pair of forceps was used to pull back

the skull, exposing the brain. The cerebral cortices were rapidly removed and placed in a sterile petri dish (Greiner Bio One Gmbh, Kremsmuenster, Austria) containing sterile phosphate buffered saline (PBS). Any meninges were carefully removed using a fine forceps and cortices were chopped into 3-4 mm pieces using a sterile disposable scalpel (Schwann-Mann, Sheffield, UK).

### 2.2.4 Dissociation procedure

Cortical tissue was incubated in 5 ml sterile PBS containing trypsin (0.25% w/v, Sigma-Aldrich, Dorset, UK) for 25 min at 37°C in $CO_2$ incubator. Trypsin digestion was followed by trituration (x5) of the dissociated neurons using 3.5 ml pasteur pipette in sterile PBS containing soyabean trypsin inhibitor (0.1% w/v, Sigma-Aldrich, Dorset, UK), DNAse (0.2mg/ml; Sigma-Aldrich, Dorset, UK) and $MgSO_4$ (0.1M; Sigma-Aldrich, Dorset, UK). The cell suspension was then passed through a sterile 40 μm nylon mesh filter (Becton Dickinson Labware Europe, France) to remove tissue clumps and centrifuged (Sigma-Aldrich, Model # 2K15C, St. Louis, USA) at 2,500 x *g* for 3 min at 20°C. The pellet was resuspended in NBM (Invitrogen, Paisley, UK), supplemented with 10% heat inactivated horse serum (Invitrogen, Paisley, UK), glutamax (2mM; Invitrogen, Paisley, UK), penicillin (100U/ml; Invitrogen, Paisley, UK), and the B27 supplement (1:50 dilution; Invitrogen, Paisley, UK). B27 was added to the NBM due to its neuroprotective antioxidant properties.

### 2.2.5 Plating of resuspended neurons

Resuspended cells in NBM were placed on the centre of each coverslip at a density of 0.25 x $10^6$ cells/coverslip and allowed to adhere to the glass coverslip for 2 hr in a humidified incubator containing 5% $CO_2$ ; 95% air at 37°C (Model # 394-048, Jencons Scientific Ltd., Bedfordshire, UK) prior to each well being flooded with 400 μl of pre-warmed supplemented NBM. Cells were incubated for 3 days *in vitro.* Media was then replaced with supplemented NBM containing 5ng/ml cytosine-arabino-furanoside (ARA-C; Sigma-Aldrich, Dorset, UK) to prevent proliferation of non-neuronal cells and maintain the purity of the cortical neuronal culture. This ensured that microglia and astrocyte contamination was less than 5% in culture

preparations. Contamination of non-neuronal cells was monitored by staining for appropriate markers. Media containing ARA-C was removed after 24 hr and replaced with supplemented NBM (200μl/well). Cells were grown in culture for up to 7 days and culture medium was changed at least every 3 days, depending on treatment conditions. The cells were exposed to $A\beta_{1-40}$ on day 7 *in vitro.* Cultured neurons were monitored by light microscopy (Nikon Labphot, Nikon Instech Co., Ltd, Kanagawa, Japan) on a daily basis to ensure that the cells appeared healthy and lacked fungal or bacterial infection. A sample image of cultured cortical neurons at 4 days *in vitro* is shown in Figure 2.1.

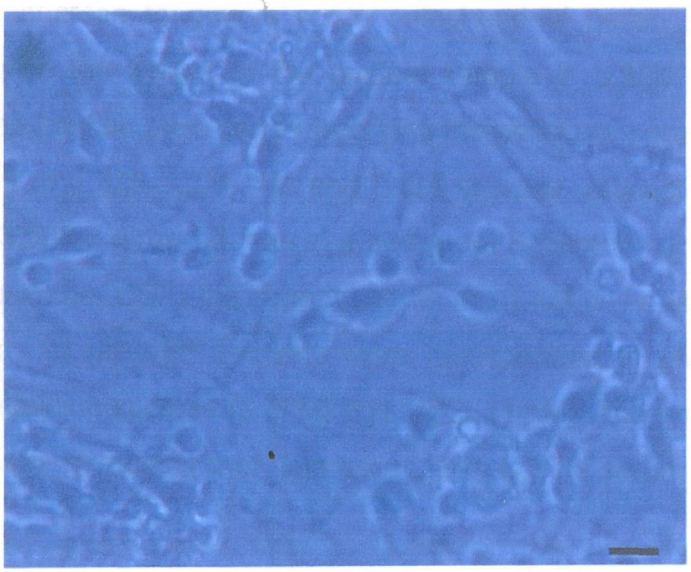

**Figure 2.1 Cultured cortical neuronal morphology**

At day 4 *in vitro* there is a dense population of neurons, displaying oval cell bodies and an extensive neurite network representative of mature neurons. Scale bar is 50μm.

## 2.3 Subcellular fractionation using dissociated cells

Suspensions of cells were prepared as described in section 2.2.3 and 2.2.4. However, in this experiment neurons were not resuspended in NBM but in filtered sterilized Hank's Balanced Salt Solution (HBSS: Sigma-Aldrich, Dorset, UK) containing HEPES (30mM), $MgSO_4$ (1mM), $CaCl_2$ (2mM), 1ml Pen/Strep pH 7.4. Cells were not allowed to adhere to coverslips, but instead were maintained in suspension in 1.5 ml sterile tubes (Sarstedt, Leicester, UK) at a concentration of 2.7 x $10^4$ cells/ml. Suspensions were then treated. Samples were spun for 3,000 x g for 10 min, the resulting pellet washed twice in 0.32M sucrose. The supernatant and washings combined were centrifuged again at 15,000 x g for 20 min, the pellet was washed in 0.32M sucrose to give a crude mitochondrial pellet. The pellet was resuspended in twice the weight of the original sample in 0.32M sucrose and a subcellular-enriched fraction prepared by overlying the pellet on a gradient consisting of layers of 0.6 ml of 1.4M, 1.2M, 1M and 0.8M sucrose, respectively. Following centrifugation at 63,500 x g for 120 min in a swing out Beckman centrifuge (TL-100 Ultracentrifuge, Beckman, USA) the pellet beneath the 1.4M layer was taken as the subcellular fraction. All pelleted fractions were resuspended in phosphate buffer (1mM), pH 6.5, containing sucrose (0.32M) and $MgCl_2$ (1mM). The protein content of all samples was measured using a protein assay, with bovine serum albumin (BSA) as standard.

## 2.4 Cell treatments

### 2.4.1 $A\beta_{1-40}$

$A\beta_{1-40}$ (BioSource International Inc, California, USA) lyophilised peptide was made up as a 1mg/ml stock solution in sterile PBS. The peptide was supplied in a form that is not neurotoxic prior to an incubation step. The appearance of toxicity in response to treatment with Aβ has been shown to correlate to the extent of beta sheet structure (Simmons, 1994), therefore the peptide was allowed to aggregate for 48 hr at 37°C. Thus, in this study the molecular and cellular signalling events induced by $A\beta_{1-40}$ were investigated. For treatment of cortical neurons, $A\beta_{1-40}$ was diluted to a final concentration of 2μM in pre-warmed NBM as previous work from our laboratory had shown this was the optimal dose required to induce cell death (Boland & Campbell, 2003).

### 2.4.2 p53 inhibitor

The p53 inhibitor, pifithrin-α (Calbiochem International, Darmstadt, Germany) was made up as a stock solution of 1mM in dimethylsulfoxide (DMSO) and was used at a final concentration of 100nM. Cells were exposed to the p53 inhibitor for 60 min prior to $A\beta_{1-40}$ treatment, as previously carried out in our laboratory (Boland & Campbell, 2003). This inhibitor is a cell permeable highly lipophilic molecule which efficiently inhibits p53-dependent transactivation of p53-responsive genes and reversibly blocks p53-mediated apoptosis (Culmsee *et al.,* 2001).

### 2.4.3 Calpain inhibitor

The calpain inhibitor, MDL 28170, (Calbiochem International, Darmstadt, Germany) was made up as a stock solution 20mM in DMSO and was used at a final concentration of 10μM. Cells were exposed to the calpain inhibitor for 60 min prior to $A\beta_{1-40}$ treatment, similar to previous studies from our laboratory (Boland & Campbell, 2003). MDL28170 is a cell permeable selective inhibitor of calpain I and II (Chard *et al.,* 1995).

### 2.4.4 Syk inhibitor

The Syk inhibitor (Calbiochem International, Darmstadt, Germany) was made up as a stock solution of 5μM in DMSO and was used at a final concentration of 50nM. Cells were exposed to the Syk inhibitor for 60 min prior to $A\beta_{1-40}$ treatment. This inhibitor is a cell permeable potent inhibitor of Syk which efficiently blocks phosphorylation of Syk substrates (Lai *et al.,* 2003).

When the cell treatment had to be made up in DMSO two controls were required. The first was treated with DMSO alone while a second control was treated with NBM alone, this allowed us to monitor and rule out any affect due to the treatment being dissolved in DMSO.

## 2.5 Protein quantification using the Bradford Assay

Protein concentration in cultured cell samples was assessed according to Bradford (1976). Standards were prepared from stock solution of 1000μg/ml BSA (Sigma-Aldrich, Dorset, UK). This was diluted in $dH_2O$ to prepare a range of standards (including a blank of $dH_2O$) from 1000μg/ml to 3.125μg/ml. Samples (10μl) and standards (10μl) were added to a 96-well plate (Sarstedt, Wexford, Ireland) in duplicate and Bio-Red dye reagent concentration (1:5 dilution in $dH_2O$, 200μl; Bio-Rad, Hertfordshire, UK) was added to both and absorbance was assessed at 600nm using a 96-well plate reader (EIA Multiwell reader, Sigma-Aldrich, Dorset, UK). The concentration of protein in samples was calculated from the regression line plotted (Instat 2.03) from the absorbance of the BSA stardards.

## 2.6 Sodium Dodecyl Sulphate-Polyacrylamide Gel Electrophoresis (SDS-PAGE)

### 2.6.1 Preparation of samples

#### (i) Preparation of total protein

To analyse total expression of protein neuronal cell cultures were washed in Tris Buffered Saline (TBS; 20mM Tris-HCl; 150mM NaCl; pH 7.6) before harvesting by scraping coverslips using the rubber end of a 1 ml syringe piston (B.Braun Medical Ltd., Melsungen, Germany) into lysis buffer (80μl/well; HEPES (25 mM), $MgSO_4$, (5mM), EDTA (5mM), dithiothreitol (DTT; 5mM), PMSF (2mM), leupeptin (2μg/ml), pepstatin (10μg/ml), aprotinin (2μg/ml); pH 7.4) on ice. Lysates were homogenized (x10 strokes) in lysis buffer on ice using a glass homogeniser (Jencons, Bedfordshire, UK). Samples were then centrifuged (13,000 x g for 15 min at 4°C) and the supernatant collected as the whole cell protein.

#### (ii) Preparation of cytosolic and mitochondrial fraction

To obtain cytosolic and mitochondrial protein fractions cells were washed in TBS before 100 μl of permeabilisation buffer (250mM sucrose, 70mM KCL, 137mMNaCl, 4.5mM $Na_2HPO_4$, 1.4mM $kH_2PO_4$, 0.1mM PMSF, 10μg/ml leupeptin, 2μg/ml aprotinin, 200μg/ml digitonin; pH 7.4) was added to each well and left on ice for 5 min. The permeabilisation buffer was then removed and collected as the cytosolic fraction. Mitochondrial buffer (100μl; 50mM Tris Base, 150mM NaCl, 2mM EGTA, 0.2% Triton-X-100, 0.3% Igepal p-40 (v/v), 0.1mM PMSF, 10μg/ml leupeptin, 2μg/ml aprotinin, pH7.2) was then added to each well before harvesting the mitochondrial protein by scraping coverslips using the rubber end of a 1 ml piston (B.Braun Medical Ltd., Melsungen, Germany). Cells were centrifuged (15, 000 x g for 20 min at 4°C) and the supernatant containing the mitochondrial fraction was collected.

Total expression of protein was assessed in all cases unless otherwise stated. All samples were prepared for SDS-polyacrylamide gel electrophoresis. Protein concentrations were assessed and samples equalized with lysis buffer. An equal

volume of sample buffer (0.5M Tris-HCl pH 6.8; 10% glycerol (v/v); 10% SDS (w/v); 5% β-mercaptoethanol (v/v); 0.05% bromophenol blue (w/v)) to sample was added to microfuge tube and samples boiled for 5 min. Samples were stored at -20°C until required

### 2.6.2 Gel electrophoresis

Polyacrylamide separation gels with a monomer concentration of either 7.5%, 10% or 12% overlaid with 4% stacking gel were cast between 10 cm wide glass plates and mounted on a mini electrophoresis unit (Sigma Techware, Dorset, UK) using spring clamps. The upper and lower reservoirs of the unit were filled with electrode running buffer (25mM Tris Base; 200mM glycine; 17 mM SDS). Samples (10μl, ≈20μg protein) were loaded into the wells using a Hamilton Microliter syringe. Prestained molecule weight standards (5μl; Sigma-Aldrich, Dorset, UK) were also loaded to verify the molecular weight of protein bands. Proteins were separated by amplification of a 32 mA current to the gel apparatus and migration of the bromophenol was monitored. The current was switched off when the blue dye band reached the bottom of the gel (approximately 30 min).

### 2.6.3 Semi-dry electrophoresis blotting

The gel was removed from the gel apparatus and washed gently in ice cold (4°C) transfer buffer (25mM Tris-Base; 192mM glycine; 20% methanol (v/v); 0.05% SDS (w/v)). The gel was placed on top of a sheet of nitrocellulose blotting paper (0.45 μm pore size; Sigma-Aldrich, Dorset, UK) wetted in transfer buffer and cut to the size of the gel. One piece of filter paper (Standard Grade No.3, Whatman, Kent, UK) was placed on top of the gel and one piece was placed beneath the nitrocellulose paper forming a "sandwich". The "sandwich" was soaked in transfer buffer and placed on the platinum coated titanium electrode (anode) of a semi-dry blotter (Sigma-Aldrich, Dorset, UK). Air bubbles were removed from the sandwich by gently rolling a pasteur pipette over it. The lid of the blotter (stainless steel cathode) was placed down firmly on top of the sandwich. The uncovered portion of the cathode was shielded with a mylar cut-out (Sigma-Aldrich, Dorset, UK), ensuring all

applied current passed directly through the sandwich. A constant current of 225 mA was applied for 90 min.

## 2.7 Western Immunoblotting

The nitrocellulose blotting paper was blocked for non-specific binding and probed with an antibody raised against the appropriate protein. This was washed off with TBS containing 0.05% Tween (TBS-T, v/v) and incubated with a secondary antibody that was horseradish peroxidase (HRP)-conjugated. A chemiluminescent detection chemical (SuperSignal Ultra; Pierce, Leiden, Netherlands) was added and the blotting paper exposed to 5 x 7 inch photographic film (Hyperfilm, Amersham, Buckinghamshire, UK) and developed using a Fuji X-ray film processor (Model # RGII. FUJIFILM Medical Systems, Stamford, USA).

### 2.7.1 Bax expression

Bax expression was assessed in cytosolic fractions. Non-specific binding was blocked by incubating nitrocellulose in TBS containing 2% BSA (w/v) overnight at 4°C. The membrane was then washed for 10 min 2 times in TBS-T. The primary antibody used was a rabbit polyclonal Bax antibody (Dako Corporation, Carpinteria, CA, USA) that recognises amino acids 43-61 of human Bax (1:200 dilution in TBS-T containing 0.1% BSA; w/v). This was incubated for 2 hr at room temperature (RT) and then washed for 20 min 3 times in TBS-T. The secondary antibody (anti-rabbit IgG-HRP, 1:2000 dilution in TBS-T containing 0.1% BSA (w/v); Sigma-Aldrich, Dorset, UK) was incubated for 90 min at RT and washed for 10 min 12 times in TBS-T. Supersignal (Pierce, Leiden, Netherlands) was added to membranes, incubated for 3 min and the membranes exposed to photographic film (Hyperfilm, Amersham, Buckinghamshire, UK) for 1 sec in the dark prior to being developed using a Fuji X-ray film processor (Model # RGII, FUJJIFILM Medical Systems, Stamford, USA).

### 2.7.2 Cathepsin-L expression

Cathepsin-L expression was assessed in cytosolic fractions. In the case of cathepsin-L expression, non-specific binding was blocked by incubating the membrane in PBS containing 5% BSA for 2 hr at RT. The primary antibody used was a polyclonal IgG antibody purified from goat serum recognising the single chain proform (31 kDa), and its double chain active form (27 kDa) (10ml; 1:1000 dilution in PBS-T containing 0.2% Marvel; Santa Cruz, California, USA). Membranes were incubated overnight at 4°C in the primary antibody and then washed for 15 min (x4) in PBS containing 0.05% Tween (PBS-T v/v). The secondary antibody (10ml; 1:1000 dilution; rabbit anti-goat IgG-HRP in PBS containing 0.1% BSA; Santa Cruz, California, USA) was added and membranes were incubated for 2 hours at RT. Membranes were washed for 15 min (x5) in PBS-T. Supersignal (Pierce, Leiden, Netherlands) was added for 5 min and membranes were exposed to photographic film (Hyperfilm, Amersham, Buckinghamshire, UK) for 1min in the dark before being developed.

### 2.7.3 ERK 2 Phosphorylation

ERK2 expression was assessed in cytosolic fractions. In order to assess ERK 2 phosphorylation, non-specific binding was blocked by incubating nitrocellulose in TBS containing 2% BSA (w/v) overnight at 4°C and then washing for 5 min 3 times in TBS-T. The primary antibody for ERK 2 expression used was a mouse monoclonal $IgG_{2b}$ anti-ERK2 antibody (Santa Cruz Biotechnology Inc, Santa Cruz, CA, USA) that recognises an epitope mapping at the C-terminus of ERK 2 MAP kinase p42 of human origin (1:1000 dilution in TBS-T containing 0.1% BSA; w/v). This was incubated overnight at 4°C and then washed for 20 min 3 times in TBS-T. The secondary antibody (goat anti-mouse IgG-HRP, 1:2000 dilution in TBS-T containing 0.1% BSA (w/v); Sigma-Aldrich, Dorset, UK) was incubated for 60 min at RT and washed for 10 min 12 times in TBS-T. Supersignal (Pierce, Leiden, Netherlands) was added to membranes, incubated for 3 min and the membranes exposed to photographic film for 1 sec in the dark prior to being developed.

### 2.7.4 Total ERK

Total ERK expression was assessed in cytosolic fractions. Following Western immunoblotting for ERK phosphorylation, blots were stripped with an antibody stripping solution as before (see section 2.7.10) and reprobed for total ERK expression in order to confirm equal loading of protein. Non-specific binding was blocked by incubating nitrocellulose membrane in TBS containing 4% BSA (w/v) for 2 hours at RT. The primary antibody used was a mouse ERK polyclonal antibody recognising ERK (1:1000 dilution in TBS-T containing 1% BSA (w/v); Santa Cruz, California, USA). Membranes were incubated overnight at 4°C in the presence of the antibody (1:2000 dilution; goat anti-mouse IgG-HRP in TBS-T containing 1% BSA (w/v); Amersham, Buckinghamshire, UK) and membranes were incubated for 1 hr at RT. Membranes were washed for 15 min 4 times in TBS-T. Supersignal (Pierce, Leiden, Netherlands) was added for 5 min and membranes were exposed to photographic film (Hyperfilm, Amersham, Buckinghamshire, UK) for 3 min in the dark before being developed.

### 2.7.5 JNK phosphorylation

JNK phosphorylation expression was assessed in cytosolic fractions. In the case of phosphorylated JNK expression, non-specific binding was blocked by incubating nitrocellulose in TBS containing 2% BSA (w/v) overnight at 4°C and then washing for 10 min 2 times in TBS-T. The primary antibody for phosphorylated JNK used was a mouse polyclonal anti-phospho-specific JNK antibody (Santa Cruz Biotechnology Inc, Santa Cruz, CA, USA) that recognises JNK1 and JNK2 isoforms of human origin phosphorylated on Thr-183 and Tyr-185 (1:2000 dilution in TBS-T containing 0.1% BSA; w/v). This was incubated for 2 hr at RT and then washed for 20 min 3 times in TBS-T. The secondary antibody (goat anti-mouse IgG-HRP, 1:4000 dilution in TBS-T containing 0.1% BSA (w/v); Sigma-Aldrich, Dorset, UK) was incubated for 90 min at RT and washed for 10 min 12 times in TBS-T. Supersignal (Pierce, Leiden, Netherlands) was added to membranes, incubated for 3 min and the membranes exposed to photographic film for 1 sec in the dark prior to being developed.

### 2.7.6 Total JNK

Total JNK expression was assessed in cytosolic fractions. Following Western immunoblotting for JNK phosphorylation, blots were stripped with an antibody stripping solution (see section 2.7.10) and reprobed for total JNK expression in order to confirm equal loading of protein. As before, non-specific binding was blocked by incubating nitrocellulose membrane in TBS containing 2% BSA (w/v) for 2 hours at RT. The primary antibody used was a rabbit JNK polyclonal antibody recognising JNK1, JNK2 and JNK3 (1:1000 dilution in TBS-T containing 0.2% BSA (w/v); Santa Cruz, California, USA). Membranes were incubated overnight at 4°C in the presence of the antibody (1:1000 dilution; goat anti-rabbit IgG-HRP in TBS-T containing 0.2% BSA (w/v); Amersham, Buckinghamshire, UK) was added and membranes were incubated for 1 hr at RT. Membranes were washed for 15 min 4 times in TBS-T. Supersignal (Pierce, Leiden, Netherlands) was added for 3 min and membranes were exposed to photographic film (Hyperfilm, Amersham, Buckinghamshire, UK) for 3 sec in the dark before being developed.

### 2.7.7 LAMP-1 Expression

LAMP-1 expression was assessed in cytosolic fractions. In order to assess LAMP-1 expression, non-specific binding was blocked by incubating the membrane in PBS containing 5% Marvel overnight at 4°C. The primary antibody used was a polyclonal IgG antibody purified from goat serum which recognises an epitope mapping at the carboxy terminus of LAMP-1 of human origin (10ml; 1:500 dilution in PBS-T containing 0.2% Marvel; Santa Cruz, California, USA). Membranes were incubated overnight at 4°C in the primary antibody and then washed for 15 min (x4) in PBS containing 0.05% Tween (PBS-T v/v). The secondary antibody (10ml; 1:1000 dilution; rabbit anti-goat IgG-HRP in PBS containing 0.1% Marvel; Santa Cruz, California, USA) was added and membranes were incubated for 2 hours at RT. Membranes were washed for 15 min (x5) in PBS-T. Supersignal (Pierce, Leiden, Netherlands) was added for 5 min and membranes were exposed to photographic film (Hyperfilm, Amersham, Buckinghamshire, UK) for 1min in the dark before being

developed using a Fuji X-ray film processor (Model # RGII, FUJJIFILM Medical Systems, Stamford, USA).

### 2.7.8 LIMP Expression

LIMP expression was assessed in a subcellular fraction. In case of LIMP expression, non-specific binding was blocked by incubating the membrane in PBS containing 5% Marvel overnight at 4°C. The primary antibody was a mouse monoclonal IgG $_{2a}$ antibody raised against purified cellular fractions from rat (10ml; 1:200 dilution in PBS-T containing 0.2% Marvel; Santa Cruz, California, USA). Membranes were incubated overnight at 4°C in the presence of the antibody and washed for 15 min 4 times in PBS-T. The secondary antibody (10ml; 1:400 dilution; mouse anti-rat IgG-HRP in PBS containing 0.2% BSA; Amersham, Buckinghamshire, UK) was added and membranes were incubated for 2 hours at RT. Membranes were washed for 15 min 5 times in PBS-T. Supersignal was added for 5 min and membranes were exposed to photographic film for 1 min in the dark before being developed.

### 2.7.9 Phosphorylated p53

Phosphorylated p53 expression was assessed in cytosolic and total cellular fractions as indicated. In the case of phospho-p53, non-specific binding was blocked by incubating membranes in TBS containing 2% BSA (w/v) overnight at 4°C. The primary antibody used was a polyclonal phospho-p53 antibody purified from rabbit serum recognising endogenous levels of p53 only when phosphorylated at residue serine 15 and does not recognize p53 phosphorylated at other sites (10ml; 1:400 dilution in TBS containing 0.05% Tween (TBS-T, v/v) containing 0.2% BSA; Cell Signalling technologies, Massachusetts, USA,. Membranes were incubated overnight at 4°C in the primary antibody and washed for 15 min (x4) in TBS-T. Then the secondary antibody (10ml; 1:1500 dilution; goat anti-rabbit IgG-HRP in TBS-T containing 0.2% BSA; Amersham, Buckinghamshire, UK) was added and incubation continued for 60 min at RT. Membranes were washed for 15 min 4 times in TBS-T. Supersignal (Pierce, Leiden, Netherlands) was added for 5 min and membranes

were exposed to photographic film (Hyperfilm, Amersham, Buckinghamshire, UK) for 10 sec in the dark before being developed using a Fuji X-ray film processor (Model # RGII, FUJJIFILM Medical Systems, Stamford, USA).

### 2.7.10 Phosphorylated Syk

Phosphorylated Syk expression was assessed in cytosolic fractions. In order to assess phospho-Syk, non-specific binding was blocked by incubating membranes in TBS containing 5% BSA (w/v) overnight at 4°C. The primary antibody used was a polyclonal phospho-Syk antibody purified from rabbit serum recognising a residue tyrosin 323. Tyrosin323 is a negative regulatory phosphorylation site within the SH-2 kinase linker region in Syk (10ml; 1:1000 dilution in TBS containing 0.05% Tween (TBS-T, v/v) containing 5% BSA; Cell Signalling technologies, Massachusetts, USA). Membranes were incubated overnight at 4°C in the primary antibody and washed for 15 min (x4) in TBS-T. The secondary antibody (10ml; 1:1000 dilution; goat anti-rabbit IgG-HRP in TBS-T containing 5 % BSA; Amersham, Buckinghamshire, UK) was added and incubation continued for 60 min at RT. Membranes were washed for 15 min 4 times in TBS-T. Supersignal (Pierce, Leiden, Netherlands) was added for 5 min and membranes were exposed to photographic film (Hyperfilm, Amersham, Buckinghamshire, UK) for 10 sec in the dark before being developed using a Fuji X-ray film processor (Model # RGII, FUJJIFILM Medical Systems, Stamford, USA).

### 2.7.11 Total Syk

Phosphorylated Syk expression was assessed in cytosolic fractions. Following Western immunoblotting for Syk phosphorylation, blots were stripped with an antibody stripping solution (1:10 dilution in deionised $H_2O$; Reblot Plus Strong antibody stripping solution; Chemicon, California, USA) and reprobed for total Syk expression in order to confirm equal loading of protein. As before, non-specific binding was blocked by incubating membranes in TBS containing 5% BSA (w/v) overnight at 4°C. The primary antibody used was a polyclonal Syk antibody purified from rabbit raised against a peptide mapping at the C-terminus of Syk of human origin (10ml; 1:1000 dilution in TBS containing 0.05% Tween (TBS-T, v/v) containing

5% BSA; Santa Cruz). Membranes were incubated overnight at 4°C in the primary antibody and washed for 15 min (x4) in TBS-T. The secondary antibody (10ml; 1:1500 dilution; goat anti-rabbit IgG-HRP in TBS-T containing 5% BSA; Amersham, Buckinghamshire, UK) was added and incubation continued for 60 min at RT. Membranes were washed for 15 min 4 times in TBS-T. Supersignal (Pierce, Leiden, Netherlands) was added for 5 min and membranes were exposed to photographic film (Hyperfilm, Amersham, Buckinghamshire, UK) for 10 sec in the dark before being developed using a Fuji X-ray film processor (Model # RGII, FUJJIFILM Medical Systems, Stamford, USA).

### 2.7.12 β-Actin expression

Following Western immunoblotting of the subcellular samples blots were stripped with an antibody stripping solution and reprobed for analysis of total β-actin expression. As before non-specific binding was blocked by incubating the membrane in TBS containing 2% BSA overnight at 4°C. The primary antibody was a mouse monoclonal IgG1 antibody corresponding to amino acid sequence mapping at the carboxy terminus of actin of human origin (10ml; 1:200 dilution in TBS-T containing 0.2% BSA; Santa Cruz, California, USA, Catalogue no. SC-8432). Membranes were incubated overnight at 4°C in the presence of the antibody and washed for 15 min 3 times in TBS-T. The secondary antibody (10ml; 1:500 dilution; goat anti-mouse IgG HRP in TBS-T containing 0.2% BSA; Santa Cruz, California, USA) was added and membranes were incubated for 60 min at RT. Membranes were washed for 15 min and membranes were exposed to photographic film for 10 sec in the dark before being developed.

### 2.7.13 Densitometry

In all cases quantification of protein bands was achieved by densitometric analysis using the Zero-Dscan Image Analysis System (Scanalytics Inc., Fairfax, USA). The procedure is semi-quantitative, a sample from each treatment was included on each blot when loading samples and values are expressed as arbitrary units.

| Protein Target | Antibody source | 2° antibody | Antibody dilution Protein | Protein band Size |
|---|---|---|---|---|
| Phospho-Syk | Rabbit | Goat anti-Rabbit IgG | **1°** 1:10000.05%BSA<br>**2°** 1:1000 5%BSA | 72 kDa |
| Syk total | Rabbit | Goat anti-Rabbit IgG | **1°** 1:1000 0.1%BSA<br>**2°** 1:1500 0.1%BSA | 72 kDa |
| Phospho-JNK1/2/3 | Mouse | Goat anti-mouse IgG | **1°** 1:200 0.1%BSA<br>**2°** 1:400 0.1%BSA | JNK1 46kDa<br>JNK2 54kDa<br>JNK3 56kDa |
| JNK total | Rabbit | Goat anti-Rabbit IgG | **1°** 1:2000 0.1%BSA<br>**2°** 1:4000 0.1%BSA | JNK1 46kDa<br>JNK2 54kDa<br>JNK3 56kDa |
| Cathepsin-L | Goat | Rabbit anti-goat IgG | **1°** 1:1000 0.2%BSA<br>**2°** 1:1000 0.2%BSA | 60 kDa |
| Bax | Rabbit | Goat anti-Rabbit IgG | **1°** 1:200 0.1%BSA<br>**2°** 1:2000 0.1%BSA | 21 kDa |
| LAMP-1 | Goat | Rabbit anti-goat IgG | **1°** 1:500 0.2%BSA<br>**2°** 1:1000 0.2%BSA | 120 kDa |
| Phospho-ERK | Mouse | Goat anti-mouse IgG | **1°** 1:200 0.2%BSA<br>**2°** 1:2000 0.2%BSA | ERK 1 44kDa<br>ERK 2 42kDa |
| ERK | Mouse | Goat anti-mouse IgG | **1°** 1:1000 0.1%BSA<br>**2°** 1:2000 0.1%BSA | ERK 1 44kDa<br>ERK 2 42kDa |
| Phospho-p53 | Rabbit | Goat anti-Rabbit IgG | **1°** 1:400 0.2%BSA<br>**2°** 1:1500 0.2%BSA | 53 kDa |
| LIMP-1 | Rat | Goat anti-Rat IgG | **1°** 1:200 0.2%BSA<br>**2°** 1:400 0.2%BSA | 105 kDa |
| β-Actin | Mouse | Goat anti-Mouse IgG | **1°** 1:200 0.2%BSA<br>**2°** 1:500 0.2%BSA | 46 k Da |

**Table 2.1 Antibodies used for Western blotting**

## 2.8 Fluorescence immunocytochemistry

### 2.8.1 LAMP fluorescence immunocytochemistry

Cells were plated onto coverslips as described in sections 2.2.3. and 2.2.4. Cells were then fixed with 4% paraformaldehyde for 30 min at RT, permeabilised with Triton-X-100 in TBS (0.2%) and refixed with paraformaldehyde for 10 min. Following washing with TBS non-reactive sites were blocked with horse serum (10%) in PBS. Cells were then incubated overnight at 4°C with a goat polyclonal anti-LAMP antibody (1:50 dilution in 10% blocking buffer; Santa Cruz, California, USA). Incubation of the secondary antibody, biotinylated horse anti-goat IgG (1:100 dilution in 10% blocking buffer; Santa Cruz, California, USA) followed washing the coverslips 3 times in PBS. Coverslips were washed several times before incubating them with ExtraAvidin conjugated FITC (1;50 dilution; Santa Cruz, California, USA) for 1 hr at RT. Coverslips were washed with $ddH_2O$ for 40 min before being mounted onto glass slides using a mounting medium for fluorescence (Vector Laboratories Inc., California, USA) and viewed under X40 magnification using a fluorescene microscope (Leitz Orthoplan Microscope, Leica, Wetzlar, Germany) in conjunction with Improvision software (Improvision, Coventry, UK). Cells were observed under excitation 490nm; emission, 520nm for FITC-associated LAMP.

### 2.8.2 Syk fluorescence immunocytochemistry

Treated cultures were fixed with 4% paraformaldehyde for 30 min at RT, permeabilised with Triton-X-100 in TBS (0.2%) and refixed with paraformaldehyde for 10 min. Following washing with TBS non-reactive sites were blocked with goat serum (10%) in PBS. Cells were then incubated overnight at 4°C with a rabbit polyclonal anti-Syk antibody (1:100 dilution in 10% blocking buffer; Santa Cruz, California, USA). Incubation of the secondary antibody, biotinylated goat anti-rabbit IgG (1:100 dilution in 10% blocking buffer; Santa Cruz, California, USA) followed washing the coverslips 3 times in PBS. Coverslips were washed several times before incubating them with ExtraAvidin conjugated FITC (1:50 dilution; Santa Cruz, California, USA) for 1 hr at RT. Coverslips were washed with $ddH_2O$ for 40 min

before being mounted onto glass slides using a mounting medium for fluorescence (Vector Laboratories Inc., California, USA) and viewed viewed under X40 magnification using a fluorescene microscope (Leitz Orthoplan Microscope, Leica, Wetzlar, Germany) in conjunction with Improvision software (Improvision, Coventry, UK). Cells were observed under excitation 490nm; emission, 520nm for FITC-associated Syk expression.

### 2.8.3 Phosphorylated Syk fluorescence immunocytochemistry

Cells were plated onto coverslips as described in sections 2.2.3, 2.2.4 and 2.2.5. Cells were then fixed with 4% paraformaldehyde for 30 min at RT, permeabilised with Triton-X-100 in TBS (0.2%) and refixed with paraformaldehyde for 10 min. Following washing with TBS non-reactive sites were blocked with goat serum (5%) in PBS. Cells were then incubated overnight at 4°C with a rabbit polyclonal anti-Syk (Tyr 323) antibody (1:200 dilution in 10% blocking buffer; Santa Cruz, California, USA). Incubation of the secondary antibody, biotinylated goat anti-rabbit IgG (1;100 dilution in 10% blocking buffer; Santa Cruz, California, USA). Coverslips were washed several times before incubating them with ExtraAvidin conjugated FITC (1;50 dilution; Santa Cruz, California, USA) for 1 hr at RT. Coverslips were washed with dd$H_2O$ for 40 min before being mounted onto glass slides using a mounting medium for fluorescence (Vector Laboratories Inc., California, USA) and viewed under X40 magnification using a fluorescene microscope (Leitz Orthoplan Microscope, Leica, Wetzlar, Germany) in conjunction with Improvision software (Improvision, Coventry, UK). Cells were observed under excitation 490nm; emission, 520nm for FITC-associated Phospho-Syk expression.

## 2.9 Localisation of intracellular organelles using fluorescence microscopy

### 2.9.1 Localisation of lysosomes and mitochondria

Fluorescent probes, LysoTracker red, MitoTracker red, (Molecular Probes, Leiden, The Netherlands) were used to visualise neuronal lysosomes and mitochondria, respectively. After neurons had undergone the desired treatment protocol, the culture media was removed from the wells and pre-warmed neurobasal medium containing either LysoTracker (1mM) or MitoTracker (400nM) was added for 25 min, to incorporate the probe. Cells were then washed in PBS and fixed in 4% paraformaldehyde/PBS for 30 min at 37°C. Coverslips were mounted onto microscope slides using a mounting medium for fluorescence (Vector Laboratories Inc., California, USA). Mounted coverslips were viewed under x40 magnification by fluorescence microscopy (Leitz Orthoplam microscope, Leica microscope AG, Wetzlar, Germany) using Improvision software or confocal microscopy. Laser scanning confocal microscopy was performed using a ZEISS LSM 510 META system with Axiovert microscope (Carl Zeiss Jena GmbH, Jena, Germany) with 40×/1.3 Oil objective, equipped with a helium/neon laser set to 543nm. The singletrack standard Rhodamine configuration was selected and cells observed under excitation, 543nm; emission, 599nm, respectively.

### 2.9.2 Co-localisation analysis

In order to assess the sub-cellular distribution of phospho-p53 and Bax, immunolocalisation of these proteins was carried out in cells which had been loaded with either LysoTracker red (1mM) or MitoTracker red (400nM) probes. Cells were permeabilised with 0.2% Triton X-100 for 10 min and refixed in a 4% paraformaldehyde for 10 min. Cells were incubated in blocking buffer 5% goat serum in PBS (phospho-p53 immunocytochemistry) and 5% horse serum in PBS (Bax immunocytochemistry) for 2 hr at RT. Coverslips were washed three times in PBS and incubated with primary antibody (1:50 dilution in 10% blocking buffer) overnight at 4°C. The phospho-p53 primary antibody used was a rabbit phospho-p53 antibody

recognising endogenous levels of p53 only when phosphorylated at residue serine 15, while the Bax primary antibody used was a mouse monoclonal IgG2b antibody raised against amino acids 1-171 of Bax$\alpha$ of mouse origin. Immunoreactivity was detected with goat anti-rabbit IgG biotinylated secondary antibody (Vector Laboratories Inc., California, USA) for phospho-p53 immunucytochemistry, horse anti-mouse IgG (Vector Laboratories Inc., California, USA) for Bax immunocytochemistry (1:50 dilution in 10% blocking buffer). Incubation proceeded for 1 hr at RT, coverslips were then washed 3 times in PBS. Cells were then incubated with Alexa Fluor 488 avidin-conjugate (1:600 dilution in 2.5% serum; Molecular Probes, The Netherlands) for 30 min at room temperature, washed 8 times with $dH_20$ to remove any unbound Alexa Fluor 488 and mounted using a mounting medium for fluorescence (Vector Laboratories Inc., California, USA). Mounted coverslips were viewed under X40 magnification using a confocal microscope. Laser scanning confocal microscopy was performed using a ZEISS LSM 510 META system with Axiovert microscope (Carl Zeiss Jena GmbH, Jena, Germany) with 40x/1.3 Oil objective, equipped with an argon, helium/neon laser set to 488nm, and 543nm, respectively. The multitrack standard FITC/Rhodamine configuration was selected, emission spectra for Alexa 488 (excitation 488 nm, emission 520 nm) and for molecular probes (excitation 543nm, emission 599nm).

## 2.10 Lysosomal integrity assay: Acridine orange (AO) relocation

The integrity of the lysosomal membrane and the maintenance of a lysosomal-cytosolic pH gradient was assessed using the AO relocation technique. In this approach, cells are incubated with a fluorogenic organic weak base which diffuses into cells and accumulates in lysosomes. This accumulation produces a change in the fluorescence emission of the probe, from green to red due to concentration-dependent stacking of the molecules. Disruption of the membrane and/or a marked change in lysosomal pH can therefore be assessed by measuring the change in emission ratio in comparison to controls and by visual inspection.

Cells were exposed to pre-warmed supplemented NBM containing AO (5μg/ml: Molecular Probes, The Netherlands) for 15 min at 37°C. Cells were then rinsed in NBM and exposed to $A\beta_{1-40}$ (2μM) for a variety of timepoints. Cells were viewed either under fluorescence microsopy (Leitz Orthoplan Microscope, Leica, Wetzlar, Germany) at an excitation wavelength of 490nm, emission 520nm and 633nm, and the pattern of AO staining evaluated using Improvision software (Improvision, Coventry, UK) or with confocal microscopy (Zeiss LSM 510 META). Visualisation of the fluorophores using confocal microscopy was achieved using the 488nm argon laser in the lambda mode with 40x/1.4 oil objective. The configuration parameters were as follows: (1) Filters: Ch3-BP 585–615, Ch2–BP 505–530, ChS1 499.3nm–670.7nm; (2) Beam Splitters: HFT 488; (3) scan zoom 1. For each digital image, 512 x 512 pixels were used.

## 2.11 Quantification

Exploiting the concentration-dependent fluorescence quenching property that AO exhibits, we observe that AO-stained cells possess both punctate staining (633nm emission), and green diffuse staining (520nm emission). Upon lysosomal membrane destabilisation (leakiness), the punctate orange AO fluorescence disappears in discrete events, rushing out of the lysosomes and into the cytosol, and the AO diffuses away into the surrounding bulk solution. To quantify lysosomal leakiness the pixel intensity at 633nm was monitored. Linear unmixing was carried out using LSM Image Examiner Software 4.0, which measures pixel intensity at any wavelength (Figure 2.2).

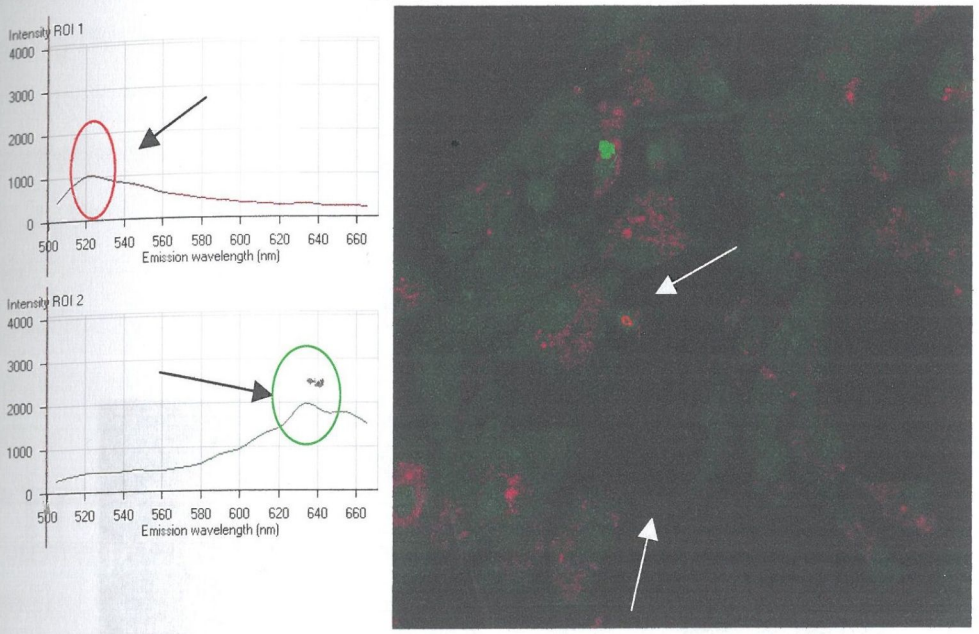


**Figure 2.2 Linear unmixing of fluorescence emissions**

The two fluorescence emissions of AO were highlighted (white arrows) and the software package unmixed the fluorescence signals (black arrows), 520nm and 633nm, as can be seen from the graphs.

A reduction in pixel intensity at fluorescence 633nm emission suggests a relocation of the probe out of the lysosomes. Fields of 5/6 cells were analysed at a time measuring pixel intensity at only the 633nm wavelength, as can be seen in Figure 2.3. In addition, the number of orange intact lysosomes were counted manually by visual inspection. Intact lysosomes of at least 60 individual cells/coverslip from at least 6 coverslips were counted for each treatment, from 4 independent experiments.

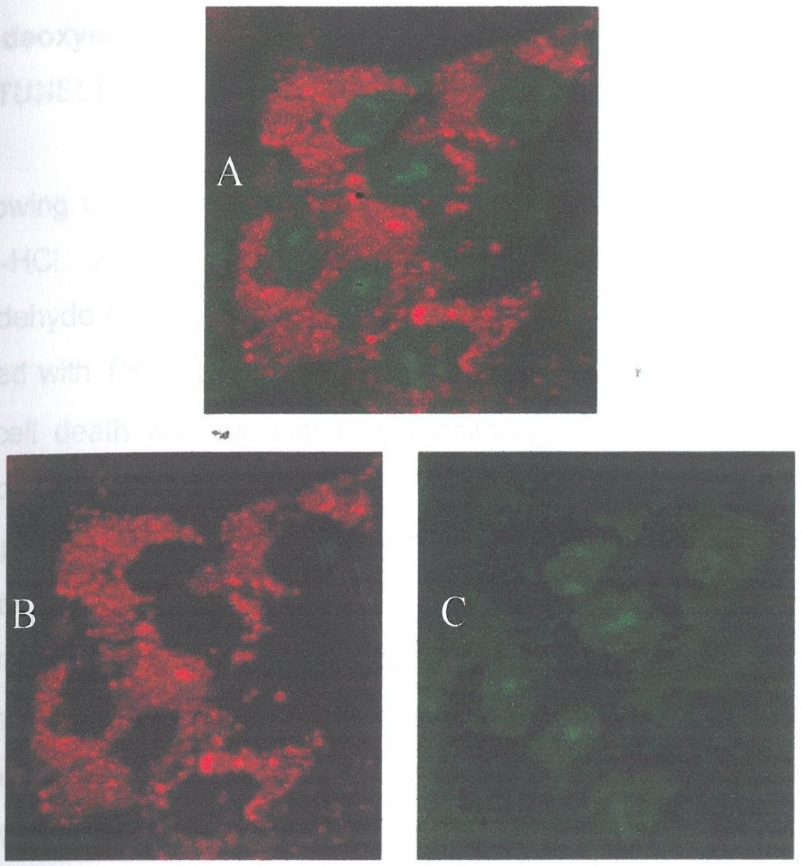


**Figure 2.3 AO staining**

Dual fluorescence emission, 520nm and 633nm can be seen in Figure A, fluorescence at 633nm emission only in Figure B and fluorescence at 520nm emission only in Figure C. The software package measured pixel intensity at 633nm emission only.

## 2.12 Live cell imaging of lysosomal integrity

Real time AO experiments were achieved using the same confocal configuration parameters as above, in addition to the following. Live cell images were acquired with a beam dwell time of 1.05 seconds, an image interval of 1 min between the 1 second acquisition with a laser transmission of 3%. Image series were scanned over 30 min, following treatment of the cells with $A\beta_{1-40}$ (2μM) for 5 hr 30 min.

## 2.13 Evaluation of neuronal viability

### Terminal deoxynucleotidyltransferase-mediated biotinylated UTP nick end labelling (TUNEL)

Following treatment of cultured cortical neurons, coverslips were washed in TBS (Tris-HCl 20mM, NaCl 150 mM, pH7.4) and fixed in 4 % (w/v) paraformaldehyde for 30 minutes at RT. The paraformaldehyde was then removed and replaced with TBS and the cells were stored at 4°C until required for analyses. Apoptotic cell death was assessed by monitoring DNA fragmentation, using the DeadEnd colorimetric apoptosis system (Promega Corporation, Madison, USA). Cells were permeabilised with Triton X-100 (0.1 % v/v), proteinase-k (1μg/ml) in TBS and refixed in 4 % paraformaldehyde for 10 min. Cells were incubated in equilibration buffer (50 μl/coverslip; 200mM potassium cacodylate (pH 6.6 at 25°C), 25 mM Tris-HCL (pH 6.6 at 25°C), 0.2 mM DTT, 0.25 mg/ml BSA, 2.5 mM cobalt chloride) for 10 min. A reaction buffer (100μl/coverslip; 1μl biotinylated nucleotide mix (25 μM biotinylated nucleotide mix, 10mM Tris-HCL, pH7.6, 1mM EDTA), 1μl Terminal deoxynucleotidyl Transferase (TdT) and 98 μl equilibration buffer, Promega Corporation, Madison, USA) was applied for 60 min at 37°C in order to incorporate the biotinylated nucleotide to the 3'–OH DNA ends of fragmented DNA strands. Horseradish-peroxidase-labelled streptavidin was then bound to the biotinylated nucleotide (100 μl; 1:100 dilution in PBS for 1 hr at RT) and this was detected using a DAB solution. Incubation proceded until cells had taken on a stained appearance (approximately 10 min). The coverslips were washed in deionised water, dehydrated through graded alcohols and mounted on slides with DPX mounting medium. Cells were then viewed under light microscopy (Nikon Laboplot, Nikon Instech Co., Ltd, Kanagawa, Japan) at approximately x100 magnification, where nuclei of TUNEL positive cells stained dark purple. Apoptotic cells (TUNEL positive) were counted and expresssed as a percentage of the total number of cells examined (400-500 cells/coverslip) from at least 6 independent experiments.

## 2.14 PCR Analysis

### 2.14.1 RNA extraction

Total RNA was isolated from cells using Tri Reagent (Sigma-Aldrich, Dorset, UK). Cultured neurons were rinsed with diethylpyrocarbonate treated PBS (DECP-treated PBS) and lysed directly by adding 50μl reagent per well and scraping coverslips using the rubber end of a 1ml syringe piston (B.Braun Medical Ltd., Melsungen, Germany). Cells were incubated for 5 min at RT. Separation was achieved by adding 0.2ml of chloroform reagent (Sigma-Aldrich, Dorset, UK) per 1ml of TRI reagent, samples were mixed by inversion and incubated at RT for 2-15 min. Cells were then centrifuged at 12000 x g for 15 min. The aqueous layer was removed and placed in a new eppendorf containing isospropanol (0.5ml per 1 ml of reagent; Sigma-Aldrich, Dorset, UK). Samples were mixed, incubated for 10 min at RT and centrifuged at 12000 x g for 20 min. RNA pellets were then washed with 75% alcohol (Sigma-Aldrich, Dorset, UK) allowed to air dry and dissolved in sterile DEPC treated water. RNA samples were stored at -80°C until required.

### 2.14.2 Gel Electrophoresis

To ensure that isolated RNA was intact and had not been degraded, samples were run on a 1% (w/v) agarose gel. The gel was prepared by dissolving fully agarose (2.0g agarose/130ml TBE) in the microwave. Ethidium bromide (10mg/ml stock) was added to this and the gel cast into the horizontal gel system and allowed to set. Samples were loaded into the wells and RNA was separated by applification of a 90V voltage to the gel appartus. The gel was visualised under UV light and photographed using a UV transilluminator to visualise the RNA.

### 2.14.3 Reverse transcription

First strand cDNA synthesis of the mRNA was carried out using Superscript II RNASE H- Reverse Transcriptase enzyme (Invitrogen, Paisley, UK). 1 μg of sample RNA was mixed with 1 μl of oligo dT Primer (Invitrogen, Paisley, UK) and 1 μl of dNTP mix (Promega, Madison, USA). This mixture was incubated at 65°C for 5 min

then moved to ice. To this reaction mixture, 5X reaction buffer (4μl), 0.1 M DTT (2μl) and Ribonuclease (RNAse) Inhibitor mix (1μl;Promega, Madison, USA) were added and the reaction was preheated to 42°C for 2 min before adding 1 μl of Superscript Reverse Transcriptase enzyme. The reaction was incubated at 42°C for 50 min for cDNA synthesis and then at 75°C for 10 min to inactivate the reverse transciptase.

### 2.14.4 Polymerase Chain Reaction

A mastermix reaction (final volume 25μl) was made up containing 10x reaction buffer (2.5μl), $MgCL_2$.(2.5-3mM), dNTP (1μl), upstream and downstream primers (1μl each), sterile $H_2O$ and Taq polymerase enzyme (0.5μl). Sample cDNA (2.5μl) was added to this mixture. The PCR was run at an initial denaturing step of 95°C followed by 25-35 cycles consisting of a denaturing step of 95°C for 1 min, an annealing step of 56°C for 1 min and an extension step of 72°C for 1 min. A final extension step of 72°C for 10 min was carried out to ensure complete extension of the PCR products. The PCR products (5μl) were loaded into the wells and separated on a 1.5% (w/v) agarose gel and visualised under UV transilluminator.

| Target Gene | Primer Sequence | Annealing Temperature | Fragment Size (base-pairs) |
|---|---|---|---|
| LAMP-1 | Fw:5'GGAGATCCTCCAAGGAGAAATC- 3'<br>Rv:3'AGTGTGAGTGACAAACAGCGTC-5' | 63°C | 297bp |
| β-actin | Fw:5'AGAAGAGCTATGAGCTGCCTGACG-3'<br>Rv: 3'-CTTCTGCATCCTGTCAGCGATGC-5' | 52°C | 236bp |

**Table 2.2 Primer pairs used for PCR**

## 2.15 Analysis of cathepsin-L concentration

The concentration of extracellular cathepsin-L was measured from supernatant collected from cells following treatment with $A\beta_{1-40}$ and analysed by an enzyme-linked immunosorbent assay (ELISA; Calbiochem, UK). The antibody-coated 96-well plate, which came pre-incubated with monoclonal anti-human cathepsin-L antibody, was washed (x3) with 300 μl of PBS containing 0.05% Tween-20, pH 7.4 (PBS-T) at RT. Standards (0-50ng/ml) were made from cathepsin-L standard diluted in sample diluent. Samples were added to the plate (50μl) in duplicate and the detection antibody (50μl; biotin-conjugate anti-cathepsin L antibody in PBS containing 0.05% Tween-20, 0.5% BSA) was added to all wells and incubated at RT for 2 hr on a rotator. The plate was washed 3 times in PBS-T and streptavidin-horseradish peroxidase conjugate (100μl;1:200 dilution in PBS containing 0.05% Tween-20, 0.5% BSA) was added and incubation continued for 20 min at RT. The plate was washed 3 times in PBS-T and substrate solution (100μl; 1:1 dilution of reagent A ($H_2O_2$) and reagent B (tetramethylbenzidine) was added to the wells and incubated in the dark for 20 min creating a colour change to blue. Stop solution (1M Phosphoric acid; 100μl) was added and the plate was read at 450nm within 30 min (Labsystems Multiskan RC). A standard curve was constructed and the concentration of cathepsin-L was extrapolated.

## 2.16 Enzyme activity analysis

### 2.16.1 Measurement of caspase-3 activity

Cleaving of the fluorogenic caspase-3 substrate (Ac-DEVD-7-amino-4-trifluoromethylcoumarin peptide (AFC); Alexis Corporation, Nottingham, UK) to its fluorescent product was used as a measure of caspase-3 activity. Following treatment the culture neurons were harvested in lysis buffer (25mM HEPES, 5mM $MgCl_2$, 5mM DTT, 5mM EDTA, 2mM PMSF, 10μg/ml leupeptin, 10μg/ml pepstatin, 10μg/ml aprotinin, pH 7.4) on ice and homogenised. Samples (50μl) were incubated in the DEVD peptide (10μM; 4μl) or incubation buffer (50μl; 50mM HEPES, 10mM dithiothreitol, 20% glycerol (v/v), pH 7.4) for 1 hr at 37°C and the fluorescence assessed (excitation, 400nm; emisson, 505 nm) using a Fluoroskan Ascent FL platereader (MSC Medical Supply Company Co. Ltd, UK).

### 2.16.2 Measurement of cathepsin-L activity

Cleaving of the fluorogenic cathepsin-L substrate (Z-Phe-Arg-AFC; Alexis, Biochemicals, Nottingham, England) to its fluorogenic product was used to measure cathepsin-L activity. This peptide is a substrate for both cathepsin-B and cathepsin-L, however inactivation of cathepsin-B activity occurs by adding 4M Urea and setting the pH of the incubation buffer to pH5, making it specific for cathepsin-L activity (Kamboj *et al.*, 1993). Following treatment cortical neurons were washed in PBS and harvested in a urea buffer (20 mM NaOAc, 4 mM EDTA, 8 mM DTT, 4 M urea; pH 5) by scrapping cells using the rubber end of a 1mL syringe piston (B.Braun Medical Ltd., Melsungen, Germany). Cell lysates were homogenised, subjected to 3 freeze-thaw cycles and centrifuged 10,000 x g for 10 min at 4°C (Sigma-Aldrich, Model # 2KI5C, St.Louis, USA). Samples of supernatant containing the cytosolic fraction (90μl) were incubated with Z-Phe-Arg conjugated to AFC (150μM; 10μl) for 1 hr at 37°C in a 96 well microtest plate (Sarstedt, Leicester, UK). Fluorescence was assessed by spectrofluorometry (excitation, 400 nm; emission, 505nm) using a Fluoroskan Ascent Fluorometer, (Labsystems, Vantaa, Finland). A standard curve was prepared from a 1 mM stock solution of AFC (Sigma-Aldrich, Dorset, UK) and

diluted in urea buffer into 1000 μM, 500 μM, 250 μM, 125 μM, 62.5 μM, 31.25 μM, 15.625 μM, 7.813 μM and 0 μM (urea buffer) standards. The enzyme activity in cell samples was calculated from the regression line plotted from the absorbance of the AFC standards and converted to pmoles AFC produced/mg/ml of protein/min (GraphPad Instat).

## 2.17 Statistical analysis

Data are expressed as means ± standard error of the means (SEM). Statistical Analysis was carried out by use of a one-way anlysis of variance, followed by a post hoc Student Newman-Kuels test when significance was indicated. When comparisons were being made between two treatments, a paired Student's t-test was performed to determine whether significant differences existed between the conditions. In all cases the alpha level was set at 0.05. All statistical analysis was carried out using Graphpad Prism software.

*Chapter 3*

## 3.1 Introduction

The nuclear phospho-protein, p53, acts as a tumour supressor, providing a protective effect against tumour growth (Zornig *et al.*, 2001). The p53 tumour suppressor gene is functionally inactivated in some 70% of human tumours (Evan *et al.*, 1995). Various stress stimuli such as cytotoxic drugs, metabolic deprivation, physiological damage and heat shock lead to p53 activation, although the primary stimulus for inducing p53 activation is DNA damage (Blatt & Glick, 2001). Normal cellular p53 concentrations are low due to its short half-life and metabolic instability when inactivated (Evan & Littlewood, 1998). Although it is largely still unknown how p53 regulates growth arrest and apoptosis, it has been shown that phosphorylation plays an important role in regulating the biological activities of p53 (Herr & Debatin, 2001). While more than a dozen phosphorylation sites have been mapped on p53, depending on the phosphorylating kinase and the stress-inducing stimulus, the phosphorylation of p53 on residue serine-15 has been shown to be a critical signal required to regulate the p53 response to stress signals. Phosphorylation at serine-15 disrupts Mdm2/p53 binding thus preventing p53 degradation. The increased stability of the p53 protein allows it to act as a transcription factor regulating stress-mediated G1 cell cycle arrest after DNA damage to enable DNA repair (Levine, 1997). However, as most neurons are in a post-mitotic state (Miller *et al.*, 2000) the cell cycle regulatory function of p53 in neurons is absent. Hence, in post-mitotic neurons in which DNA fragmentation is occuring following a toxic insult, the regulation of p53 expression is associated with mechanisms underlying cellular apoptosis rather than recovery from the insult (Enokido *et al.*, 1996; Jordan *et al.*, 1997; Karpinich *et al.*, 2002).

Indeed, accumulating evidence from our own laboratory and others now support a role for p53 in neuronal apoptosis. Assessment of DNA fragmentation, PARP cleavage and caspase-3 activation all confirmed the involvement of p53 in apoptosis (McCormack *et al.*, submitted, 2006). Furthermore, p53 was found to induce apoptosis in post-mitotic hippocampal cells (Jordan *et al.*, 1997) following X-irradiation and in cortical neurons (Xiang *et al.*, 1996) following glutamate exposure. Expression of the p53 protein was

increased in neuronal tissue following experimental traumatic brain injury (Napieralski *et al.*, 1999). In addition, other *in vitro* studies have shown that knocking out the p53 gene protects hippocampal neurons from seizure-induced cell death (Morrison *et al.*, 1996). So, involvement of p53 is an emerging factor in neuronal apoptosis.

There is evidence for an up-regulation of p53 in AD brains (Seidl *et al.*, 1999) and in Down syndrome patients with Alzheimer-like neuropathologic lesions (Kitamura *et al.*, 1997). Upregulation of p53 expression was found in neurons associated with plaques resident in AD brains (de la Monte *et al.*, 1997). Activation of p53 and DNA fragmentation has been reported in transgenic mice that overexpress Aβ (LaFerla *et al.*, 1996), suggesting that Aβ drives p53 accumulation. Culmsee and colleagues (2001) demonstrated that $A\beta_{1-42}$ peptide-mediated neuronal apoptotic cell death occurs through a p53-dependent pathway, thereby supporting the *in vitro* data reported previously in our laboratory which indicates an association between Aβ and enhanced expression of p53 (Fogarty *et al.*, 2003). However, the exact mechanism by which p53 mediates Aβ-induced apoptosis remains to be elucidated. Interestingly, in non-neuronal cells p53 has been found to induce lysosomal destabilisation upstream of a temperature-dependent cell death pathway (Yuan *et al.*, 2002), suggestig that p53 impacts on the lysosomal branch of apoptosis.

Disruption of intracellular organelles is a common event in apoptosis. As well as the mitochondria being involved in apoptosis, there is an increasing body of evidence to suggest a role for lysosomes in the apoptotic process (Li *et al.*, 2000; Brunk *et al.*, 2001). However the role of lysosomes in apoptosis is less well understood. Lysosomes are membrane-bound acidic organelles containing a plethora of hydrolytic enzymes. Lysosomes are normally concerned with cellular housekeeping, removing damaged macromolecules, or organelles, and bacterium from the cellular environment and converting them into reusable products, thus replenishing pools of amino acids and glucose for new protein synthesis. Until recently lysosomes were believed to be static stable organelles seemingly intact even in the latter stages of apoptosis. However, advances in technology has allowed a more

comprehensive study and revealed lysosomes to be dynamic organelles capable of membrane permeabilisation with subsequent apoptotic consequences. Depending on the extent of the lysosomal membrane permeabilisation and the amount of active cathepsins relesed into the cytoplasm, a variety of death morphologies, from classic apoptosis to necrosis, can be triggered. The cellular mechanisms responsible for lysosomal membrane permeabilisation (LMP) remain largely unknown. However, LMP is know to cause translocation of lysosomal proteases such as cathepsins, to the cytosol (Guicciardi *et al.*, 2004) where they induce apoptotic signalling (Leist & Jaattela, 2001b). Although it is accepted that p53 can regulate mitochondrial events during apoptosis, the role of p53 in regulating the lysosomal branch of the apoptotic pathway is less clear. The p53 protein can directly associate with the mitochondrial membrane and form complexes with the anti-apoptotic Bcl-2 protein to induce permeabilisation of the outer mitochondrial membrane, resulting in cytochrome *c* release (Mihara *et al.*, 2003). Because the p53 protein regulates mitochondrial permeabilisation it is plausible that p53 may mediate lysosomal permeabilisation in a similar manner.

The experimental work carried out in this chapter aimed to establish a role for p53 in lysosomal membrane permeabilisation in cortical neurons exosed to $A\beta_{1-40}$. The rationale behind this approach was based on the hypothesis that Aβ-mediates numerous signalling cascades in neuronal cells and that p53 is activated in response to diverse cellular stress including Aβ exposure. Expression of p53 was assessed at the protein level by western immunoblot and confocal fluorescence microscopy. Given that p53 was found to induce lysosomal destabilisation (Yuan *et al.*, 2002) I investigated the involvement of p53 on $A\beta_{1-40}$-induced lysosomal membrane integrity, and assessed if p53 associates with lysosomes. In addition I considered if p53 impacted on lysosomal membrane proteins, in particular LAMP1 expression, since downregulation of LAMP1 could possibly result in destabilisation of lysosomal membrane integrity. Following on from this I assessed the role of p53 on cathepsin-L secretion. To investigate the events which occur downstream of p53 in $A\beta_{1-40}$-treated neurons, the synthetic p53 inhibitor,

pifithrin-α, was applied to cells. This reversible inhibitor has been shown to have antiapoptotic effects in a number of systems (Gudkov & Komarova, 2005) by preventing p53 transactivation (Komarov *et al.*, 1999) and inhibiting Bax expression (Culmsee *et al.*, 2001). More recently, pifithrin-α, has been demonstrated to inhibit p53 phosphorylation and subsequent apoptosis (Chua *et al.*, 2006).

# Chapter 3 Results

## 3.1 $A\beta_{1-40}$-induces the phosphorylation of p53 at residue serine-15 in cultured cortical neurons

Phosphorylation of p53 at specific residues has been demonstrated to stabilise p53 by preventing ubiquitin-mediated degradation, thereby allowing it to act as a transcription factor to enhance and repress genes involved in the apoptotic process (Miyashita & Reed, 1995). Phosphorylation of p53 at residue serine-15, a key site for p53 stabilisation (Appella & Anderson, 2001) was assessed following treatment of cultured neurons with $A\beta_{1-40}$ (Figure 3.1A). Cells were treated with $A\beta_{1-40}$ (2$\mu$M) for 5 min or 1 hr, and p53 phosphorylation was assessed by western immunoblot using an antibody that specifically detects p53 only when phosphorylated at serine 15 (phospho-$p53^{ser\ 15}$). $A\beta_{1-40}$ increases phospho-$p53^{ser\ 15}$ expression from 0.58 ± 0.055 (mean band width ± SEM; arbitrary units) to 1.03 ± 0.116 ($p<0.01$, student's paired t-test, n=8) at 5 min, and from 0.837 ± 0.02 to 1.265 ± 0.118 ($p<0.05$, student's paired t-test, n=8) at 1 hr. Previous work in this laboratory has already shown that $A\beta_{1-40}$-induces an increase in total p53 expression in cultured neurons at 1hr (Fogarty *et al.*, 2003). This result suggests that $A\beta_{1-40}$ increases p53 protein by stabilisation of the protein via phosphorylation at serine-15. A sample immunoblot demonstrating that phospho-$p53^{ser\ 15}$ expression is increased by $A\beta_{1-40}$ is shown in Figure 3.1B.

A.

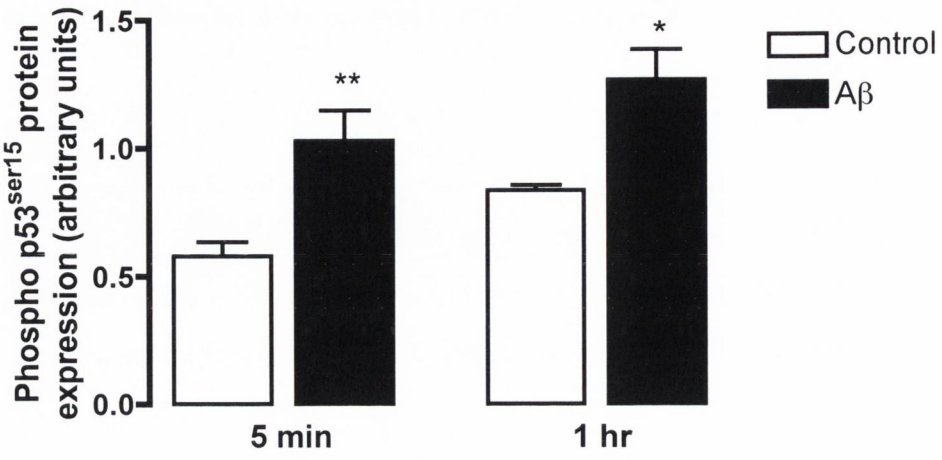


B.

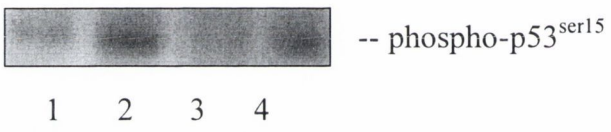


**Figure 3.1 $A\beta_{1-40}$ mediates phosphorylation of p53 at residue serine-15.**

A. Cortical neurons were treated with $A\beta_{1-40}$ (2μM) for 5 min and 1 hr or NBM alone. p53 phosphorylation at residue serine-15 was examined by western immunoblot. $A\beta_{1-40}$ significantly increased p53 phosphorylation at 5 min and 1 hr. Results are expressed as mean ± SEM for 8 observations, student's paired t-test, *$p<0.05$, **$p<0.01$.

B. Sample western immunoblot demonstrating levels of phosphorylated p53 in control (lane 1) and $A\beta_{1-40}$-treated cells (lane 2; 5 min), and control (lane 3) and $A\beta_{1-40}$-treated cells (lane 4; 1 hr).

## 3.2 Association of Phospho-p53 at the lysosome mediated by $A\beta_{1-40}$

In order to investigate whether p53 impacts on the lysosomal system, expression of phospho-$p53^{ser\ 15}$ was assessed by immunocytochemistry. Cells were incubated with $A\beta_{1-40}$ (2μM) for 30 min, 6 hr or 24 hr, prior to a 30 min incubation with the lysosomal marker, Lysotracker red (1mM). Phospho-$p53^{ser\ 15}$ expression was detected by immunocytochemistry using an antibody which specifically recognises p53 phosphorylated at serine-15, and cells were visualised by confocal microscopy. Figure 3.2A represents phospho-$p53^{ser15}$ immunostaining in control cells and in (B) phospho-$p53^{ser15}$ immunofluorescence in $A\beta_{1-40}$-treated cells at 1hr. Distribution of lysosomes in cultured cells are shown in control (C) and $A\beta_{1-40}$-treated cells at 1 hr (D). Co-localisation analysis of phospho-$p53^{ser15}$ and lysosomes are respresented in control (E) and $A\beta_{1-40}$-treated cells (F). $A\beta_{1-40}$ treatment appears to have no effect on the distribution of phospho-$p53^{\ ser\ 15}$ in cortical neurons at this early timepoint of 1 hr.

In contrast, when cells were exposed to $A\beta_{1-40}$ for 6 hr, phospho-$p53^{ser\ 15}$ was observed to co-localise with the lysosomal compartment. Thus, Figure 3.3A demonstrates phospho-$p53^{ser\ 15}$ immunostaining in control cells and this phospho-$p53^{ser\ 15}$ immunofluorescence was increased in $A\beta_{1-40}$-treated cells at 6 hr (B). Distribution of lysosomes in cultured cells are shown in control (C) and $A\beta_{1-40}$-treated cells (D). Furthermore, in $A\beta_{1-40}$-treated cells increased co-localisation of phospho-$p53^{ser15}$ expression with lysosomes was observed at 6 hr (Figure 3.3F). This result indicates that the $A\beta_{1-40}$-mediated increase in phospho-$p53^{ser15}$ expression is coupled with increased association of phospho-$p53^{ser15}$ at the lysosome.

Similarly, Figure 3.4A demonstrates phospho-$p53^{ser\ 15}$ immunostaining in control cells and this phospho-$p53^{ser\ 15}$ immunofluorescence was increased in cells treated with $A\beta_{1-40}$ for 24 hr (B). Location of lysosomes in cultured cells are shown in control (C) and $A\beta_{1-40}$-treated cells (D). Furthermore, in $A\beta_{1-40}$-treated cells increased co-localisation of phospho-$p53^{ser15}$ expression with lysosomes was observed at 24 hr (Figure 3.4F). This result indicates that the $A\beta_{1-40}$-mediated increase in phospho-$p53^{ser15}$ expression is coupled with

increased association of phospho-p53$^{ser15}$ at the lysosome within 6 hr and this association is still present at 24 hr.

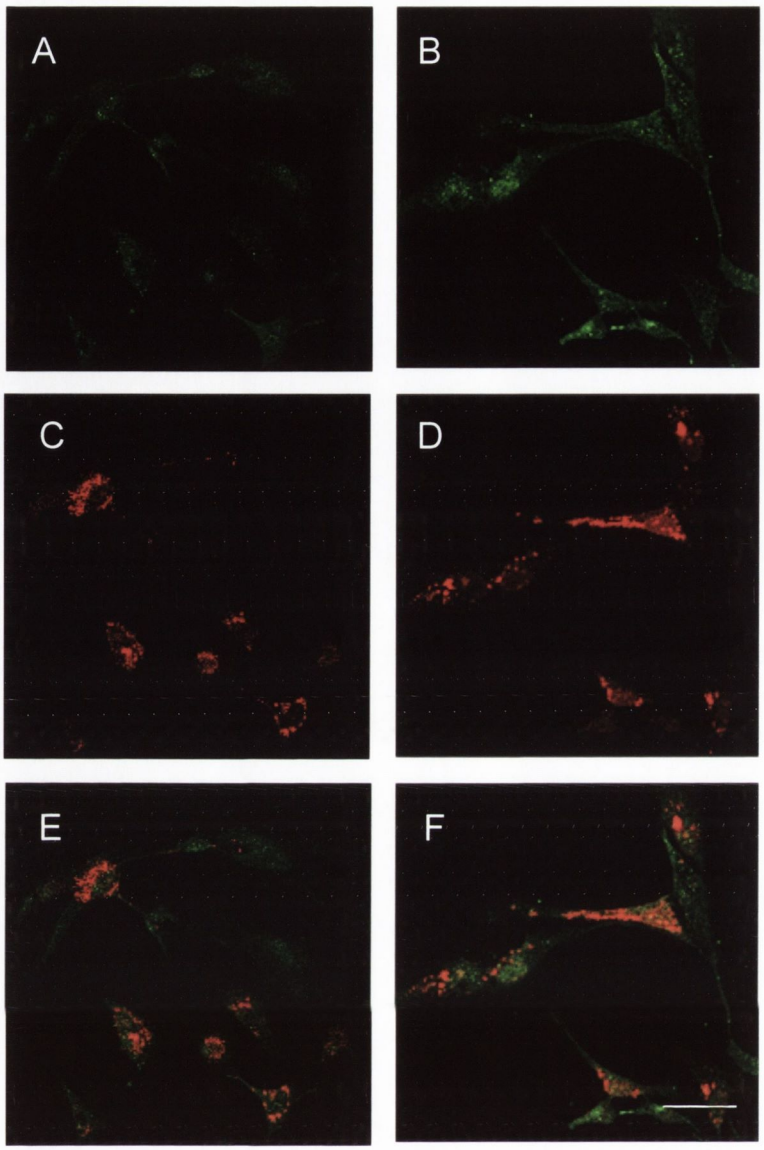


**Figure 3.2 Distribution of Phospho-p53 in cortical neurons at 30 min.**

Confocal microscopy was used to visualise the distribution of phospho-p53$^{ser15}$ within cortical neurons following treatment with A$\beta_{1-40}$ (2$\mu$M) for 30 min. Cells were double labelled with the lysosomal specific agent, Lysotracker red, and a Alexa 488-labelled phospho-p53$^{ser15}$ antibody. Analysis of phospho-p53$^{ser15}$ expression in control (A) and A$\beta_{1-40}$-treated cells (B) (excitation 488nm; emission, 520nm). Lysotracker red staining represents the distribution of lysosomes in control (C) and A$\beta_{1-40}$-treated cells (D) (excitation 543 nm; emission, 599nm). Co-localisation analysis of phospho-p53$^{ser15}$ and lysosomes in control (E), A$\beta_{1-40}$-treated cells (F), Scale bar 50$\mu$m.

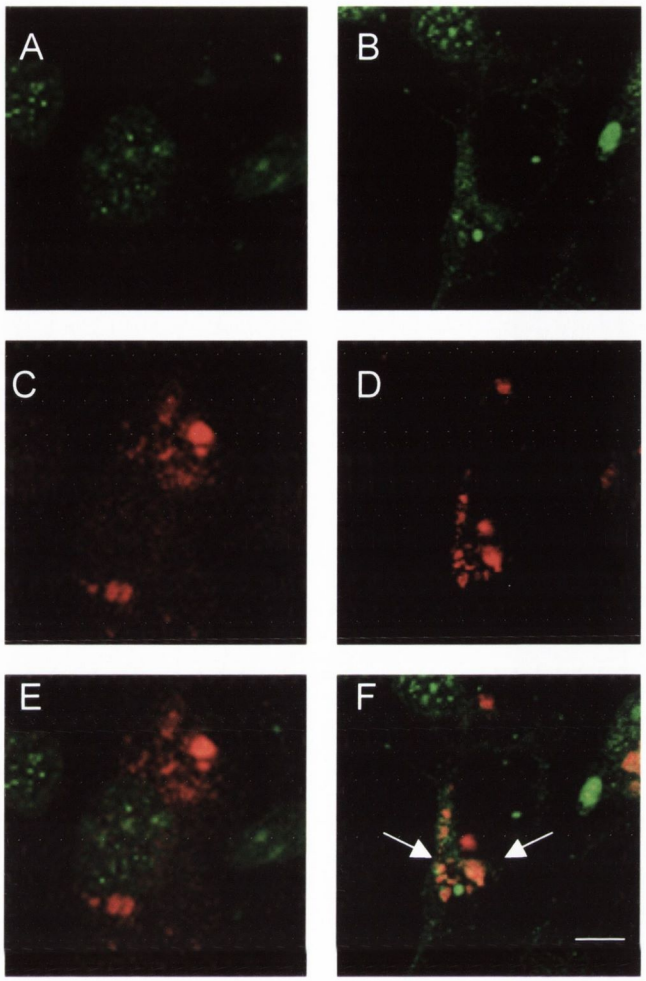


**Figure 3.3 Phospho-p53 expression co-localises with ysosomes in $A\beta_{1-40}$-treated cells at 6 hr.**

Confocal microscopy was used to visualise the distribution of phospho-$p53^{ser15}$ within cortical neurons following treatment with $A\beta_{1-40}$ (2μM, 6 hr). Cells were double labelled with the lysosomal specific marker, Lysotracker red, and an Alexa 488-labelled phospho-$p53^{ser15}$ antibody. Analysis of phospho-$p53^{ser15}$ expression in control (A) and $A\beta_{1-40}$-treated cells (B) (excitation 488nm; emission, 520nm). Lysotracker red staining represents the distribution of lysosomes in control (C) and $A\beta_{1-40}$-treated cells (D) (excitation 543 nm; emission, 599nm). Co-localisation analysis of phospho-$p53^{ser15}$ and lysosomes in control (E), $A\beta_{1-40}$-treated cells (F) revealed increased localization of phospho-$p53^{ser15}$ at the lysosomes in $A\beta_{1-40}$-treated cells. Arrows indicate regions within cells displaying co-localisation. Scale bar 50μm.

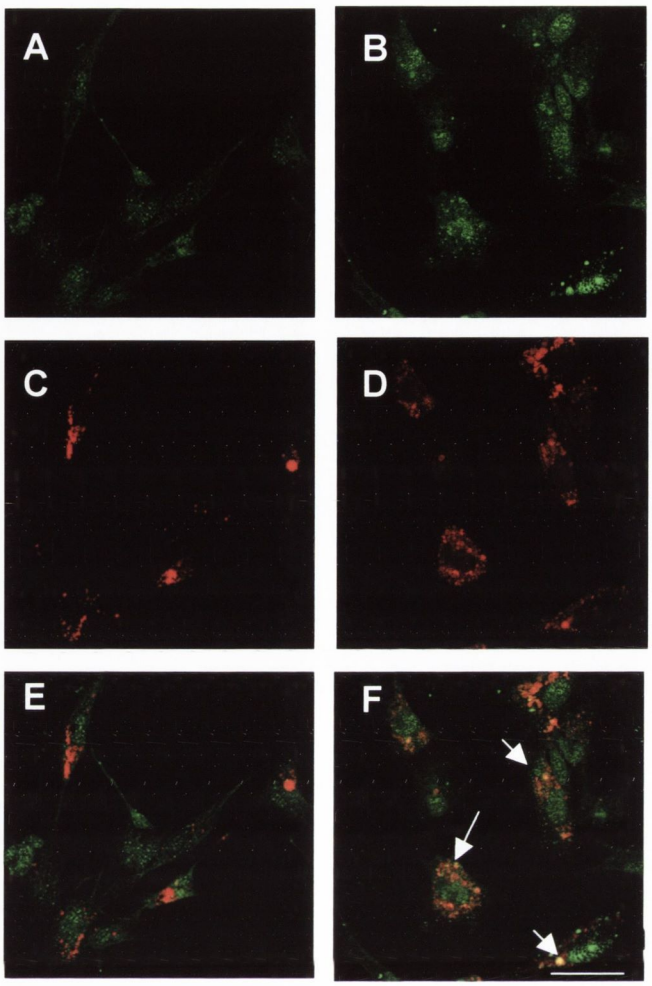


**Figure 3.4 Phospho-p53 expression co-localises with lysosomes in $A\beta_{1-40}$-treated cells at 24 hr.**

Confocal microscopy was used to visualise the distribution of phospho-$p53^{ser15}$ within cortical neurons following treatment with $A\beta_{1-40}$ (2μM, 24 hr). Cells were double labelled with the lysosomal specific marker, Lysotracker Red, and an Alexa 488-labelled phospho-$p53^{ser15}$ antibody. Analysis of phospho-$p53^{ser15}$ expression in control (A) and $A\beta_{1-40}$-treated cells (B) (excitation 488nm; emission, 520nm). Lysotracker Red staining represents the distribution of lysosomes in control (C) and $A\beta_{1-40}$-treated cells (D) (excitation 543 nm; emission, 599nm). Co-localisation analysis of phospho-$p53^{ser15}$ and lysosomes in control (E), $A\beta_{1-40}$-treated cells (F) revealed increased localisation of phospho-$p53^{ser15}$ at the lysosomes in $A\beta_{1-40}$-treated cells. Arrows indicate regions within cells displaying co-localisation. Scale bar 50μm.

## 3.3 Analysis of subcellular fraction

We have shown that $A\beta_{1-40}$ induces an increase in expression of phospho-$p53^{ser15}$ and confocal microscopy indicated that p53 co-localises to the lysosome. Therefore, it was necessary to establish whether p53 is contained within subcellular compartments. To accomplish this we obtained a purified subcellular fraction using gradient density fractionation. To verify that the methology used was sufficient to achieve desired subcellular fractionation, western immunoblot for lysosomal-integrated membrane protein (LIMP), a marker of lysosomal integrity, and cathepsin-L, a lysosomal enzyme, was assessed. LIMP-1 is a heavily glycosylated protein that is bound to the luminal surface of lysosomal membranes, where it functions to protect the membrane from attack by lysosomal enzymes. A sample immunoblot in Figure 3.5A, demonstrates the presence of LIMP protein and Figure 3.5B shows a sample immunoblot of cathepsin-L. Immuoblotting for β-actin, a cytosolic protein, showed that there was no cytosolic contamination in the subcellular fraction (Figure 3.5C). These results confirm that we had indeed a subcellular fraction.

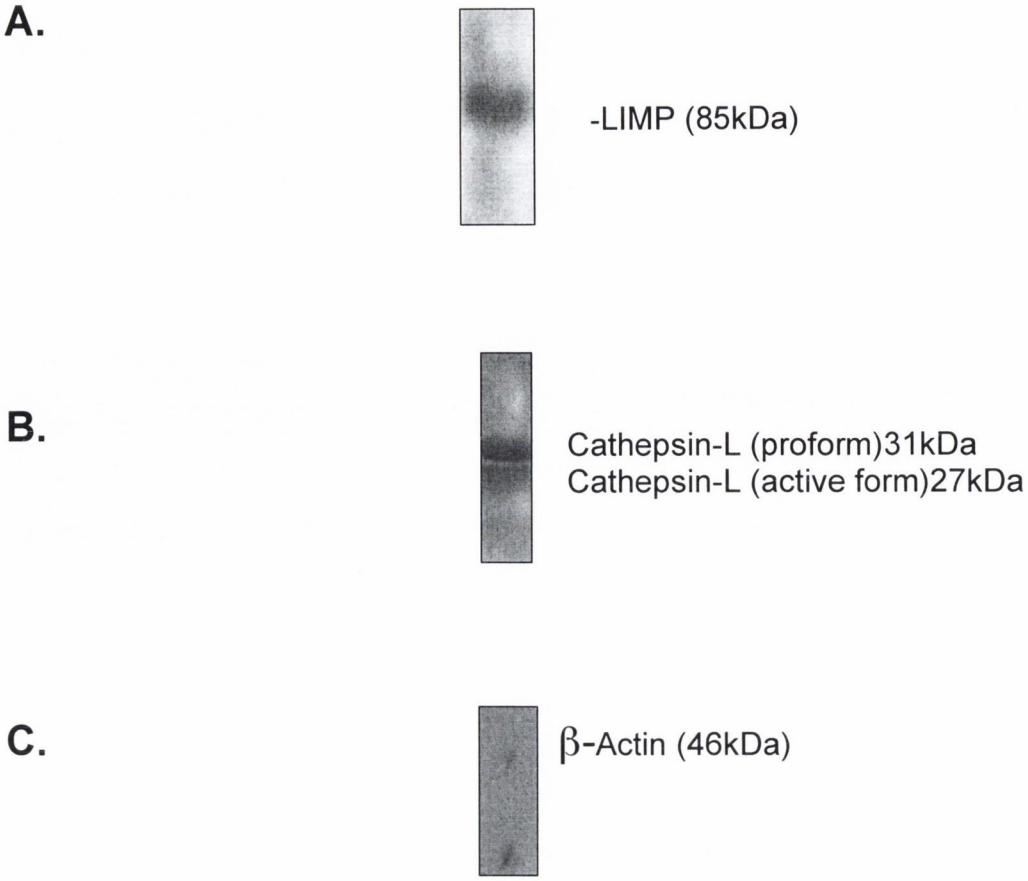


**Figure 3.5 Analysis of subcellular fraction**

Subcellular fractions were isolated from cells as described in methods. Samples were probed for LIMP and cathepsin-L to verify that the methodology used to achieve a subcellular fraction was successful.

A. A sample western immunoblot demonstrating presence of LIMP protein in the subcellular fraction

B. A sample western immunoblot indicating cathepsin-L protein in the purified fraction

C. A sample western immunoblot demonstrating absence of β-actin expression from the subcellular fraction

### 3.4 $A\beta_{1-40}$ increases expression of phospho-p53 in subcellular fractions

Since we found that $A\beta_{1-40}$-mediates the translocation of phospho-p53 to the lysosome, we further verified this observation by examining p53 expression in subcellular fractions prepared from cells using gradient density fractionation. Cortical neurons were treated with $A\beta_{1-40}$ (2μM) for 2 hr after which time subcellular fractions were prepared. The subcellular fractions were equalised for protein expression and prepared for western immunoblot analysis in order to examine phosphorylation of p53 at residue serine-15, a key target site for p53 stabilisation. In Figure 3.6A, analysis of densitometric data demonstrates that $A\beta_{1-40}$ induced a significant increase in subcellular expression of phospho-$p53^{ser\ 15}$ at 2 hr. Thus, phospho-$p53^{ser\ 15}$ expression in control cells was 1638 ± 121 (mean band width ± SEM; arbitrary units) and this was significantly increased to 2679 ± 256 by Aβ ($p<0.01$, student's *t* test, n=6). This result indicates that $A\beta_{1-40}$ promotes the association of phospho-$p53^{ser15}$ with subcellular compartments in cultured cortical neurons, suggesting that p53 may play an important role in the regulation of lysosomal function during the neurodegenerative process. A sample western blot illustrating the effect of $A\beta_{1-40}$ treatment on subcellular phospho-$p53^{ser\ 15}$ expression is shown in Figure 3.6B.

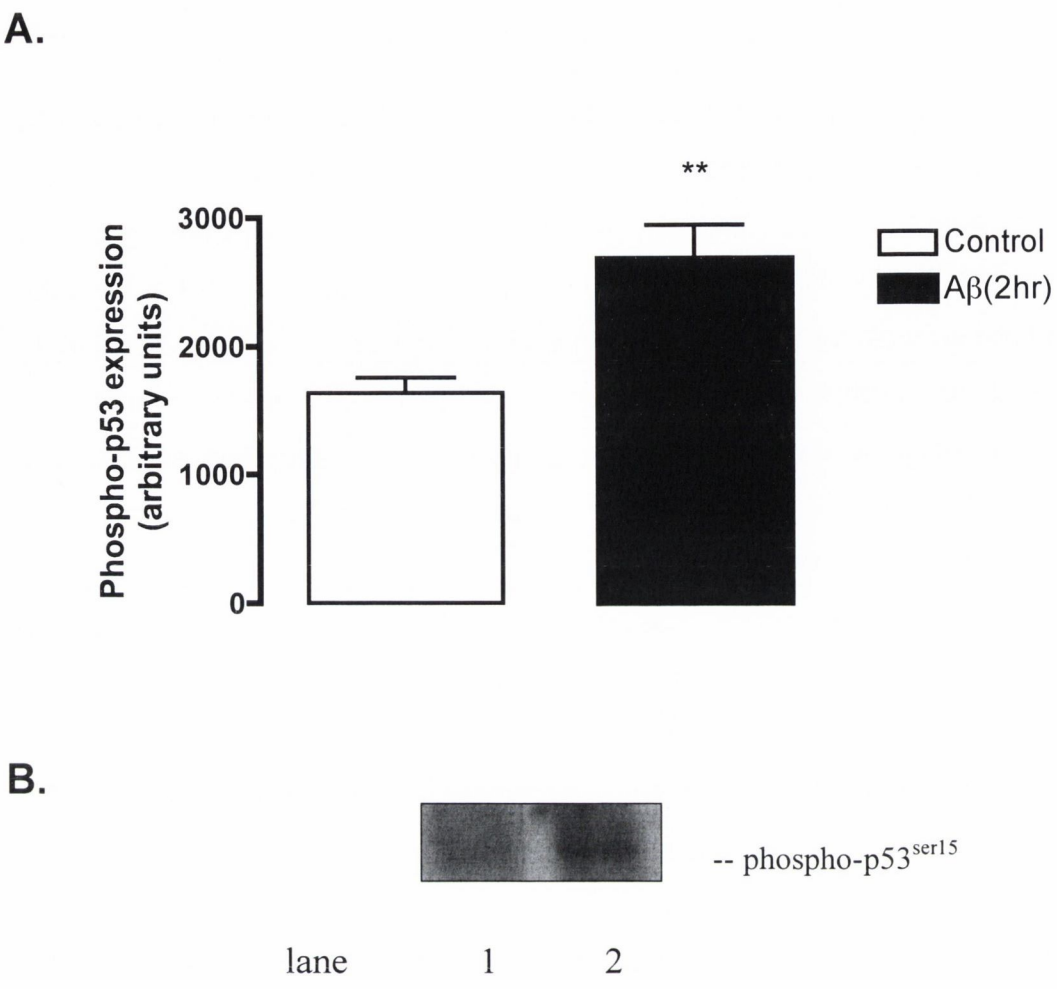


**Figure 3.6 $A\beta_{1-40}$ increases subcellular phospho-p53$^{ser15}$**

A. Cortical neurons were treated with $A\beta_{1-40}$ (2μM) for 2 hr. p53 phosphorylation at residue serine-15 was assessed by western immunoblot in a subcellular fraction. $A\beta_{1-40}$ significantly increased phospho-p53 $^{ser15}$ expression. Results are expressed as mean ± SEM for 6 observations. ** $P<0.01$, student's *t* test, n=6.

B. Sample western immunoblot demonstrating levels of phosphorylated p53 in control (lane 1) and $A\beta_{1-40}$-treated cells (lane 2).

## 3.5 The $A\beta_{1-40}$-mediated increase in subcellular p53 is calpain dependent

Calpain is a $Ca^{2+}$-dependent protease. Reports suggest that calpain can activate p53 in response to DNA damage (Sedarous *et al.*, 2003). Figure 3.7A demonstrates that $A\beta_{1-40}$ induced a significant increase in subcellular expression of phospho-$p53^{ser\ 15}$ at 2 hr. Thus, phospho-$p53^{ser\ 15}$ expression in control cells was 1637 ± 121 (mean band width ± SEM; arbitrary units) and this was significantly increased to 2679 ± 256 by Aβ ($p<0.01$, one-way ANOVA, n=6). Neurons treated with calpain inhibitor, MDL28170, (10μM) alone (2073 ± 126; mean band width ± SEM; arbitrary units) and $A\beta_{1-40}$ in the presence of MDL28170 (1435 ± 72; $p<0.01$, one-way ANOVA, n=6) displayed a level of phospho-$p53^{ser15}$ expression comparable to control. This finding suggests that the $A\beta_{1-40}$-induced increase in lysosomal phospho-p53 is mediated by calpain. A sample western blot illustrating the effect of the calpain inhibitor, MDL28170, on phospho-$p53^{ser\ 15}$ expression is shown in Figure 3.7B.

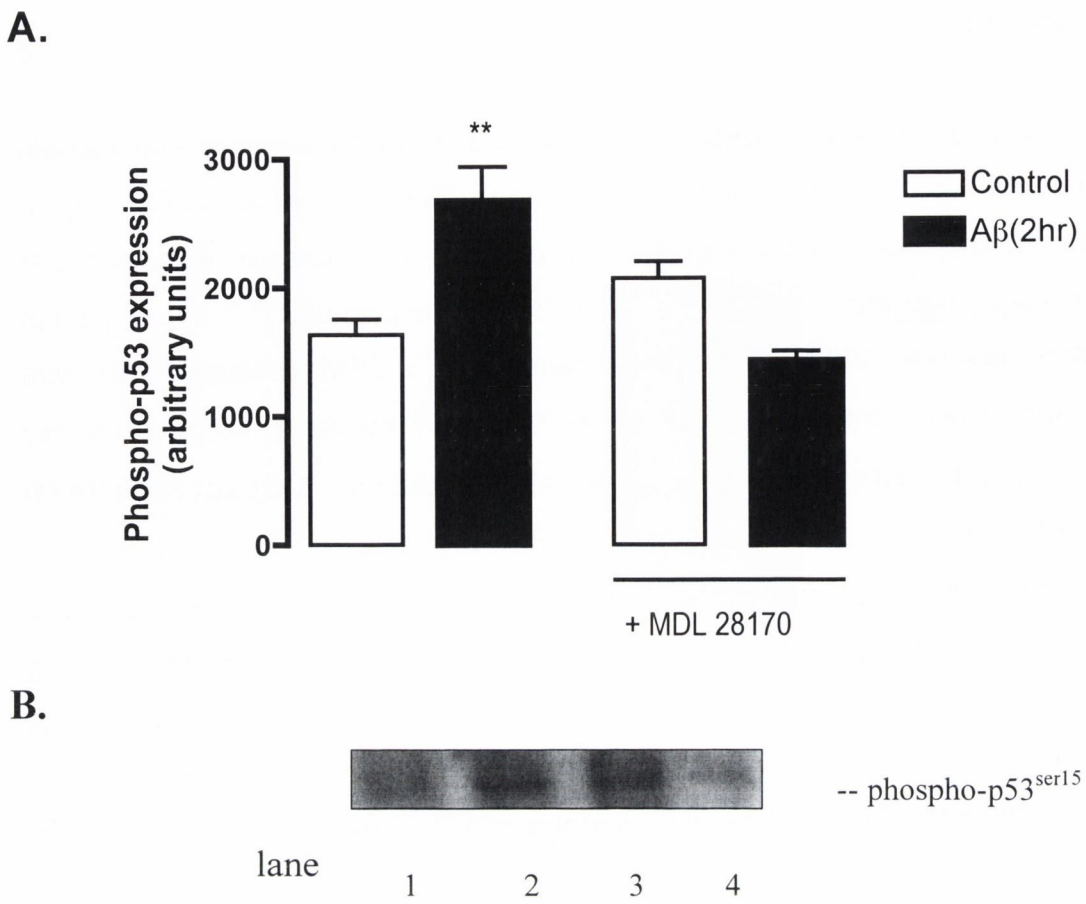


**Figure 3.7 The $A\beta_{1-40}$-induced increase in subcellular expression of phospho-$p53^{ser15}$ is calpain-dependent**

A. Cortical neurons were treated with Aβ (2μM) in the presence or absence of calpain inhibitor, MDL28170 (10μM) for 2 hr. p53 phosphorylation at residue serine-15 was assessed in a subcellular fraction by western immunoblot. $A\beta_{1-40}$ significantly increased phospho-$p53^{ser15}$protein expression at 2 hr. In the presence of MDL28170 the $A\beta_{1-40}$-mediated increased in phospho-$p53^{ser15}$protein expression was significantly reduced. Results are expressed as mean ± SEM for 6 observations. ** $P<0.01$, ANOVA, n=6

B. Sample western immunoblot demonstrating levels of phosphorylated p53 in control (lane1), Aβ (lane2), MDL28170 (lane3) and Aβ+ MDL28170 (lane4).

### 3.6 Effect of $A\beta_{1-40}$ on lysosomal membrane integrity using fluorescence microscopy

Lysosomal rupture can contribute to apoptosis of the cell (Li *et al.*, 2000). AO uptake is used as a method to investigate integrity of lysosomes. It can diffuse across cellular membranes becoming protonated in acidic environments. Once protonated, it is prevented from passing through the hydrophobic membrane layer and so accumulates and thus labels lysosomes. In Figure 3.8 and Figure 3.9 cortical neurons were treated with AO (5μg/ml) for 15 min prior to incubation with $A\beta_{1-40}$ (2μM) for 1 hr or 6 hr, respectively. Relocation of AO from lysosomes into the cell was assessed using fluorescent microscopy. In control cells, AO displays an orange granular fluorescence due to accumulation in the acidic lysosomal vesicles at 1 hr Figure 3.8 (i) and 6 hr Figure 3.9 (i), respectively. Exposure of cells to $A\beta_{1-40}$ (2μM) for 1 hr Figure 3.8 (ii) and 6 hr Figure 3.9 (ii), resulted in reduced orange fluorescence and increased diffuse green fluorescence, suggesting that AO had leaked out of lysosomes. Cells treated with the p53 inhibitor, pifithrin-α (100nM), for 1 hr Figure 3.8 (iii and iv) and 6 hr Figure 3.9 (iii and iv) resulted in punctate orange fluorescence suggesting AO remained within the lysosomal compartment. This result indicates that the $A\beta_{1-40}$-induced destabilisation of lysosomal integrity is p53-dependent.

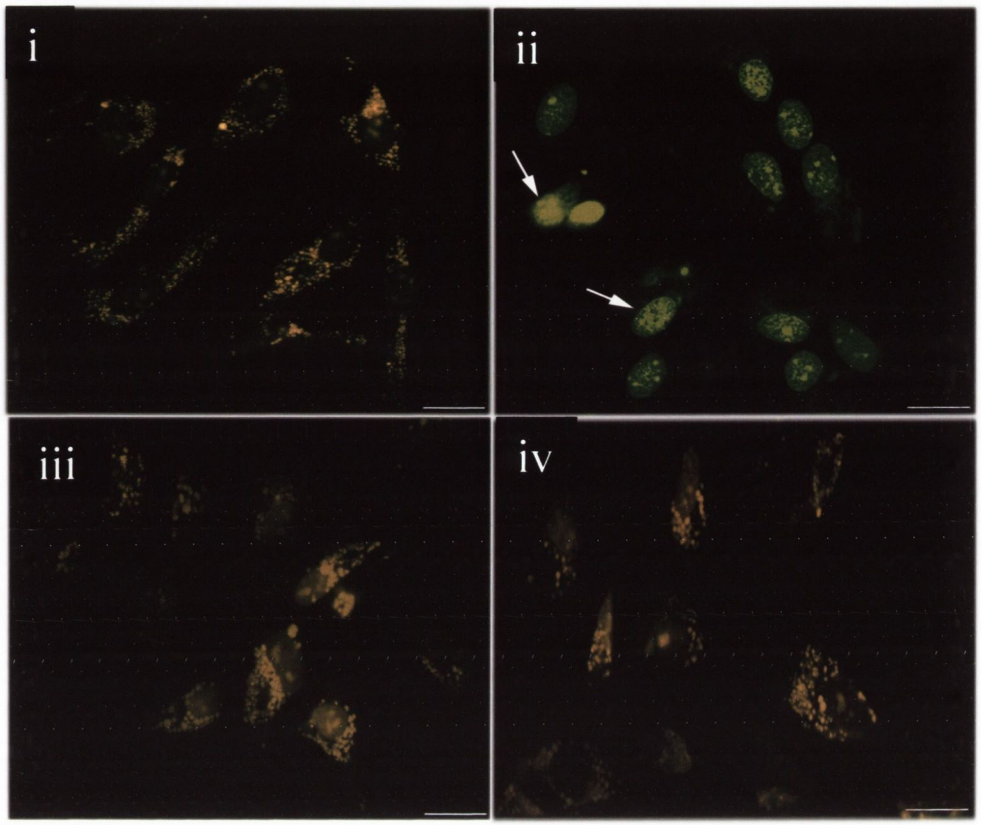


**Figure 3.8 Effect of $A\beta_{1-40}$ on lysosomal membrane integrity at 1hr**

Cortical neurons were exposed to AO (5μg/ml) for 15 min prior to incubation with $A\beta_{1-40}$ (2μM) for 1 hr in the presence or absence of the p53 inhibitor, pifithrin-α (100nM; 60 min pretreatment). Relocation of AO from the lysosomes to cytosol was assessed. AO displayed an orange fluorescence and was localised in discrete punctate compartments within the cell suggesting lysosomal distribution of AO (i). Exposure to $A\beta_{1-40}$ for 1 hr resulted in the disappearance of AO orange fluorescence and an increase in diffuse cytosolic fluorescence (ii). Cells treated with pifithrin-α (iii) and $A\beta_{1-40}$ in the presence of pifithrin-α (iv) displayed an orange fluorescence suggesting AO remained localised in the lysosomal compartment. Arrows indicate cells displaying green AO fluorescence demonstrating an impairment of lysosomal integrity. Scale bar is 10μm.

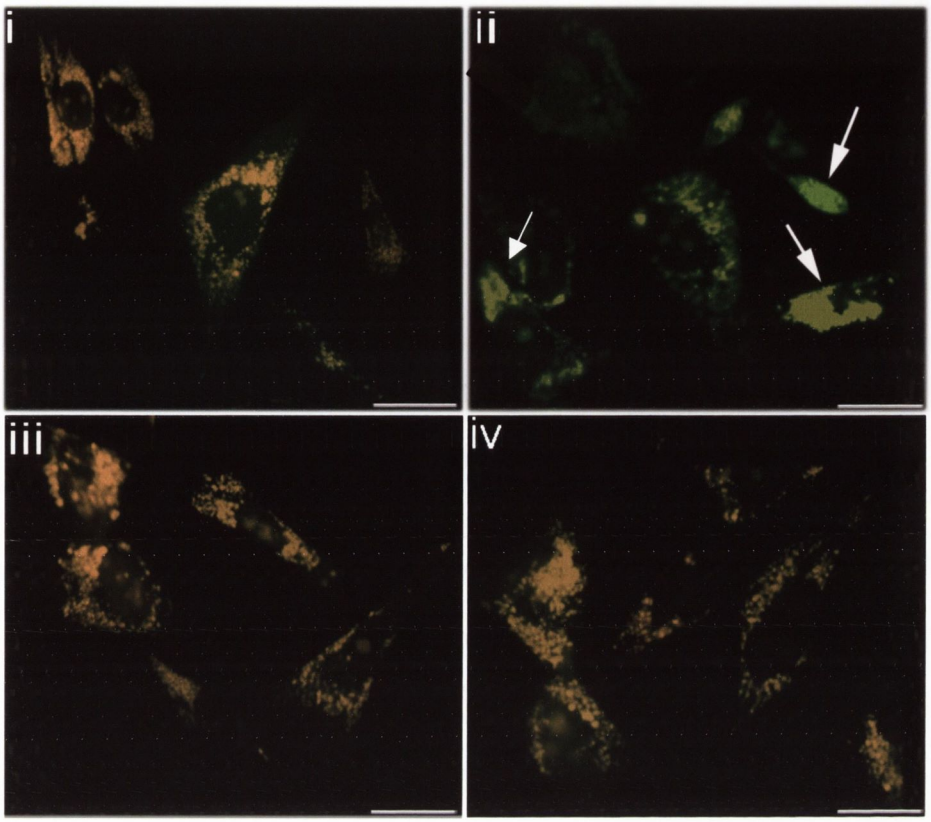


**Figure 3.9 Effect of $A\beta_{1-40}$ on lysosomal membrane integrity at 6 hr**

Cortical neurons were exposed to AO (5μg/ml) for 15 min prior to incubation with $A\beta_{1-40}$ (2μM) for 6 hr in the presence or absence of the p53 inhibitor, pifithrin-α (100nM; 60 min pretreatment). Relocation of AO from the lysosomes to cytosol was assessed. AO displayed an orange fluorescence and was localised in discrete punctate compartments within the cell suggesting lysosomal distribution of AO (i). Exposure to $A\beta_{1-40}$ for 6 hr resulted in the disappearance of AO orange fluorescence and an increase in diffuse cytosolic fluorescence (ii). Cells treated with pifithrin-α (iii) and $A\beta_{1-40}$ in the presence of pifithrin-α (iv) displayed an orange fluorescence suggesting AO remained localised in the lysosomal compartment. Arrows indicate cells displaying green AO fluorescence demonstrating an impairment of lysosomal integrity. Scale bar is 10μm.

## 3.7 Effect of $A\beta_{1-40}$ on lysosomal membrane integrity using confocal microscopy

Confocal laser scanning microscopy became available to me after I had used a conventional fluorescence microscope to analyse AO relocation. Confocal microscopy is a relatively new technique (1980) that has a wide range of applications in the biological sciences. It possesses several advantages over conventional microscopy. It produces images of improved resolution, up to 1.4 times greater, it has a higher level of sensitivity and it is a less invasive form of imaging due to the use of high-power gas laser illumination. It also removes out-of-focus glare and allows observation of discrete intracellular structures. All of this culminates to produce sharper, superior images than conventional fluorescence microscopy.

Utilising confocal laser microscopy I assessed relocation of AO from lysosomes following treatment with $A\beta_{1-40}$ (2$\mu$M) for a variety of time points. In Figure 3.10, Figure 3.12 and Figure 3.14 cortical neurons were treated with AO (5$\mu$g/ml) for 15 min prior to incubation with $A\beta_{1-40}$ (2$\mu$M) for 1 hr, 6 hr and 24 hr, respectively. Neurons were also pre-treated with the p53 inhibitor, pifithrin-$\alpha$, (100nM) for 60 min prior to $A\beta_{1-40}$ exposure to determine if the effect of $A\beta_{1-40}$ on lysosomal membrane integrity was mediated via p53. At 1 hr (Figure 3.10) in control cells (Figure 3.10A) AO displayed a granular orange fluorescence and was localised in discrete punctate compartments within the cell, suggesting lysosomal distribution of AO. Exposure to $A\beta_{1-40}$ for 1 hr had no effect on the distribution of AO (Figure 3.10B). Pre-treatment with pifithrin-$\alpha$ alone (Figure 3.10C) or $A\beta_{1-40}$ in the presence of pifithrin-$\alpha$ (Figure 3.10 D) had no effect on AO distribution and yielded comparable staining to controls. This data demonstrates that exposure of neurons to $A\beta_{1-40}$ for 1 hr has no effect on lysosomal membrane integrity.

Lysosomal membrane integrity was also monitored and quantified by measuring mean pixel intensity at 633nm, the emission wavelength AO emits when it accumulates in lysosomes. Figure 3.11A demonstrates the mean pixel intensity at 633nm; there is no effect following $A\beta_{1-40}$ treatment for 1 hr, where control pixel intensity at 633nm emission is 527.5 $\pm$ 47.82 and in neurons

treated with $A\beta_{1-40}$ mean pixel intensity at 633nm is 486.33 ± 73.42 (P>0.05, ANOVA, n=4 cultures, 100 cells analysed per culture). Pre-treatment with pifithrin-α alone (421.18 ± 35.44) or $A\beta_{1-40}$ in the presence of pifithrin-α (480.66 ± 52.63; P>0.05, ANOVA, n=4 cultures, 100 cells analysed per culture), had comparable pixel intensity at 633nm to control cells. In addition, intact lysosomes were counted by visual inspection. There was no difference in the number of intact lysosomes counted at this time point, where the average number of lysosomes in control cells was 74.3 ± 4.68 (mean ± S.E.M.) and 78.5 ± 3.81 in cells exposed to $A\beta_{1-40}$ (2μM) for 1 hr (P>0.05, ANOVA, n=4; Figure 3.11B). Neurons treated with pifithrin-α alone had 79.38 ± 2.68 lysosomes per cell and 81.75 ± 5.39 lysosomes per cells in neurons exposed to $A\beta_{1-40}$ in the presence of pifithrin-α. This demonstrates that $A\beta_{1-40}$ does not compromise the lysosomal membrane at 1 hr. This finding is in direct contrast to my previous result, which indicated that treatment with $A\beta_{1-40}$ for 1 hr causes AO to translocate from the lysosome. I will comment on this in the discussion.

Neurons were incubated with $A\beta_{1-40}$ (2μM) for a duration of 6 hr, in control cells (Figure 3.12A) AO accumulated in the acidic compartments and displayed a punctuate orange fluorescence. Exposure to $A\beta_{1-40}$ for 6 hr (Figure 3.12B) resulted in the disappearance of AO fluorescence and an increase in diffuse green fluorescence suggesting a loss of lysosomal integrity. Furthermore, mean pixel intensity at 633nm emission decreased significantly in cells treated with $A\beta_{1-40}$ for 6 hr (Figure 3.13A), from 484 ± 58.94 (mean ± S.E.M.) to 313 ± 17.49 (P<0.05, ANOVA, n=4 cultures, 100 cells analysed per culture). There is also a reduction in the number of intact lysosomes counted manually (Figure 3.13B), where the number of lysosomes in control cells was 76 ± 7.17 (mean ± S.E.M.) and this decreased to 17.63 ± 5.14 (P<0.001, ANOVA, n=4) lysosomes per cell in cells treated with $A\beta_{1-40}$ for 6 hr. These results suggest leakage of the dye from the lysosomal compartment, possibly as a result of a disruption in lysosomal integrity and a loss of lysosomal acidification. Neurons were also pre-treated with pifithrin-α prior to $A\beta_{1-40}$ exposure to determine if the effect of $A\beta_{1-40}$ on lysosomal

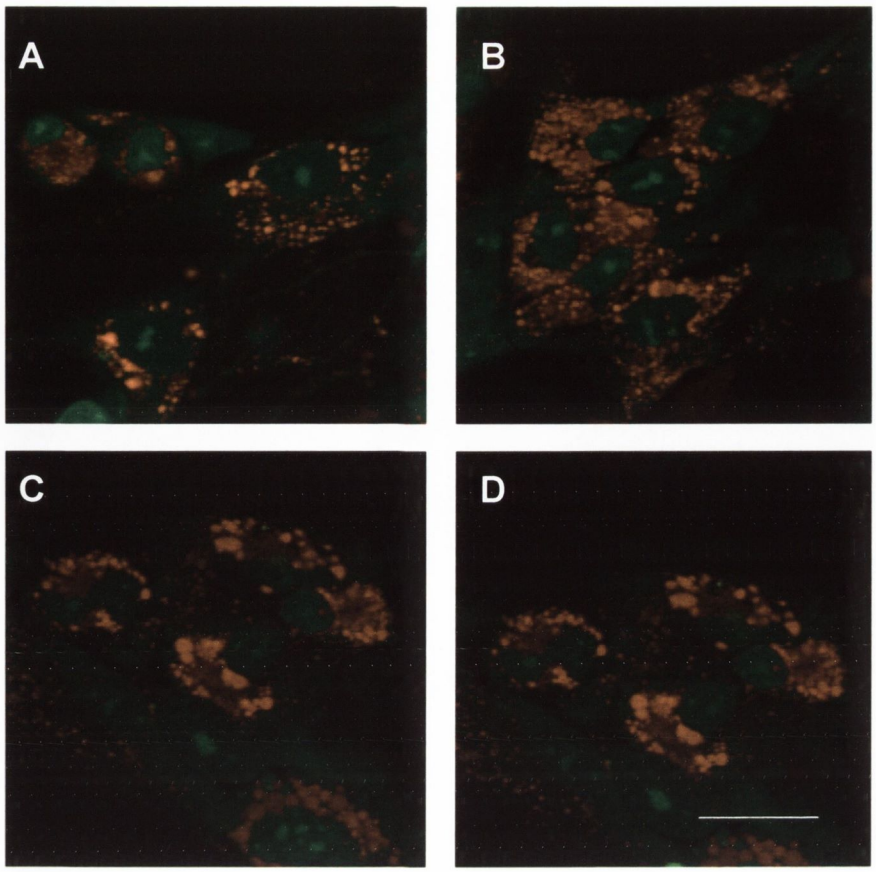


**Figure 3.10 Effect of $A\beta_{1-40}$ on lysosomal membrane integrity at 1 hr**

Cortical neurons were exposed to AO (5μg/ml) for 15 min prior to incubation with $A\beta_{1-40}$ (2μM) for 1 hr in the presence or absence of the p53 inhibitor, pifithrin-α (100nM; 60 min pretreatment). Relocation of AO from the lysosomes to cytosol was assessed. A, in control cells AO displayed an orange fluorescence and was localised in discrete punctate compartments within the cell suggesting lysosomal distribution of AO. B, exposure to $A\beta_{1-40}$ for 1 hr had no effect on the appearance of AO orange fluorescence. C, cells treated with pifithrin-α and D, $A\beta_{1-40}$ in the presence of pifithrin-α displayed an orange fluorescence similar to controls, suggesting that AO remained localised in the lysosomal compartment. Scale bar is 10μm.

A.

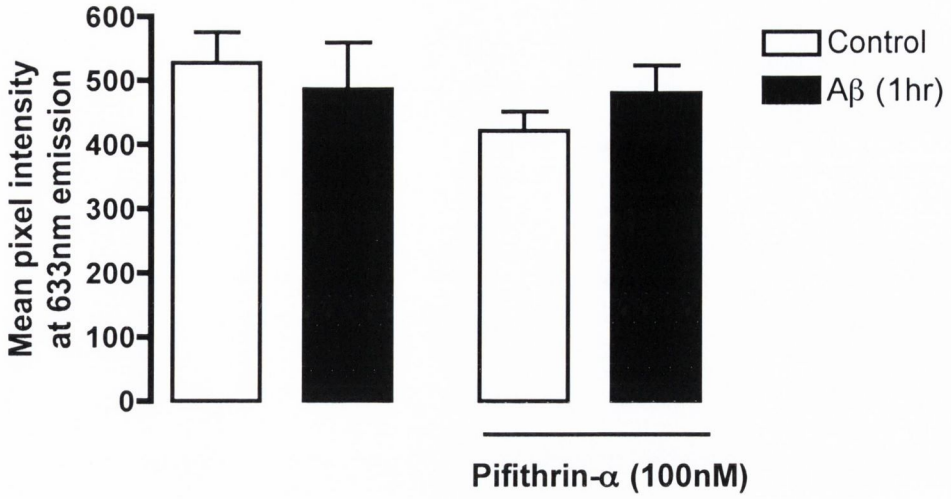


B.

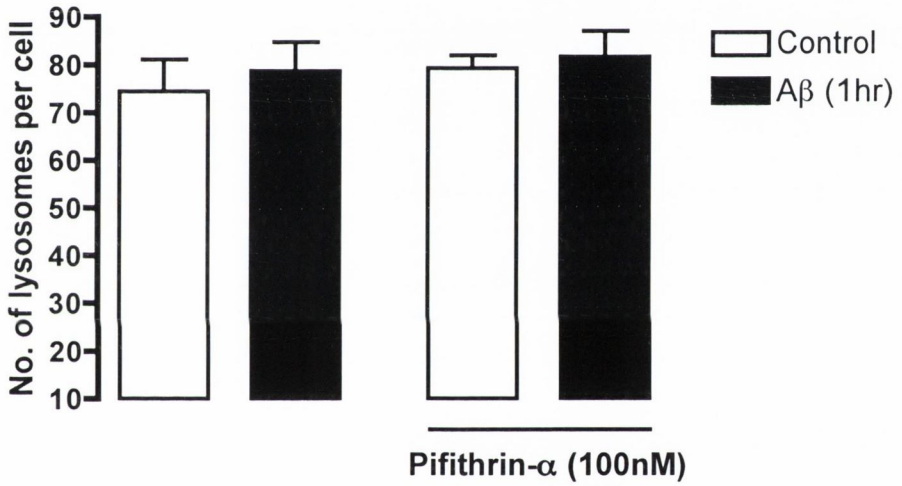


**Figure 3.11 $A\beta_{1-40}$ has no effect on lysosomal membrane integrity at 1 hr**

A. Intact lysosomes accumulate AO and emit at 633nm. By measuring the mean pixel intensity of pixels at this wavelength we can monitor disruption of the lysosomal membrane due to leakage of the probe. $A\beta_{1-40}$ (2μM) has no effect on the fluorescence emission at 633nm at 1 hr.

B. The number of intact lysosomes per cell were counted. Treatment with $A\beta_{1-40}$ (2μM) for 1 hr had no effect on the number of lysosomes observed. Results are expressed as the mean ± SEM of 4 independent observations.

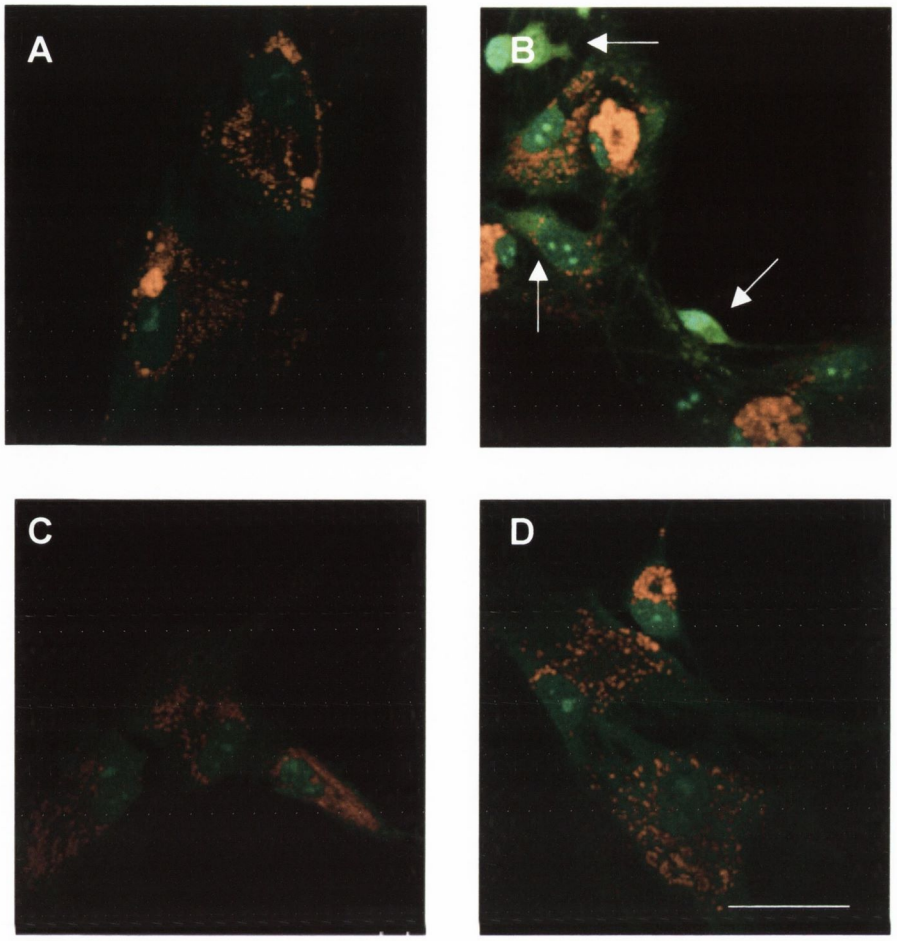


**Figure 3.12 $A\beta_{1-40}$-mediated alteration in lysosomal membrane integrity is p53-dependent at 6 hr**

Neurons were exposed to AO (5ug/ml) for 15 min prior to incubation with $A\beta_{1-40}$ (2μM) for 6 hr in the presence or absence of the p53 inhibitor, pifithrin-α (100nM; 60 min pretreatment). Relocation of AO from the lysosomes to cytosol was assessed. A, in control cells AO displayed an orange fluorescence and was localised in discrete punctate compartments within the cell reflecting lysosomal distribution of AO. B, exposure to $A\beta_{1-40}$ for 6 hr resulted in the reduction of AO orange fluorescence and in increase in diffuse cytosolic green fluorescence. C, treatment with pifithrin-α alone had no effect on AO fluorescence. D, co-incubation with $A\beta_{1-40}$ + pifithrin-α had no effect on AO fluorescence. Arrows indicate cells displaying green AO fluorescence demonstrating an impairment of lysosomal integrity. Scale bar is 50μm.

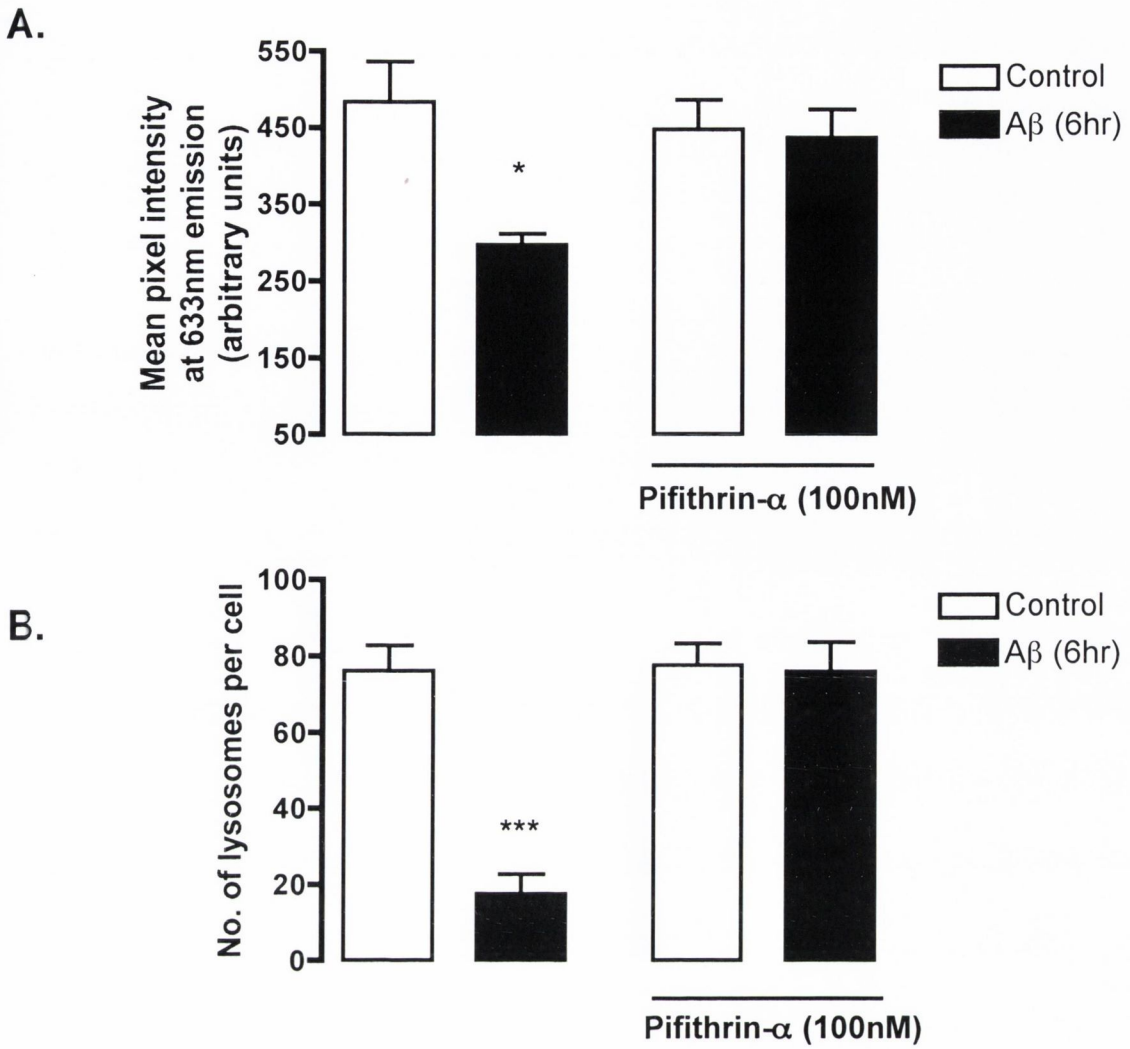


**Figure 3.13 $A\beta_{1-40}$ impacts lysosomal membrane integrity at 6 hr**

A Intact lysosomes accumulate AO and emit at 633nm. By measuring the intensity of pixels at this wavelength we can monitor disruption of the lysosomal membrane due to leakage of the probe. $A\beta_{1-40}$ (2μM) reduces the pixel intensity at 6 hr, pretreatment with pifithrin-α (100nM) abolished the $A\beta_{1-40}$-induced reduction (*$p<0.05$, ANOVA, n=4).

B. The number of intact lysosomes per cell were counted. Following treatment with $A\beta_{1-40}$ (2μM) for 6 hr a reduction in the number of lysosomes was observed. Pretreatment with pifithrin-α (100nM) abolished the $A\beta_{1-40}$-induced reduction in the number of lysosomes (***$p<0.001$, ANOVA, n=4). Results are expressed as the mean ± SEM of 4 independent observations.

membrane integrity was mediated via p53. Cells treated with pifithrin-α alone or $A\beta_{1-40}$ in the presence of pifithrin-α for 6 hr (Figure 3.12 C and D) resulted in punctate orange fluorescence suggesting AO remained within the lysosomal compartment. Thus, mean pixel intensity at 633nm emission in cells treated with pifithrin-α alone for 6 hr was 448.16 ± 35.45 (mean ± S.E.M.) and 437.13 ± 39.27 ($P<0.001$, ANOVA, n=4 cultures, 100 cells analysed per culture) in cells treated with $A\beta_{1-40}$ + pifithrin-α (Figure 3.13A). Furthermore, pifithrin-α prevented the $A\beta_{1-40}$-mediated decrease in number of intact lysosomes per cell; where lysosomal number was (77.5 ± 5.77) (n=4 cultures, 100 cells analysed per culture) in cells treated with pifithrin-α alone and 75.87 ± 7.75 lysosomes per cell in neurons exposed to $A\beta_{1-40}$ in the presence of pifithrin-α at 6 hr (Figure 3.13B). Therefore, the $A\beta_{1-40}$-induced disruption of the lysosomal membrane is p53-sensitive at 6 hr.

Similarly, when neurons were incubated with $A\beta_{1-40}$ (2μM) for a duration of 24 hr, in control cells (Figure 3.14A) AO accumulated in the acidic compartments and displayed a punctuate orange fluorescence. Exposure to $A\beta_{1-40}$ for 24 hr (Figure 3.14B) resulted in the disappearance of AO fluorescence and an increase in diffuse green fluorescence suggesting a loss of lysosomal integrity. Furthermore, mean pixel intensity at 633nm emission decreased significantly in cells treated with $A\beta_{1-40}$ for 24 hr (Figure 3.15A), from 481.81 ± 45.16 (mean ± S.E.M.) to 285.3 ± 18.07 ($P<0.05$, ANOVA, n=4 cultures, 100 cells analysed per culture). There is also a reduction in the number of intact lysosomes counted manually (Figure 3.15B), where the number of lysosomes in control cells was 70.25 ± 8.1 (mean ± S.E.M.) and this decreased to 15 ± 1.9 ($P<0.001$, ANOVA, n=4 cultures, 100 cells analysed per culture) lysosomes per cell in cells treated with $A\beta_{1-40}$ for 24 hr. These results suggest leakage of the dye from the lysosomal compartment, possibly as a result of a disruption in lysosomal integrity and a loss of lysosomal acidification. Neurons were also pre-treated with pifithrin-α prior to $A\beta_{1-40}$ exposure to determine if the effect of $A\beta_{1-40}$ on lysosomal membrane integrity was mediated via p53. Cells treated with pifithrin-α alone or $A\beta_{1-40}$ in

the presence of pifithrin-α for 24 hr (Figure 3.14 C and D) resulted in punctate orange fluorescence suggesting AO remained within the lysosomal compartment. Thus, mean pixel intensity at 633nm emission in cells treated with pifithrin-α alone for 24 hr was 429.3 ± 44.5 (mean ± S.E.M.) and 485.14 ± 36.96 ($P<0.001$, ANOVA, n=4 cultures, 100 cells analysed per culture) in cells treated with $A\beta_{1-40}$ + pifithrin-α (Figure 3.15A). Furthermore, pifithrin-α prevented the $A\beta_{1-40}$-mediated decrease in number of intact lysosomes per cell; where lysosomal number was (65.6 ± 7.6) (n=4 cultures, 100 cells analysed per culture) in cells treated with pifithrin-α alone and 69.16 ± 7.39 lysosomes per cell in neurons exposed to $A\beta_{1-40}$ in the presence of pifithrin-α at 24 hr (Figure 3.15B). Therefore, the $A\beta_{1-40}$-induced disruption of the lysosomal membrane is reliant on p53 at 24 hr.

### 3.8 AO images

As the previous results indicated $A\beta_{1-40}$ alters lysosomal integrity before 6 hr, I utilised the real time imaging capability of the confocal microscope and filmed cells for 30 min. At 5 hr 30 min post $A\beta_{1-40}$ treatment, cells were moved to the confocal microscope and scanned every minute until the end of the treatment, ie for 30 min. Figure 3.16A shows the first scan. AO displayed an orange fluorescence and was localised in discrete punctate compartments within the cell suggesting lysosomal distribution of AO. Figure 3.16B demonstrates the last scan. Continued exposure to $A\beta_{1-40}$ for the final 30 min resulted in reduction of AO orange fluorescence and in increase in diffuse cytosolic green fluorescence, demonstrating an impairment of lysosomal integrity.

The movie of this real time scan (30sec) can be seen on the cd attached at back of thesis (3.16movie).

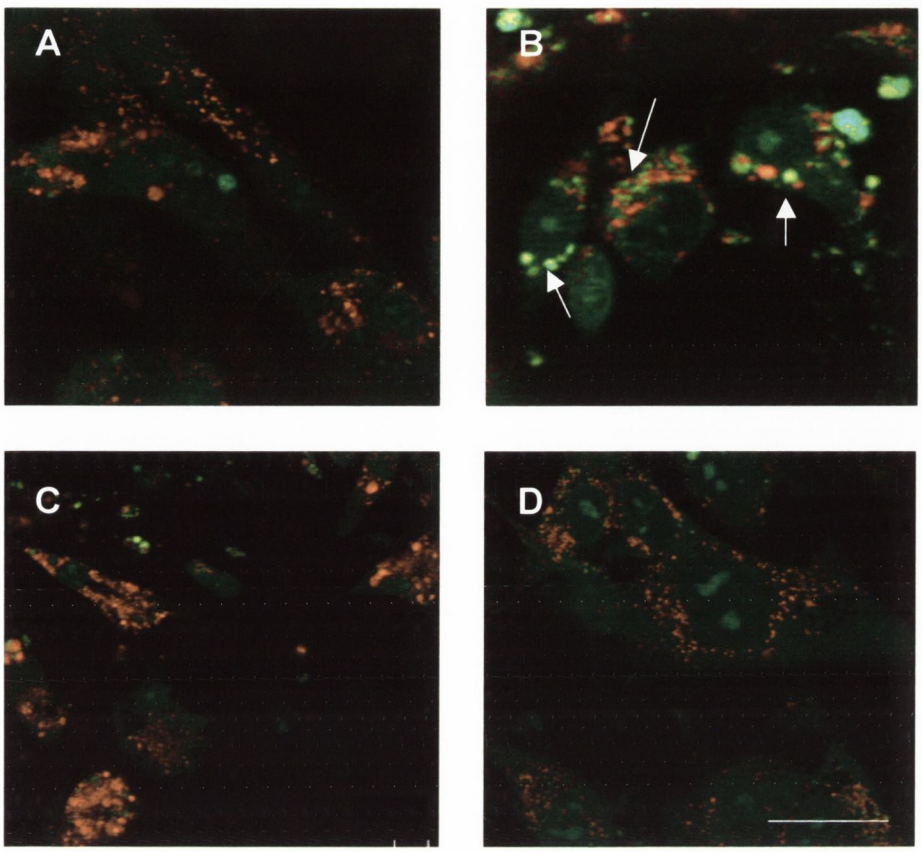


**Figure 3.14 $A\beta_{1-40}$-mediated alteration in lysosomal membrane integrity is p53 dependent at 24 hr**

Neurons were exposed to AO (5ug/ml) for 15 min prior to incubation with $A\beta_{1-40}$ (2μM) for 24 hr in the presence or absence of the p53 inhibitor, pifithrin-α (100nM; 60 min pretreatment). Relocation of AO from the lysosomes to cytosol was assessed. A, in control cells AO displayed an orange fluorescence and was localised in discrete punctate compartments within the cell reflecting lysosomal distribution of AO. B, exposure to $A\beta_{1-40}$ for 24 hr resulted in the reduction of AO orange fluorescence and in increase in diffuse cytosolic green fluorescence. C, treatment with the p53 inhibitor, pifithrin-α, alone had no effect on AO fluorescence. D, co-incubation with $A\beta_{1-40}$ + pifithrin-α resulted in AO displaying an orange fluorescence suggesting AO remained localised in the lysosomal compartment. Arrows indicate cells displaying green AO fluorescence demonstrating an impairment of lysosomal integrity. Scale bar is 50μm.

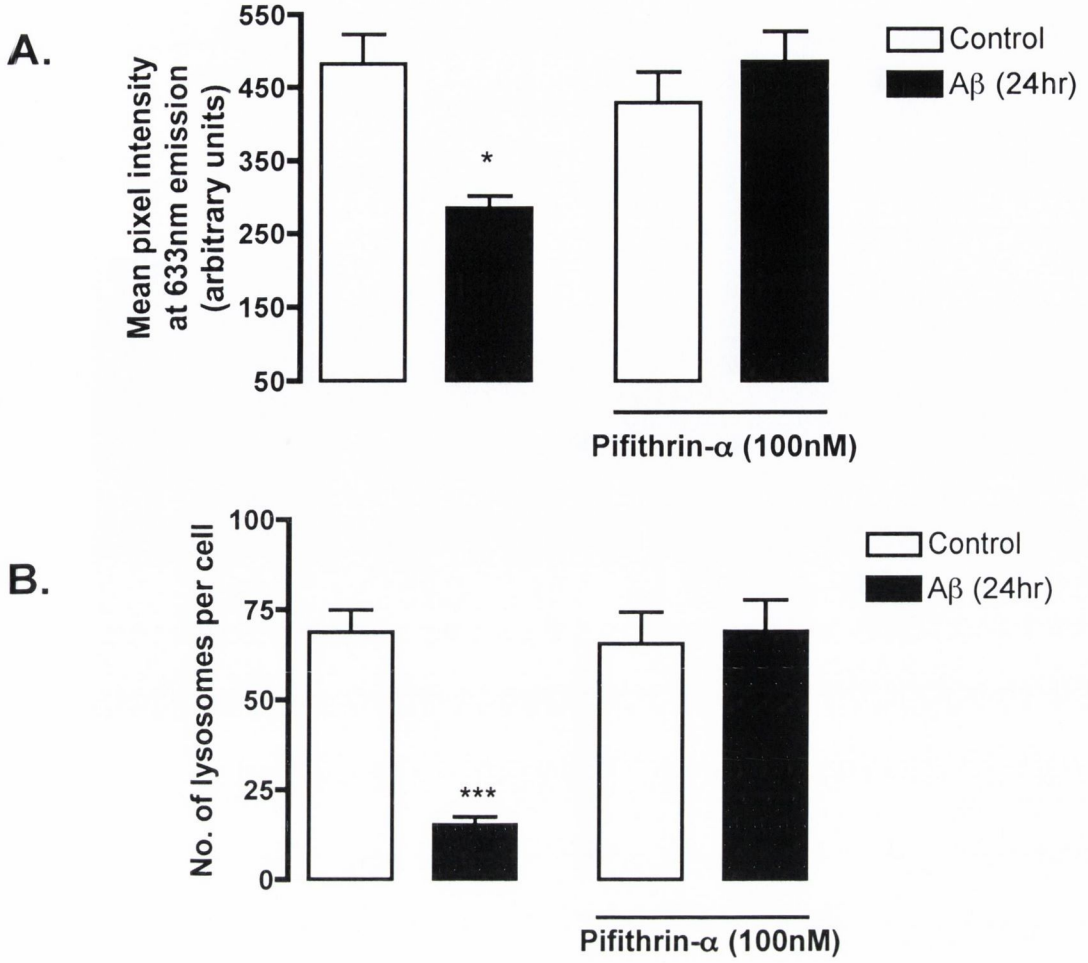


**Figure 3.15 $A\beta_{1-40}$ compromises lysosomal membrane integrity at 24 hr**

A. Intact lysosomes accumulate AO and emit at 633nm. By measuring the mean pixel intensity at this wavelength we can monitor disruption of the lysosomal membrane due to leakage of the probe. $A\beta_{1-40}$ (2μM) reduces the mean pixel intensity at 633nm at 24 hr and pretreatment with the p53 inhibitor, pifithrin-α, (100nM) abolished the $A\beta_{1-40}$-induced reduction in emission at 633nm (*$p<0.05$, ANOVA, n=4)

B. The number of intact lysosomes per cell were counted. Treatment with $A\beta_{1-40}$ (2μM) for 24 hr induced a reduction in the number of lysosomes. Pretreatment with pifithrin-α (100nM) abolished the $A\beta_{1-40}$-induced reduction (***$p<0.001$, ANOVA, n=4). Results are expressed as the mean ± SEM of 4 independent observations.

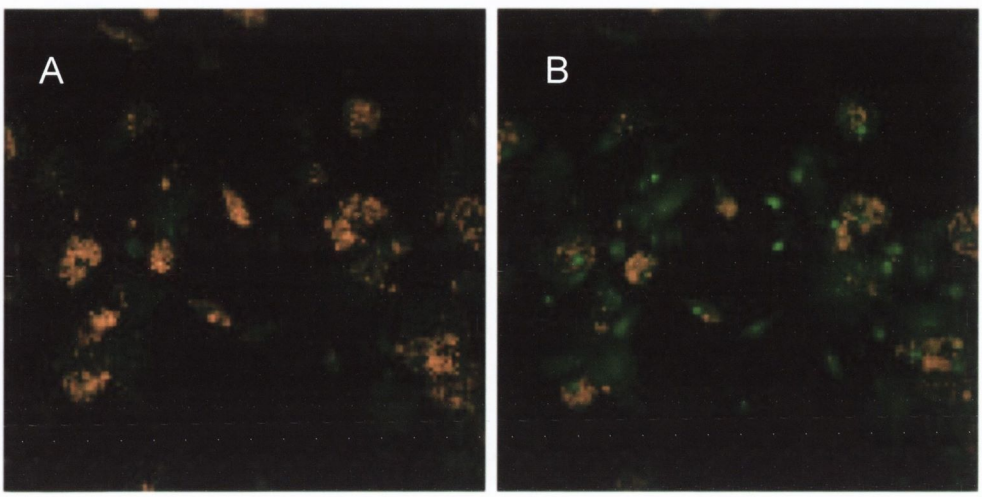


**Figure 3.16 AO images**

Cortical neurons were exposed to AO (5μg/ml) for 15 min prior to incubation with $A\beta_{1-40}$ (2μM) for 6 hr. Relocation of AO from the lysosomes to cytosol was assessed. At 5 hr 30 min post $A\beta_{1-40}$ treatment, cells were moved to the confocal microscope and scanned every minute until the end of the treatment, ie for 30 min. Image **A** shows the first scan. AO displayed an orange fluorescence and was localised in discrete punctate compartments within the cell suggesting lysosomal distribution of AO. **B** demonstrates the last scan. Continued exposure to $A\beta_{1-40}$ for final 30 min resulted in reduction of AO orange fluorescence and in increase in diffuse cytosolic green fluorescence, demonstrating an impairment of lysosomal integrity.

The movie of this real time scan (30sec) can be seen on the cd attached at back of thesis (3.16movie).

### 3.9 $A\beta_{1-40}$ downregulates LAMP expression in neuronal cells at 2 hr, 6 hr and 24 hr

There are two main types of lysosomal membrane proteins, lysosomal associated membrane protein (LAMP) and lysosomal integrated membrane protein (LIMP), accounting for 50% of total membrane proteins (Marsh, 1987). One of the many functions of membrane proteins is to protect the membrane from attack by lysosomal enzymes and so prevent the leakage of enzymes into the cytosol, where they could induce apoptotic signalling (Leist & Jaattela, 2001a). To determine whether $A\beta_{1-40}$-induced destabilisation of lysosomal membrane involved modulation of lysosomal proteins, cortical neurons were exposed to $A\beta_{1-40}$ (2μM) for 2 hr, 6 hr and 24 hr, and LAMP-1 immunofluorescence was monitored. Visualisation of LAMP by fluorescence immunocytochemistry used LAMP-1 antibody, which recognises an epitope mapping at the carboxy terminus of LAMP-1 of human origin (Figure 3.17). In control cells, LAMP-1 immunoreactivity was detected at 2 hr (A) 6 hr (B) and 24 hr (C). However, in cells treated with $A\beta_{1-40}$ (2μM) for 2 hr (D), 6 hr (E) and 24 hr (F), a lower intensity of LAMP-1 immunoreactivity was observed. This finding suggests that $A\beta_{1-40}$ reduces expression of LAMP-1 in cultured cortical neurons.

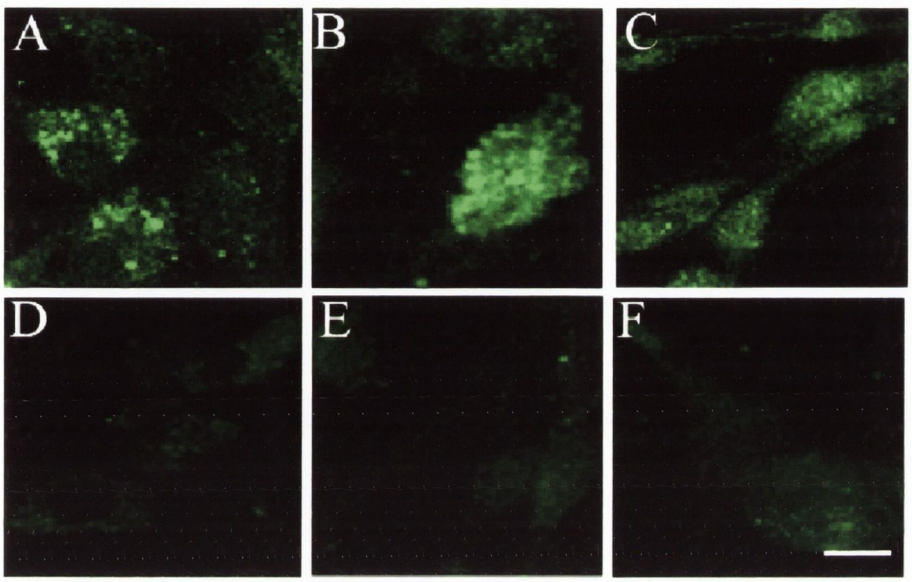


**Figure 3.17 Effect of $A\beta_{1-40}$ on LAMP-1 expression in neuronal cells.**

Fluorescence microscopy was used to visualise the distribution of LAMP within cortical neurons following treatment with $A\beta_{1-40}$ (2μM) for 2 hr, 6 hr and 24 hr. Punctate LAMP-1 immunoreactivity was observed in control cells at 2 hr (A), 6 hr (B) and 24 hr (C). Treatment with $A\beta_{1-40}$ for 2 hr (D), 6 hr (E) and 24 hr (E) resulted in reduced LAMP-1 immunoreactivity. Scale bar 50μm.

### 3.10 Effect of the p53 inhibitor, pifithrin-α, on the $A\beta_{1-40}$-mediated decrease in LAMP-1 expression

To determine whether p53 played a role in the $A\beta_{1-40}$-mediated decrease in LAMP-1 expression observed at 2 hr, 6 hr and 24 hr, cells were treated with the p53 inhibitor, pifithrin-α (100nM), for 1 hr prior to treatment with $A\beta_{1-40}$ (2μM). LAMP-1 expression was assessed by both fluorescence immunocytochemistry (Figure 3.18) and western immunoblot (Figure 3.19 and 3.20). Figure 3.18 illustrates the expression of LAMP-1 in control cells at 2 hr (A), 6 hr (B), and 24 hr (C) and in $A\beta_{1-40}$-treated cells at 2 hr (D), 6 hr (E) and 24 hr (F). Cells treated with pifithrin-α alone at 2 hr (G), 6 hr (H) and 24 hr (I), had no effect on LAMP-1 expression. However, in cells exposed to $A\beta_{1-40}$ in the presence of pifithrin-α for 2 hr (J), 6 hr (K) and 24 hr (L), LAMP-1 expression was also reduced.

The $A\beta_{1-40}$-mediated regulation of the LAMP-1 expression was also assessed by western immunoblot. Exposure of cortical neurons to $A\beta_{1-40}$ (2μM) for 6 hr (Figure 3.19) and 24 hr (Figure 3.20) produced a significant reduction in the expression of LAMP-1 from 51.89 ± 2.31 (mean ± SEM) to 29 ± 5.0 in cells exposed to $A\beta_{1-40}$ for 6 hr ($p<0.05$, ANOVA, n=5) and from 32.9 ± 1.74 to 23.19 ± 1.12 in cells treated with $A\beta_{1-40}$ for 24 hr ($p<0.05$, ANOVA, n=5). While pifithrin-α at 6 hr had no effect on LAMP-1 expression (47.79 ± 4.15), it did not prevent the $A\beta_{1-40}$-induced reduction in LAMP-1 expression; where LAMP-1 expression was 33.94 ± 3.6 in cells treated with $A\beta_{1-40}$ in the presence of pifithrin-α (n=5). In cells treated for 24 hr with pifithrin-α alone, LAMP-1 expession was 28.71 ± 3.26 and the $A\beta_{1-40}$-induced reduction in LAMP-1 expression was not prevented when cells were treated with $A\beta_{1-40}$ in the presence of pifithrin-α (17.92 ± 2.3). These results demonstrate that $A\beta_{1-40}$ impacts on LAMP-1 expression, possibly indicating that $A\beta_{1-40}$ causes a destabilisation of lysosomal membrane integrity via downregulation of LAMP-1. Furthermore, this $A\beta_{1-40}$-induced reduction in LAMP expression is not

dependent on p53. This is in contrast to my finding that the $A\beta_{1-40}$-mediated destabilisation of the lysosomal membrane is p53-dependent.

### 3.11 $A\beta_{1-40}$-induced decrease in LAMP-1 mRNA expression

To establish whether the $A\beta_{1-40}$-mediated decrease in expression of LAMP-1 protein was due to decreased transcription of the LAMP-1 gene, cortical neurons were incubated with $A\beta_{1-40}$ (2μM) for 30 min, 6 hr and 24 hr. Levels of LAMP-1 mRNA expression were examined by RT-PCR, with gene-specific primers for LAMP-1 and β-actin (Figure 3.21). In Figure 3.19, analysis of densitometric data demonstrates that $A\beta_{1-40}$ induced a significant reduction in LAMP-1 mRNA expression at 6 hr where LAMP mRNA was reduced from 2.591 ± 1.053 (mean band width ± SEM; arbitrary units) to 0.052 ± 0.014 ($p<0.05$, one way ANOVA; n=6) by $A\beta_{1-40}$. No statistically relevant changes occurred at 30 min, control (0.848 ± 0.072) and $A\beta_{1-40}$-treated (1.790 ± 0.733) or the 24 hr timepoint, control (0.060 ± 0.042) and $A\beta_{1-40}$-treated (90.042 ± 0.024). This result suggests that $A\beta_{1-40}$ modulates transcription of the LAMP-1 gene within 6 hr. The mRNA expression of LAMP-1 was normalised to that of the housekeeping gene β-actin. A sample agarose gel demonstrating that LAMP-1 mRNA expression is reduced by $A\beta_{1-40}$ is shown in Figure 3.21B.

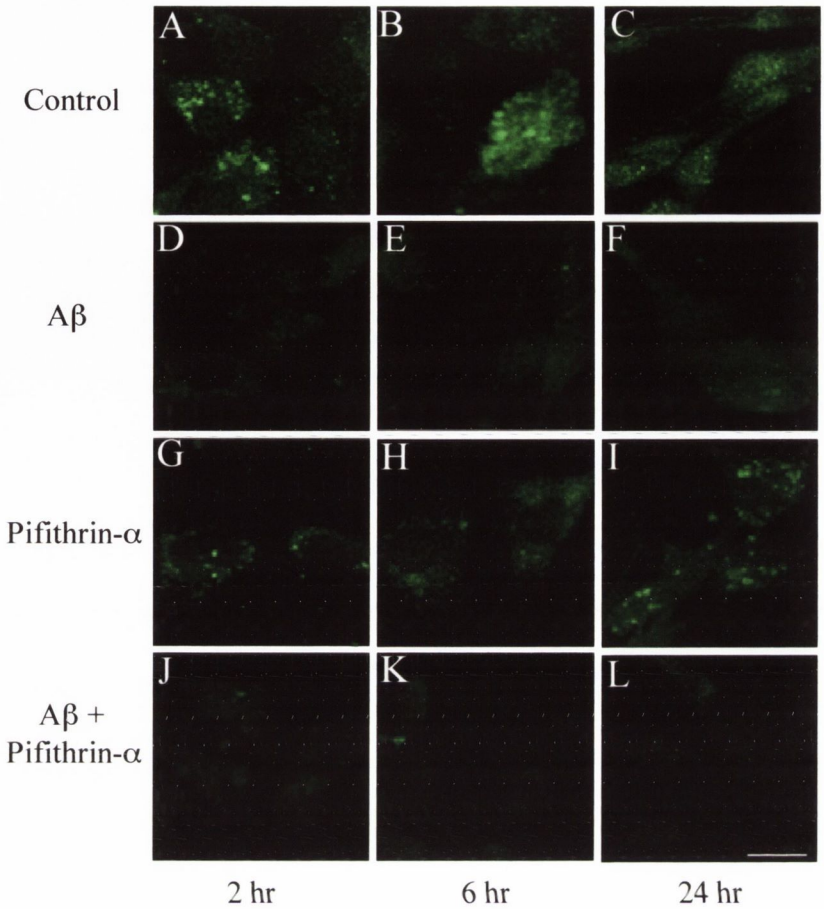


**Figure 3.18 Effect of p53 on $A\beta_{1-40}$-mediated reduction in LAMP-1 expression in neuronal cells.**

Fluorescent microscopy was used to visualise the distribution of LAMP-1 within cortical neurons following treatment with $A\beta_{1-40}$ (2μM) in the presence or absence of pifithrin-α (100nM) for 2 hr, 6 hr and 24 hr. Punctate LAMP-1 immunoreactivity was observed in control cells at 2 hr (A), 6 hr (B) and 24 hr (C). Following treatment with $A\beta_{1-40}$ for 2 hr (D), 6 hr (E) and 24 hr (E), LAMP-1 immunoreactivity was markedly reduced. In cells treated with pifithrin-α for 2 hr (G), 6 hr (H) and 24 hr (I) LAMP immunoreactivity was similar to control cells. However, in cells exposed to $A\beta_{1-40}$ in the presence of pifithrin-α for 2 hr (J), 6 hr (K) and 24 hr (L) LAMP immunoreactivity was reduced. Scale bar 50μm

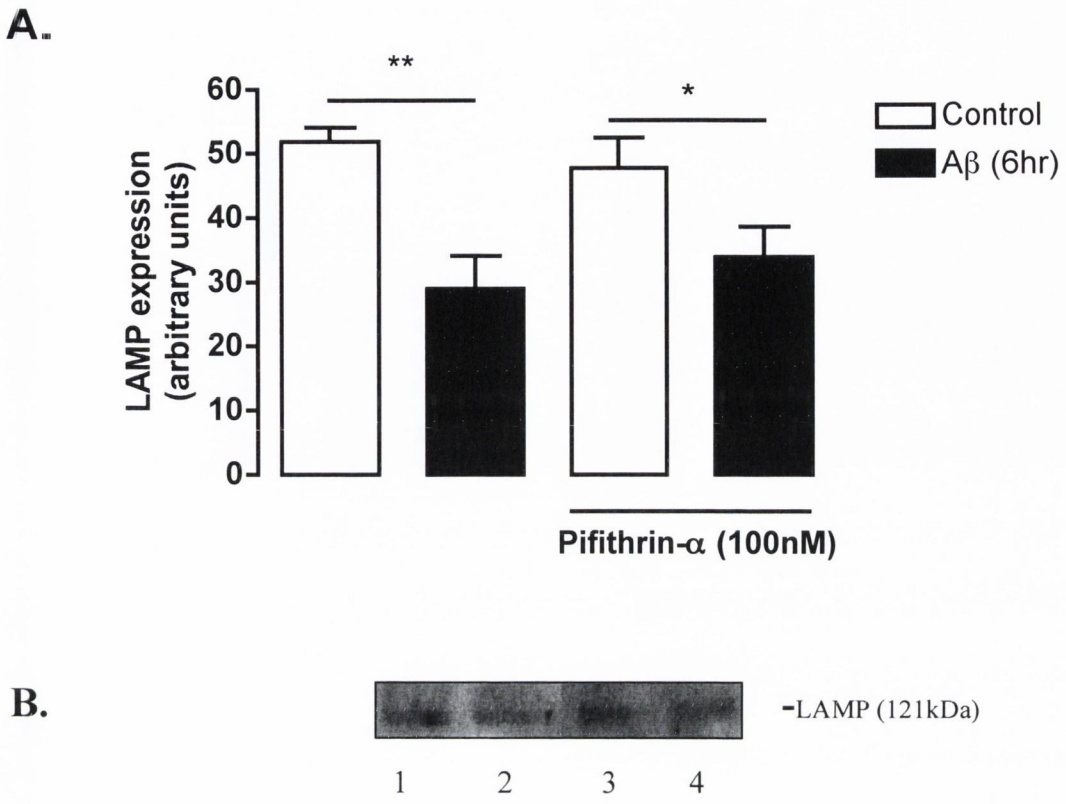


**Figure 3.19 Aβ reduces LAMP expression in neuronal cells at 6 hr**

A. Cortical neurons were treated with Aβ (2μM), in the presence or absence of the p53 inhibitor, pifithrin-α (100nM) for 6 hr. LAMP expression was examined by western immunoblot. Aβ significantly reduced LAMP expression at 6 hr. In the presence of pifithrin-α, the Aβ-mediated decrease in LAMP expression remained. Pifithrin-α alone had no effect on LAMP expression. Results are expressed as mean ± SEM for 5 observations, ANOVA, *$p<0.05$, **$p<0.01$

B. Sample western immunoblot demonstrating LAMP expression in control (lane 1) and Aβ -treated cells (lane 2;), and pifithrin-α (lane 3) and Aβ+pifithrin-α-treated cells (lane 4).

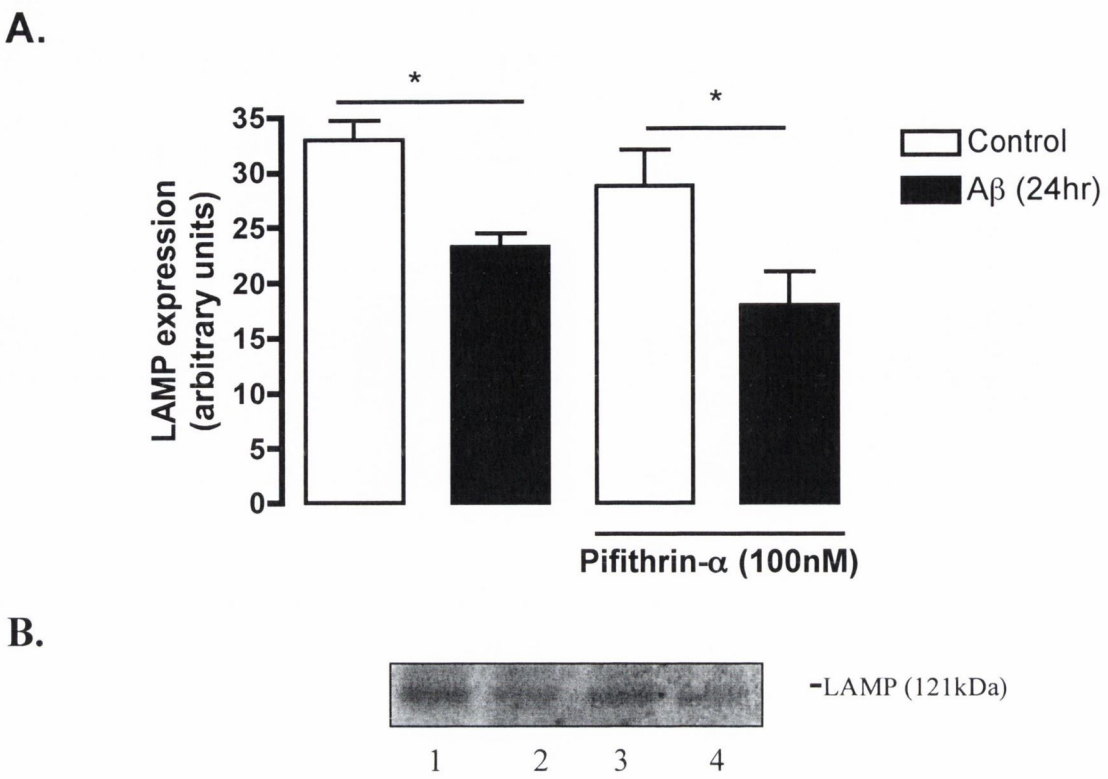


**Figure 3.20 $A\beta_{1-40}$ reduces LAMP-1 expression in neuronal cells at 24hr**

A. Cortical neurons were treated with $A\beta_{1-40}$ (2μM), in the presence or absence of the p53 inhibitor, pifithrin-α (100nM) for 24 hr. LAMP-1 expression was examined by western immunoblot. $A\beta_{1-40}$ significantly reduced LAMP-1 expression at 24 hr. In the presence of pifithrin-α, the $A\beta_{1-40}$-mediated decrease in LAMP-1 expression remained. Pifithrin-α alone had no effect on LAMP-1 expression. Results are expressed as mean ± SEM for 5 observations, ANOVA, *$p<0.05$.

B. Sample western immunoblot demonstrating LAMP-1 expression in control (lane 1) and $A\beta_{1-40}$-treated cells (lane 2), and pifithrin-α, (lane 3) and $A\beta_{1-40}$ + pifithrin-α,-treated cells (lane 4).

A.

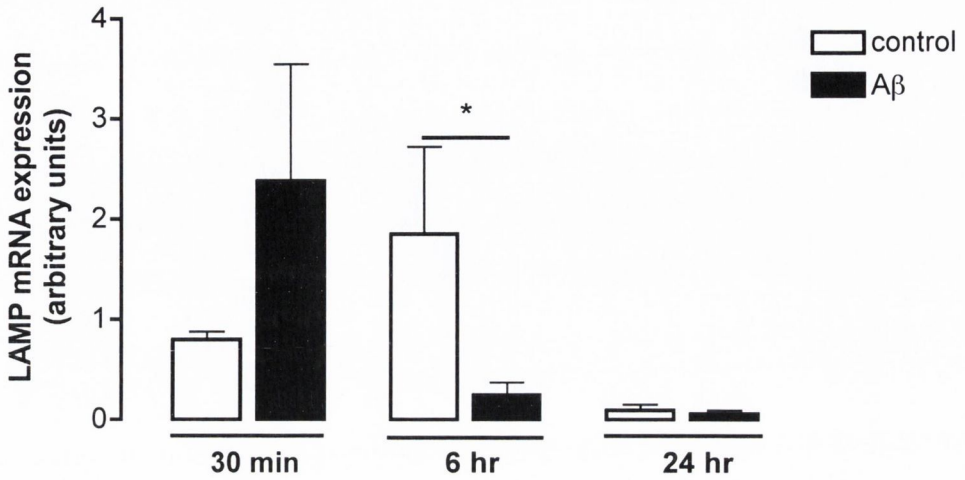


B.

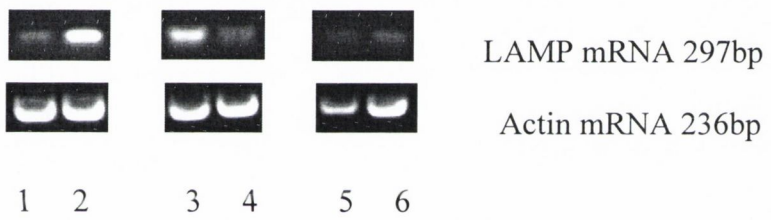


**Figure 3.21 $A\beta_{1\text{-}40}$ decreases expression of LAMP-1 mRNA**

A. Cortical neurons were treated with $A\beta_{1\text{-}40}$ (2μM) for 30 min, 6 and 24 hr and LAMP-1 mRNA expression was assessed using RT-PCR. $A\beta_{1\text{-}40}$ significantly reduced mRNA expression of LAMP-1 at the 6 hr timepoint. No changes were observed at 30 min or 24 hr. Results are expressed as mean ± SEM for 5 or more observations, ANOVA, *$p<0.05$.

B. Representative image of agarose gel demonstrating levels of LAMP-1 and β-actin mRNA expression in control 30 min (lane 1); $A\beta_{1\text{-}40}$-treated cells 30 min (lane 2); control 6 hr (lane 3); $A\beta_{1\text{-}40}$-treated cells 6 hr (lane 4); control 24 hr (lane 5) and $A\beta_{1\text{-}40}$-treated cells 24 hr (lane 6).

### 3.12 Effect of $A\beta_{1-40}$ on cellular cathepsin-L

A destabilisation of the lysosomal membrane can result in release of lysosomal proteases and subsequent increase in lysosomal protease activity within the cytosol. Previous studies from this laboratory have shown that $A\beta_{1-40}$ significantly increases cytosolic cathepsin-L activity within 6 hr of treatment (Boland & Campbell, 2004). We investigated whether cytosolic cathepsin-L could relocate to the extracellular compartment. To examine whether $A\beta_{1-40}$ evoked a release of cathepsin-L into the extracellular medium, expression of cathepsin-L was assessed in supernatants collected from cultured neuronal cells treated with $A\beta_{1-40}$ (2$\mu$M) for 30 min, 2 hr and 6 hr (Figure 3.22). The presence of extracellular cathepsin-L was measured using an enzyme linked immunosorbant assay specific for cathepsin-L. Figure 3.22 demonstrates that during the time points studied no appreciable level of cathepsin-L was released by cells, with or without $A\beta_{1-40}$. This result suggests that cathepsin-L is not released from lysosomes into the extracellular environment within the time periods studied.

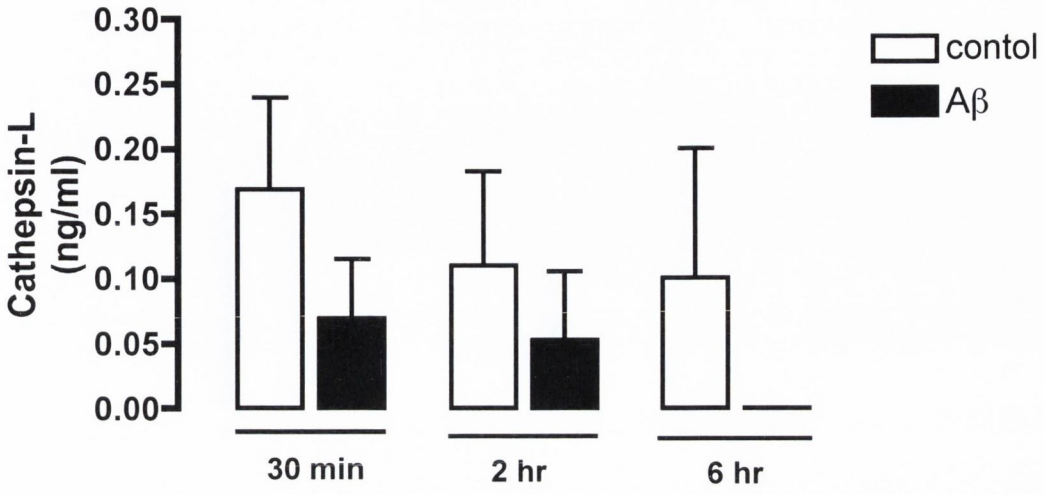


**Figure 3.22 Effect of $A\beta_{1-40}$ cathepsin-L secretion**

The concentration of cathepsin-L was analysed from the extracellular medium of cultured cortical neuronal cells over a range of timepoints. $A\beta_{1-40}$ (2μM) had no effect on the concentration of cathepsin-L in the extracellular environment. Results are expressed as ng/ml and are means ± SEM of 6 independent observations

### 3.3 Discussion

The aim of this study was to examine the role of the cell cycle regulatory protein, p53, in the $A\beta_{1-40}$-mediated regulation of the lysosomal system in cultured cortical neurons. The results demonstrate that $A\beta_{1-40}$ increases expression of phospho-$p53^{ser15}$ as early as 5 min and furthermore phospho-$p53^{ser15}$ associates with lysosomes at 6 hr and 24 hr. The $A\beta_{1-40}$-induced increase in lysosomal phospho-$p53^{ser15}$ found at 2 hr was calpain-dependent, indicating an interaction between calpain and p53. Timecourse experiments revealed that $A\beta_{1-40}$ induces destabilisation of the lysosomal membrane at 6 hr and 24 hr. The proclivity of $A\beta_{1-40}$ to promote disruption of lysosomal stability was dependent on p53, suggesting that p53 may play an important role in the regulation of the release of lysosomal constituents during the neurodegenerative process. Expression of LAMP was significantly reduced following $A\beta_{1-40}$ treatment at 6 hr and 24 hr, however, this was not reliant on p53. Furthermore, analysis of cathepsin-L secretion demonstrated that $A\beta_{1-40}$ does not regulate the release of cathepsin-L from lysosomes into the extracellular compartment within 6 hr. The p53 inhibitor, pifithrin-$\alpha$, was used to determine the role of p53 in regulating downstream effectors in $A\beta_{1-40}$-induced signalling. Treatment of cortical neurons with pifithrin-$\alpha$ blocked the effects of $A\beta_{1-40}$ on lysosomal stability indicating that the integrity of the lysosomal membrane is regulated by p53 in $A\beta_{1-40}$ neuronal signalling. Use of pifithrin-$\alpha$ revealed that p53 is not involved in $A\beta_{1-40}$-mediated reduction in LAMP expression, although my previous result found that the $A\beta_{1-40}$-mediated destabilisation of the lysosomal membrane was p53-dependent. Overall this study indicates that $A\beta_{1-40}$ regulates p53 signal transduction in cultured cortical neurons and that this pathway contributes to the loss of lysosomal membrane integrity.

The concentration of $A\beta_{1-40}$ that was selected for the experimental work carried out in this thesis was 2$\mu$M. Previous results from this laboratory have established that $A\beta_{1-40}$ used at this concentration is sufficient to induce significant levels of neuronal apoptosis within 72 hours of treatment (Boland & Campbell, 2003).

In response to cellular stress, alterations in neuronal p53 expression have been reported by many studies. The data presented here indicate that $A\beta_{1-40}$ treatment of cultured neuronal cells increases phosphorylation of p53 at residue serine-15. Following exposure with $A\beta_{1-40}$, p53 phosphorylation at serine-15 was increased by 44% at 5 min and 34% at 1 hr. Up-regulation of p53 occurs in models of oxidative stress (Strosznajder *et al.*, 2005) damaged neurons in acute models of injury such as ischemia (Li *et al.*, 1994; Miller *et al.*, 2000) and in brain tissue samples derived from animal models and patients with chronic neurodegenerative diseases (LaFerla *et al.*, 1996; de la Monte *et al.*, 1997). Furthermore, p53-associated neuronal death in $A\beta_{42}$ transgenic mice (LaFerla *et al.*, 1996) and p53-dependent apoptosis of primary neurons injected cytosolically with $A\beta_{1-40}$ (Zhang *et al.*, 2002) have been reported, suggesting that p53 may play a role in AD pathology. However, Maeda and colleagues (2001) have shown an aggravation of brain injury after transient focal ischemia in p53-deficient mice. It seems that the beneficial effects of p53 inhibition on neuronal survival closely depend on the intensity and type of oxidative stress. Increased p53 expression can occur as a result of increased transcription of the p53 gene or stabilisation of the protein by post-translational modification (Zornig *et al.*, 2001). There is evidence that p53 phosphorylated on residue serine-15 occurs following cellular stress, disrupting the association of p53 with its negative regulator, Mdm2, which in turn prevents the degradation of the p53 protein (Shieh *et al.*, 1997). Post-translational modifcations can also occur at the carboxy-terminus of p53 at residue serine-392 in response to DNA damage (Lu *et al.*, 1998). In either event, p53 accumulates in the nucleus and activates transcription of its target genes. Hence, up-regulation of phospho-$p53^{ser15}$ is an early signalling event and therefore a potential modulator of downstream signalling cascades. The results presented here support an interaction between p53 and Aβ, as other studies have shown (Culmsee *et al.*, 2001; Velez-Pardo *et al.*, 2002; Ohyagi *et al.*, 2005; Strosznajder *et al.*, 2005). Although the mechanism behind this is unknown several potential molecules have been suggested. It has been proposed that Aβ directly or acting as a minor transcription co-factor with other nuclear proteins, may bind and activate the p53 promoter in a

sequence–specific manner (Ohyagi *et al.*, 2005). Our laboratory has previously shown that the Aβ-mediated increase in p53 was JNK-1 dependent (Fogarty *et al.*, 2003). Other candidate molecules including ERK and DNA-PK (Lees-Miller *et al.*, 1990; Adler *et al.*, 1997) have been cited, however this shall be investigated more throughly in chapter 6.

The mechanism of p53-induced apoptosis has been extensively studied. It involves the activation of the mitochondrial/caspase pathway (Marchenko *et al.*, 2000; Bonini *et al.*, 2004), regulation of the Fas receptor (Bennett *et al.*, 1998) and the transcription of genes involved in regulating the redox state of the cell (Polyak *et al.*, 1997). Recently, several studies have indicated a potential role for the lysosomal system in cell death mediated by the p53 protein (Zhao, 2001; Yuan *et al.*, 2002). The results obtained herein demonstrated that phospho-p53$^{ser15}$ was increased possibly at the lysosome following A$\beta_{1\text{-}40}$ treatment for 2 hr. A subcellular fraction were prepared using gradient density fractionation from cortical cells which had been previously treated with A$\beta_{1\text{-}40}$. Under normal cellular conditions, p53 is distributed within the cytosol or at the nucleus, and my finding that p53 can associate with lysosomes is extremely interesting. Accumulation of p53 at the mitochondria during the cell death cascade has been well documented in the literature. The p53 protein directly associates with the mitochondrial membrane and forms complexes with the anti-apoptotic Bcl-2 protein to induce permeabilisation of the outer mitochondrial membrane, resulting in cytochrome *c* release (Mihara *et al.*, 2003). Yuan and colleagues (2002) have documented that p53 initiates lysosomal destabilisation, with subsequent apoptosis in myeloid leukemic cells. Whether the lysosomal-associated p53 we found in this study plays a role in regulating lysosomal stability, akin to the role of p53 in inducing cytochrome *c* release from the mitochondria, is unclear. This will be discussed later.

Pre-treatment with the calpain inhibitor, MDL2170, prevented the A$\beta_{1\text{-}40}$-induced increase in lysosomal phospho-p53$^{ser15}$ expression, revealing that the A$\beta_{1\text{-}40}$-mediated association of p53 at the lysosome is calpain dependent. Calpains are calcium-dependent neutral proteases that have been implicated in a variety of physiological and pathological conditions, including regulation of

cell cycle progression, neuronal plasticity and initiation of neuronal cell death. Calpains are reported to modulate a wide variety of intracellular signalling pathways by targeted cleavage of substrate proteins such as NFκB inhibitor, Iκβ (Shumway *et al.*, 1999) and early genes c-fos and c-Jun (Hirai *et al.*, 1991). Interestingly, calpain has been demonstrated to be activated at the lysosomal membrane and to cause release of cathepsins from lysosomes via proteolysis of the lysosomal membrane (Yamashima *et al.*, 1998). Calpain has also been shown to underlie apoptotic death in neurons (Bradford, 1976) and glia (Cheng *et al.*, 1999). Calpain requires an increase in $[Ca^{2+}]_i$ to induce its activation (Ishiura *et al.*, 1978). Previous studies from our laboratory have shown a Aβ-induced increase in $[Ca^{2+}]_i$ (MacManus *et al.*, 2000) and have demonstrated the involvement of calpain in the Aβ-mediated apoptosis (Boland & Campbell, 2004). There is evidence that $Ca^{2+}$ may control lysosomal function in exocytosis by inducing fusion of lysosomes with the plasma membrane (Rodriguez *et al.*, 1997) and in dendritic cells, $Ca^{2+}$-mediated lysosomal exocytosis is followed by release of cathepsins (Gardella *et al.*, 2001). Although it is unclear how calpain activation modulates p53 levels, it is unlikely that it has a direct effect on p53 stability. First, calpain does not effect the p53 regulator Mdm2 (Benetti *et al.*, 2001). Second, calpain inhibitors have been shown to upregulate p53 levels (Kubbutat & Vousden, 1997), the opposite to what is reported here. This difference may be due to the cellular context of proliferating cells in that study versus neuronal systems in this model. In 2003, a study by Sedarous and colleagues found that calpain activated p53 in response to DNA damage and this was believed to occur through the regulation of the NFκB pathway. NFκβ can activate p53 through direct transcriptional means (Wu *et al.*, 1994). Alternatively, p53 stability via calpain could involve the phosphatidylinositol 3-kinase-like ATM/ATR family of kinases. Reports indicate these kinases phosphorylate p53 directly on serine-15 (Hirai, 2000). The high level of calpain activation in individuals with familial AD, in conjunction with other findings, suggest that calpain activity is contributing to the neurodegeneratve process and not simply a consequence of it. In conclusion, this result demonstrates an interaction between p53 and

calpain as supported by others (Raynaud & Marcilhac, 2006), although the exact nature of this interaction in Aβ signalling requires further investigation.

My previous finding showed an increase in lysosomal phospho-p53$^{ser15}$, and in an attempt to clarify this increase I employed a specific lysosomal marker, Lysotracker red. Lysotracker probes are fluorescent acidotropic probes for labelling and tracing acidic organelles in live and fixed cells. They are freely permeable to cell membranes and typically have high selectively for acidic organelles such as lysosomes, therefore they concentrate in these organelles. Fluorescence confocal microscopy indicated that phospho-p53$^{ser15}$ associated with lysosomes at both 6 hr and 24 hr following A$\beta_{1-40}$ exposure. This suggests that following treatment with A$\beta_{1-40}$, p53 is redirected to the lysosome in agreement with our previous finding. Indeed, the significance of these findings are unclear, but suggest a role for p53 in the regulation of the lysosomal system which may be pertinent to the Aβ-induced neurodegeneration. Although it is accepted that p53 can regulate mitochondrial events during apoptosis, including the release of cytochrome *c*, the role of p53 in regulating the lysosomal branch of the apoptotic pathway is less clear.

To this end, the integrity of the lysosomal membrane and the maintenance of a lysosomal-cytosolic pH gradient was assessed using the AO relocation technique. In this approach, cells are incubated with a fluorogenic organic weak base which diffuses into cells and accumulates in lysosomes producing a change in the fluorescence emission of the probe, due to concentration-dependent stacking of the molecules. Disruption of the membrane and/or a marked change in lysosomal pH can therefore be assessed by measuring the change in emission ratio in comparison to controls and by visual inspection. It is generally accepted that leakage of AO from lysosomes to the cytosol is representative of decreased lysosomal membrane integrity (Li *et al.*, 2000; Yuan *et al.*, 2002). First, I have to account for the difference in results I obtained using a conventional fluorescence microscope as opposed to the LSM 510 META confocal microscope at the 1 hr timepoint. Using conventional fluorescence microscopy the results suggested that treatment with A$\beta_{1-40}$ for 1 hr caused lysosomal membrane

integrity to be compromised. However, confocal laser scanning microscopy became available to me after I had used a conventional fluorescence microscope and I re-analysed AO relocation at this timepoint. I obtained a result that was in direct contrast to my previous one. I believe this was due entirely to the difference in equipment used. Confocal fluorescence microscopy possesses several advantages over conventional microscopy. It produces images of improved resolution with a higher degree of magnification, it has a higher level of sensitivity and it is a less invasive form of imaging due to the use of high-power gas laser illumination. All of this culminates to produce superior images than conventional fluorescence microscopes and allows greater numbers of cells to be analysed. I believe this increased sensitivity accounts for the difference in results and would argue that the confocal findings are more reliable.

The results of the study demonstrate that in control cells AO fluorescence exhibited a punctate distribution, reflective of a lysosomal distribution of AO. The mean pixel intensity when AO is sequestered within the lysosome (633nm; complete uncompromised lysosomes) was monitored and quantified and the number of intact orange lysosomes per cell was counted manually. These three measurements allowed us to comment on lysosomal integrity. In contrast to control cells, a diffuse green pattern of AO fluorescence was observed in $A\beta_{1-40}$-treated cells at both 6hr and 24hr, reflecting leakage of the dye from the lysosomal compartment. Fluorescence at 633nm emission significantly decreased, indicating relocation of the dye from the lysosome to the cytosol and this correlated with a reduction in the number of intact lysosomes per cell. The consequences of this increased lysosomal permeability may be the release of lysosomal enzymes into the cytoplasm to initiate apoptotic pathways. For example, cathepsins translocate from lysosomes to the cytosol during apoptosis induced by TNF-$\alpha$ (Werneburg *et al.*, 2002) or oxidative stress (Kagedal *et al.*, 2001). The redistribution of cathepsins is suspected to be an important initiating event of apoptosis (Reiners *et al.*, 2002). However, the requirement for lysosomal permeability and cathepsin translocaion has been questioned in other models. TNF-$\alpha$-induced apoptosis demonstrated a lack of lysosomal permeability and

translocation of cathepsin D, despite a requirement for cathepsin D activity during apoptosis (Demoz *et al.*, 2002). It is evident however, that not all cells undergoing lysosomal permeability proceed to DNA fragmentation at the same time.

Interestingly, treatment with the p53 inhibitor, pifithrin-$\alpha$, revealed that the $A\beta_{1-40}$-mediated destabilisation of the lysosomal membrane was p53-dependent. Given the fact that I had already shown that p53 translocates to the lysosome following treatment with $A\beta_{1-40}$ for 2 hr, this finding indicates that p53 has an important role in regulating lysosomal membrane permeability and suggests a possible mechanism whereby p53 contributes to a lysosomal branch of the apoptotic pathway. The release of lysosomal enzymes may cause mitochondrial damage directly (Zhao *et al.*, 2001) or indirectly (Stoka *et al.*, 2001), followed by cytochrome *c* release, apoptosome formation with Apaf-1 and caspase activation. There may also be a direct activation of caspases by lysosomal cathepsins (Vancompernolle *et al.*, 1998; Ishisaka *et al.*, 1999). There is evidence for the existence of crosstalk between lysosomes and mitochondria during apoptosis. Reports suggest that lysosomal membrane permeabilisation occurs upstream of mitochondrial membrane permeabilisation in apoptosis (Boya *et al.*, 2003). The work presented here suggests the apoptotic effector, p53, associates with the lysosomal membrane early in the cell death cascade. The mechanism by which p53 mediates lysosomal membrane instability has yet to be elucidated. It may directly compromise the lysosomal membrane by inserting itself in the membrane or indirectly by altering some of the lysosomal membrane proteins. The next part of our experiment focused on addressing these questions.

Given that $A\beta_{1-40}$ alters the integrity of the lysosomal membrane, it was pertinent to investigate the role of $A\beta_{1-40}$ in the regulation of lysosomal membrane proteins. Our results presented here reveal a decrease in LAMP-1 expression in neurons exposed to $A\beta_{1-40}$ for 2 hr, 6 hr and 24 hr. Treatment with the p53 inhibitor, pifithrin-$\alpha$, had no effect on the $A\beta_{1-40}$-mediated reduction in LAMP-1 expression, indicating that this event was independent of p53. Furthermore, primers for LAMP-1 mRNA were designed to clarify the effect of $A\beta_{1-40}$ on LAMP-1 expression. The findings demonstrate that $A\beta_{1-40}$

induced a signifcant decrease in LAMP-1 mRNA at 6hr, indicating that $A\beta_{1-40}$ can modulate the transcription of LAMP-1. Western immunoblot analysis also confirmed a significant reduction in LAMP-1 expression in cortical neurons following exposure of cells to $A\beta_{1-40}$ at 6 hr and 24 hr. Pre-treatment with pifithrin-$\alpha$ did not prevent the $A\beta_{1-40}$-induced decrease, again suggesting that p53 is not involved in modulating LAMP-1 expression in neuronal cells. This is in contrast to my finding that the $A\beta_{1-40}$-mediated destabilisation of the lysosomal membrane is p53-dependent. Although our results indicate no role for p53 in LAMP-1 regulation, this does not negate a role for p53 in regulating other membrane proteins, which govern lysosomal integrity (LAMP-2, LIMP I/II, LAP) and this warrants further investigation. While much is known about the structure of lysosomal membrane proteins (Kundra & Kornfeld, 1999), their proposed physiological functions are only of a hypothetical nature. One speculation is that LAMP-2 is a receptor for the uptake and degradation of cytosolic proteins (Cuervo & Dice, 1996). It has been suggested that lysosomal membrane proteins function to protect the lysosomal membrane from proteolysis by lysosomal hydrolases (Kornfeld & Mellman, 1989; Fukuda, 1991; Eskelinen *et al.*, 2003). This function is attributed to the heavy glycosylation of these proteins which prevents the degrading enzymes access through this glycocalix. The loss of LAMP-1/LAMP-2 protein in a double knockout transgenic model has been reported to lead to embryonic lethality (Andrejewski *et al.*, 1999), demonstrating the importance of these proteins in lysosomal stability and cell viability. *lamp1*-deficient mice were found to be viable and fertile, however results revealed an up-regulation of LAMP-2 protein pointing to a compensatory effect of LAMP-2 in response to *lamp1* deficiency. This indicates that LAMP-2 can partially compensate for the loss of *lamp1* and that expression of these proteins is tighly regulated (Andrejewski *et al.*, 1999). In contrast to the relatively mild phenotype in *lamp1* knockout mice, a deficiency of *lamp2* caused severe symptoms; about half of all LAMP-2-deficient mice died at the age of 20-40 days post partum. The physiological importance of LAMP-2 is supported by the finding that LAMP-2 deficiency is the primary defect in Danon disease, a lysosomal glycogen storage disorder (Tanaka *et al.*, 2000). Danon disease is characterised by fatal

cardiomyopathy, variable mental retardation and mild skeletal myopathy. In contrast to the above studies which support a role for LAMPs in protection of the lysosomal membrane, Kundra and Kornfeld (1999) found that deglycosylated LAMP-1 and LAMP-2 are rapidly degraded while lysosomes maintain their acidic pH and membrane stability. They propose that the lysosomal membrane itself is resistant to the constituent lipases due to the presence of the unique lipid lysobisphosphatidic acid. Nevertheless, they note that they cannot totally exclude the possibility that a fraction of LAMP molecules retained their glycosylation state and that this small number of LAMP molecules are sufficient to maintain lysosomal function. There is further evidence for alterations in expression of lysosomal membrane proteins. A progressive age-related decrease in the levels of the LAMP-2 was observed in rat livers, which correlated with a reduction in autophagy (Cuervo & Dice, 2000). The study also found an increase in the number of lysosomes. They attributed the increase in the number of lysosomes to an attempt to compensate for the reduced autophagy. The mechanism for this $A\beta_{1-40}$-induced reduction in LAMP remains unclear. Levels of LAMP at the lysosomal membrane are regulated by two different mechanisms, degradation of LAMP at the lysosomal membrane and changes in the dynamic distribution of LAMP between the lysosomal membrane and lysosomal matrix (Cuervo & Dice, 2000). Could changes in oxidative agents induced by $A\beta_{1-40}$ result in the altered function of LAMP protein? Interestingly, up-regulation of the lysosomal system in AD has been reported by others (Cataldo *et al.*, 1996). This up-regulation is also evident in presymptomatic subjects, 2-3 years before the onset, so that it should be considered an early event in the pathogenesis of AD. In summary, I have demonstrated that $A\beta_{1-40}$ reduces LAMP expression and since I also demonstrated a concomitant loss of membrane stability by $A\beta_{1-40}$, it is possible that this LAMP reduction may contribute to the loss of lysosomal membrane integrity. In support of this hypothesis, Brasseur and colleagues (1997) postulate that the partial cleavage of LAMP-2 at the lysosomal membrane might have a direct effect on the permeabilisation of the lysosomal membrane.

Whereas the importance of caspases in apoptosis is firmly established, recent studies have shown that several other types of proteases, including some lysosomal proteases, may also play a role in programmed cell death (Bursch, 2001; Guicciardi *et al.*, 2004). We analysed supernatant from cells treated with $A\beta_{1-40}$ for 30 min, 2 hr and 6 hr for cathepsin-L secretion and our findings presented here show no appreciable levels of cathepsin-L in the extracellular medium. Previous findings from our laboratory reported a $A\beta_{1-40}$-induced increase in cytosolic cathepsin-L activity (Boland & Campbell, 2003), suggestive of a $A\beta_{1-40}$-mediated translocation of cathepsin-L from the lysosome to the cytosol. In addition, inhibition of cathepsin-L prevented the $A\beta_{1-40}$-mediated increase in caspase-3 activity, PARP cleavage and DNA fragmentation, all indicators of apoptosis (Boland & Campbell, 2004). Increases in cathepsin D expression have been observed in the brain of rats treated with kainate, particularly in regions that showed features of neurodegeneration (Hetman *et al.*, 1995). These results support emerging evidence indicating that cathepsins have interesting functions outside of the lysosomal compartment. They are involved in execution of programmed cell death when released into the cytosol and interestingly, studies have shown cathepsins are involved in degradation of the extracellular matrix when they secreted into the extracellular space (Koblinski *et al.*, 2000). Secretion of lysosomal enzymes has been observed in several cell types capable of digesting extracellular matrices, such as macrophages, osteoclasts and tumour cells (Baron, 1989). In cancer cells, cathepsin B degrades components of the extracellular matrix (laminin, fibronectin and collagen) (Buck *et al.*, 1992) and it is proposed that proteolysis of extracellular matrix liberates growth factors (bFGF, EGF, IGF) with subsequent cell proliferation. Furthermore, it is generally accepted that organic constituents of bone are degraded by lysosomal enzymes secreted by osteoclast cells (Baron, 1989). Several lines of evidence suggest that activated microglia secrete cathepsins to induce neuronal death (Petanceska *et al.,* 1996; Ryan *et al.,* 1995; Kingham and Pocock, 2001), by degrading extracellular matrix proteins (Nakanishi, 2003). We postulated that $A\beta_{1-40}$ may not only induce the release of cathepsins from lysosomes to the cytosol as we have previously shown

(Boland & Campbell, 2004), but that Aβ may result in secretion of cathepsins to the extracellular compartment. It has been suggested that Aβ-induced toxicity is mediated by microglia, the resident macrophage population in the brain. Activated microglia can secrete a host of interleukins including IL-1β, IL-1α, and TNF-α, all of which can mediate the inflammatory response and possibly cause the demise of neurons (McGeer & McGeer, 2003). Over-expression of the pro-inflammatory cytokine, IL-1β, in the AD brain (Griffin *et al.*, 1989) has been proposed to contribute to the additional processing of Aβ in neurons (Forloni *et al.*, 1992). In addition, work by Minogue et al (2003) has demonstrated an increase concentration of IL-1β in cortical neurons exposed to Aβ and that inhibition of IL-1β prevents the Aβ-mediated activation of JNK, caspase-3 and DNA fragmentation, indicating a role for IL-1β in Aβ-induced signalling. The accumulation of microglia at the site of amyloid plaques is a strong indication that microglia play a major role in AD pathogenesis (Eikelenboom, 2002). If cathepsins were secreted extracellularly could they activate microglia thus initiating the inflammatory response with subsequent cell death? Although our results showed no indications of cathepsin secretion in cortical neurons, the time points measured were early, only up to 6 hr. Indeed, if cathepsins are being released into the extracellular environment it may take them substantially longer to translocate from the lysosome through the cytosol and out into the extracellular medium. Furthermore, we only analysed one cathepsin and only in its active state. It is possible that a different cathepsin or a cathepsin in its native form is being secreted, as was indicated in ovarian carcinomas by Pagano and colleagues (1989). Several mechanisms have been suggested to be responsible for the secretion of cathepsins, downregulation of mannose-6-phosphate receptor, altered glycosylation, impaired internalisation of mannose-6-phosphate receptor, and functional deficiency of mannose 6-phosphate ligand binding activity (Achkar *et al.*, 1990). On the other hand alterations in the cytoskeleton has also been proposed to be responsible for secretion (Honn *et al.*, 1994). Nevertheless, our results indicate no cathepsin-L secretion from neuronal populations within 6 hr.

In conclusion, $A\beta_{1-40}$ increased the association of phospho-$p53^{ser15}$ at the lysosome and this was concominant with a disruption in lysosomal membrane integrity, which was prevented by pifithrin-$\alpha$. These data suggest that p53 may be intricately linked with the regulation of lysosomal stability. Since an alteration in endosomal-lysosomal systems is an early event in AD and lysosomal leakage is thought to be one of the earliest detectable event during apoptosis (Cataldo *et al.*, 1996), so the finding that p53 is involved in destablisation of the lysosomal membrane may offer a target for therapeutic intervention at an early stage. While the reduction in LAMP-1 expression evoked by $A\beta_{1-40}$ was not dependent upon p53, it is possible that other lysosomal membrane proteins may be regulated by p53 to control lysosomal membrane integrity and this warrants further investigation. $A\beta_{1-40}$ did not evoke release of cathepsin-L into the extracellular environment at the timepoint studied. Since secretion of neuronal cathepsins could possibly lead to microglial activation this may represent a mechanism for the neuroinflammation associated with AD, and further experiments are required to investigate the effect of $A\beta_{1-40}$ on secretion of a broader range of cathepsin enzymes.

*Chapter 4*

## 4.1 Introduction

Bax is a pro-apoptotic member of the Bcl-2 family of proteins. This family contains both pro-apoptotic members such as Bax and Bid, and anti-apoptotic members such as Bcl-2 and Bcl-$X_L$. Bcl-2 family members act as an upstream checkpoint of caspase activation by controlling cytochrome *c* release from the mitochondria. Bax and Bid are predominantly soluble proteins, whereas Bcl-2 is associated with membranes of various organelles including endoplasmic reticulum, mitochondria and nuclei (Krajewski *et al.*, 1994) and Bcl-$X_L$ exists in both soluble and membrane forms. In response to an apoptotic stimulus, Bax translocates to mitochondria (Wolter *et al.*, 1997), and undergoes a conformational change (Desagher *et al.*, 1999), such as dimerisation or oligomerisation and inserts into mitochondria membrane (Zha *et al.*, 1996), forming a pore allowing the release of cytochrome *c*. Once in the cytosol, cytochrome *c* binds the caspase adaptor, apaf-1, in the presence of ATP, and thus activates the inactive precursor, pro-caspase-9. This leads to the initiation of a caspase cascade culminating in activation of the effector caspase, caspase-3 and induction of DNA fragmentation and apoptosis (Raff, 1998).

Modulation of intracellular organelles is a common phenomenom during apoptosis. Although most studies focus on the mitochondrial regulation of apoptosis, several reports indicate a role for lysosomes. Lysosomes were first described in 1955 by de Duve and his collaborators–a discovery that won him the Nobel prize–as cellular organelles full of acid hydrolases and potentially harmful for the cell (De Duve, 1976). The lysosome is the primary reservoir of nonspecific proteases in the mammalian cell. Although previously described as 'suicide bags' in the cell that release unspecific digestive enzymes following cell damage, recent observations have implicated these organelles and their constituents in the regulation of different modes of cell death (Mathiasen & Jaattela, 2002; Turk *et al.*, 2002). Destabilisation of the lysosomal membrane and translocation of enzymes from the lysosomal compartment to the cytosol has been reported during apoptosis induced by varying stimuli such as the synthetic retinoid, CD437 (Zang *et al.*, 2001), oxidative stress (Roberg & Ollinger, 1998; Antunes *et al.*, 2001),

staurosporine (Kagedal *et al.*, 2001), TNF-α (Guicciardi *et al.*, 2000) and p53 (Yuan *et al.*, 2002). Indeed, previous studies have also implicated endosomal or lysosomal abnormalities as a component of AD pathogenesis (Bowen *et al.*, 1973; Cataldo & Nixon, 1990). Not only has lysosomal dysfunction been found in disease states but also in normal aged control brains (Nakamura *et al.*, 1989; Estus *et al.*, 1992). In many cases of apoptosis induction, partial rupture of the lysosomal membrane allowing selective release of lysosomal enzymes appears to be an early event, occuring either before mitochondrial transmembrane loss or caspase activation (Roberg *et al.*, 1999; Guicciardi *et al.*, 2000; Li *et al.*, 2000; Erdal *et al.*, 2005). However, it is generally believed that a necrotic cell death can be triggered by complete or too strong lysosomal membrane permeabilisation, resulting in the release of high concentrations of lysosomal enzymes in the cytosol (Li *et al.*, 2000). Thus, the release of lysosomal enzymes into the cytosol activates steps in the death cascade possibly resulting in apoptosis. Previous work from our laboratory has documented that $A\beta_{1-40}$-induces cathepsin-L release into the cytosol with downstream activation of caspase-3 in the cytosol (Boland & Campbell, 2004), indicating that Aβ may modulate lysosomal membrane integrity as part of the neurodegenerative process. In a neuronal cell line lysosomal instability, and subsequent apoptosis, was mediated by $A\beta_{1-42}$ (Ji *et al.*, 2002) and $A\beta_{1-42}$ amyloid fragment was found to accumulate in lysosomal compartments preceding death (Yang *et al.*, 1995).

It has been suggested that there exist similar mechanisms for release of lysosomal and mitochondrial constituents to the cytosol during cell death. Previous results from this laboratory has demonstrated that Aβ mediates the release of cathepsin-L from lysosomes and cytochrome *c* from mitochondria, possibly due to Aβ altering the membrane integrity of these organelles. One proposed mechanism for the release of lysosomal enzymes into the cytosol is the opening of pores similar to that induced by Bax following its oligomerisation and insertion into the mitochondrial membrane (Gross *et al.*, 1998). One recent study has found that Bax translocates to lysosomes upon activation of apoptosis, although Bax targeted lysosomes to a lesser extent than it targeted to mitochondria (Kagedal *et al.*, 2005).That study also showed

that Bax and not other proteins can target and insert into lysosomal membranes. Alternative mechanisms that can cause lysosomal instability have been suggested, including oxidative stress (Antunes *et al.*, 2001), Bid (Guicciardi *et al.*, 2005), and p53 (Yuan *et al.*, 2002), however the exact pathway remains to be elucidated.

Abnormalities in both mitochondria and lysosomes occur in AD. Reduced rate of brain metabolism, due to compromised mitochondrial function is one of the best documented abnormalitites in AD (Blass, 2001). Up-regulation of the lysosomal system is an early event seen in almost all pyramidal neurons in prefrontal and hippocampal areas. It is evident in presymptomatic subjects 2-3 years before the onset of the disease, so is an early event in the pathogenesis of AD (Cataldo *et al.*, 1996). This up-regulation is due to an accumulation of lysosomes and an increase in the amount of lysosomal hydrolases. A feature common to lysosomes and mitochondria is their increased membrane permeability in the early phase of apoptosis (Mathiasen & Jaattela, 2002). The experimental work in this chapter aimed to assess the effect of $A\beta_{1-40}$ on Bax association with mitochondria and lysosomes. Expression of Bax was assessed in cortical neurons to investigate whether Aβ influenced the expression of this pro-apoptotic protein. The association of Bax with mitochondrial and lysosomal membranes was assessed by confocal immunocytochemistry in conjunction with the specific mitochondrial dye, Mitotracker red and the specific lysosomal dye, Lysotracker red. To examine the role of p53 in $A\beta_{1-40}$-regulated Bax expression and to investigate whether p53 is involved in distribution of Bax within cortical neurons, cells were pre-treated with the p53 inhibitor, pifithrin-$\alpha$.

# Chapter 4 Results

## 4.1 Pifithrin-α abolishes the $A\beta_{1-40}$-mediated increase in Bax protein expression

There is evidence that p53 mediates apoptosis by modulating the expression of the Bcl-2 family of mitochondrial-associated proteins (Marchenko *et al.*, 2000). Since pro-apoptotic Bax is a transcriptional target of p53, the effects of $A\beta_{1-40}$ (2μM) on Bax expression were investigated in this study. Neurons were treated with $A\beta_{1-40}$ for 6 hr and Bax expression was assessed by western immunoblot using an antibody which recognises the full form of Bax. To establish whether or not p53 had a role in Bax protein expression, cells were pretreated with pifithrin-α (100nM) for 1 hr, prior to treatment with $A\beta_{1-40}$ (2μM) for 6 hr. In Figure 4.1, analysis of densitometric data demonstrate that $A\beta_{1-40}$ induced a significant increase in Bax protein expression at 6 hr. Thus, Bax protein expression in controls cells was 1.00 ± 0.02 (mean ± SEM; arbitrary units) and this was significantly increased to 1.35 ± 0.09 by Aβ ($p<0.01$, one-way ANOVA, n=8). Pifithrin-α alone had no effect on Bax protein expression (1.03 ± 0.03, n=8) but it abolished the $A\beta_{1-40}$-mediated increase in Bax protein expression; where Bax protein expression was 0.95 ± 0.04 ($p<0.05$, one-way ANOVA, n=8) in cells which were co-incubated with $A\beta_{1-40}$ + pifithrin-α. This data indicates that p53 contributes to the $A\beta_{1-40}$-mediated increase in Bax protein expression at 6 hr. A sample immunoblot illustrating the effect pifithrin-α treatment of Bax protein expression is shown in Figure 4.1B.

A.

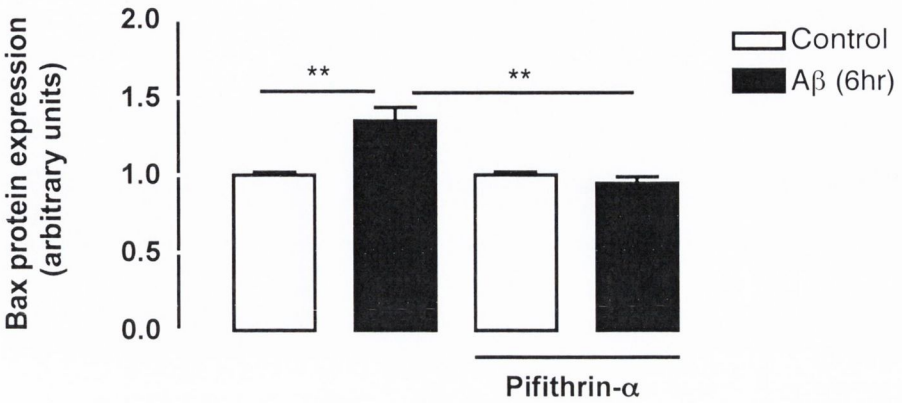


B.

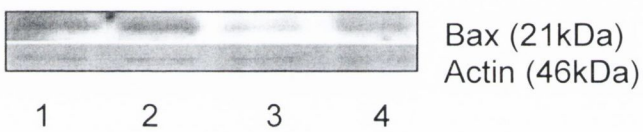


**Figure 4.1 $A\beta_{1-40}$-mediated increase in Bax protein expression is p53-dependent**

A Cortical neurons were treated with $A\beta_{1-40}$ (2μM) in the presence or absence of pifithrin-α (100nM) for 6 hr. Bax protein expression was examined by western immunoblot. $A\beta_{1-40}$ significantly increased Bax protein expression at 6 hr. In the presence of pifithrin-α the $A\beta_{1-40}$-mediated increase in Bax expression was abolished. Results are expressed as mean ± SEM for 8 observations, ANOVA,**$p<0.01$.

B Sample western immunoblot demonstrating levels of Bax and β-actin protein in control (lane 1) and $A\beta_{1-40}$-treated cells (lane 2); pifithrin-α-treated (lane 3) and $A\beta_{1-40}$± pifithrin-α treated cells (lane 4).

## 4.2 Effect of $A\beta_{1-40}$ on Bax expression at mitochondria at 30 min, 6 hr and 24 hr

There is evidence that following a death signal, a dramatic change occurs in the intracellular localisation of Bax, specifically, Bax moves from the cytosol to the mitochondrial membrane (Wolter *et al.,* 1997; Gross *et al.*, 1998). Once at the mitochondria, there is evidence that Bax inserts in the mitochondrial membrane and orchestrates a programme of mitochondrial dysfunction including cytochrome *c* release that results in apoptosis (Gross *et al.*, 1998). In this study, the effect of $A\beta_{1-40}$ on the cellular distribution of Bax was assessed in association with the specific mitochondrial marker, Mitotracker red. Cells were incubated with $A\beta_{1-40}$ (2μM) for 30 min, 6 hr and 24 hr, prior to incubation with Mitotracker red (400nM) for 30 min. Bax expression was detected by immunocytochemistry using a monclonal Bax-specific antibody and cells were visualised by confocal microscopy. Bax immunostaining in control cells is represented in Figure 4.2 (A) and this Bax immunofluorescence was similar in $A\beta_{1-40}$-treated cells at 30 min (Figure 4.2B). In Figure 4.2, (C) and (D) demonstrate the location of mitochondria in control and $A\beta_{1-40}$-treated cells at 30 min following loading with Mitotracker red. Furthermore, in $A\beta_{1-40}$-treated cells increased co-localisation of Bax expression with mitochondria at 30 min (Figure 4.2F) was observed. This result indicates that Bax expression is associated with increased association of Bax at the mitochondria following $A\beta_{1-40}$-treatment. However, regions remained in the cell where Bax expression did not co-localise with mitochondria, indicating alternative intracellular sites for Bax perhaps the nucleus or mitochondria.

Similarly, cells treated with $A\beta_{1-40}$ for 6 hr (Figure 4.3D) and control cells (Figure 4.3C) demonstrate the location of mitochondria following loading with Mitotracker red. Figure 4.3 (A) represents Bax immunostaining in control cells at 6 hr, and in $A\beta_{1-40}$-treated cells (Figure 4.3B). Furthermore, in cells treated with $A\beta_{1-40}$ for 6 hr, co-localisation was observed between Bax expression and mitochondria distribution. This result indicates that treatment with $A\beta_{1-40}$ for 6 hr results in association between Bax and mitochondria.

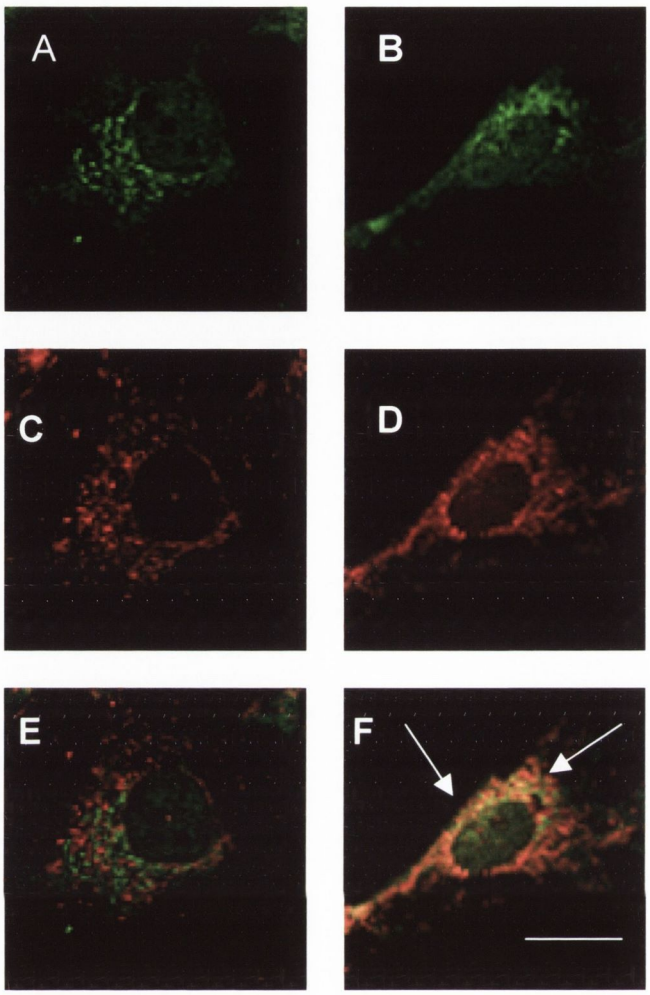


**Figure 4.2 Mitochondrial localisation of Bax induced by $A\beta_{1-40}$ at 30 min**

Confocal microscopy was used to visualised the distribution of Bax within cortical neurons following treatment with $A\beta_{1-40}$ (2μM; 30 min). Cells were double labelled with the mitochondrial-specific marker, Mitotracker Red, and an Alexa 488nm-labelled Bax antibody. Analysis of Bax expression in (i) control and (ii) $A\beta_{1-40}$-treated cells (excitation 488nm; emission, 520nm). Mitotracker Red staining represents the distribution of mitochondria in (iii) control and (iv) $A\beta_{1-40}$-treated cells (excitation 579nm; emission, 599nm). Co-localisation analysis of Bax and mitochondria in (v) control and (vi) $A\beta_{1-40}$-treated cells revealed increased localisation of Bax with mitochondria following $A\beta_{1-40}$-treatment. Scale bar is 10μm.

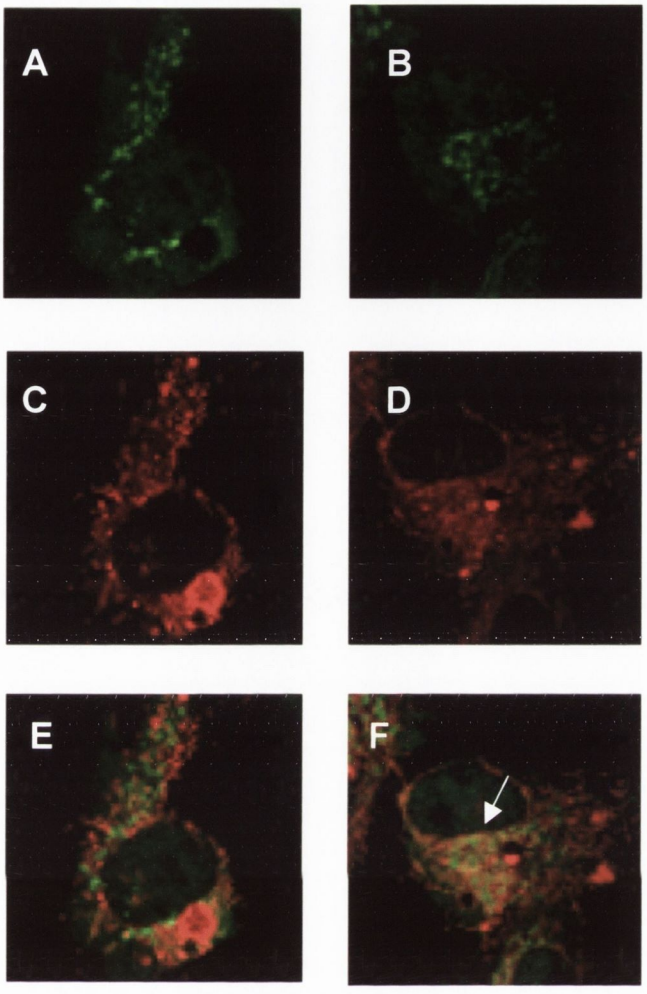


**Figure 4.3 Effect of $A\beta_{1-40}$ on distribution of Bax at 6 hr**

Confocal microscopy was used to visualised the distribution of Bax within cortical neurons following treatment with $A\beta_{1-40}$ (2μM; 6 hr). Cells were double labelled with the mitochondrial-specific marker, Mitotracker Red, and an Alexa 488nm-labelled Bax antibody. Analysis of Bax expression in (i) control and (ii) $A\beta_{1-40}$-treated cells (excitation 488nm; emission, 520nm). Mitotracker Red staining represents the distribution of mitochondria in (iii) control and (iv) $A\beta_{1-40}$-treated cells (excitation 579nm; emission, 599nm). Co-localisation analysis of Bax and mitochondria in (v) control and (vi) $A\beta_{1-40}$-treated cells revealed localisation of Bax with mitochondria following $A\beta_{1-40}$-treatment. Scale bar is 50μm.

In Figure 4.4, (C) and (D) demonstrate the location of mitochondria in control and $A\beta_{1-40}$-treated cells respectively at 24 hr following loading with Mitotracker red. Figure 4.4 (A) represents Bax immunostaining in control cells at 24 hr and in $A\beta_{1-40}$-treated cells (Figure 4.4B). Furthermore, in $A\beta_{1-40}$-treated cells increased co-localisation of Bax expression with mitochondria at 24 hr (Figure 4.4F) was observed. This result indicates that the $A\beta_{1-40}$-mediated increase in Bax expression is associated with increased association of Bax at the mitochondria. However, regions remained in the cell where Bax expression did not co-localise with mitochondria, indicating alternative intracellular sites for Bax.

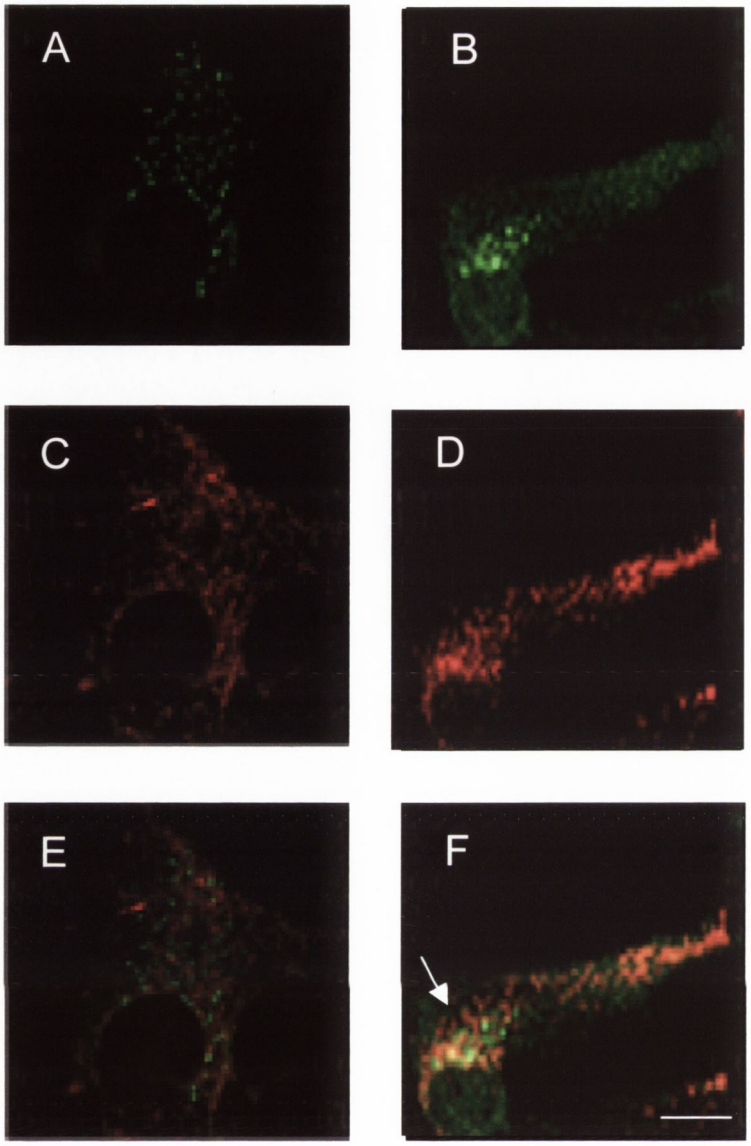


**Figure 4.4 $A\beta_{1-40}$-induces association of Bax at mitochondria at 24 hr**

Confocal microscopy was used to visualised the distribution of Bax within cortical neurons following treatment with $A\beta_{1-40}$ (2μM; 24 hr). Cells were double labelled with the mitochondrial-specific marker, Mitotracker Red, and an Alexa 488nm-labelled Bax antibody. Analysis of Bax expression in (i) control and (ii) $A\beta_{1-40}$-treated cells (excitation 488nm; emission, 520nm). Mitotracker Red staining represents the distribution of mitochondria in (iii) control and (iv) $A\beta_{1-40}$-treated cells (excitation 579nm; emission, 599nm). Co-localisation analysis of Bax and mitochondria in (v) control and (vi) $A\beta_{1-40}$-treated cells revealed increased localisation of Bax with mitochondria following $A\beta_{1-40}$-treatment (arrows). Scale bar is 10μm.

## 4.3 Pifithrin-α prevents the $A\beta_{1-40}$-induced co-localisation of Bax with mitochondria at 30 min

To determine if the association of Bax with mitochondria (Figure 4.2) was a consequence of $A\beta_{1-40}$-induced regulation of p53, neurons were treated with the p53 inhibitor, pifithrin-α (100nM) for 60 min prior to $A\beta_{1-40}$ (2μM; 30 min) treatment and Bax expression and distribution was assessed. Cells were viewed by confocal microscopy at an excitation wavelength of 488nm for Alexa labelled-Bax and 534nm for Mitotracker red. Figure 4.5 represents Bax staining in control (A), $A\beta_{1-40}$-treated (B), pifithrin-α (C) and $A\beta_{1-40}$ + pifithrin-α (D) treated cells at 30 min. The distribution of mitochondria in control (E), $A\beta_{1-40}$-treated (F), pifithrin-α (G) and $A\beta_{1-40}$ + pifithrin-α (H) treated cells, respectively, following loading with Mitotracker red is also demonstrated. In $A\beta_{1-40}$-treated cells increased co-localisation of Bax expression with mitochondria was observed (Figure 4.5J) compared to control (Figure 4.5I). This association of Bax with mitochondria was abolished in cells pre-treated with pifithrin-α (Figure 4.5L). Treatment with pifithrin-α alone resulted in no association of Bax with mitochondria (Figure 4.5K). This finding indicates that the $A\beta_{1-40}$-induced association of Bax with mitochondria at 30 min is mediated by p53.

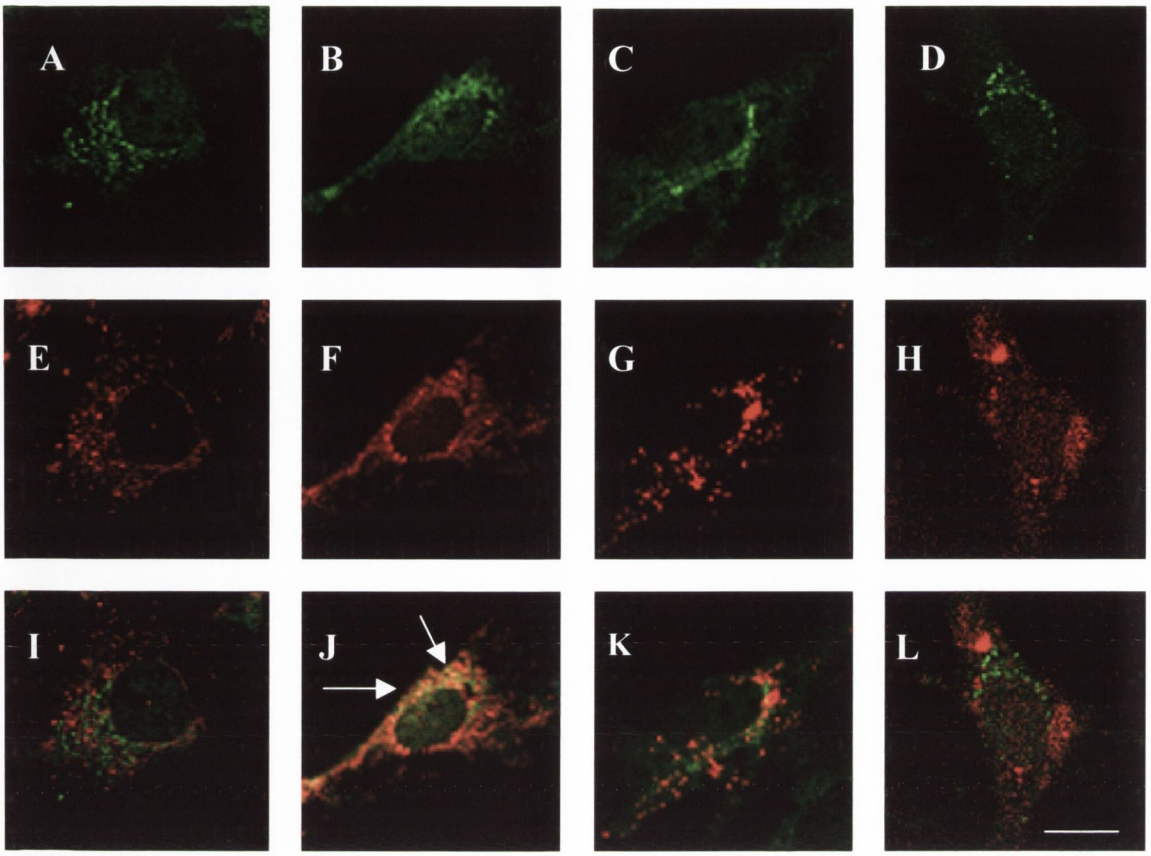


**Figure 4.5 Pifithrin-α prevents $A\beta_{1-40}$-induced association of Bax at mitochondria at 30 min**

Confocal microscopy was used to visualised the distribution of Bax within cortical neurons following treatment with $A\beta_{1-40}$ (2μM; 30 min). Cells were double labelled with the mitochondrial-specific marker, Mitotracker Red, and an Alexa 488nm-labelled Bax antibody. Analysis of Bax expression in (A) control (B) $A\beta_{1-40}$-treated cells, (C) pifithrin-α treated cells, (D) and $A\beta_{1-40}$+pifithrin-α treated cells (excitation 488nm; emission 520nm). Mitotracker red staining represents the distribution of mitochondria in (E) control, (F) $A\beta_{1-40}$-treated cells, (G) pifithrin-α treated cells and (H) $A\beta_{1-40}$+pifithrin-α treated cells (excitation 579nm; emission, 599nm). Co-localisation analysis of Bax and mitochondria in (I) control and (J) $A\beta_{1-40}$-treated cells revealed increased localisation of Bax with mitochondria. Treatment with pifithrin-a alone (K) had no effect on Bax while treatment with pifithrin-α (L) abolished the $A\beta_{1-40}$-induced association of Bax with mitochondria. Arrows indicate cells displaying co-localisation. Scale bar is 10μm.

### 4.4 Effect of pifithrin-α on Bax expression at mitochondria at 6 hr

To further examine the role of p53 on $A\beta_{1-40}$-induced redistribution of Bax, neurons were treated with the p53 inhibitor, pifithrin-α (100nM) for 60 min prior to $A\beta_{1-40}$ (2μM; 6 hr) treatment and Bax expression and distribution was assessed. Fixed cells were viewed by confocal microscopy. Figure 4.6 represents Bax staining in control (A), $A\beta_{1-40}$-treated (B), pifithrin-α (C) and $A\beta_{1-40}$ + pifithrin-α (D) treated cells at 6 hr. Figure 4.6 demonstrates distribution of mitochondria in control (E), $A\beta_{1-40}$-treated (F), pifithrin-α (G) and $A\beta_{1-40}$ + pifithrin-α (H) treated cells, respectively, following loading with Mitotracker red. In $A\beta_{1-40}$-treated cells increased co-localisation of Bax expression with mitochondria was observed (Figure 4.6J) compared to control (Figure 4.6I). This association of Bax with mitochondria was abolished in cells pre-treated with pifithrin-α (Figure 4.6L). Treatment with pifithrin-α alone resulted in no association of Bax with mitochondria (Figure 4.6K). This finding indicates that the $A\beta_{1-40}$-induced association of Bax with mitochondria at 6 hr is dependent on p53.

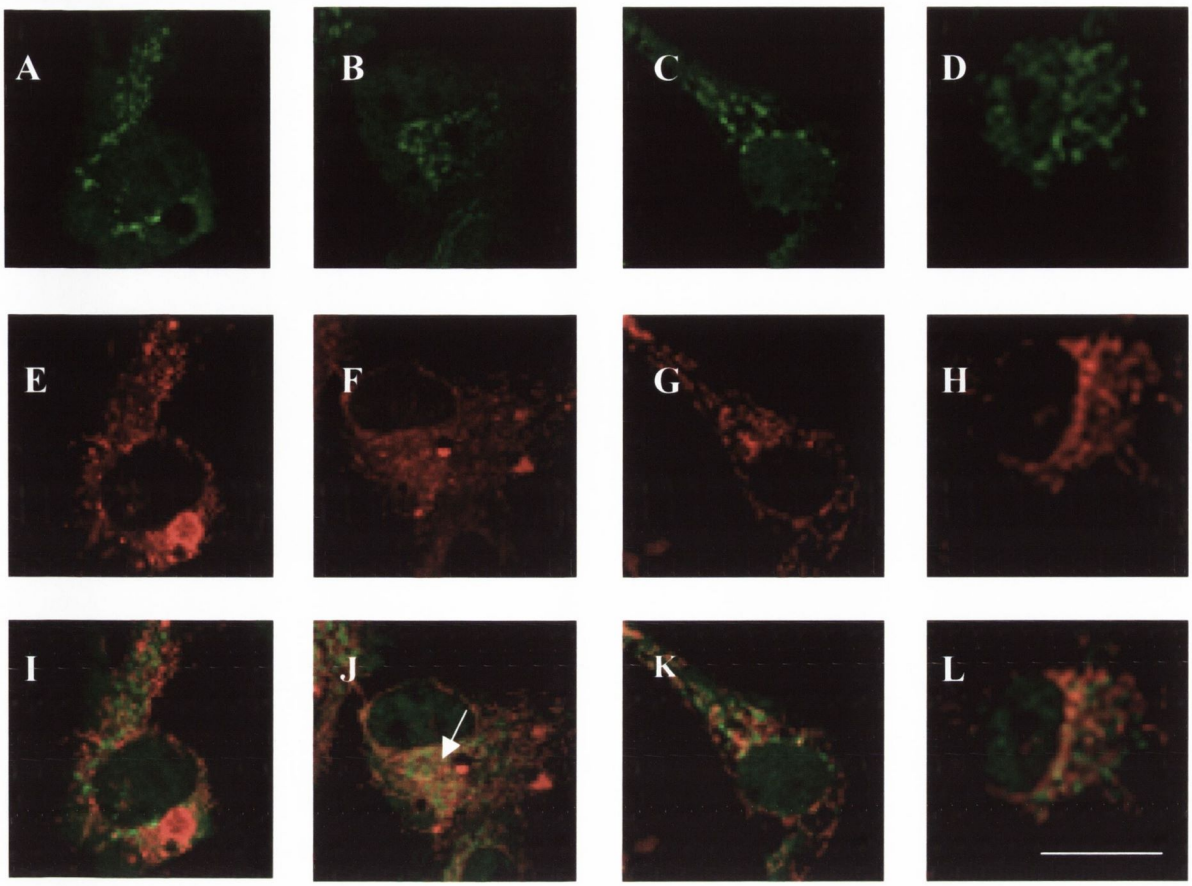


**Figure 4.6 Role of pifithrin-α on $A\beta_{1-40}$ regulation of Bax at mitochondria at 6 hr**

Confocal microscopy was used to visualised the distribution of Bax within cortical neurons following treatment with $A\beta_{1-40}$ (2μM; 6 hr). Cells were double labelled with the mitochondrial-specific marker, Mitotracker red, and an Alexa 488nm-labelled Bax antibody. Analysis of Bax expression in (A) control, (B) $A\beta_{1-40}$-treated, (C) pifithrin-α and (D) $A\beta_{1-40}$+pifithrin-α treated cells (excitation 488nm; emission, 520nm). Mitotracker red staining represents the distribution of mitochondria in (E) control, (F) $A\beta_{1-40}$-treated cells, (G) pifithrin-α treated and (H) $A\beta_{1-40}$+pifithrin-α treated cells. (excitation 579nm; emission, 599nm). Co-localisation analysis of Bax and mitochondria in (I) control and (J) $A\beta_{1-40}$-treated cells revealed increased localisation of Bax with mitochondria. Treatment with pifithrin-α alone (K) had no effect on Bax while treatment with pifithrin-α (L) abolished the $A\beta_{1-40}$-induced association of Bax with mitochondria. Arrows indicate regions within the cell displaying co-localisation. Scale bar is 10μm.

### 4.5 The $A\beta_{1-40}$-induced co-localisation of Bax with mitochondria is p53 dependent at 24 hr

The role of p53 in $A\beta_{1-40}$-induced redistribution of Bax, was also assessed in neurons treated with $A\beta_{1-40}$ (2μM) for 24 hr. Cultured cells were treated with the p53 inhibitor, pifithrin-α (100nM) for 60 min prior to $A\beta_{1-40}$ (2μM) treatment and Bax expression and distribution was assessed. Fixed cells were viewed by confocal microscopy. Figure 4.7 represents Bax staining in control (A), $A\beta_{1-40}$-treated (B), pifithrin-α (C) and $A\beta_{1-40}$ + pifithrin-α (D) treated cells at 24 hr. Figure 4.7 demonstrates distribution of mitochondria in control (E), $A\beta_{1-40}$-treated (F), pifithrin-α (G) and $A\beta_{1-40}$ + pifithrin-α (H) treated cells, respectively, following loading with Mitotracker red. In $A\beta_{1-40}$-treated cells increased co-localisation of Bax expression with mitochondria was observed (Figure 4.7J) compared to control (Figure 4.7I). This association of Bax with Mitochondria was abolished in cells pre-treated with pifithrin-α (Figure 4.7L). Treatment with pifithrin-α alone resulted in no association of Bax with mitochondria (Figure 4.7K). This finding indicates that the $A\beta_{1-40}$-induced association of Bax with mitochondria at 24 hr is dependent on p53.

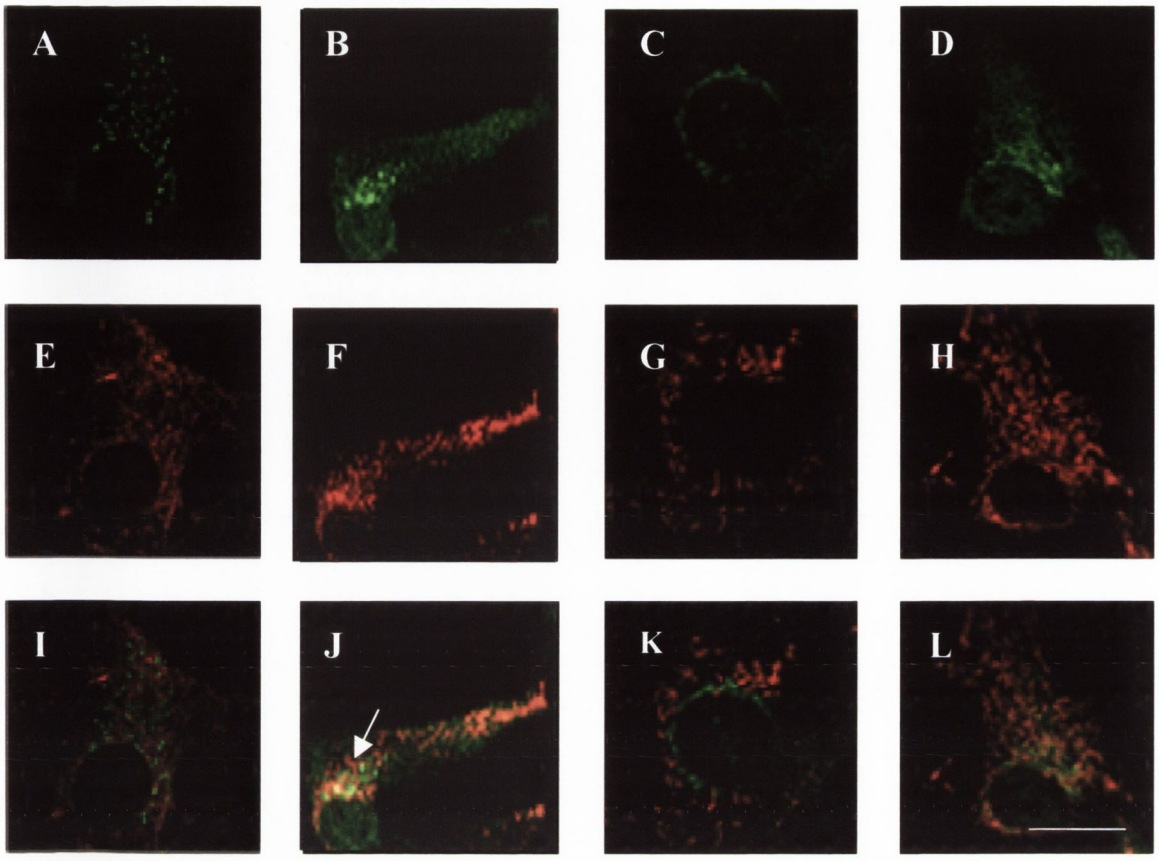


**Figure 4.7 Pifithrin-α prevents $A\beta_{1-40}$-induced association of Bax at mitochondria at 24 hr**

Confocal microscopy was used to visualised the distribution of Bax within cortical neurons following treatment with $A\beta_{1-40}$ (2μM; 24 hr). Cells were double labelled with the mitochondrial-specific marker, Mitotracker red, and an Alexa 488nm-labelled Bax antibody. Analysis of Bax expression in (A) control, (B) $A\beta_{1-40}$-treated, (C) pifithrin-α and (D) $A\beta_{1-40}$+pifithrin-α treated cells (excitation 488nm; emission, 520nm). Mitotracker red staining represents the distribution of mitochondria in (E) control, (F) $A\beta_{1-40}$-treated cells, (G) pifithrin-α treated and (H) $A\beta_{1-40}$+pifithrin-α treated cells (excitation 579nm; emission, 599nm). Co-localisation analysis of Bax and mitochondria in (I) control and (J) $A\beta_{1-40}$-treated cells revealed increased localisation of Bax with mitochondria. Treatment with pifithrin-α alone (K) had no effect on Bax while treatment with pifithrin-α (L) abolished the $A\beta_{1-40}$-induced association of Bax with mitochondria. Arrows indicate regions within the cell displaying co-localisation. Scale bar is 10μm.

### 4.6 The role of p53 inhibitor, pifithrin-α, on lysosomal Bax expression

In order to determine whether Bax impacts on the lysosomal system, expression of Bax was assessed in association with the lysosomal specific dye, Lysotracker red. Fluorescence confocal microscopy was used to visualise the distribution of Bax within cortical neurons following treatment with $A\beta_{1-40}$ (2μM) for 30 min, 6 hr and 24 hr in the presence or absence of pifithrin-α (100nM) for 60 min, prior to incubation with Lysotracker red (1mM) for 30 min. Bax expression was detected by immunocytochemistry using a monoclonal Bax-specific Alexa 488nm-antibody. Figure 4.8 represents Bax immunostaining in control (A) and $A\beta_{1-40}$-treated (B) cells at 30 min. Figure 4.8 also demonstrates the location of lysosomes in control (E) and $A\beta_{1-40}$-treated treated cells (F). No association of Bax with lysosomes was observed following $A\beta_{1-40}$-treatment at 30 min (Figure 4.8J). To examine the role of p53 on Bax expression, neurons were treated with the p53 inhibitor, pifithrin-α (100nM) alone (Figure 4.8C) or prior to $A\beta_{1-40}$ (2μM; 30 min) treatment (Figure 4.8D). Co-localisation analysis of Bax with lysosomes in pifithrin-α (K) and $A\beta_{1-40}$ + pifithrin-α (L) reveal no association of Bax with lysosomes. This finding indicates that at 30 min there is no association of Bax with lysosomes.

In contrast, Figure 4.9 demonstrates Bax immunostaining in control (A) and $A\beta_{1-40}$-treated (2μM) (B) at 6 hr. The location of lysosomes is demonstrated in control (E) and $A\beta_{1-40}$-treated treated cells (F). In cells incubated with $A\beta_{1-40}$ for 6 hr, staining revealed increased localisation of Bax at the lysosomes (J). To determine if the association of Bax with lysosomes was a consequence of $A\beta_{1-40}$-induced regulation of p53, neurons were treated with the p53 inhibitor, pifithrin-α (100nM) for 60 min prior to $A\beta_{1-40}$ (2μM; 6 hr) treatment. Bax staining is illustrated in pifithrin-α (C) and $A\beta_{1-40}$ + pifithrin-α (D) treated cells at 6 hr. Figure 4.9 also demonstrates distribution of lysosomes in control pifithrin-α (G) and $A\beta_{1-40}$ + pifithrin-α (H) treated cells, respectively. Co-localisation analysis of Bax with lysosomes in cells pre-treated with pifithrin-α (L) revealed that pifithrin-α abolished the $A\beta_{1-40}$-induced association Bax with lysosomes. This finding indicates that the $A\beta_{1-40}$-induced association of Bax with lysosomes at 6 hr is mediated by p53.

On the contrary, Figure 4.10 demonstrates Bax immunostaining in control (A) and $A\beta_{1-40}$-treated (2μM) (B) at 24 hr. The location of lysosomes is demonstrated in control (E) and $A\beta_{1-40}$-treated treated cells (F). In cells incubated with $A\beta_{1-40}$ for 24 hr, no localisation of Bax at the lysosomes (J) was observed. In cells pre-treated with pifithrin-α no association of Bax with lysosomes is observed in cells treated with pifithrin-α alone (Figure 4.10K) or $A\beta_{1-40}$ + pifithrin-α (Figure 4.10L). This finding indicates that at 24 hr there is no association of Bax with lysosomes.

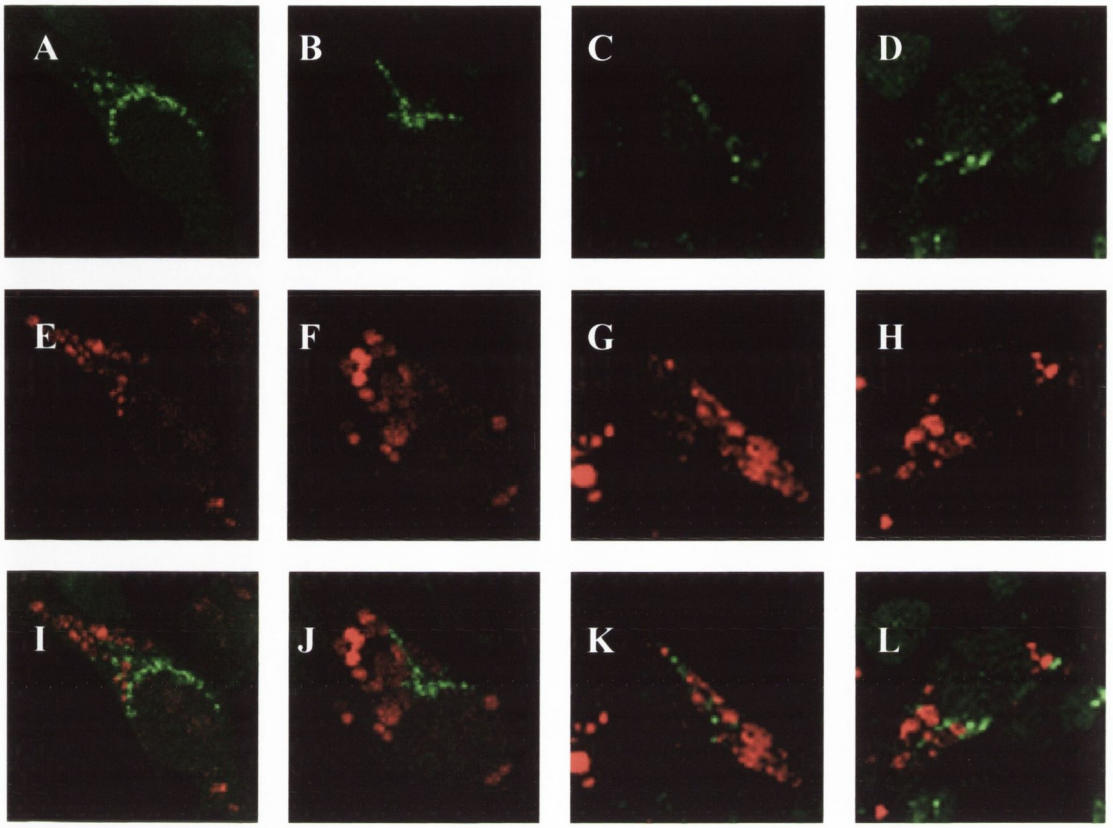


**Figure 4.8 $A\beta_{1-40}$ does not induce Bax association with lysosomes at 30 min**

Fluorescent confocal microscopy was used to visualise the distribution of Bax within cortical neurons following treatment with $A\beta_{1-40}$ (2μM) for 30 min. Cells were double labeled with the lysosomal specific agent, Lysotracker red, and a Alexa 488nm-labelled Bax antibody. Analysis of Bax expression in control (A), $A\beta_{1-40}$-treated (B), pifithrin-α treated (C) and $A\beta_{1-40}$+Pifithrin-α treated cells (D) (excitation 488nm; emission, 520nm). Lysotracker red staining represents the distribution of lysosomes in control (E), $A\beta_{1-40}$-treated cells (F), pifithrin-α treated cells (G) and $A\beta_{1-40}$ +pifithrin-α treated cells (H) (excitation 579 nm; emission, 599nm). Co-localisation analysis of Bax expression with lysosomes is shown in control (I), $A\beta_{1-40}$-treated (J), pifithrin-α (K) and $A\beta_{1-40}$ + pifithrin-α (L) treated cells. Scale bar 10μm.

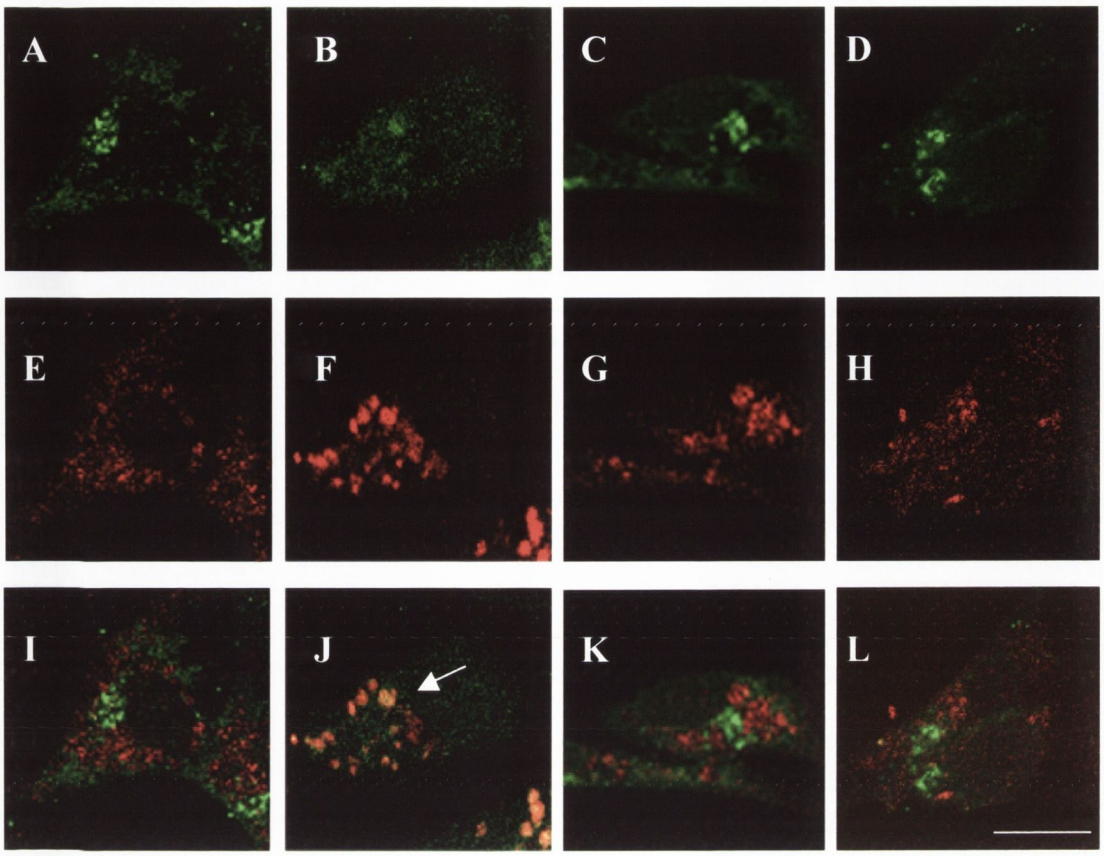


**Figure 4.9 $A\beta_{1-40}$ induces Bax association with lysosomes at 6 hr via p53**

Fluorescence confocal microscopy was used to visualise the distribution of Bax within cortical neurons following treatment with $A\beta_{1-40}$ (2μM) for 6 hr. Cells were double labeled with the lysosomal specific agent, Lysotracker red, and a Alexa 488nm-labelled Bax antibody. Analysis of Bax expression in control (A), $A\beta_{1-40}$-treated (B), pifithrin-α treated (C) and $A\beta_{1-40}$+Pifithrin-α treated cells (D) (excitation 488 nm; emission, 520nm). Lysotracker red staining represents the distribution of lysosomes in control (E), $A\beta_{1-40}$-treated cells (F), pifithrin-α treated cells (G) and $A\beta_{1-40}$ +pifithrin-α treated cells (H) (excitation 579 nm; emission, 599nm). Co-localisation analysis of Bax expression with lysosomes is shown in control (I), $A\beta_{1-40}$-treated (J), pifithrin-α (K) and $A\beta_{1-40}$ + pifithrin-α (L) treated cells. Arrows indicate association between Bax and lysosomes. Scale bar 10μm.

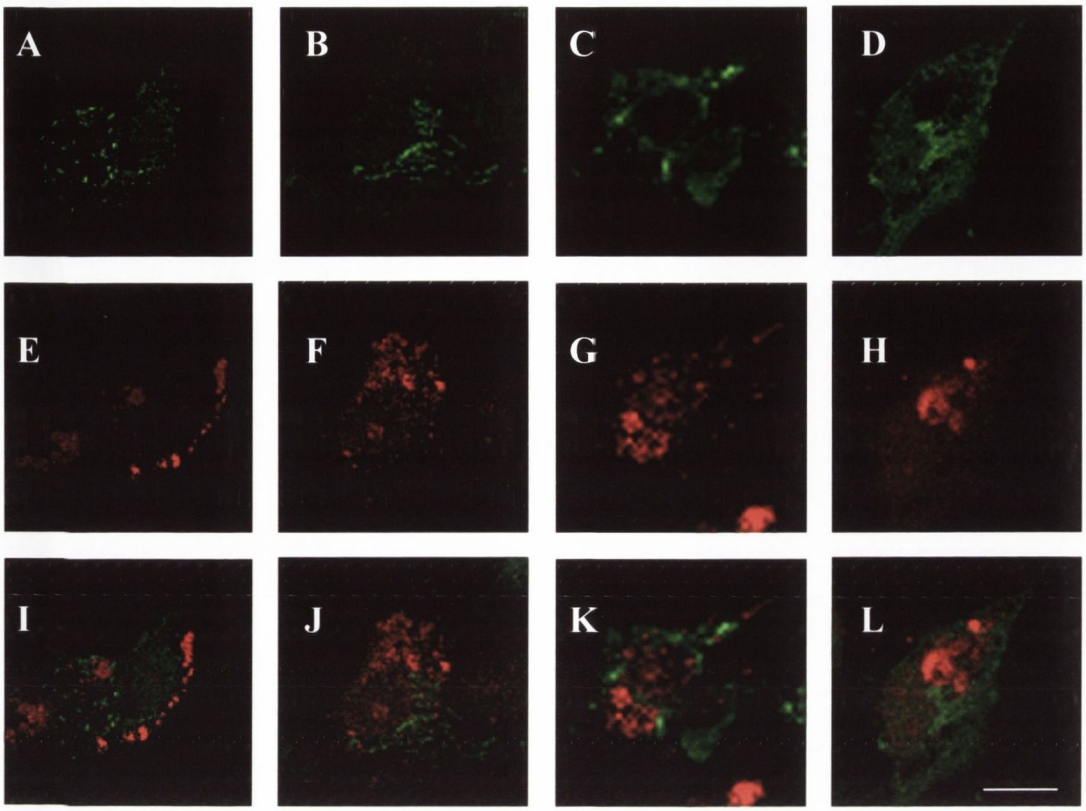


**Figure 4.10 $A\beta_{1-40}$ has no effect on lysosomal Bax expression at 24 hr**

Fluorescence confocal microscopy was used to visualise the distribution of Bax within cortical neurons following treatment with $A\beta_{1-40}$ (2μM) for 24 hr. Cells were double labeled with the lysosomal specific agent, Lysotracker red and a Alexa 488nm-labelled Bax antibody. Analysis of Bax expression in control (A), $A\beta_{1-40}$-treated (B), pifithrin-α treated (C) and $A\beta_{1-40}$+Pifithrin-α treated cells (D) (excitation 488 nm; emission, 520nm). Lysotracker red staining represents the distribution of lysosomes in control (E), $A\beta_{1-40}$-treated cells (F), pifithrin-α treated cells (G) and $A\beta_{1-40}$ +pifithrin-α treated cells (H) (excitation 579 nm; emission, 599nm). Results show no localisation of Bax with lysosomes in control (I), $A\beta_{1-40}$-treated (J), pifithrin-α (K) and $A\beta_{1-40}$ + pifithrin-α (L) treated cells. Scale bar 10μm.

## 4.3 Discussion

The experimental work carried out in this chapter investigated the effect of $A\beta_{1-40}$ on the subcellular distribution of the pro-apoptotic protein, Bax. The data provide evidence that $A\beta_{1-40}$ induces a significant increase in the expression of Bax protein at 6 hr and this increase was mediated by the tumour supressor protein, p53. $A\beta_{1-40}$ promoted Bax translocation from the cytosol to mitochondrial membranes and exposure of cells to the p53 inhibitor, pifithrin-$\alpha$, abolished this association. Additionally, Bax co-localised with lysosomal membranes following $A\beta_{1-40}$ treatment for 6 hr and this translocation was mediated by p53. These results indicate that Bax can not only associate with mitochondria but also associates with lysosomes in cultured cortical neurons, suggesting that Bax may play an important role in the regulation of the release of lysosomal and mitochondrial constituents during the neurodegenerative process.

The previous chapter demonstrated the crucial role of p53 in regulating the stability of cellular organelles, specifically lysosomes. In this chapter we investigate if the p53 transcription factor, Bax, translocates from the cytosol to mitochondria or lysosomes following $A\beta_{1-40}$ exposure. Bax is a pro-apoptotic member of the Bcl-2 family of proteins that can induce (Bax, Bid) or inhibit (Bcl-2, Bcl-xl) apoptosis, by virtue of their ability to associate with the mitochondrial membrane thereby inducing or blocking cytochrome *c* release, respectively. In order to determine whether $A\beta_{1-40}$ can modulate Bax expression in cultured cortical neurons, expression of Bax protein was assessed by western immunoblot analysis. A significant increase in Bax protein was observed at 6 hr post $A\beta_{1-40}$ treatment. Similar observations have been reported in the literature, $A\beta_{1-42}$ upregulates Bax expression when applied intra- (Zhang *et al.*, 2002) or extracellularly (Culmsee *et al.*, 2001) and $A\beta_{1-40}$ increased mitochondrial expression of Bax in the CA1 region of the hippocampus (Minogue *et al.*, 2003). However, another study found that in hippocampal neurons Bax expression was unaffected by $A\beta_{1-40}$ (Paradis *et al.*, 1996). Thus, the regulatory effects of A$\beta$ on Bax may be dependent on the nature of the A$\beta$ species and cell type, although the observation that Bax

expression is increased in regions of the AD brain (MacGibbon *et al.*, 1997) is suggestive of a role for Bax in the disease process. The mechanism underlying Aβ-induced Bax expression is unclear. Several studies show that Bax is transcriptionally regulated by p53. To investigate whether p53 played a role in this Aβ-induced increase, the p53 inhibitor, pifithrin-α, was incubated in cells prior to Aβ treatment. Our results demonstrate that pifithrin-α abolished the Aβ-mediated increase in Bax expression indicating that the Aβ-induced increase in Bax expression was mediated by p53. The previous chapter demonstrated that Aβ increased phospho-p53$^{ser\text{-}15}$ in cultured cortical neurons. Increased p53 expression has been found in transgenic neurons which express Aβ cytosolically, and in neurons from the brains of AD patients (LaFerla *et al.*, 1996; de la Monte *et al.*, 1997).

As Bax is a pro-apoptotic member of the Bcl-2 family, the probable consequences of this Aβ-induced Bax expression is neuronal cell death. Bax has been found to evoke rapid neuronal cell death through overexpression (Bounhar *et al.*, 2001) and upregulation of Bax has been reported in Aβ-mediated apoptosis (Zhang *et al.*, 2002). Mitochondria are considered key players in the regulation of apoptotic cell death. It is well known that Bax activates caspases by promoting the release of mitochondrial cytochrome *c* which forms an apoptosome with a number of other factors including caspases (Adrain & Martin, 2001). To further examine the distribution of Bax in $A\beta_{1\text{-}40}$-treated neurons, confocal immunofluorescence microscopy was employed. This technique represents a more sensitive approach with which to monitior protein expression in a single cell monolayer. Expression of Bax was monitored in association with the fluorescent mitochondrial marker, Mitotracker red. The results herein reveal increased expression of Bax at the mitochondria in $A\beta_{1\text{-}40}$-treated cells. In additon, $A\beta_{1\text{-}40}$ promoted the association of Bax with the mitochondrial membrane at 30 min, 6 hr and 24 hr compared with a cytosolic distribution of Bax in control cells. Pre-treatment with the p53 inhibitor, pifithrin-α, prevented the $A\beta_{1\text{-}40}$-mediated localisation of Bax with mitochondria suggesting that the association of Bax with mitochondria is dependent on p53. Bax normally resides in the cytoplasm and translocates to the mitochondria during apoptosis. It is therefore likely that this

association of Bax at the mitochondria contributes to the Aβ–mediated release of cytochrome *c* demonstrated in previous studies (Minogue *et al.*, 2003). In its inactive state there is evidence suggesting that the C-and N-termini of Bax interact and that upon triggering of apoptosis there is a conformational change in Bax, exposing these two domains and thus enabling Bax insertion into the mitochondria. Indeed, there is evidence that Bax can form channels in artifical membranes (Minn *et al.*, 1997; Schlesinger *et al.*, 1997), furthermore, its structure is similar to the pore forming domains of some bacterial toxins (Muchmore *et al.*, 1996). It is therefore possible that Bax may form channels in the mitochondrial outer membrane allowing the release of cytochrome *c*. There are alternative proposed mechanisms for mitochondrial release of cytochrome *c*. Another potential pathway is the opening of the mitochondrial permeability transition pore. The components of this pore include the voltage-dependent anion channel and ANT, which is located in the inner mitochondrial membrane and functions as an ATP/ADP carrier (Narita *et al.*, 1998). Opening of this pore can be induced by atractyloside, an agonistic ligand to ANT (Kroemer *et al.*, 1997). Another proposed mechanism for mitochondrial release is caspase-8-mediated activation of Bid, which has been shown to induce release of cytochrome *c* (Li *et al.*, 1998).

The mechanism of Bax recruitment to intracellular organelles is not yet fully understood. Recent studies indicate that permeabilisation of the mitochondria by Bax requires interaction of a BH3-domain–only protein, such as Bid with the negatively charged phospholipid cardiolipin (Epand *et al.*, 2002). Also, the Bax translocation process seems to involve its dimerisation and/or a conformational change in the structure of Bax (Nechushtan *et al.*, 1999). Once in the cytosol, cytochrome *c* complexes with the cytosolic factor Apaf-1 which triggers the activation of the cysteine protease caspase-3, which contributes to the drastic morphological changes associated with apoptosis by disabling a number of key substrates (Zou *et al.*, 1997). In addition to cytochrome *c*, several other proteins are released from mitochondria during apoptosis, including apoptosis-inducing factor (AIF) and Smac/Diablo (Zornig *et al.*, 2001). AIF redistributes from the mitochondria to the nucleus during apoptosis and induces some of the nuclear morphological changes associated with apoptosis in a caspase-independent manner (Herr & Debatin,

2001). The Smac/Diablo molecule inactivates caspase inhibitors and thereby relieves inhibition of caspase acitvation by IAP inactivation (Zornig *et al.*, 2001).

Although mitochondria are considered key players in the regulation of apoptotic cell death, in recent years increased knowledge about the complexity of PCD has shed light on many new components, and lysosomes or lysosomes constituents have been implicated in some cell death programmes. To elucidate whether Bax could be a mediator of lysosomal membrane permeability, the subcellular location of Bax was studied using confocal immunofluorescence microscopy. The lysosomal specific marker, Lysotracker red was used to visualise distribution of lysosomes within cortical neurons. Prior to $A\beta_{1-40}$ exposure cells showed a diffuse cytosolic staining of Bax, while no co-localisation of Bax with lysosomes was detected. In reponse to $A\beta_{1-40}$ treatment for 6 hr, punctate distribution of Bax, that in part co-localised with lysosomes was detected by yellow staining. The result suggests that Bax translocates from the cytosol to lysosomes following $A\beta_{1-40}$ exposure to cells. However, at 24 hr there was no observable association between Bax and lysosomes. This transient association between Bax and lysosomes may mediate specific signals within culltured cortical neurons. Previous findings from this laboratory have reported a $A\beta_{1-40}$-mediated release of cathepsins at this timepoint (Boland & Campbell, 2004). In addition, this timepoint occurs upstream of $A\beta_{1-40}$-mediated apoptosis (see chapter 5). Therefore, this early colocalisation could initiate cell death through release of cathepsins. The mechanisms of lysosomal rupture or destabilisation are not yet completely understood. Indeed, it is still unclear whether there is general leakage of lysosomal contents or whether the permeabilisation is rather selective. A selective release based on molecular size has been indicated by the analysis of staurosporine-treated cells loaded with FITC-labelled dextran particles of increasing size (Kroemer & Jaattela, 2005). Faster release of cathepsins (approx. 40kDa) than that of the higher molecular weight β-hexosaminidase (over 200kDa) supports this view. Lysosomal membrane permeabilisation and translocation of enzymes from lysosomes to cytosol has been reported following apoptosis induced by various stimuli. Previous results from this

laboratory have demonstrated that Aβ promotes release of cathapsin-L from lysosomes (Boland & Campbell, 2004). Interestingly, a common feature to lysosomes and mitochondria is their increased membrane permeability in the early phase of apoptosis (Mathiasen & Jaattela, 2002). It is therefore possible that lysosomal-associated Bax plays a role in destabilising the lysosomal membrane promoting cathepsin release in a similar way to the role of Bax in inducing cytochrome *c* release from mitochondria. In support of this an increase in Bax expression correlates with deficiencies in lysosomal integrity during glioblastoma apoptosis (Chen *et al.*, 2001). Recently, one publication has mentioned that Bax localises with lysosomes in response to staurosporine-induced apoptosis at 4 hr (Kagedal *et al.*, 2005), thus supporting our hypothesis and findings. Bcl-2 family members have long been known to control permeabilisation of the mitochondrial membrane during apoptosis, but involvement of these proteins in lysosomal membrane permeabilisation was not considered until recently. There is an increasing body of evidence to suggest a functional interaction between the Bcl-2 family of proteins and lysosomes. Phosphorylation of Bcl-2 has been demonstrated to block oxidative stress-induced apoptosis by stabilising lysosomes (Zhao *et al.*, 2001) and cleavage of Bcl-2 by the calcium-dependent protease, calpain, is thought to be another likely mechanism for the disruption of lysosomal membrane integrity (Wang, 2000). Thus, Bcl-2 proteins may be intricately linked with lysosomal stability. The results from this study demonstrate that Aβ increases Bax association with lysosomes suggesting that Bax may play a key role in Aβ-mediated alterations in lysosomal membrane integrity. Pre-treatment with the p53 inhibitor, pifithrin-α, abolished the association of Bax with lysosomes, indicating the this co-localisation is reliant on p53.

An alternative mechanism suggests that intracellular sphingosine could promote partial lysosomal rupture (Kagedal *et al.*, 2001). Sphingosine production is stimulated by different death inducers such as TNF-α, which triggers lysosomal destabilisation (Schutze *et al.*, 1999; Guicciardi *et al.*, 2000). Given its detergent and lysosomotropic properties, the sphingosine accumulated in lysosomes could permeabilise lysosomal membranes and facilitate the relocation of some lysosomal proteases to the cytosol (Kagedal

*et al.*, 2001). Other possible mechanisms involved in inducing lysosomal destabilisation have implicated a role for the pro-apoptotic protein, Bid. Bid is required for Bax to intergrate into mitocondrial membranes causing pore formation. Studies have found that caspase-8 can induce the release of cathepsin-B from isolated lysosomes via Bid (Guicciardi *et al.*, 2005). Furthermore, lysosomal membranes are rich in lysobisphosphatidic acid which is structurally related to the phospholipid cardiolipin, which was found to interact with Bid (Wherrett & Huterer, 1972). Another explanation for triggering lysosomal rupture implicates the production of reactive oxygen species (ROS). Oxidative stress can induce lysosomal destabilisation very fast, resulting in the release of cathepsins, *in vitro* (Kalra *et al.*, 1988) and *in vivo* (Ollinger & Brunk, 1995). Lysosomes are organelles particularly vunerable to oxidative stress since they contain the most important pool of reactive iron in the cell (Antunes *et al.*, 2001). On the other hand, atractyloside, an agonistic ligand to ANT, which is a component of permeability transition pore in mitochondria, was reported to cause lysosomal membrane permeability and release of cathepsin-B into the cytosol (Vancompernolle *et al.*, 1998). This result was repeated by Kagedal and collaborators (2005) however they had to use very high concentrations to obtain a result. Finally, the previous chapter implicated downregulation of LAMP, a lysosomal membrane protein, as a potential cause of lysosomal membrane permeabilisation. Whether these different mechanisms indeed play an active role in lysosomal rupture and how they are controlled remains to be clarified.

The relationship between lysosomes and mitochondria is complicated. Some studies present evidence indicating lysosomal instability precedes mitochondria dysfunction (Yuan *et al.*, 2002; Boya *et al.*, 2003), however, the extent of mitochondrial input into lysosomal-induced cell death is unknown. During apoptosis induced by sphingosine and lysosomotropic reagents, cathepsin B was found to be translocated to the cytosol prior to mitochondrial damage and cytochrome c release (Turk *et al.*, 2000; Leist & Jaattela, 2001). Cytosolic cathepsins have been shown to interact with the Bcl-2 family of proteins and promote apoptosis. In a cell free system it was found that pro-apoptotic Bid was cleaved in the presence of lysosomal enzymes (Stoka *et al.*, 2001). Cleaved Bid went on to induce cytochrome *c* release. Bid-

independent pathways have also been suggested, implicating Bax and Bak (Boya *et al.*, 2003). Cathepsin-D has been shown to trigger Bax activation in human T lymphocytes with resulting apoptosis (Bidere *et al.*, 2003). Furthermore, lysosomes and mitochondria seem to share mechanisms that precede membrane permeabilisation. This was demonstrated by Zhao and colleagues in which overexpression of Bcl-2, which is known to inhibit mitochondrial release of cytochrome *c*, was found to prevent lysosomal destabilisation (Zhao *et al.*, 2000b). These findings highlight the complexity of the relationship between mitochondria and lysosomes.

While there are still many issues that need clarification for a better understanding of the precise participation of lysosomes in cell death, accumulating studies point to a lysosomal component of apoptosis in addition to the classical mitochondrial pathway of apoptosis. Apoptosis in various cell lines triggered by various lysosomotropic reagents and oxidative stress suggests a route for pathological activation of the apoptotic machinery. Indeed the sensitivity of lysosomes toward oxidative stress could predispose them to a number of pathological conditions, such as certain forms of neurodegeneration when oxidation plays a role. Spreading of hydrolytic enzymes from lysosomes into the cytoplasm due to the lysosomal membrane injury or rupture has been suggested in both heart (Brachfeld, 1969; Ichihara *et al.*, 1987) and brain (White *et al.*, 1993) ischemia injuries.

The results presented here suggest a possible mechanism for disruption of mitochondrial and lysosomal membrane integrity induced by $A\beta_{1-40}$ reported in the previous chapter. Association of Bax at the mitochondria and lysosome in response to $A\beta_{1-40}$ hints at a role for this pro-apoptotic protein in the regulation of mitochondrial and lysosomal stability.

# *Chapter 5*

## 5.1 Introduction

The family of PTKs includes non-receptor type proteins such as the Syk family (Syk and ZAP-70), the Src family (Lyn, Fyn, Lck, Blk and Fgr) in addition to Csk and Btk of the Tec family. The activation of tyrosine kinases is the initial step in regulating a variety of cellular processes, including proliferation, differentiation and inflammatory responses. The Syk family comprises Syk and ZAP-70 and is characterised by the presence of two adjacent SH2 domains, separted by a long linker (linker B) from a C-terminal catalytic domain (Turner *et al.*, 2000). Unlike Src-family kinases, Syk family members lack an SH3 domain. Syk and ZAP-70 can function downstream of the Src family kinases to amplify the signal and are focal points for the assembly of signalling complexes. Syk is expressed in a wide variety of hematopoietic cells, including T cells, B cells, myeloid cells and platelets, whereas ZAP-70 expression is restricted to T cells and natural killer cells (Chan *et al.*, 1994).

Syk was first recognised as a 40 kDa proteolytic fragment derived from a p72 tyrosine kinase present in spleen thymus and lung (Zioncheck *et al.*, 1988). Originally cloned from porcine spleen (Taniguchi *et al.*, 1991), Syk has been almost exclusively studied in hematopoietic cells such as B and T lymphocytes, natural killer cells, mast cells, macrophages and platelets (Sada *et al.*, 2001). In these cells, Syk is involved in the proximal signalling downstream of activated immunorecepetors, such as BCR, TCR and Fc receptors. Upon receptor cross-linking the tandem SH2 domains of Syk bind two phosphorylated tyrosines in the conserved ITAMs in immune response receptors. Subsequent phosphorylation of Syk induces its activation, leading to the binding and/or phosphorylation of adapter proteins and downstream effectors (Ding *et al.*, 2000), orchestrating a complex series of cellular responses such as cell proliferation, differentiation, survival and phagocytosis. Syk can activate several signalling effectors including PLC$\gamma$, calcium mobilisation, the Ras-Raf-Mek-ERK pathway, as well as the PI3K (Agarwal *et al.*, 1993; Benhamou *et al.*, 1993; Kiener *et al.*, 1993; Kurosaki *et al.*, 1994).

Increasing evidence indicates that Syk also has fundamental cellular functions that are receptor and ITAM independent. The first evidence for a

role of Syk in non-immune cells came from its targeted disruption in mice. Homozygous Syk mutants suffered severe hemorrhaging as embryos and died perinatally, indicating that Syk has a critical role in maintaining vascular integrity or wound healing during embryogenesis (Cheng *et al.*, 1995; Turner *et al.*, 1995). Since then, recent work has shown that Syk exhibits a more widespread expression pattern and is found in various non-hematopoietic cells including epithelial cells (Fluck *et al.*, 1995), hepatocytes (Tsuchida *et al.*, 2000), fibroblasts (Wang & Malbon, 1999), breast tissue (Coopman *et al.*, 2000), vascular endothelial cells (Turner *et al.*, 2000) and neuron-like cells (Tsuchida *et al.*, 2000), suggesting a general physiological role for this kinase.

Cellular location and distribution of Syk appears to depend on the cell type and state of the cell. In lymphoid and epithelial cells, Syk has been reported to reside in both the nucleus and cytoplasm (Ma *et al.*, 2001), as has its close family member Zap-70. In breast cancer cells, the expression of Syk and its localisation to the nucleus have been correlated with the repression of invasive tumor growth (Wang *et al.*, 2003). In B cells, engagement of the BCR recruits Syk from both the cytoplasm and nucleus to the aggregated BCR complex. Syk returns rapidly to both compartments following receptor internalisation (Ma *et al.*, 2001). Little is known as to how the movement of Syk between the cytoplasm and nucleus is regulated, although, one recent study identified an unconventional shuttling sequence near the junction of the catalytic domain and the linker B region that accounts for Syk's subcellular localisation (Zhou *et al.*, 2006). They also suggest that the subcellular localisation of Syk can influence how B cells respond to external stimuli. The pathways involved in this process are unknown but under investigation.

Growing evidence suggests a relationship between trafficking of BCR and lysosomes (Bonnerot *et al.*, 1998; He *et al.*, 2005). An important step, after the engagement of immunoreceptors by their ligands, is their internalisation and delivery to lysosomes. Thus, signal transduction and internalisation/lysosomal transport are initiated simultaneously after immunoreceptor engagement. The cytosolic effectors of cell signalling have been analysed extensively, but very little is known about the pathways and effectors of immunoreceptor internalisation and lysosomal transport. Studies carried out in macrophages show that the FcR-associated λ-chain and Syk

are involved in phagocytosis (Bonnerot *et al.*, 1998), however the mechanism is not clear

To conclude, the function of Syk varies depending on the cell type, stimulus involved and cellular location of Syk. Therefore the aim of this study was to firstly investigate whether or not Syk is present in primary cortical neurons and if so to examine its distribution. Second, to assess if $A\beta_{1-40}$ regulates expression of Syk, and investigate the role of Syk in Aβ-mediated signalling, including cell death as previously shown in our laboratory. Finally, experiments were performed to elucidate a relationship between Syk and lysosomes in cortical neuronal cells.

# Chapter 5 Results

## 5.1 $A\beta_{1-40}$-induces an increase in Syk expression in neuronal cells

Syk, a nonreceptor protein kinase initially believed to be expressed in hemopoietic cells only, has recently been found expressed in nonhemopoietic cells (Coopman *et al.*, 2000; Tsuchida *et al.*, 2000). Expression of Syk was investigated using immunofluorescence microscopy in cultured cortical neurons. Syk immunofluorescence was visualised by probing neurons with an anti-Syk antibody which recognises a peptide mapping at the carboxy terminus of Syk of human origin, and a fluorescein-conjugated secondary antibody. Cells were then examined under a fluorescence microscope at an excitation wavelength of 505nm. Figure 5.1 depicts the changes in Syk expression, evoked by $A\beta_{1-40}$ at 30 min and 2 hr. In control cells, Syk immunoreactivity was detected within the cytosol (Figure 5.1 A and C), reflecting a basal level of Syk expression at 30 min and 2 hr, repectively. However, in cells treated with $A\beta_{1-40}$ (2μM) for 30 min or 2 hr (Figure 5.1 B and D), a higher intensity of Syk immunoreactivity was observed within the cytosol. This result demonstrates the $A\beta_{1-40}$ increases Syk expression in cultured cortical neurons. This is the first time Syk expression has been demonstrated in cultured cortical neurons.

## 5.2 $A\beta_{1-40}$ increases phospho-Syk expression in neuronal cells

Since $A\beta_{1-40}$ mediated an increase in total Syk expression, this study investigated whether the increase was due to a posttranslational modification event. Phosphorylation of Syk at residue tyrosine 323, was assessed following treatment of cells with $A\beta_{1-40}$ (2μM). Cells were treated with $A\beta_{1-40}$ (2μM) for 30 min and 2 hr, and Syk phosphorylation was assessed by immunostaining using an antibody which specifically recognises Syk phosphorylated at residue tyrosine-323. Figure 5.2 depicts the changes in phospho-Syk expression, evoked by $A\beta_{1-40}$ at 30 min and 2 hr. In control cells,

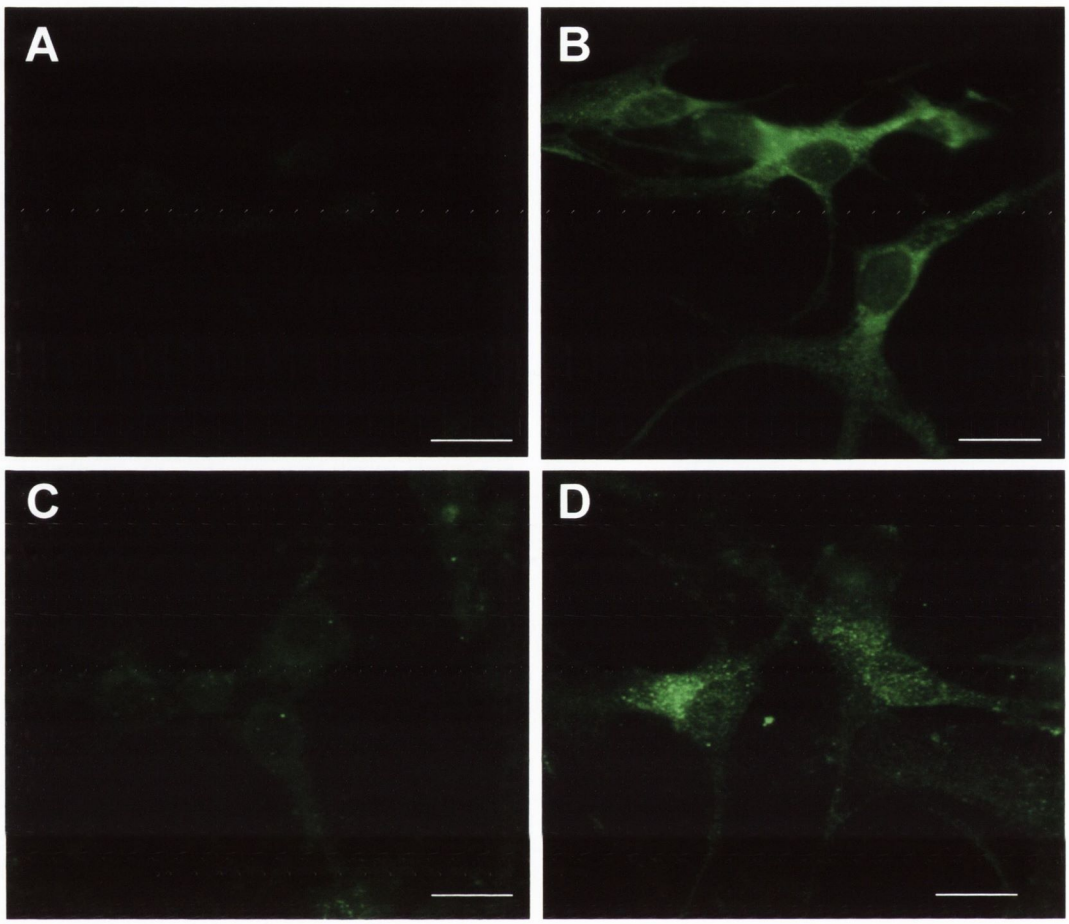


**Figure 5.1 $A\beta_{1-40}$ increases Syk expression in neuronal cells**

Fluorescence microscopy was used to visualise the distribution of Syk within cortical neurons following treatment with $A\beta_{1-40}$ (2μM) for 30 min and 2 hr. Analysis of Syk expression in (A) control (B) $A\beta_{1-40}$-treated (30 min) (C) control and (D) $A\beta_{1-40}$-treated (2 hr) cells demonstrated increased expression of Syk in $A\beta_{1-40}$-treated cells. Scale bar is 20 μm.

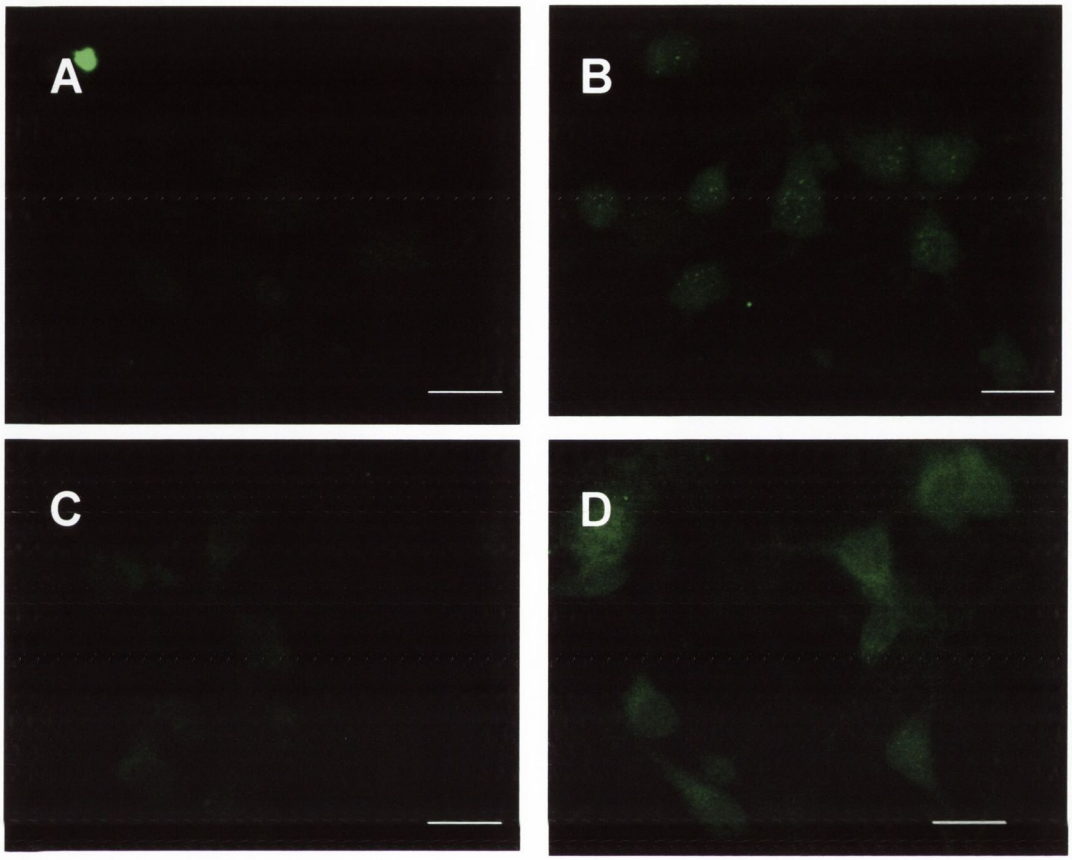


**Figure 5.2 $A\beta_{1-40}$ increases phospho-Syk expression in neuronal cells**

Fluorescence microscopy was used to visualise the distribution of phospho-Syk within cortical neurons following treatment with $A\beta_{1-40}$ (2μM) for 30 min and 2 hr. Analysis of phospho-Syk expression in (A) control (B) $A\beta_{1-40}$-treated (30 min) (C) control and (D) $A\beta_{1-40}$-treated (2 hr) demonstrated increased expression of phospho-Syk in $A\beta_{1-40}$-treated cells. Scale bar is 20 μm.

phospho-Syk immunoreactivity was detected within the cytosol (Figure 5.2 A and C), reflecting a basal level of phospho-Syk expression at 30 min or 2 hr, respectively. However, in cells treated with $A\beta_{1-40}$ (2μM) for 30 min or 2 hr (Figure 5.2 B and D), a higher intensity of phospho-Syk immunoreactivity was observed within the cytosol. This result demonstrates the $A\beta_{1-40}$ induces Syk phosphorylation in cultured cortical neurons.

## 5.3 Time course of $A\beta_{1-40}$-induced activation of Syk

To further confirm Syk expression in neuronal cells, and to quantify the effect of $A\beta_{1-40}$ on Syk expression, western immunoblot analysis was performed on cortical neurons exposed to $A\beta_{1-40}$ (2μM) over a range of time-points from 30 min to 6 hr. Results are expressed as % of phospho-Syk expression over total Syk (pSyk/tSyk) expression. Analysis of mean densitometric data (Figure 5.3 A) demonstrates that $A\beta_{1-40}$ evoked a significant increase in Syk activity at all timepoints. Exposure of $A\beta_{1-40}$ to cultures for 30 min produced a significant increase in pSyk/tSyk from a value of 0.39 ± 0.21 (mean band width ± SEM; arbitrary units) in control cells to 0.84 ± 0.21 in $A\beta_{1-40}$-treated cells ($p<0.01$, ANOVA, n=6). Similarly, pSyk/tSyk expression at 2 hr was 0.41 ± 0.18 in untreated cells and this was significantly increased to 0.96 ± 0.12 by $A\beta_{1-40}$ ($p<0.001$, ANOVA, n=6). At the 6 hr time-point pSyk/tSyk expression was 0.51 ± 0.43 in control cells and this was significanlty increased to 1.29 ± 0.41 ($p<0.001$, ANOVA, n=6) following $A\beta_{1-40}$ treatment for 6 hr. Figure 5.3 B shows a sample western blot showing phospho- and total Syk expression.

**A.**

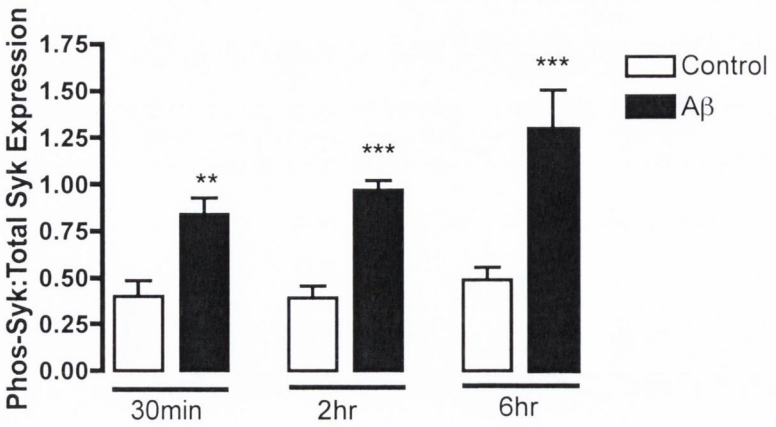


**B.**

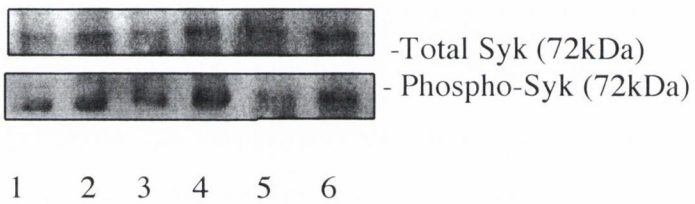


**Figure 5.3 Time course of $A\beta_{1-40}$-induced increase in Syk phosphorylation**

A. Cultured cortical neurons were exposed to $A\beta_{1-40}$ (2μM) for 30min, 2 hr and 6 hr. Cells were harvested and analysed for Syk using western immunoblot. A significant increase in phospho-Syk expression, expressed as a ratio of total-Syk expression was found following treatment with $A\beta_{1-40}$ at 30 min, 2 hr and 6 hr timepoints. Results are expressed as the mean ± SEM for 3 observations, **p<0.01, ***p<0.001, ANOVA.

B. Sample western blot showing phospho-Syk and total Syk expression in control cells (30 min, lane 1); $A\beta_{1-40}$-treated cells (30 min, lane 2); control (2 hr, lane 3); $A\beta_{1-40}$-treated cells (2 hr, lane 4); control (6 hr, lane 5); $A\beta_{1-40}$-treated cells (6 hr, lane 6).

## 5.4 $A\beta_{1-40}$-induced activation of caspase-3 is mediated by Syk

The downstream consequences of Syk activation in neurons are as yet unclear. Some evidence has suggested that Syk activation could potentially lead to the commitment of a cell to the apoptotic pathway (Arndt *et al.*, 2004). Caspase-3 is a key executioner of apoptosis and is cleaved following treatment with $A\beta_{1-40}$ (2μM; 24 hr) (Boland & Campbell, 2003). The ability of Syk to impact on Aβ-induced caspase-3 activation was assessed by measuring cleavage of a fluorogenic caspase-3 peptide, DEVD, to its fluorescent product following $A\beta_{1-40}$ exposure (Figure 5.4). Figure 5.4 demonstrates that $A\beta_{1-40}$ increased activity of caspase-3 from 20.66 ± 4.35 nmol AFC produced/mgprotein/min (mean ± SEM) to 35.76 ± 8.34 pmol AFC produced/mgprotein/min ($p<0.05$, ANOVA, n=4). The Syk inhibitor (50nM) alone, which is cell permeable and efficiently blocks phosphorylation of Syk substrates (Lai *et al.*, 2003), had no effect on caspase-3 activity (17.90 ± 5.81 nmole AFC produced/mgprotein/min, n=6), but it abolished the $A\beta_{1-40}$-mediated increase in caspase-3 activity, where caspase-3 activity was 18.63 ± 7.26 (nmol AFC produced/mgprotein/min, n=6) in cells which were pre-treated with $A\beta_{1-40}$ + Syk inhibitor. A DMSO control was included since the Syk inhibitor was made up in DMSO, but it had no effect on caspase-3 activity 11.86 ± 11.53 (nmol AFC produced/mgprotein/min, n=6). This result provides evidence that Syk is involved in coupling $A\beta_{1-40}$ to induction of caspase-3 in cultured cortical neurons.

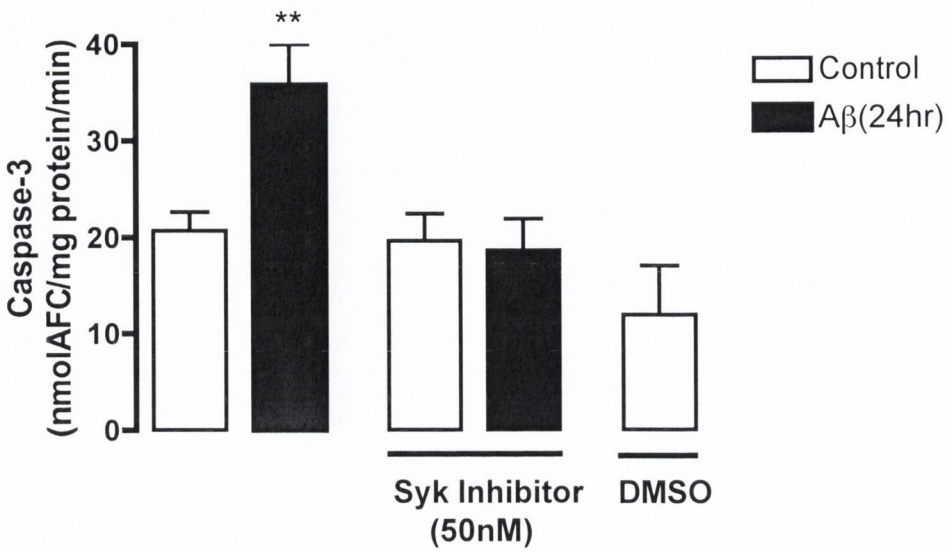


**Figure 5.4 $A\beta_{1-40}$-induced activation of caspase-3 is mediated by Syk**

Cultured cortical neurons were treated with $A\beta_{1-40}$ (2μM; 24hr) and caspase-3 activity was assessed by the measuring cleavage of the fluorogenic DEVD substrate. Treatment of cells with $A\beta_{1-40}$ for 24 hr increased caspase-3 activity compared to vehicle-treated cells. The stimulatory effect of $A\beta_{1-40}$ on caspase-3 activity was prevented by the Syk inhibitor (50nM), indicating the involvement of Syk. Exposure of cells to the Syk inhibitor alone and DMSO alone had no effect on caspase-3 activity. Results are expressed as the mean ± SEM for 5 observations, **$p<0.01$, ANOVA.

## 5.5 $A\beta_{1-40}$-mediated DNA fragmentation is Syk dependent

To further demonstrate a role for Syk in $A\beta_{1-40}$-mediated neuronal apoptosis, levels of DNA fragmentation were assessed in cells which were pre-treated with the Syk inhibitor (50nM) for 1 hr, prior to treatment with $A\beta_{1-40}$ (2μM) for 48 hr (Figure 5.5). TUNEL analysis was carried out to measure the percentage of cells displaying fragmented DNA. DNA cleavage into oligonucleosomal fragments is a distinguishing feature of apoptosis (Lee, 1993) that can readily be detected using the colorimetric TUNEL system. Exposure of neurons to $A\beta_{1-40}$ significantly increased the percentage of TUNEL positive cells from 7.74 ± 2.42 % (mean ± SEM) to 20.80 ± 4.99 % ($p<0.001$, ANOVA, n=6). The percentage of TUNEL positive cells was 9.33 ± 3.90 % in the presence of the Syk inhibitor (50nM) alone (n=6) and the $A\beta_{1-40}$-mediated increase in the percentage of TUNEL positive cells was significantly reduced to 8.96 ± 4.90 % in cells co-treated with $A\beta_{1-40}$ + Syk inhibitor ($p<0.001$, ANOVA, n=6). The percentage of TUNEL positive cells was 7.02 ± 1.43 % in the presence of DMSO alone (n=6). This result demonstrates the involvement of Syk in the $A\beta_{1-40}$-mediated induction of DNA fragmentation in cortical neurons. A sample photo demonstrating the apoptotic effect of $A\beta_{1-40}$ in cultured cortical cells ar 48 hr is shown in Figure 5.5 B.

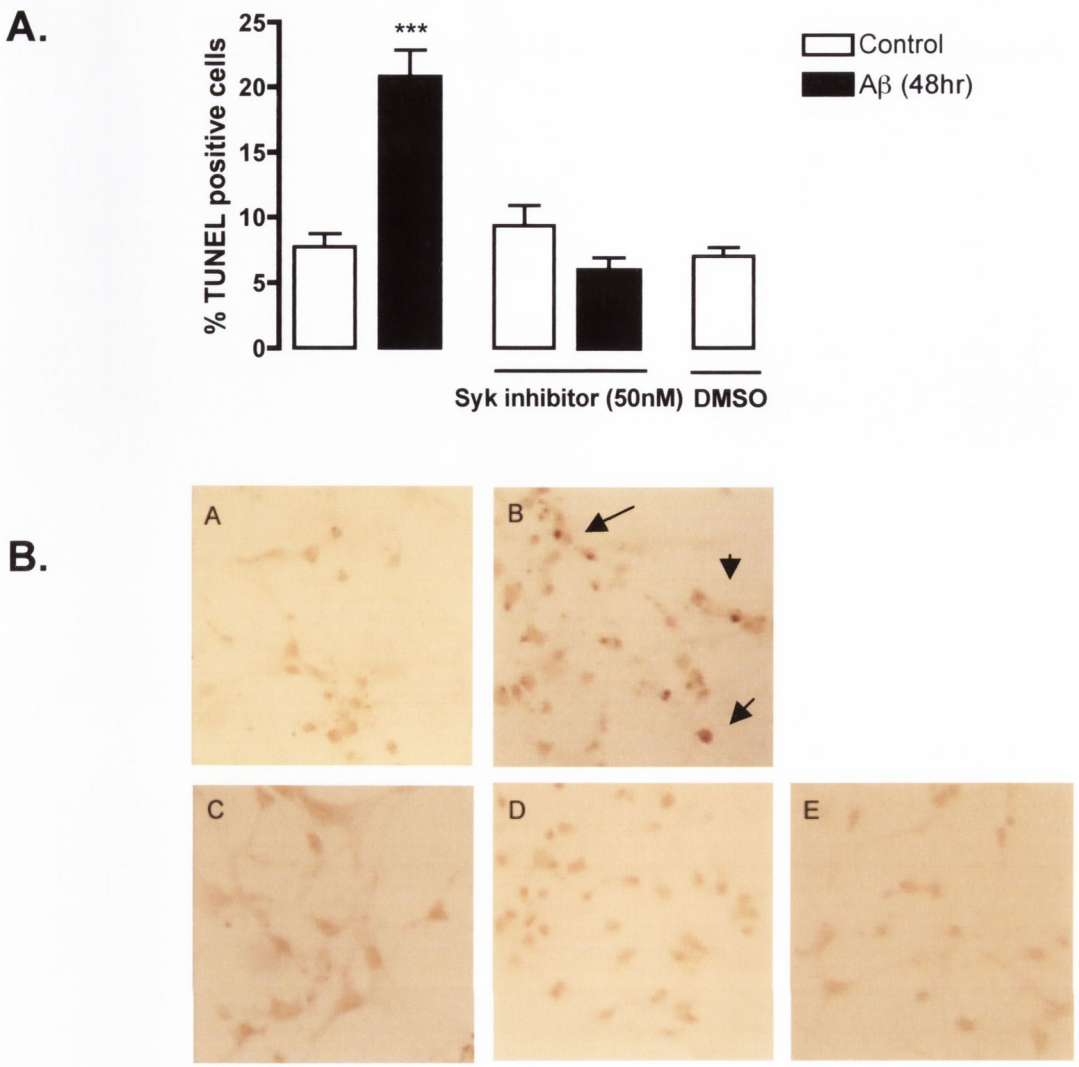


**Figure 5.5 $A\beta_{1-40}$-mediated DNA fragmentation is Syk dependent**

A. Cultured cortical neurons were treated with $A\beta_{1-40}$ (2μM) in the presence or absence of Syk inhibitor (50nM) for 48 hr and DNA fragmentation was assessed using TUNEL analysis. $A\beta_{1-40}$ significantly increased DNA fragmentation at 48 hr. In the presence of Syk inhibitor, the $A\beta_{1-40}$-induced increase in DNA fragmentation was abolished. DMSO had no effect on DNA fragmentation. Results are expressed as the mean ± SEM for 6 independent observations, *** $p<0.001$.

B. Representative image of cortical neurons stained for DNA fragmentation. Arrows indicate TUNEL positive cells following exposure to (A) vehicle control (B) $A\beta_{1-40}$ (C) Syk inhibitor (D) $A\beta_{1-40}$ + Syk inhibitor and (E) DMSO control. Scale is 10X.

## 5.6 $A\beta_{1-40}$-mediated increase in cathepsin-L activity is Syk dependent

To further characterise a role for Syk in cultured cortical neurons, the ability of Syk to impact on the lysosomal system was investigated. Since it had been previously demonstrated in our laboratory that $A\beta_{1-40}$ significantly increases cathepsin-L activity within 6 hr of treatment (Boland & Campbell, 2004), cathepsin-L activity was assessed in cells pre-treated with the Syk-inhibitor. Cells were treated with Syk inhibitor (50nM) for 1 hr, prior to treatment with $A\beta_{1-40}$ (2$\mu$M) for 6 hr and activity of cathepsin-L was assessed by measuring cleavage of a fluorogenic cathepsin-L substrate. Figure 5.6 demonstrates that $A\beta_{1-40}$ significantly increased activity of cytosolic cathepsin-L from 3.80 ± 0.79 pmolAFCproduced/mg protein/min (mean ± SEM) to 13.76 ± 1.67 pmolAFCproduced/mg protein/min ($p<0.001$, ANOVA, n=6). Syk inhibitor alone had no effect on cathepsin-L activity (5.42 ± 1.34 pmole AFC produced/mg protein/min, n=6), but it abolished the $A\beta_{1-40}$-mediated increase in cathepsin-L activity, where cathepsin-L activity was 6.09 ± 1.04 (n=5) in cells which were co-incubated with $A\beta_{1-40}$ + Syk inhibitor. This result provides evidence that $A\beta_{1-40}$-mediated lysosomal disruption is dependent on Syk.

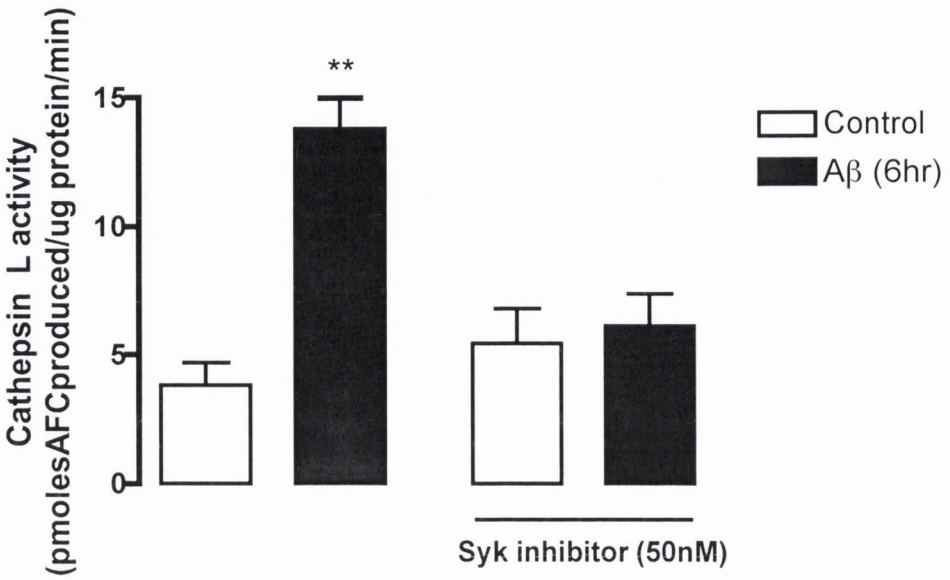


**Figure 5.6 $A\beta_{1-40}$-mediated increase in cathepsin-L activity is Syk-dependent**

Cortical neurons were treated with $A\beta_{1-40}$ (2μM) in the presence or absence of Syk inhibitor (50nM) for 6 hr and cathepsin-L activity was measured using the fluorogenic substrate Arg-Phe-AFC. $A\beta_{1-40}$ significantly increased cathepsin-L activity at 6 hr. In the presence of Syk inhibitor, the $A\beta_{1-40}$-mediated increase in cathepsin-L activity was significantly reduced. Results are expressed as mean ± SEM for 6 observations, **$p<0.01$.

## 5.7 Phospho-Syk localises with lysosomes following $A\beta_{1-40}$ exposure

As the previous result suggested an involvement of Syk with the lysosomal system, this study examined whether Syk associates with lysosomes following exposure of cells to $A\beta_{1-40}$. Confocal microscopy was used to visualise Phospho-Syk expression in cortical neurons and the lysosomal specific marker, Lysotracker red was used to visualised distribution of lysosomes (Figure 5.7). Cells were exposed to $A\beta_{1-40}$ (2μM) for 2 hr prior to a 30 min incubation with Lysotracker red (1mM). Figure 5.7 (A) represents Phospho-Syk immunostaining in control cells and this immunofluorescence was increased in $A\beta_{1-40}$-treated cells (B). Distribution of lysosomes in cultured cells are shown in control (C) and $A\beta_{1-40}$-treated cells (D). Colocalisation analysis of Phospho-Syk with lysosomes are represented in control (E) and association of Phospho-Syk with lysosomes was increased in $A\beta_{1-40}$-treated cells (F). This finding provides further evidence the Syk has a role to play in modulating the lysosomal sytem.

## 5.8 p53 does not modulate association of Phospho-Syk with lysosomes induced by $A\beta_{1-40}$

The p53 inhibitor, pifithrin-α (100nM), was pre-incubated with cultures for 60 min to determine if p53 played a role in $A\beta_{1-40}$-induced localisation of Phospho-Syk to lysosomes, as demonstrated in the previous result (Figure 5.7). Confocal microscopy was used to visualised Phospho-Syk expression in cortical neurons and the lysosomal specific marker, Lysotracker red was used to visualised distribution of lysosomes (Figure 5.8). Phospho-Syk immunostaining is represented in control cells (Figure 5.8 A), $A\beta_{1-40}$-treated cells (B), pifithrin-α-treated cells (C) and $A\beta_{1-40}$ + pifithrin-α-treated cells (D). Distribution of lysosomes in cultured cells are shown in control (E), $A\beta_{1-40}$-treated cells (F), pifithrin-α-treated cells (G) and $A\beta_{1-40}$ + pifithrin-α-treated cells (H). Similarly, exposure of $A\beta_{1-40}$ (2μM) for 2 hr promotes the association of Phospho-Syk with lysosomes (J). Treatment with pifithrin-α alone had no

effect on Phospho-Syk co-localisation (K). Cells exposed to $A\beta_{1-40}$ + pifithrin-$\alpha$ continued to show association of Phospho-Syk and lysosomes (L). This finding indicates that p53 is not involved in the $A\beta_{1-40}$-induced association of Phospho-Syk with lysosomes.

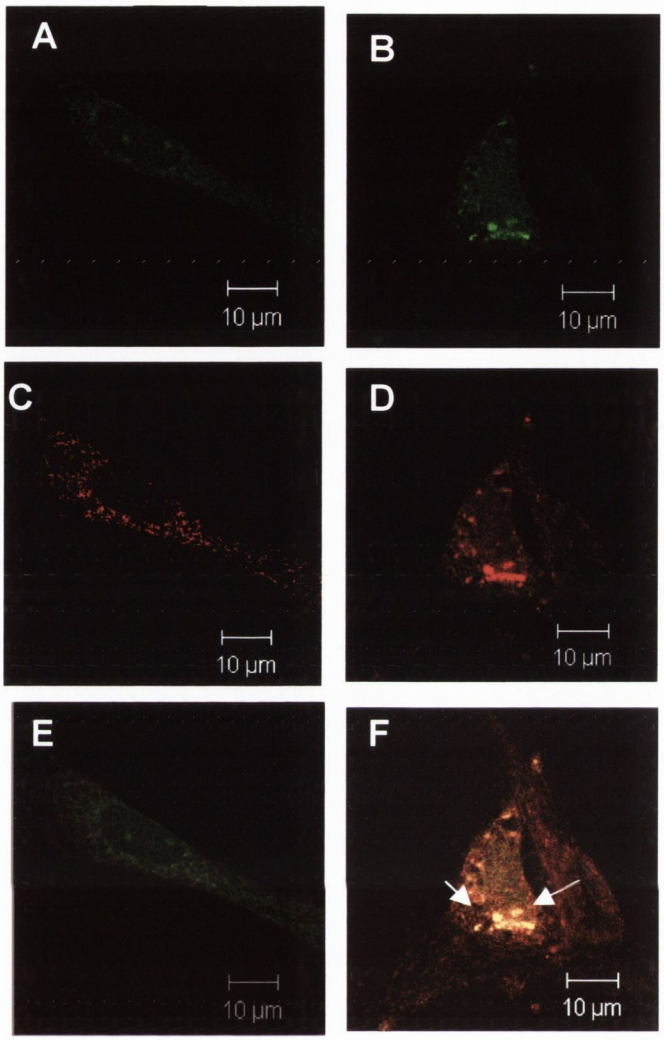


**Figure 5.7 $A\beta_{1-40}$-induces localisation of Phospho-Syk to lysosomes in cortical neurons at 2 hr**

Cells were double labelled with the lysosomal specific agent, Lysotracker red, and a Alexa-labelled Phospho-Syk antibody. Analysis of Phospho-Syk expression in control (A) and $A\beta_{1-40}$-treated cells (B), Lysotracker red staining representing the distribution of lysosomes in control (C) and $A\beta_{1-40}$-treated cells (D) and co-localisation analysis of Phospho-Syk and lysosomes in control (E) and $A\beta_{1-40}$-treated (F).The Syk protein was localised throughout the cytoplasm and nucleus and localised to lysosomes following $A\beta_{1-40}$ treatment. Arrows indicate cells displaying co-localisation. Scale 10µm.

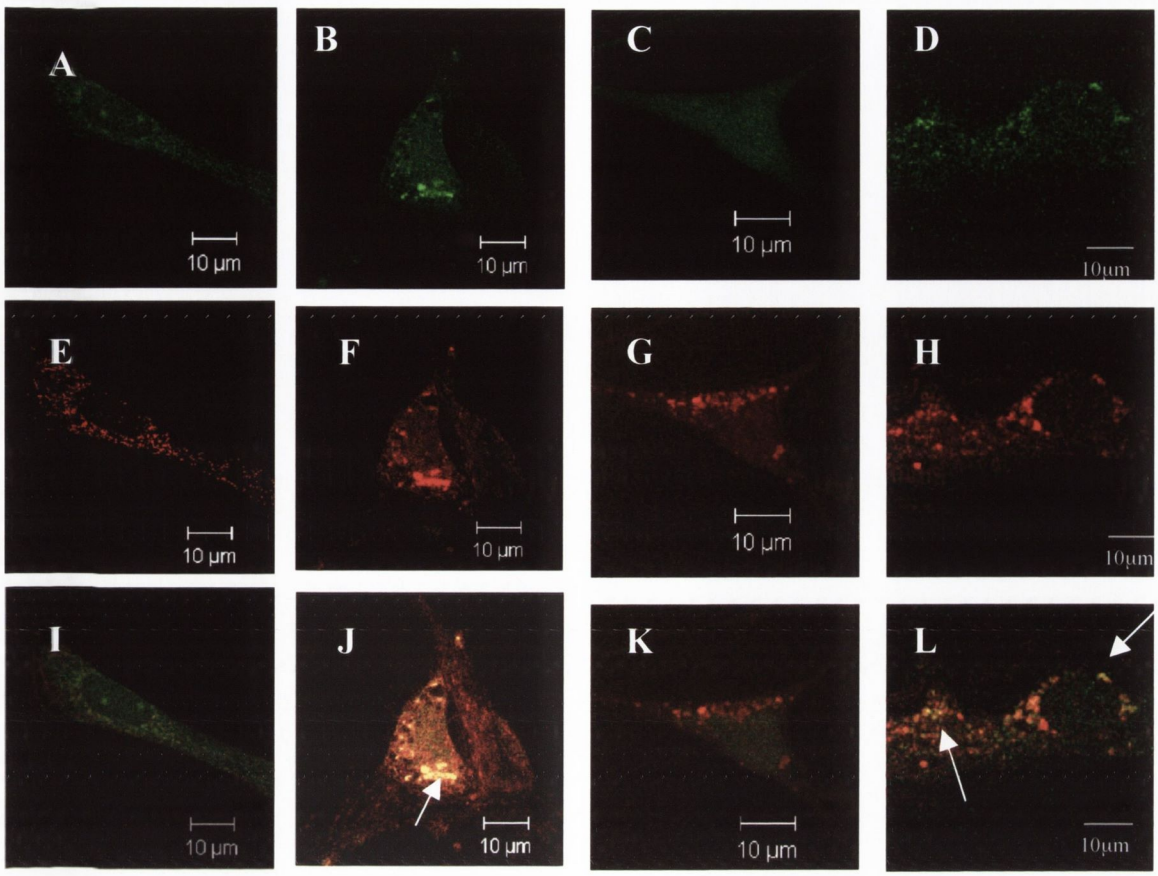


**Figure 5.8 The $A\beta_{1-40}$-induced association of phospho-Syk at lysosomes is p53-independent at 2 hr**

Cells were double labeled with the lysosomal specific agent, Lysotracker red, and a Alexa-labelled Phospho-Syk antibody. Analysis of Phospho-Syk expression in (A) control cells, (B) $A\beta_{1-40}$-treated cells, (C) pifithrin-$\alpha$-treated cells, and (D) $A\beta_{1-40}$ + pifithrin-$\alpha$-treated cells (excitation 579 nm; emission, 599nm). Lysotracker red staining represents the distribution of lysosomes in (E) control cells, (F) $A\beta_{1-40}$-treated cells, (G) pifithrin-$\alpha$ treated cells and (H) $A\beta_{1-40}$ + pifithrin-$\alpha$-treated cells (excitation 579 nm; emission, 599nm). Co-localisation of Phospho-Syk expression with lysosomes is shown in (J) $A\beta_{1-40}$-treated cells, where $A\beta_{1-40}$-induces association of Phospho-Syk with lysosomes. Treatment with $A\beta_{1-40}$ + pifithrin-$\alpha$ (L) did not abolish the $A\beta_{1-40}$-induced association. Arrows indicate cells displaying co-localisation. Scale bar 10$\mu$m.

## 5.9 Determination of the involvement of Syk on the stability of lysosomal membrane integrity

Changes in lysosomal permeability were evaluated by the translocation of AO out of lysosomes. This weakly basic dye accumulates within acidic compartments (lysosomes) due to protonation at low pH. At high concentrations it exists in a stacked form that emits red fluorescence (633nm) when excited by blue light. The intensity of red fluorescence is reflective of the lysosomal concentration of AO, which decreases in acridine orange-loaded cells upon lysosomal rupture or deprotonation of AO during impairment of the proton gradient. We determined the ability of Syk pretreatment to influence the lysosomal partitioning of AO.

Confocal laser microscopy was used to assess relocation of AO from lysosomes following treatment with $A\beta_{1-40}$ (2μM) for 1 hr. In Figure 5.9 cortical neurons were treated with AO (5μg/ml) for 15 min prior to incubation with $A\beta_{1-40}$ for 1 hr. Neurons were also pre-treated with Syk inhibitor (50nM) prior to $A\beta_{1-40}$ exposure to determine if the effect of $A\beta_{1-40}$ on lysosomal membrane integrity was mediated via Syk. At 1 hr, (Figure 5.9A) AO displayed a granular orange fluorescence and was localised in discrete punctate compartments within the cell, suggesting lysosomal distribution of AO in control cells. Exposure to $A\beta_{1-40}$ for 1 hr (Figure 5.9B) had no effect on the distribution of AO Pre-treatment with Syk inhibitor alone Figure 5.9 (C) or $A\beta_{1-40}$ in the presence of Syk inhibitor Figure 5.9 (D) had no effect on AO and yielded comparable staining to controls.

Lysosomal membrane integrity was also monitored by measuring pixel intensity at 633nm, the emission wavelength AO emits when it accumulates in lysosomes. Figure 5.10A demonstrates the mean pixel intensity at 633nm; there is no difference in mean pixel intensity following treatment of $A\beta_{1-40}$ at 1 hr, where control is 578.77 ± 70.42 and neurons treated with $A\beta_{1-40}$ is 459.30 ± 81.63 ($P>0.05$, ANOVA, n=4). Pre-treatment with Syk inhibitor alone (555.75 ± 44.55) or $A\beta_{1-40}$ in the presence of Syk inhibitor 525.58 ± 40.14 ($P>0.05$, ANOVA, n=4), had comparable levels of pixel intensity to controls.

In addition, intact lysosomes were counted by visual inspection (Figure 5.10B). There is no change in the number of intact lysosomes counted at this timepoint; control 64.28 ± 6.17 (mean ± S.E.M.) and $A\beta_{1-40}$-treated cells 56.50 ± 6.25 ($P>0.05$, ANOVA, n=4). Neurons treated with Syk inhibitor alone (69.75 ± 4.25) and $A\beta_{1-40}$ in the presence of Syk inhibitor (61.00 ± 5.33) for 1 hr had comparable numbers of intact lysosomes to control. This demonstrates that $A\beta_{1-40}$ does not compromise the lysosomal membrane at 1 hr.

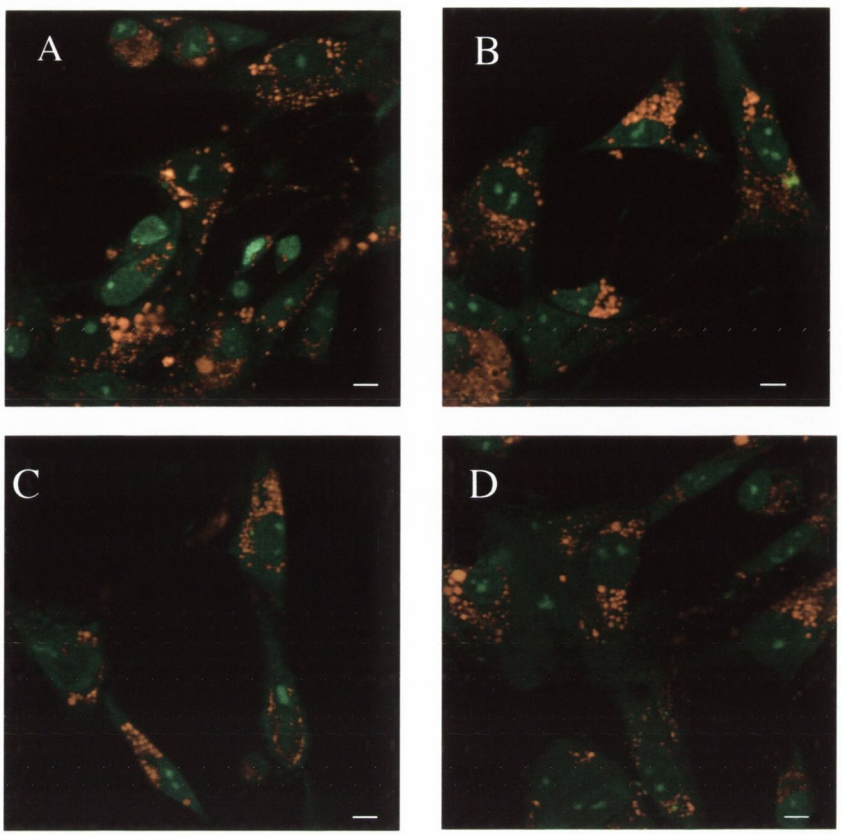


**Figure 5.9 $A\beta_{1-40}$ does not mediate alterations in lysosomal membrane integrity at 1 hr**

Neurons were exposed to AO (5ug/ml) for 15 min prior to incubation with Syk inhibitor (50nM) in the presence or absence of $A\beta_{1-40}$ (2μM) for 1 hr. Relocation of AO from the lysosomes to cytosol was assessed. In control cells (A) AO displayed an orange fluorescence and was localised in discrete punctate compartments within the cell reflecting lysosomal distribution of AO. Exposure to $A\beta_{1-40}$ for 1 hr (B) had no effect on the fluorescence emitted by AO, indicating that the lysosomes remained intact. Treatment with Syk inhibitor alone (C) had no effect on AO fluorescence. Co-incubation with $A\beta_{1-40}$ + Syk inhibitor (D) resulted in AO displaying an orange fluorescence. Scale bar is 10μm.

A

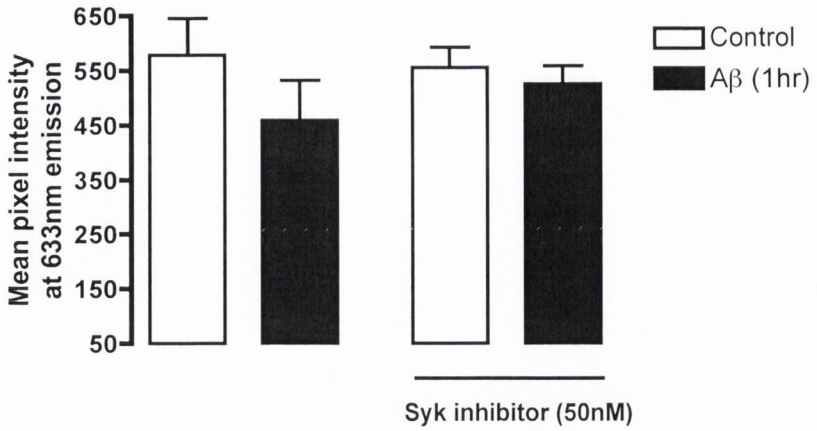


B

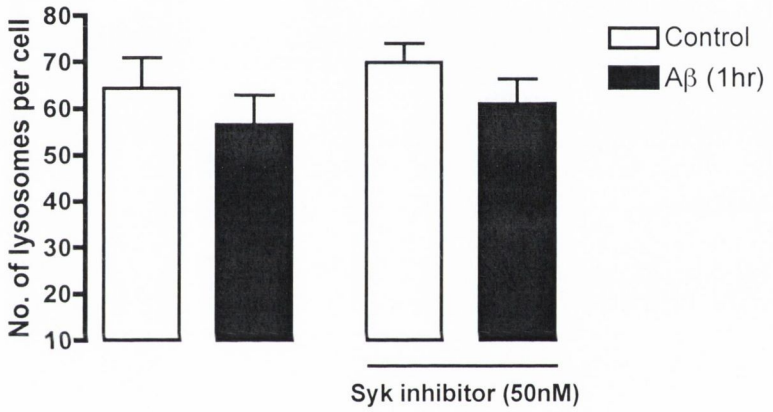


**Figure 5.10 $A\beta_{1-40}$ and Syk inhibitor have no effect on lysosomal membrane integrity at 1 hr**

A. Intact lysosomes accumulate AO and emit at fluorescence 633nm. By measuring the intensity of pixels at this wavelength we can monitor disruption of the lysosomal membrane due to leakage of the probe. Neither $A\beta_{1-40}$ (2μM) or Syk inhibitor (50nM) had no effect on mean pixel intensity at 1 hr.

B. The number of intact lysosomes per cell were counted. Treatment with $A\beta_{1-40}$ (2μM) for 1 hr or the Syk inhibitor (50nM) had no effect on the number of lysosomes counted. Results are expressed as mean ± SEM of 6 independent observations.

## 5.10 $A\beta_{1-40}$-induced modulation of lysosomal membrane integrity is Syk-dependent at 6 hr

The role of Syk in destabilisation of lysosomal membrane integrity was assessed using the AO technique. Exposure of cells to $A\beta_{1-40}$ (2μM) for 6 hr (Figure 5.11B) resulted in increased diffuse green fluorescence and a reduction in orange punctate staining. Furthermore, mean pixel intensity at 633nm decreased significantly following $A\beta_{1-40}$ treatment at 6 hr (Figure 5.12 A), from 524.71 ± 54.34 (mean ± S.E.M.) to 313 ± 16.36 ($P<0.05$, ANOVA, n=4). There is also a reduction in the number of intact lysosomes counted manually. The number of lysosomes in control cells at 6 hr (Figure 5.12 B), was 85.83 ± 7.16 (mean ± S.E.M.) and this decreased to 17.70 ± 5.21 ($P<0.001$, ANOVA, n=4) in cells treated with $A\beta_{1-40}$. These results suggest leakage of the dye from the lysosomal compartment, possibly as a result of a disruption in lysosomal integrity and a loss of lysosomal acidification.

Neurons were also pre-treated with Syk inhibitor (50nM) prior to $A\beta_{1-40}$ exposure to determine if the effect of $A\beta_{1-40}$ on lysosomal membrane integrity was mediated via Syk. Cells treated with Syk inhibitor alone or $A\beta_{1-40}$ in the presence of Syk inhibitor (Figure 5.11C and D) for 6 hr resulted in punctate orange fluorescence suggesting AO remained within the lysosomal compartment. Thus, in Figure 5.12A, mean pixel intensity at fluorescence 633nm in cells treated with Syk inhibitor alone was 600.71 ± 55.60 (mean ± S.E.M.) and 541.50 ± 63.18 ($P<0.001$, ANOVA, n=4) in cells treated with $A\beta_{1-40}$ + Syk inhibitor for 6 hr. Furthermore, treatment with Syk inhibitor (Figure 5.12B) prevented the $A\beta_{1-40}$-mediated decrease in number of intact lysosomes; where lysosomal number was (74.00 ± 9.48) (n-4) in cells treated with Syk inhibitor alone and (82.83 ± 5.36) in cells treated with $A\beta_{1-40}$ in the presence of Syk inhibitor at 6 hr. Therefore, the $A\beta_{1-40}$-induced disruption of the lysosomal membrane is Syk-sensitive at 6 hr.

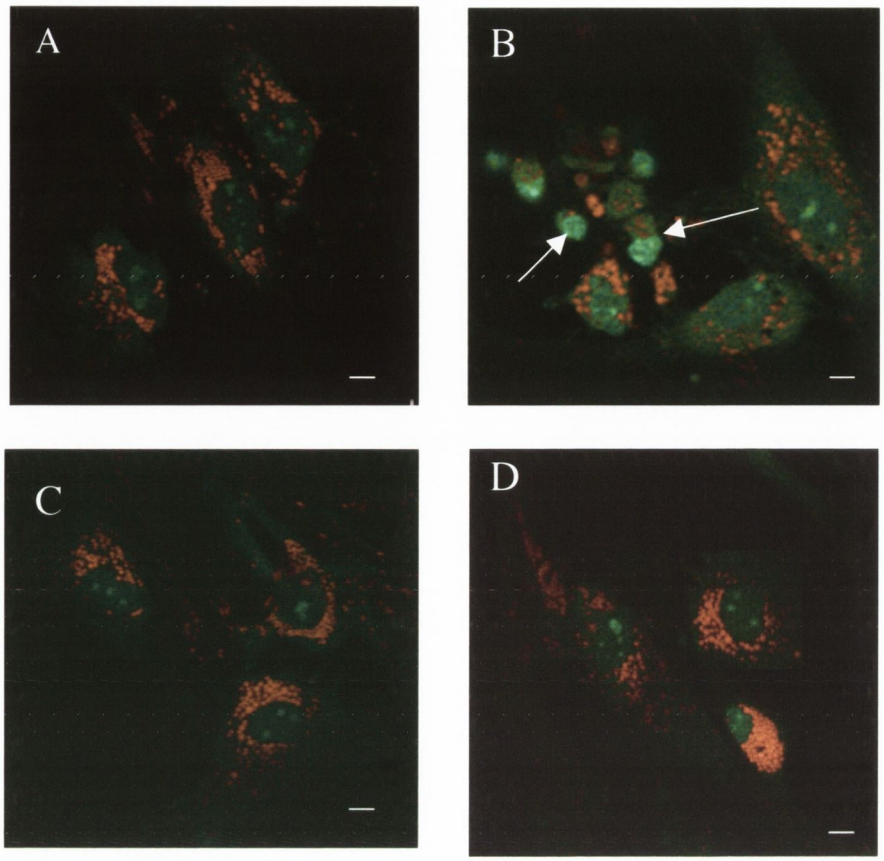


**Figure 5.11 $A\beta_{1-40}$-mediated alteration in lysosomal membrane integrity is Syk dependent at 6 hr**

Neurons were exposed to AO (5ug/ml) for 15 min prior to incubation with Syk inhibitor (50nM) in the presence or absence of $A\beta_{1-40}$ (2μM) for 6 hr. Relocation of AO from lysosomes to cytosol was assessed. In control cells (A) AO displayed an orange fluorescence and was localised in discrete punctate compartments within the cell reflecting lysosomal distribution of AO. Exposure to $A\beta_{1-40}$ for 6 hr (B) resulted in the reduction of AO orange fluorescence and in increase in diffuse cytosolic green fluorescence. Treatment with Syk inhibitor alone (C) had no effect on AO fluorescence. Co-incubation with $A\beta_{1-40}$ + Syk inhibitor (D) resulted in AO displaying an orange fluorescence similar to control cells. Arrows indicate cells displaying destabilisation. Scale bar is 10μm.

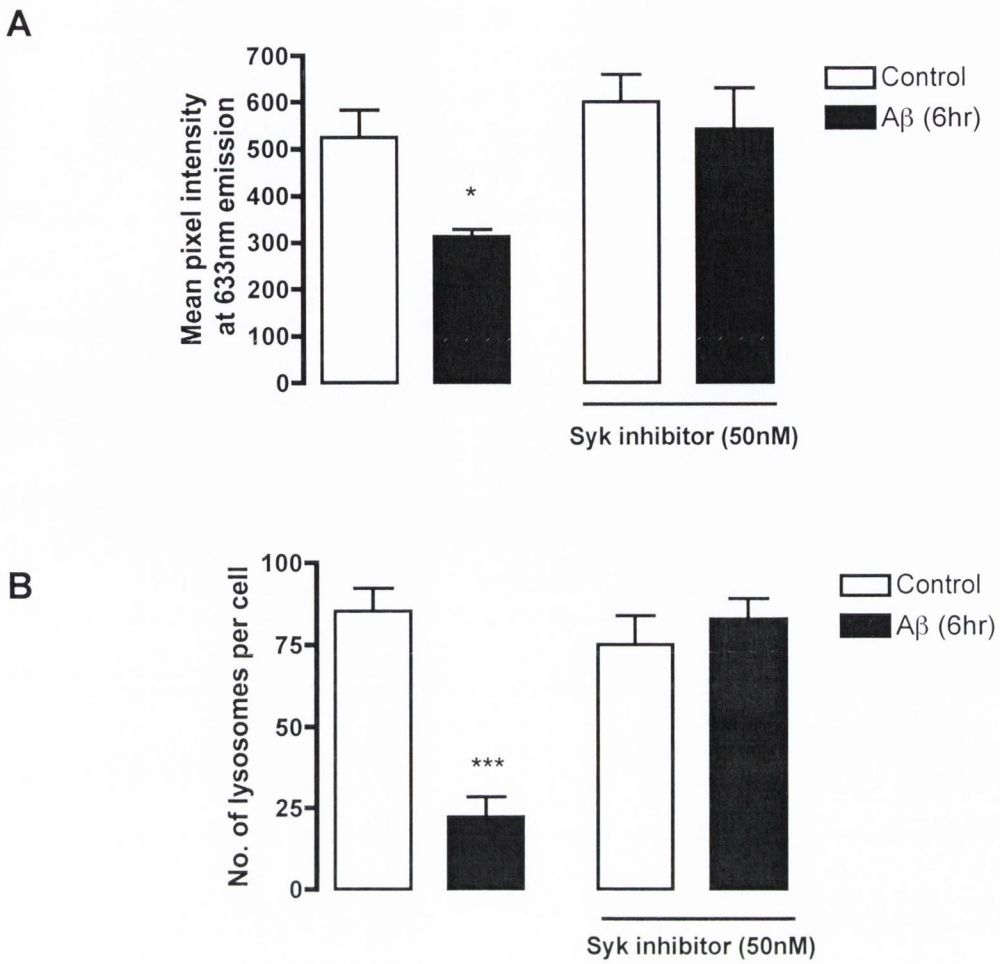


**Figure 5.12 The $A\beta_{1-40}$-mediated destabilisation of lysosomes at 6 hr is Syk-dependent**

A. Intact lysosomes accumulate AO and emit at fluorescence 633nm. By measuring the intensity of pixels at this wavelength we can monitor disruption of the lysosomal membrane due to leakage of the probe. $A\beta_{1-40}$ (2μM) reduces the mean pixel intensity at 6 hr and pre-treatment with Syk inhibitor (50nM) abolished the $A\beta_{1-40}$-induced reduction in mean pixel intensity (*$p<0.05$, ANOVA, n=4)

B. The number of intact lysosomes per cell were counted. Treatment with $A\beta_{1-40}$ (2μM) for 6 hr caused a reduction in the number of lysosomes observed. Pre-treatment with Syk inhibitor (50nM) abolished the $A\beta_{1-40}$-induced reduction in lysosomal number (***$p<0.001$, ANOVA, n=4).

## 5.11 Lysosomal destabilisation induced by $A\beta_{1-40}$ is reliant on Syk at 24 hr

To determine the contribution of Syk in $A\beta_{1-40}$-mediated destabilisation of the lysosomal membrane, the AO technique was used. Exposure of cells to $A\beta_{1-40}$ (2$\mu$M) for 24 hr (Figure 5.13 B) resulted in increased diffuse green fluorescence and a reduction in orange punctate staining. Furthermore, mean pixel intensity at 633nm decreased significantly following $A\beta_{1-40}$ treatment at 24 hr (Figure 5.14A) from 481.81 ± 47.90 (mean ± S.E.M.) to 285.30 ± 19.16 ($P<0.05$, ANOVA, n=4). There was also a reduction in the number of intact lysosomes counted manually. The number of lysosomes in control cells at 24 hr (Figure 5.14B), was 74.37 ± 8.80 (mean ± S.E.M.) and this decreased to 23.00 ± 3.24 ($P<0.001$, ANOVA, n=4) in cells treated with $A\beta_{1-40}$. These results suggest leakage of the dye from the lysosomal compartment, possibly as a result of disruption in lysosomal integrity and a loss of lysosomal acidification.

Neurons were also pre-treated with Syk inhibitor (50nM) prior to $A\beta_{1-40}$ exposure to determine if the effect of $A\beta_{1-40}$ on lysosomal membrane integrity was mediated via Syk. Cells treated with Syk inhibitor alone or $A\beta_{1-40}$ in the presence of Syk inhibitor for 24 hr (Figure 5.13C and D) resulted in punctate orange fluorescence suggesting AO remained within the lysosomal compartment. Thus, in Figure 5.14A, mean pixel intensity at fluorescence 633nm in cells treated with Syk inhibitor alone was 459.00 ± 49.51 (mean ± S.E.M.) and 531.83 ± 79.44 ($P<0.001$, ANOVA, n=4) in cells treated with $A\beta_{1-40}$ + Syk inhibitor for 24 hr Furthermore, in Figure 5.14B treatment with Syk inhibitor prevented the $A\beta_{1-40}$-mediated decrease in number of intact lysosomes; where lysosomal number was (68.60 ± 9.64) (n=4) in cells treated with Syk inhibitor alone and (96.27 ± 10.31) in cells treated with $A\beta_{1-40}$ in the presence of Syk inhibitor at 24 hr Therefore, the $A\beta_{1-40}$-induced disruption of the lysosomal membrane is Syk-sensitive at 24 hr.

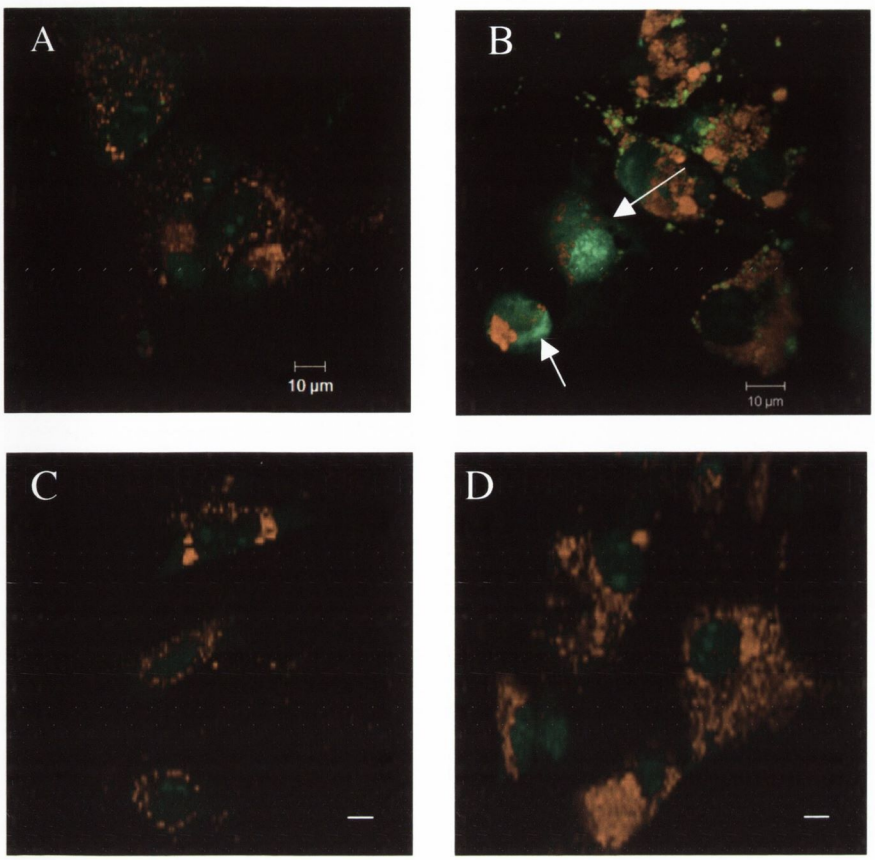


**Figure 5.13 The $A\beta_{1-40}$-mediated destabilisation of lysosomes at 24 hr is Syk-dependent**

Neurons were exposed to AO (5ug/ml) for 15 min prior to incubation with Syk inhibitor (50nM) in the presence or absence of $A\beta_{1-40}$ (2μM) for 24 hr. Relocation of AO from the lysosomes to cytosol was assessed. In control cells (A) AO displayed an orange fluorescence and was localised in discrete punctate compartments within the cell reflecting lysosomal distribution of AO. Exposure to $A\beta_{1-40}$ for 24 hr (B) resulted in the reduction of AO orange fluorescence and in increase in diffuse cytosolic green fluorescence. Treatment with Syk inhibitor alone (C) had no effect on AO fluorescence. Co-incubation with $A\beta_{1-40}$ + Syk inhibitor (D) resulted in AO displaying an orange fluorescence similar to that observed in control cells. Arrows indicate cells displaying destabilisation. Scale bar is 10μm.

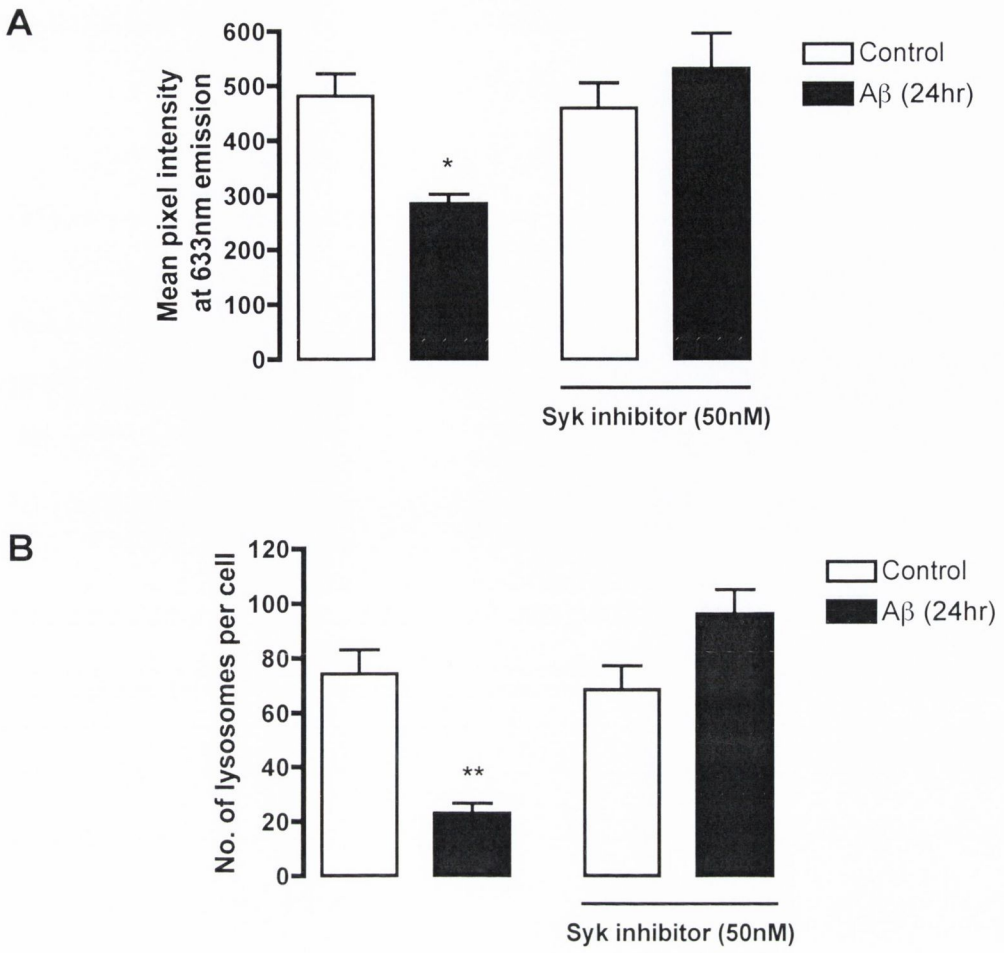


**Figure 5.14 The $A\beta_{1-40}$-mediated impact on lysosomal membrane integrity at 24 hr is Syk-dependent**

A. Intact lysosomes accumulate AO and emit at 633nm. By measuring the intensity of pixels at this wavelength we can monitor disruption of the lysosomal membrane due to leakage of the probe. $A\beta_{1-40}$ reduces the pixel intensity at 24 hr, pre-treatment with Syk inhibitor (50nM) abolished the $A\beta_{1-40}$-induced reduction in mean pixel intensity (*$p<0.05$, ANOVA, n=4)

B. The number of intact lysosomes per cell were counted. Treatment with $A\beta_{1-40}$ (2$\mu$M) for 24 hr caused a reduction in the number of lysosomes observed. Pre-treatment with Syk inhibitor (50nM) abolished the $A\beta_{1-40}$-induced reduction in lysosomal number (**$p<0.01$, ANOVA, n=4).

## 5.12 Destabilisation of the lysosomal membrane induced by $A\beta_{1-40}$ is Syk-dependent at 48 hr

To assess the role of Syk in $A\beta_{1-40}$-mediated destabilisation of the lysosomal membrane at 48 hr the AO technique was used. Exposure of cells to $A\beta_{1-40}$ (2μM) for 48 hr (Figure 5.15B) resulted in increased diffuse green fluorescence and a reduction in orange punctate staining. Furthermore, mean pixel intensity at 633nm decreased significantly following $A\beta_{1-40}$ treatment at 48 hr (Figure 5.16A), from 571.50 ± 74.83 (mean ± S.E.M.) to 252.00 ± 11.58 ($P<0.01$, ANOVA, n=4). There is also a reduction in the number of intact lysosomes counted manually. The number of lysosomes in control cells at 48 hr (Figure 5.16B), was 72.18 ± 8.74 (mean ± S.E.M.) and this decreased to 15.45 ± 2.72 ($P<0.001$, ANOVA, n=4) in cells treated with $A\beta_{1-40}$. These results suggest leakage of the dye from the lysosomal compartment, possibly as a result of a disruption in lysosomal integrity and a loss of lysosomal acidification.

Neurons were also pre-treated with Syk inhibitor (50nM) prior to $A\beta_{1-40}$ exposure to determine if the effect of $A\beta_{1-40}$ on lysosomal membrane integrity was mediated via Syk. Cells treated with Syk inhibitor alone or $A\beta_{1-40}$ in the presence of Syk inhibitor for 48 hr (Figure 5.15C and D) resulted in punctate orange fluorescence suggesting AO remained within the lysosomal compartment. Thus, in Figure 5.16A mean pixel intensity at fluorescence 633nm in cells treated with Syk inhibitor alone was 568.45± 97.02 (mean ± S.E.M.) and 670.16 ± 72.34 ($P<0.001$, ANOVA, n=4) in cells treated with $A\beta_{1-40}$ + Syk inhibitor for 48 hr Furthermore, in Figure 5.16B treatment with Syk inhibitor prevented the $A\beta_{1-40}$-mediated decrease in number of intact lysosomes; where lysosomal number was (86.66 ± 1.59) (n=4) in cells treated with Syk inhibitor alone and (78.20 ± 8.30) in cells treated with $A\beta_{1-40}$ in the presence of Syk inhibitor at 48 hr Therefore, the $A\beta_{1-40}$-induced disruption of the lysosomal membrane is Syk-sensitive at 48 hr.

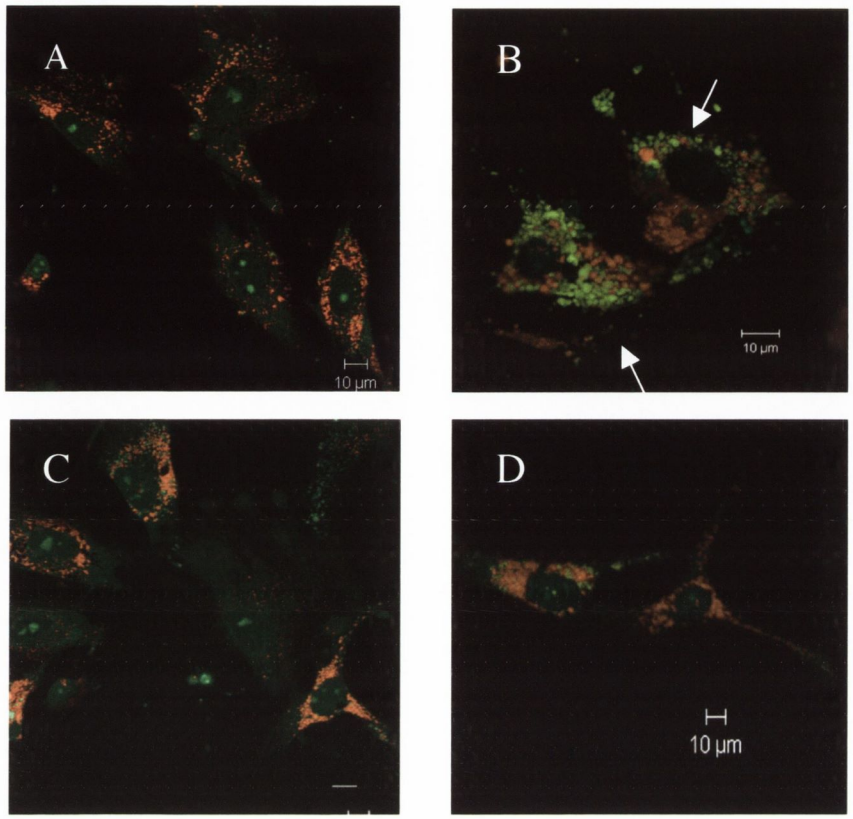


**Figure 5.15 The $A\beta_{1-40}$-mediated destabilisation of lysosomes at 48 hr is Syk-dependent**

Neurons were exposed to AO (5ug/ml) for 15 min prior to incubation with $A\beta_{1-40}$ (2μM) in the presence or absence of Syk inhibitor (50nM) for 48 hr. Relocation of AO from the lysosomes to cytosol was assessed. In control cells (A) AO displayed an orange fluorescence and was localised in discrete punctate compartments within the cell reflecting lysosomal distribution of AO. Exposure to $A\beta_{1-40}$ for 24 hr (B) resulted in the reduction of AO orange fluorescence and an increase in diffuse cytosolic green fluorescence. Treatment with Syk inhibitor alone (C) had no effect on AO fluorescence. Co-incubation with $A\beta_{1-40}$ + Syk inhibitor (D) resulted in AO displaying an orange fluorescence similar to control cells. Arrows indicate cells displaying destabilisation. Scale bar is 10μm.

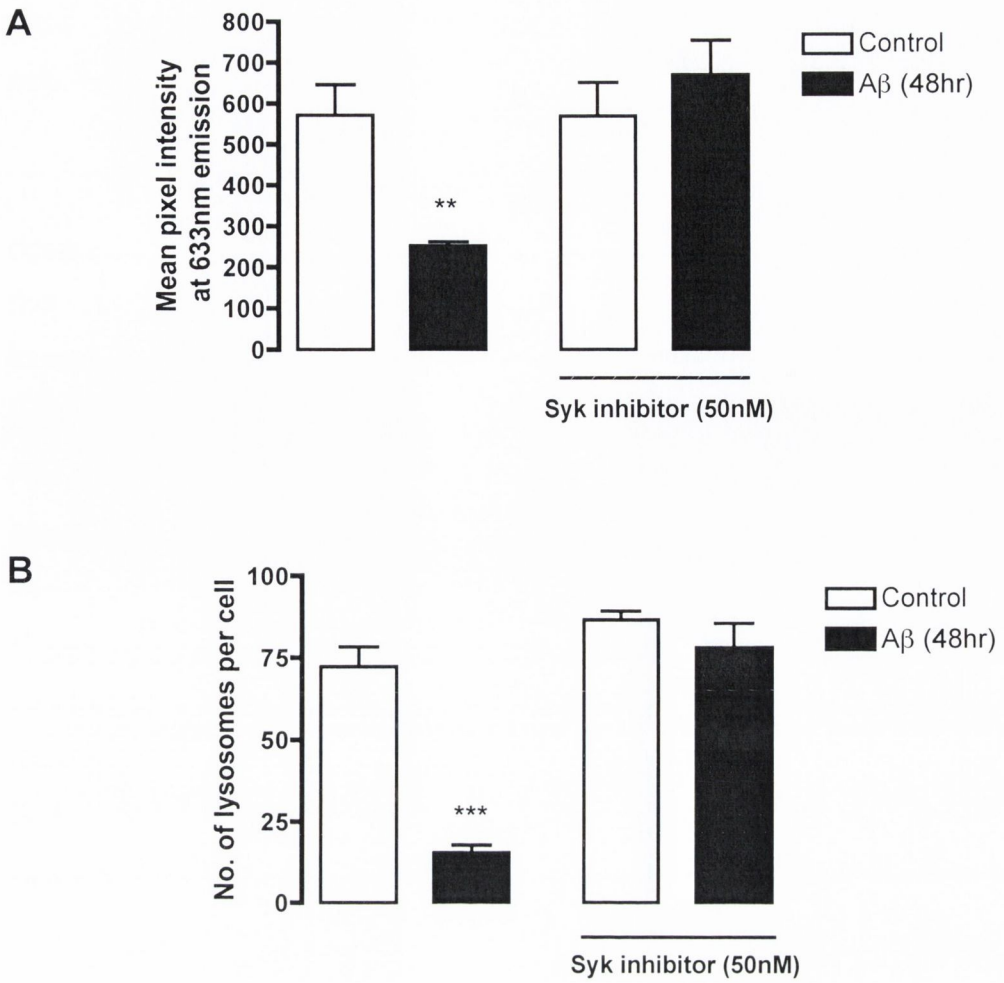


**Figure 5.16 The $A\beta_{1-40}$-mediated impact on lysosomal membrane integrity at 48 hr is Syk-dependent**

A. Intact lysosomes accumulate AO and emit at 633nm. By measuring the intensity of pixels at this wavelength we can monitor disruption of the lysosomal membrane due to leakage of the probe. $A\beta_{1-40}$ (2μM) reduces the pixel intensity at 48 hr, pre-treatment with Syk inhibitor (50nM) abolished the $A\beta_{1-40}$-induced reduction in mean pixel intensity (*$p<0.05$, ANOVA, n=4).

B. The number of intact lysosomes per cell were counted. Treatment with $A\beta_{1-40}$ (2μM) for 48 hr resulted in a reduction in the number of lysosomes observed. Pre-treatment with Syk inhibitor (50nM) abolished the $A\beta_{1-40}$-induced reduction in lysosomal number (***$p<0.001$, ANOVA, n=4).

## 5.13 Syk inhibitor prevents the $A\beta_{1-40}$-induced localisation of Bax with mitochondria at 30 min

The ability of $A\beta_{1-40}$ to promote Bax localisation with mitochondria was demonstrated in Chapter 4. It has been suggested that Bax association with the mitochondria can mediate apoptosis (Gross *et al.*, 1998). This study investigates whether Syk is involved in this $A\beta_{1-40}$-mediated localisation of Bax with mitochondria. Neurons were treated with the Syk inhibitor (50nM) prior to $A\beta_{1-40}$ (2μM; 30 min) treatment and Bax expression and distribution was assessed. Cells were viewed by confocal microscopy at an excitation wavelength of 488nm for Alexa-labelled Bax and 534nm for Mitotracker red. Figure 5.17 represents Bax staining in control (A), $A\beta_{1-40}$-treated (B), Syk inhibitor (C) and $A\beta_{1-40}$ + Syk inhibitor (D) treated cells at 30 min. Figure 5.17 demonstrates distribution of mitochondria in control (E), $A\beta_{1-40}$-treated (F), Syk inhibitor (G) and $A\beta_{1-40}$ + Syk inhibitor (H) treated cells, respectively, following loading with Mitotracker red. Furthermore, in $A\beta_{1-40}$-treated cells increased co-localisation of Bax expression with mitochondria was observed (Figure 5.17J) compared to control (Figure 5.17I). This association of Bax with mitochondria was abolished in cells pre-treated with Syk inhibitor (Figure 5.17 L). Treatment with Syk inhibitor alone resulted in no association of Bax with mitochondria (Figure 5.17K). This finding indicates that the $A\beta_{1-40}$-induced association of Bax with mitochondria at 30 min is mediated by Syk.

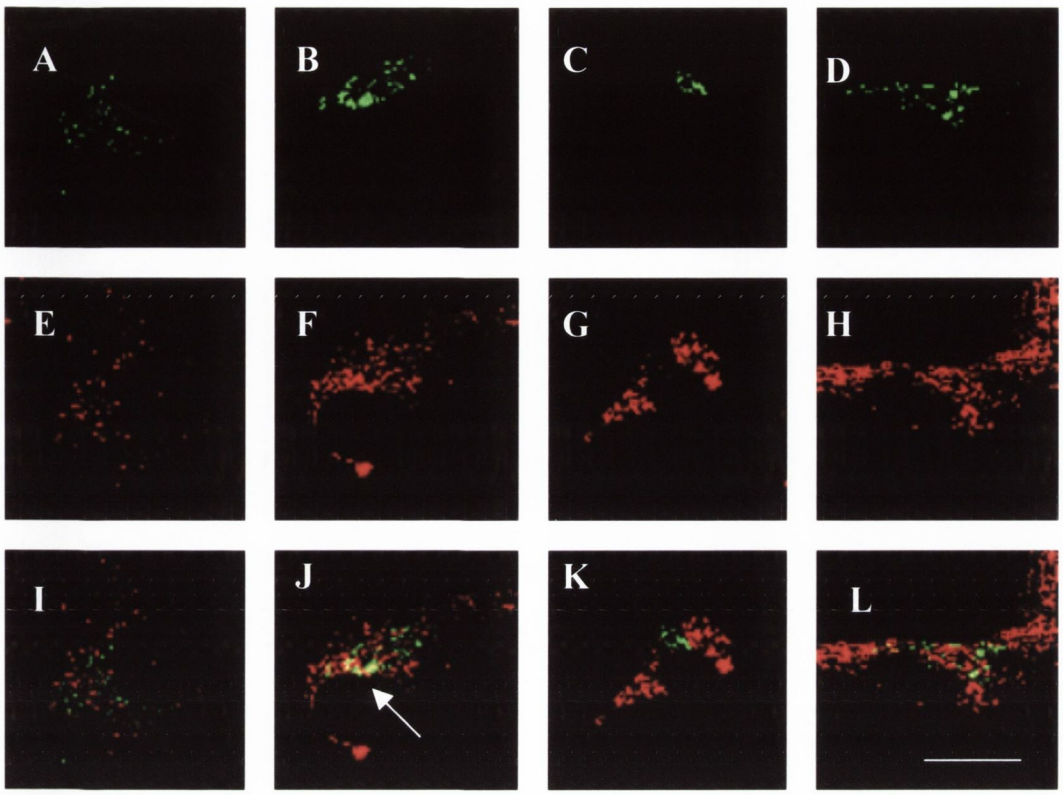


**Figure 5.17 Syk inhibitor prevents $A\beta_{1-40}$-induced association of Bax at mitochondria at 30 min**

Confocal microscopy was used to visualise the distribution of Bax within cortical neurons following treatment with $A\beta_{1-40}$ (2μM; 30 min). Cells were double labelled with the mitochondrial-specific marker, Mitotracker red, and an Alexa 488nm-labelled Bax antibody. Analysis of Bax expression in (A) control (B) $A\beta_{1-40}$-treated, (C) Syk inhibitor treated and (D) Aβ+ Syk inhibitor (50nM) treated cells (excitation 488nm; emission, 520nm). Mitotracker red staining represents the distribution of mitochondria in (E) control, (F) $A\beta_{1-40}$-treated, (G) Syk inhibitor treated and (H) $A\beta_{1-40}$+ Syk inhibitor treated cells (excitation 579nm; emission, 599nm). Co-localisation analysis of Bax and mitochondria in (J) $A\beta_{1-40}$-treated cells revealed increased localisation of Bax with mitochondria. Treatment with Syk inhibitor alone (K) had no effect and treatment with $A\beta_{1-40}$+ Syk inhibitor (L) abolished the $A\beta_{1-40}$-induced association of Bax with mitochondria. Arrows indicate cells displaying co-localisation. Scale bar is 10μm.

## 5.14 Syk inhibitor prevents the $A\beta_{1-40}$-induced localisation of Bax with mitochondria at 24 hr

To determine if the increase in Bax protein expression (see Figure 4.1) and the association of Bax with mitochondria (see Figure 4.2) was a consequence of $A\beta_{1-40}$-induced regulation of Syk, neurons were treated with the Syk inhibitor (50nM) prior to $A\beta_{1-40}$ (2μM; 24 hr) treatment and Bax expression and distribution was assessed. Cells were viewed by confocal microscopy at an excitation wavelenghth of 488nm for Alexa-labelled Bax and 534nm for Mitotracker red. Figure 5.18 represents Bax staining in control (A), $A\beta_{1-40}$-treated (B), Syk inhibitor (C) and $A\beta_{1-40}$ + Syk inhibitor (D) treated cells at 30 min. Figure 5.18 demonstrates distribution of mitochondria in control (E), $A\beta_{1-40}$-treated (F), Syk inhibitor (G) and $A\beta_{1-40}$ + Syk inhibitor (H) treated cells, respectively, following loading with Mitotracker red. Furthermore, in $A\beta_{1-40}$-treated cells increased co-localisation of Bax expression with mitochondria was observed (Figure 5.18J) compared to control (Figure 5.18I). This association of Bax with mitochondria was abolished in cells pre-treated with Syk inhibitor (Figure 5.18L). Treatment with Syk inhibitor alone resulted in no association of Bax with mitochondria (Figure 5.18K). This finding indicates that the $A\beta_{1-40}$-induced association of Bax with mitochondria at 24 hr is mediated by Syk.

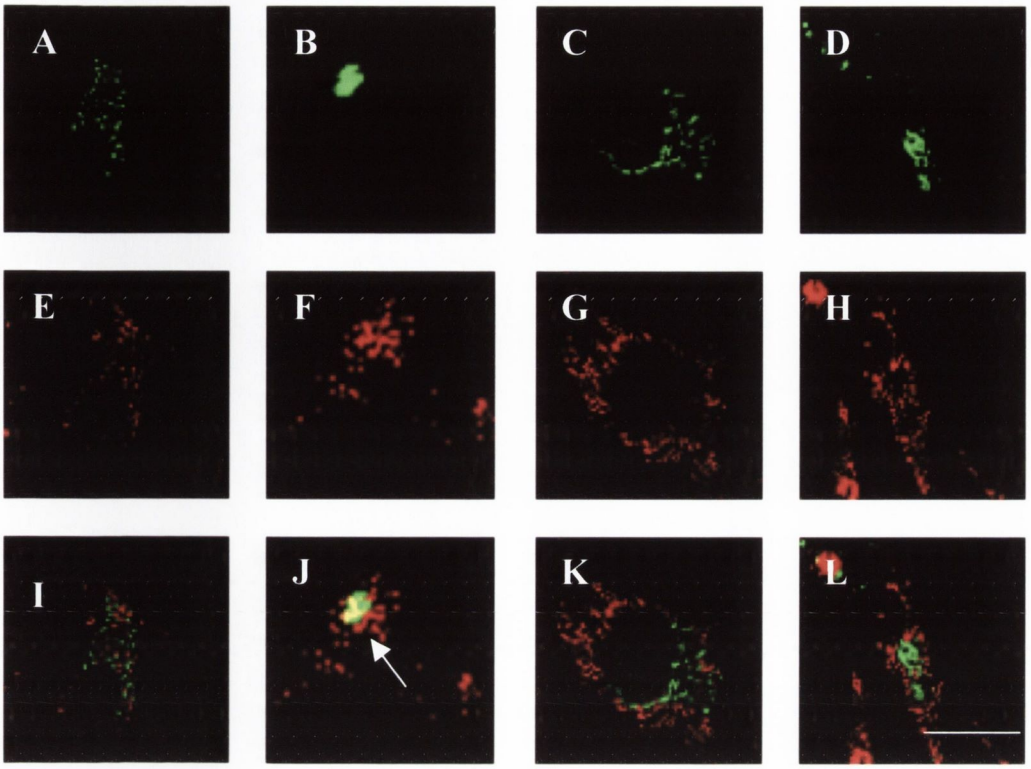


**Figure 5.18 Syk inhibitor prevents $A\beta_{1-40}$-induced association of Bax at mitochondria at 24 hr**

Confocal microscopy was used to visualise the distribution of Bax within cortical neurons following treatment with $A\beta_{1-40}$ (2μM; 24 hr). Cells were double labelled with the mitochondrial-specific marker, Mitotracker red, and an Alexa 488nm-labelled Bax antibody. Analysis of Bax expression in (A) control, (B) $A\beta_{1-40}$-treated, (C) Syk inhibitor and (D) $A\beta_{1-40}$ + Syk inhibitor treated cells (excitation 488nm; emission, 520nm). Mitotracker red staining represents the distribution of mitochondria in (E) control, (F) Aβ-treated cells, (G) Syk inhibitor treated and (H) $A\beta_{1-40}$+ Syk inhibitor treated cells (excitation 579nm; emission, 499nm). Co-localisation analysis of Bax and mitochondria in (J) $A\beta_{1-40}$-treated cells revealed increased localisation of Bax with mitochondria. Treatment with Syk inhibitor alone (K) had no effect and treatment with $A\beta_{1-40}$+ Syk inhibitor (L) abolished the $A\beta_{1-40}$-induced association of Bax with mitochondria. Arrows indicate cells displaying co-localisation. Scale bar is 10μm.

### 5.15 The role of Syk on Bax expression at the lysosome at 30 min

To examine the role of Syk on Bax expression at the lysosome, neurons were treated with the Syk inhibitor (50nM) prior to $A\beta_{1-40}$ (2μM; 30 min) treatment. Bax expression was assessed by confocal microscopy in fixed cells. Figure 5.19 represents Bax staining in control (A), $A\beta_{1-40}$-treated (B), Syk inhibitor (C) and $A\beta_{1-40}$ + Syk inhibitor (D) treated cells at 30 min. Figure 5.19 demonstrates distribution of lysosomes in control (E), $A\beta_{1-40}$-treated (F), Syk inhibitor (G) and $A\beta_{1-40}$ + Syk inhibitor (H) treated cells, respectively. Co-localisation analysis of Bax with lysosomes in control (I) and $A\beta_{1-40}$-treated cells (J) reveal no association of Bax with lysosomes. Treatment with Syk inhibitor alone (K) or $A\beta_{1-40}$ + Syk inhibitor (L) resulted in no association of Bax with lysosomes. This finding indicates that at 30 min there is no association of Bax with lysosomes.

### 5.16 Syk inhibitor abolishes the $A\beta_{1-40}$-induced localisation of Bax with lysosomes at 6 hr

To determine if the association of Bax with lysosomes (see Figure 4.9) was a consequence of $A\beta_{1-40}$-induced regulation of Syk, neurons were treated with the Syk inhibitor (50nM) prior to Aβ (2μM; 6 hr) treatment. Bax expression was assessed by confocal microscopy in fixed cells. Figure 5.20 represents Bax staining in control (A), $A\beta_{1-40}$-treated cells (B), Syk inhibitor-treated cells (C) and $A\beta_{1-40}$ + Syk inhibitor-treated cells (D) at 6 hr. Figure 5.20 demonstrates distribution of lysosomes in control (E), $A\beta_{1-40}$-treated cells (F), Syk inhibitor-treated cells (G) and $A\beta_{1-40}$ + Syk inhibitor-treated cells (H), respectively. Co-localisation analysis of Bax with lysosomes in control (I) and $A\beta_{1-40}$-treated cells (J) reveal increased association of Bax with lysosomes in $A\beta_{1-40}$-treated cells. This association of Bax with lysosomes was abolished in cells pre-treated with Syk inhibitor (Figure 5.20L). Treatment with Syk inhibitor alone resulted in no association of Bax with lysosomes (Figure 5.20K). This

finding indicates that the $A\beta_{1-40}$-induced association of Bax with lysosomes at 6 hr is mediated by Syk.

### 5.17 Effect of Syk inhibitor on Bax expression at lysosomes in cortical neurons at 24 hr

To examine the role of Syk on Bax expression, neurons were treated with the Syk inhibitor (50nM) prior to $A\beta_{1-40}$ (2μM; 24 hr) treatment. Bax expression was assessed by confocal microscopy in fixed cells. Figure 5.21 represents Bax staining in control (A), $A\beta_{1-40}$ (B), Syk inhibitor (C) and $A\beta_{1-40}$ + Syk inhibitor (D) at 24 hr. Figure 5.21 demonstrates distribution of lysosomes in control (E), $A\beta_{1-40}$ (F), Syk inhibitor (G) and $A\beta_{1-40}$ + Syk inhibitor (H), respectively. Co-localisation analysis of Bax with lysosomes in control (I) and $A\beta_{1-40}$ (J) reveal no association of Bax with lysosomes. Treatment with Syk inhibitor alone (K) or $A\beta_{1-40}$ + Syk inhibitor (L) resulted in no association of Bax with lysosomes. This finding indicates that at 24 hr there is no association of Bax with lysosomes.

### 5.18 $A\beta_{1-40}$ does not mediate an association between Phospho-p53 and lysosomes at 30 min

In order to investigate whether p53 impacts on the lysosomal system, expression of phospho-$p53^{ser\ 15}$ was assessed by immunocytochemistry. Cells were incubated with $A\beta_{1-40}$ (2μM) for 30 min prior to a 30 min incubation with the lysosomal marker, Lysotracker red (1mM). Phospho-$p53^{ser\ 15}$ expression was detected by immunocytochemistry using an antibody which specifically recognises p53 phosphorylated at serine-15 and cells were visualised by confocal microscopy. Neurons were also pre-treated with Syk inhibitor (50nM) prior to $A\beta_{1-40}$ exposure to determine if the effect of $A\beta_{1-40}$ on Phospho-p53 was Syk mediated. Figure 5.22 (A) represents p53 immunostaining in control (A), $A\beta_{1-40}$ (B), Syk inhibitor (C) and $A\beta_{1-40}$ + Syk inhibitor (D) at 30 min. Figure 5.22 demonstrates distribution of lysosomes in control (E), $A\beta_{1-40}$ (F),

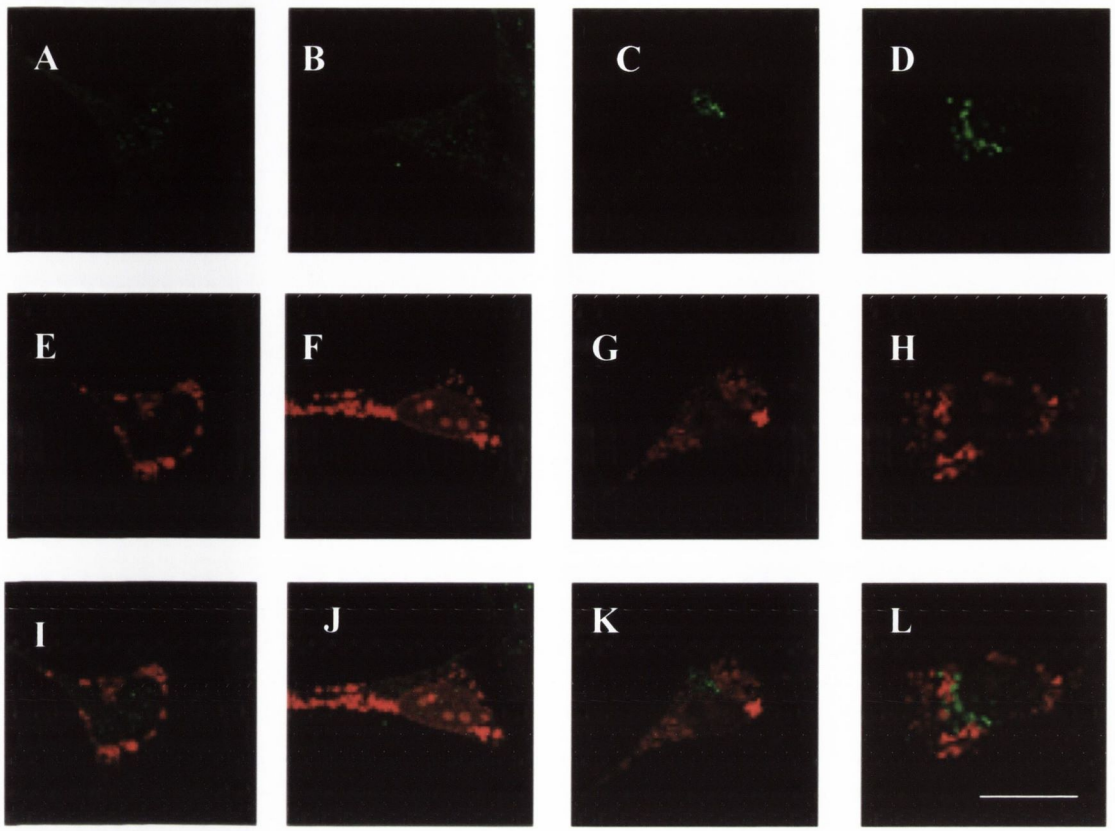


**Figure 5.19 Role of Syk on Bax expression at the lysosome at 30 min**

Fluorescence confocal microscopy was used to visualise the distribution of Bax within cortical neurons following treatment with $A\beta_{1\text{-}40}$ (2μM) for 30 min. Cells were double labeled with the lysosomal specific agent, Lysotracker red, and a Alexa-labelled Bax antibody. Analysis of Bax expression in control (A), $A\beta_{1\text{-}40}$-treated (B), Syk inhibitor treated (C) and $A\beta_{1\text{-}40}$+ Syk inhibitor treated cells (D) (excitation 488 nm; emission, 520nm). Lysotracker red staining represents the distribution of lysosomes in control (E), $A\beta_{1\text{-}40}$-treated cells (F), Syk inhibitor treated cells (G) and $A\beta_{1\text{-}40}$ + Syk inhibitor treated cells (H) (excitation 579 nm; emission, 599nm). Co-localisation analysis of Bax expression with lysosomes is shown in control (I), $A\beta_{1\text{-}40}$-treated (J), Syk inhibitor (K) and $A\beta_{1\text{-}40}$ + Syk inhibitor (L) treated cells, where $A\beta_{1\text{-}40}$-treatment has no effect. Scale bar 10μm.

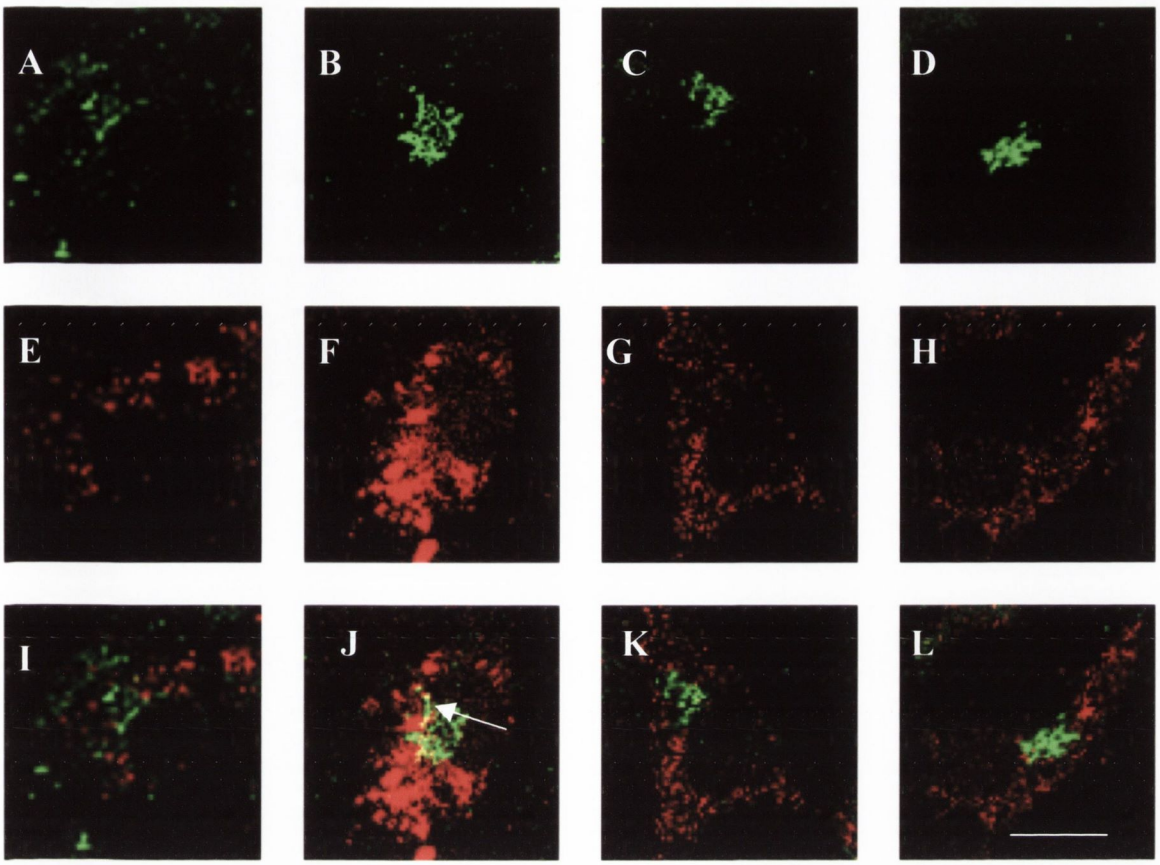


**Figure 5.20 Role of Syk on Bax association with lysosomes in cortical cells at 6 hr**

Fluorescence confocal microscopy was used to visualise the distribution of Bax within cortical neurons following treatment with $A\beta_{1-40}$ (2μM) for 6 hr. Cells were double labeled with the lysosomal specific agent, Lysotracker red, and a Alexa-labelled Bax antibody. Analysis of Bax expression in control (A), $A\beta_{1-40}$-treated (B), Syk inhibitor treated (C) and $A\beta_{1-40}$+ Syk inhibitor treated cells (D) (excitation 579 nm; emission, 599nm). Lysotracker red staining represents the distribution of lysosomes in control (E), $A\beta_{1-40}$-treated cells (F), Syk inhibitor treated cells (G) and $A\beta_{1-40}$ + Syk inhibitor treated cells (H) (excitation 579 nm; emission, 599nm). Co-localisation analysis of Bax expression with lysosomes is shown in control (I), $A\beta_{1-40}$-treated (J), Syk inhibitor (K) and Aβ + Syk inhibitor (L) treated cells, where $A\beta_{1-40}$-treated-mediated association of Bax with lysosomes. Pre-treatment with Syk inhibitor prevents the $A\beta_{1-40}$-mediated localisation of Bax with lysosomes at 6 hr. Arrows indicate cells displaying co-localisation. Scale bar 10μm.

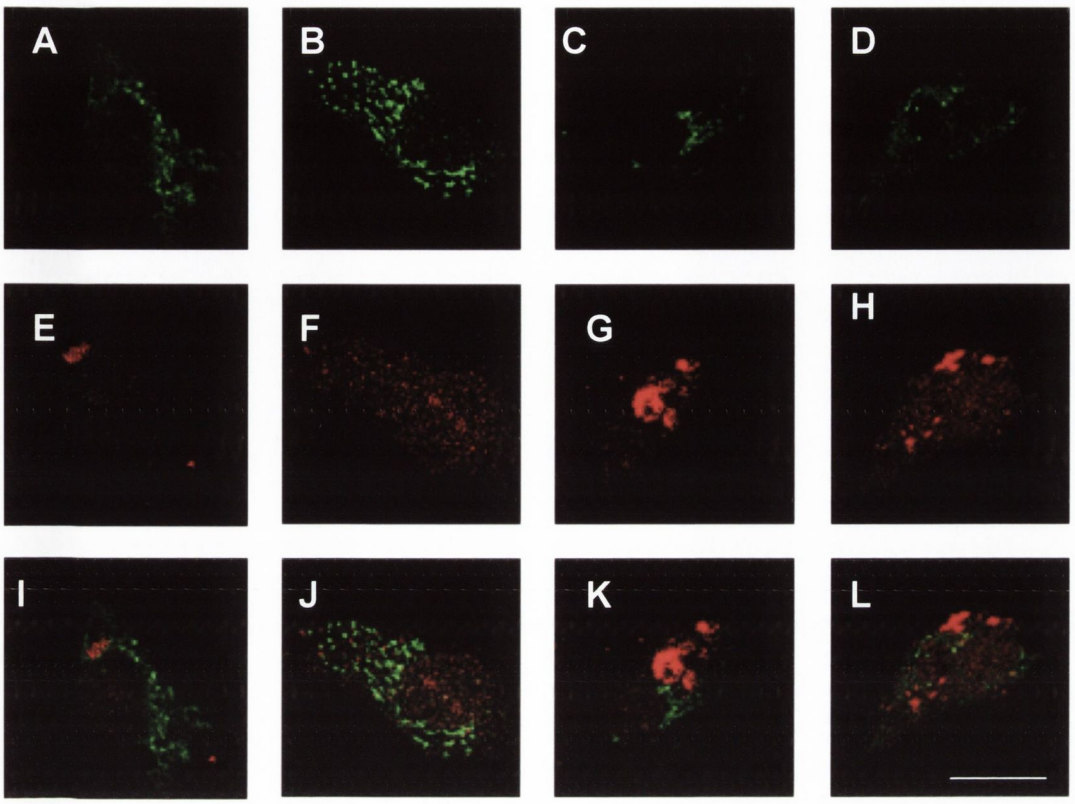


**Figure 5.21 Role of Syk on Bax expression at lysosomes in cortical cells at 24 hr**

Fluorescence confocal microscopy was used to visualise the distribution of Bax within cortical neurons following treatment with $A\beta_{1-40}$ (2μM) for 24 hr. Cells were double labeled with the lysosomal specific agent, Lysotracker red, and a Alexa-labelled Bax antibody. Analysis of Bax expression in (A) control cells, (B) $A\beta_{1-40}$-treated cells, (C) Syk inhibitor-treated cells and (D) $A\beta_{1-40}$+ Syk inhibitor treated cells (excitation 488 nm; emission, 520nm). Lysotracker red staining represents the distribution of lysosomes in (E) control cells, (F) $A\beta_{1-40}$-treated cells, (G) Syk inhibitor treated cells and (H) $A\beta_{1-40}$ + Syk inhibitor treated cells (excitation 579 nm; emission, 599nm). Co-localisation analysis of Bax expression with lysosomes is shown in (I) control cells, (J) $A\beta_{1-40}$-treated cells, (K) Syk inhibitor-treated cells and (L) $A\beta_{1-40}$ + Syk inhibitor treated cells. Treatment with $A\beta_{1-40}$ does not induce localisation of Bax with lysosomes at 24 hr. Scale bar 10μm.

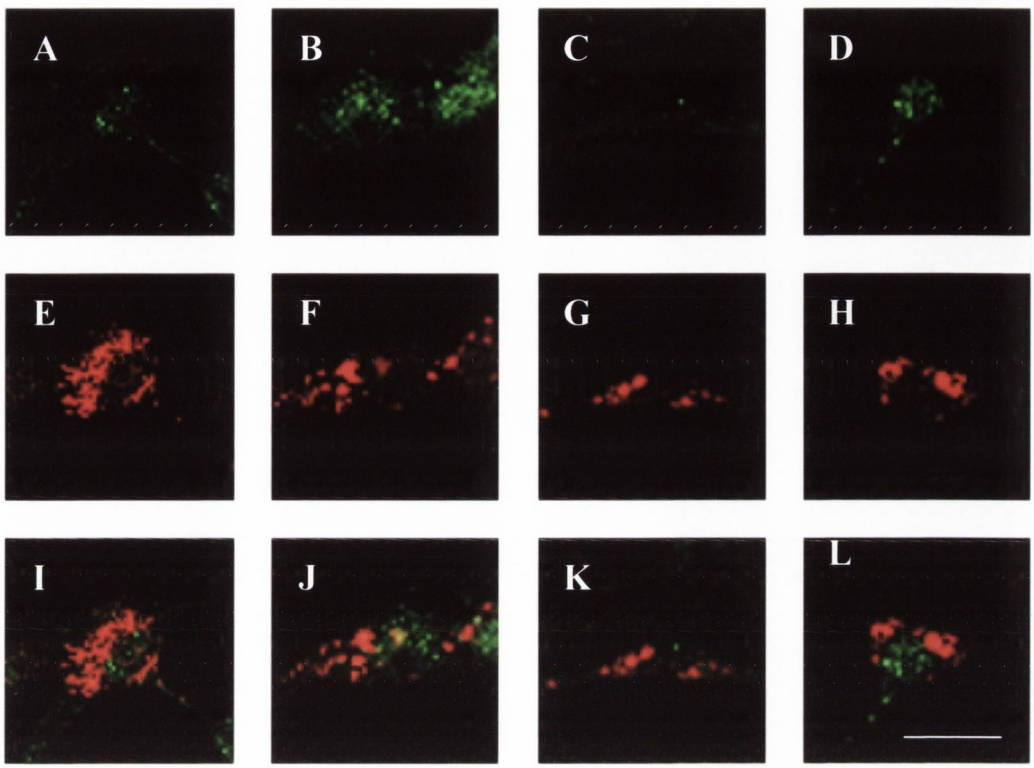


**Figure 5.22 The effect of Syk inhibitor on $A\beta_{1-40}$-mediated localisation of Phospho-p53$^{ser15}$ at the lysosome at 30 min**

Cells were double labeled with the lysosomal specific agent, Lysotracker red, and an Alexa-labelled Phospho-p53 antibody. Analysis of Phospho-p53 expression in control (A) $A\beta_{1-40}$-treated (B) Syk inhibitor alone (C) and $A\beta_{1-40}$ + Syk inhibitor (D) treated cells (excitation 488 nm; emission, 520nm). Lysotracker red staining represents the distribution of lysosomes in control (E), $A\beta_{1-40}$-treated cells (F), Syk inhibitor treated cells (G) and $A\beta_{1-40}$ + Syk inhibitor treated cells (H) (excitation 579 nm; emission, 599nm). Co-localisation analysis of Bax expression with lysosomes is shown in control (I), Aβ-treated (J), Syk inhibitor (K) and $A\beta_{1-40}$ + Syk inhibitor (L) treated cells. There is no observable localisaiton of Phospho-p53$^{ser15}$ with lysosomes. Scale bar 10μm.

Syk inhibitor (G) and $A\beta_{1-40}$ + Syk inhibitor (H), respectively. Co-localisation analysis of Phospho-p53$^{ser\ 15}$ with lysosomes in control (I) and $A\beta_{1-40}$-treated cells (J) reveal no association of Phospho-p53$^{ser\ 15}$ with lysosomes. Treatment with Syk inhibitor alone (K) or $A\beta_{1-40}$ + Syk inhibitor (L) resulted in no association of Phospho-p53$^{ser\ 15}$ with lysosomes. This finding indicates that at 30 min there is no association of Phospho-p53$^{ser\ 15}$ with lysosomes.

### 5.19 $A\beta_{1-40}$-induced association of Phospho-p53 with lysosomes at 6 hr is Syk dependent

Cells were incubated with $A\beta_{1-40}$ (2$\mu$M) for 6 hr prior to a 30 min incubation with the lysosomal marker, Lysotracker Red (1mM). Phospho-p53 $^{ser\ 15}$ expression was detected by immunocytochemistry using an antibody which specifically recognises p53 phosphorylated at serine-15 and cells were visualised by confocal microscopy. Neurons were also pre-treated with Syk inhibitor (50nM) prior to $A\beta_{1-40}$ exposure to determine if the effect of $A\beta_{1-40}$ on Phospho-p53 was Syk mediated. Figure 5.23 (A) represents p53 immunostaining in control (A), $A\beta_{1-40}$ (B), Syk inhibitor (C) and $A\beta_{1-40}$ + Syk inhibitor (D) at 6 hr. Figure 5.23 demonstrates distribution of lysosomes in control (E), $A\beta_{1-40}$ (F), Syk inhibitor (G) and $A\beta_{1-40}$ + Syk inhibitor (H), respectively. Co-localisation analysis of Phospho-p53 $^{ser\ 15}$ with lysosomes in $A\beta_{1-40}$ (J) reveal localisation of Phospho-p53 $^{ser\ 15}$ with lysosomes. Treatment with Syk inhibitor alone (K) or $A\beta_{1-40}$ + Syk inhibitor (L) prevented the $A\beta_{1-40}$-induced association of Phospho-p53$^{ser\ 15}$ with lysosomes. Therefore, the $A\beta_{1-40}$-mediated association of Phospho-p53$^{ser15}$ at lysosomes is mediated via Syk.

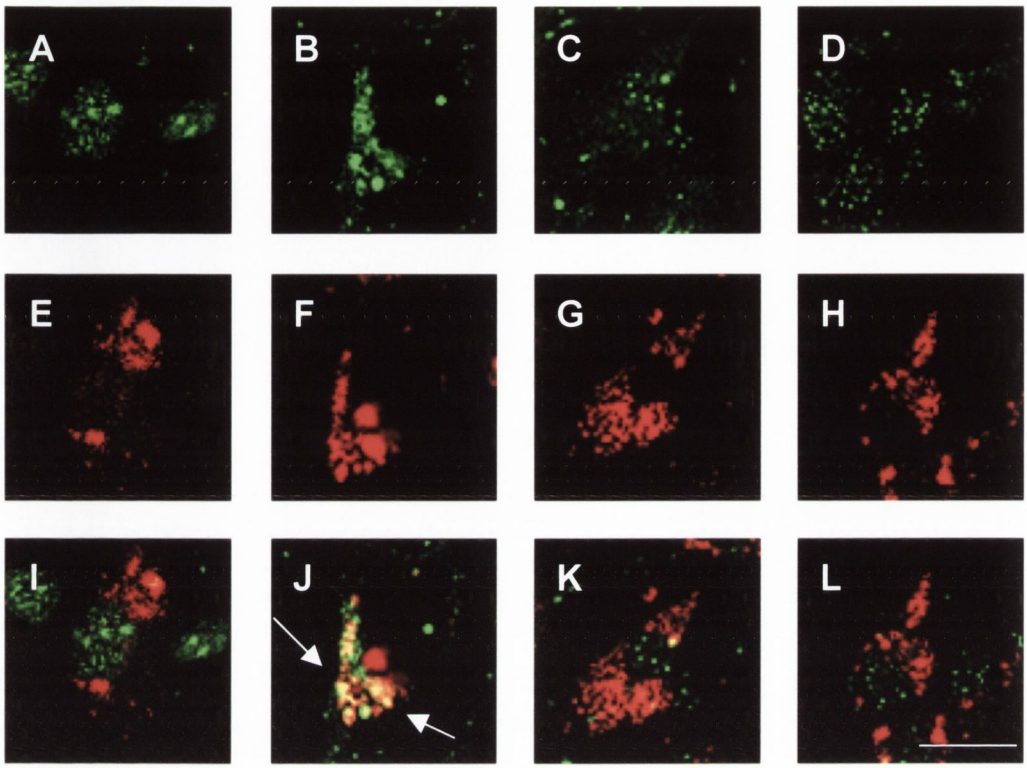


**Figure 5.23 The effect of Syk inhibitor on $A\beta_{1-40}$-mediated localisation of Phospho-p53$^{ser15}$ at the lysosome at 6 hr**

Cells were double labeled with the lysosomal specific agent, Lysotracker red, and an Alexa-labelled Phospho-p53 antibody. Analysis of Phospho-p53 expression in control (A) $A\beta_{1-40}$-treated (B) Syk inhibitor alone (C) and $A\beta_{1-40}$ + Syk inhibitor (D) treated cells (excitation 579 nm; emission, 599nm). Lysotracker red staining represents the distribution of lysosomes in control (E), $A\beta_{1-40}$-treated cells (F), Syk inhibitor treated cells (G) and $A\beta_{1-40}$ + Syk inhibitor treated cells (H) (excitation 579 nm; emission, 599nm). Co-localisation of Bax expression with lysosomes is shown in control (I), $A\beta_{1-40}$-treated (J), Syk inhibitor (K) and $A\beta_{1-40}$ + Syk inhibitor (L) treated cells, where $A\beta_{1-40}$-treated-mediates association of Phospho-p53$^{ser15}$ at lysosomes at 6 hr. Arrows indicate cells displaying co-localisation. Scale bar 10μm.

## 5.3 Discussion

The aim of this study was to investigate whether or not the protein tyrosine kinase, Syk, was expressed in primary cortical neurons and if so, to examine the role of Syk in $A\beta_{1-40}$-induced signalling in these cells. Furthermore, the involvement of Syk in $A\beta_{1-40}$-mediated regulation of the lysosomal system was also examined. The results herein demonstrate that Syk is expressed in cortical neurons, and the data show that $A\beta_{1-40}$ has the proclivity to modulate expression of Syk in a time-dependent manner. The ability of $A\beta_{1-40}$ to induce DNA fragmentation was dependent on Syk, indicating that $A\beta_{1-40}$ neurotoxicity is mediated through Syk signalling in cortical neurons. $A\beta_{1-40}$ significantly increased the activity of the cell death protease, caspase-3, and this increase was abated by the Syk inhibitor. Hence, the results suggest that Syk may be pertinent in mediating the neurotoxic properties of $A\beta_{1-40}$. Syk was also found to associate at lysosomes, following treatment with $A\beta_{1-40}$. Subsequently, cytosolic cathepsin-L activity was increased by $A\beta_{1-40}$ in an Syk-dependent manner, suggesting that Syk association at the lysosome could modulate release of cathepsins into the cytosol. In addition, destabilisation of lysosomal integrity, as assessed by the AO relocation technique, induced by $A\beta_{1-40}$ was abolished by the Syk inhibitor, indicating that Syk is involved in regulating the stability of lysosomes. Finally, the $A\beta_{1-40}$-induced association of the pro-apoptotic protein, Bax, at the mitochondria and lysosome was prevented by the Syk inhibitor, demonstrating a link between the $A\beta_{1-40}$-mediated increase in Syk expression and loss of lysosomal membrane integrity. Overall, these results implicate the protein tyrosin kinase, Syk, in a wide variety of signalling events induced by $A\beta_{1-40}$ in cortical neurons, suggesting that Syk could be a potential target in the neurodegeneration process.

Through extensive biochemical and genetic studies, Syk has been well characterised as an essential component of the machinery required for signalling through multiple immune recognition receptors. In the past 10 years or so, several studies have investigated the expression of, and a role for, Syk in non-hematopoietic cells and results have found that Syk is expressed in

various non-immune cells including epithelial cells (Fluck *et al.*, 1995), hepatocytes (Tsuchida *et al.*, 2000), fibroblasts (Wang & Malbon, 1999) breast tissue (Coopman *et al.*, 2000), vascular endothelial cells (Turner *et al.*, 1995) and neuron-like cells (Tsuchida *et al.*, 2000), suggestive of a general physiological role for this kinase. This is the first study that has investigated whether Syk is present in primary cortical cells. The results herein demonstrate expression of Syk in cortical neurons, and expression appears to be localised to the cytosol. In hematopoietic cells, Syk, along with other protein tyrosine kinases, function at the plasma membrane where the receptors to which it is recruited are located, it would therefore be expected to localise at the plasma membrane. However, studies have shown that in unstimuled cells this kinase distributes to cytoplasmic and nuclear compartments, in support of our findings (Ma *et al.*, 2001).

In this study, exposure of neurons to $A\beta_{1-40}$ for 30 min, 2 hr and 6 hr resulted in the upregulation of Syk in a time-dependent manner, as shown by both immunofluorescence and western immunoblot analysis. This is the first report that we know of, suggesting an interaction between Aβ and Syk in neuronal cells. Several studies have identified a relationship between Aβ and Syk in another type of brain cell, the microglia. Microglia, the main immune effector cells within the brain (Leong & Ling, 1992) are the predominant glial cell type present within senile plaques (Itagaki *et al.*, 1989). Microglia that are in direct contact with senile plaques exhibit an activated phenotype as evidenced by elevated expression of HLA-DR, complement receptors, and immunoglobulin receptors (McGeer *et al.*, 1989; McGeer *et al.*, 1993). Importantly, they also exhibit high levels of tyrosin-phosphorylated proteins (Wood & Zinsmeister, 1991). It has been reported that exposure of microglia to fibrillar forms of Aβ resulted in the activation of numerous tyrosine kinases, including Syk (McDonald *et al.*, 1997; Combs *et al.*, 1999). Upon further investigation, these responses were found to be independent of the scavenger receptors, the receptor for advanced glycation end product, or the serpin-enzyme complex receptor, all of which are known to interact with Aβ. Those studies provide evidence that in microglia Aβ may interact with other membrane proteins linked to intracellular signal transduction pathways. In this

study, I did not examine the mechanism behind the $A\beta_{1-40}$-mediated activation of Syk in cortical neuronal cells, however, several mechanisms could potentially target Aβ to cellular elements. In this regard, cell surface-binding sites are logical to consider for multiple reasons: their capacity to concentrate Aβ at the plasma membrane, where it could directly damage membranes; the possibility that they could function as receptors which engage in intracellular signalling mechanisms; and, their ability to trigger endocytosis, potentially concentrating toxic species in the endolysosomal pathway where disruption of lysosomal integrity could induce severe cellular damage (Yang *et al.*, 1998). As might be expected for a pleiotropic peptide such as Aβ, many cell surface interaction sites have been reported, neuronal RAGE receptors (Yan *et al.*, 1996), p75 neurotrophin receptor (Yaar et al., 1997), amyloid precursor protein (Lorenzo *et al.*, 2000), and the nicotinic acetylcholine receptor (Dineley *et al.*, 2001). Aβ could also penetrate directly into membranes - spontaneously integrating into the bilayers of neuronal membranes forming aqueous pores (Singer & Dewji, 2006), as one study recently suggested. In addition, Aβ could indirectly activate Syk by activating a kinase, such as ERK (Dineley *et al.*, 2001) or JNK (Fogarty *et al.*, 2003).

Syk activation has been shown to involve several mechanisms including a conformational change due to ITAM binding (Turner *et al.*, 2000), autophosphorylation (Chu *et al.*, 1998) and phosphorylation by other kinases (Latour & Veillette, 2001). Classically, Syk has been studied in haematopoietic cells. Stimulation of B lymphocytes through their antigen receptor (BCR) results in rapid increases in tyrosine phosphorylation on a number of proteins. Since none of the BCR subunits possess intrinsic PTK activity, cytoplasmic PTKs associate with BCR complexes. Thus, activation of Syk occurs via binding of ligands to their receptors, allowing the rapid phosphorylation of an immunoreceptor tyrosine activation motif (ITAM), which constitutes a binding site for the two Src homology 2 (SH2) domains of Syk (Songyang *et al.*, 1994). Subsequently Syk is autophosphorylated (Rowley *et al.*, 1995) and/or phosphorylated by Src kinases and its intrinsic kinase activity increases (Kurosaki *et al.*, 1994). The binding of growth factors and cytokines to their cognate receptors, also activate Syk in a similar fashion (Taniguchi, 1995).

Indeed, it has been reported that extracellular stress such as LPS, ionising radiation, UV irradiation, $H_2O_2$ and genotoxic agents all activate the Syk family (Kharbanda *et al.*, 1994; Hardwick & Sefton, 1995; Brumell *et al.*, 1996; Arndt *et al.*, 2004; Zou *et al.*, 2004). The molecular basis of Syk activation in non-immune cells remains to be clarified as expression of receptors containing ITAMs is absent in these cells. However, recent evidence suggests that components of the ITAM-based signalling are also present in a number of non-immune cells. A number of molecules expressed in non-hematopoietic cells carry ITAM-like sequences. The PSGL-1 adhesion molecule has been shown to activate Syk (Urzainqui *et al.*, 2002). Tamalin, a metabotropic glutamate receptor-associated neuronal scaffolding protein also known as GRASP (Kitano *et al.*, 2002), contains an ITAM sequence, which becomes phosphorylated by the Scr-family kinases, Src and Fyn, leading to the recruitment of the Syk tyrosine kinase (Hirose *et al.*, 2004). The TNF-α receptor-related death domain containing apoptosis receptor WSL-1 also contains an ITAM sequence (Lohi & Lehto, 1998). Intriguingly, stimulation of Syk in haematopoietic cells does not always involve interaction with ITAMs. Various alternative pathways resulting in the stimulation of Syk have been reported. Syk can associate with the phosphorylated intracellular component of the erythropoietin receptor, which does not contain an ITAM but has several tyrosine residues (Duprez *et al.*, 1998). The IL-15Rα does not contain an ITAM but has one tyrosine residue (Anderson *et al.*, 1995); thus, only one of the two SH2 domains of Syk is capable of binding the intracellular part of IL-15Rα. Syk has also been reported to be activated through integrins, which do not contain ITAMs, suggesting a unique role for integrins in Syk function (Gao *et al.*, 1997). Furthermore, activation of Syk induced by hydrogen peroxide is independent of ITAM (Schieven *et al.*, 1993), suggesting that $H_2O_2$ is likely to act on cellular components that regulate Syk activity. Since, $H_2O_2$ is known to inhibit phosphotyrosine phosphatases (Hecht & Zick, 1992), one possiblity to be considered is that inhibition of phosphatases activity leads to Syk activation. It is also possible that Syk may be activated by direct interaction with Lyn, an Src protein kinase, because Syk has been shown to be coimmunoprecipitated with Lyn (Sidorenko *et al.*, 1995). Therefore, there

are multiple ways in which Aβ could stimulate Syk in cortical neuronal cells and further study is required to elucidate this interaction.

Activation of Syk results in a diverse range of signalling cascades, including cell activation, proliferation, differentiation and cell death, depending on cell type and stimulus involved. Caspases act as molecular instigators of apoptosis (Zou *et al.*, 1997). Caspase-3 is the most extensively studied apoptotic caspase. The enzyme exists as a proenzyme (32kDa) in most cells, including neurons, and is processed and activated by caspase-9 to the heterodimeric form (17kDa and 12kDa) during apoptosis (Slee *et al.*, 1999). The role of caspase-3 in Aβ-neurodegeneration has been proposed to be brain-region specific (Selznick *et al.*, 1999). While inhibition of caspase-3 was found to protect cortical neurons from Aβ-mediated cell death, caspase-3 was found to have no role in Aβ-mediated hippocampal cell death (Troy *et al.*, 2000). Our results demonstrate that following Aβ-treatment for 24 hr, caspase-3 activation is significantly increased, supporting previous work from our laboratory (Boland & Campbell, 2004). The Aβ-induced caspase-3 activation was blocked by the Syk inhibitor, suggesting that the neurotoxic effects of Aβ are mediated by coupling of Aβ to Syk and caspase-3 activation. In support of this result, there is evidence that Syk expression in immune cells couples to caspase-3 activation (Zhou *et al.*, 2006), however the pathways involved in this process are unknown.

Apoptosis is characterised by distinct morphological and biochemical changes to the cell, including the internucleosomal cleavage of DNA (Behl, 2000). The ability of Aβ to induce DNA fragmentation was assessed by TUNEL staining. The TUNEL technique provides an quantitative method of determining cell death in cultured cell populations. Aβ induced DNA fragmentation in the nucleus of cultured neurons, reflecting an apoptotic response profile to Aβ. The ability of Aβ to induce DNA fragmentation was blocked by the Syk inhibitor, indicating that Aβ neurotoxicity is mediated through Syk in cortical neurons. These results indicate that Syk is involved in Aβ-mediated cell death suggestive of a role for Syk in neurodegeneration. The exact involvement of Syk in Aβ-induced apoptosis is unclear. In the literature there is conflicting evidence as to the role of Syk in cell death. In immature B

cells the binding of an antigen to the BCR in the absence of costimulatory signals leads to induction of apoptosis, mediated by Syk (Tsubata *et al.*, 1993). TNFα activates Syk in T cells, myeloid cells, epithelial cells and neuronal cells (Combs *et al.*, 2001; Takada & Aggarwal, 2004) with subsequent apoptosis, suggestive of a role for Syk in apoptosis. Indeed, there is evidence that Syk can activate certain cytokines, particularly TNF-α and IL-1β and increase c-fos expression (Combs *et al.*, 2001), supporting a role for this kinase in the regulation of cell death. A Syk signalling cascade has also been identified in microglial lineage cells, activated by exposure of the cells to Aβ (McDonald *et al.*, 1997; McDonald *et al.*, 1998; Combs *et al.*, 1999) and is directly responsible for the production of neurotoxic factors (including PKC, MEK, Lyn) and toxic superoxide radicals. A chicken cell line, DT40, deficient in Syk did not respond by apoptosis to receptor crosslinking, whereas the wild-type DT40 cells underwent apoptosis (Takata *et al.*, 1994). Taken together, these findings indicate that Syk plays an important role in the early signalling cascade eventually leading to apoptosis in cells. In contrast, other reports suggest that Syk is not involved in apoptosis but decreases a cells mitotic index inhibiting their proliferation rate (Moroni *et al.*, 2004). Syk was found to localise to the centrosomes and exhibit catalytic activity, demonstrating that Syk may be a novel centrosomal kinase that negatively affects cell division, thus controlling cell proliferation. Furthermore, there is evidence of an essential role for Syk in the activation of the antiapoptotic pathways that are stimulated through the IL-3/IL-5/GM-CSF receptor β subunit in human eosinphils (Yousefi *et al.*, 1996). Paradoxically, Syk expression in B cells also protects cells from apoptosis induced by ceramide, osmotic stress, or oxidative stress (Qin *et al.*, 1997a; Qin *et al.*, 1997b; Ding *et al.*, 2000; Takano *et al.*, 2002). Thus, the role of Syk in regulating apoptosis remains controversial and appears to be cell and stimulus dependent.

Cathepsins are thought to play a significant role in oxidative stress (Roberg & Ollinger, 1998; Yuan *et al.*, 2000) and age-related neurodegeneration (Nakamura *et al.*, 1991). Previous work from this laboratory has demonstrated that Aβ promotes an increase in cytosolic expression of cathepsin-L in cultured cortical neurons (Boland & Campbell,

2004). In addition, the proclivity of Aβ to induce apoptotic changes, such as caspase-3 activation, cleavage of the DNA repair enzyme, poly-ADP ribose polymerase, and DNA fragmentation, was prevented by the selective cathepsin-L inhibitor. Thus, the role of Syk in regulating the lysosomal component of Aβ-mediated apoptosis was assessed. The translocation of lysosomal cathepsin-L into the cytoplasm induced by Aβ at 6 hr was abolished by the Syk inhibitor, suggestive of an interaction between Syk and lysosomes. Previous studies using the immature B cell line, DT40, demonstrated that cascades driven by the activation of Syk were esential for BCR-induced apoptosis (Takata *et al.*, 1994), however the precise mechanism by which Syk was involved in BCR-induced apoptosis was unclear. Another cell line, WEHI-231, demonstrated the involvement of BCR-induced disruption of mitochondrial transition pore followed by postmitochondrial activation of cathepsin-B (Katz *et al.*, 2001; Katz *et al.*, 2004). A recent study by He and colleagues (2005) showed that after BCR-crosslinking lysosomal membrane permeability was enhanced with the concomitant release of lysosomal enzymes correlated with early apoptotic hallmarks. Destabilisation of the lysosomal membrane was not detected in Syk-deficient cells, suggesting that loss of lysosomal integrity is a primary step in BCR-induced apoptosis and that Syk is responsible for the disruption to lysosomal integrity. While my study found an increase in cytosolic cathepsin-L activity, results from B cell lines reveal that an alternative cathepsin, cathepsin-B, was released from lysosomes to the cytosol (He *et al.*, 2005). Cathepsin proteases are normally active in the acidic enviroment of the lysosome however, certain cathepsins, such as cathepsin-L and cathepsin-B, can also be active at neutral pH (Ishisaka *et al.*, 1999). It is suggested that cytosolic cathepsins may activate key proteases involved in the apoptotic cascade, such as caspase-3, via direct (Ishisaka *et al.*, 1999) or indirect (Stoka *et al.*, 2001) mechanisms. Although the exact cause underlying the Syk-dependent Aβ-mediated release of cathepsin-L from the lysosomal compartment is unclear, several theories have been suggested and will be discussed further in the discussion. Expression of cathepsin-L is upregulated in Alzheimer's disease brains (Cataldo *et al.*, 1995; Yoshiyama *et al.*, 2000) and cathepsin-D has been

shown to play a role in processing of Aβ precursor protein (Sadik *et al.*, 1999). These alterations in cathepsin-L activity and cellular distribution occur prior to evidence of Aβ-mediated cell death, indicating that Syk activation and release of cathepsin-L into the cytoplasm are upstream events in this apoptotic cascade. Given that the Syk inhibitor blocks the Aβ-mediated release of cathepsin-L, Syk appears to play a significant role in regulating the lysosomal system and possibly modulating apoptosis in cortical neurons.

Few studies have focused on the intracellular distribution of Syk or the trafficking of it between subcellular compartments and the role this plays on its cellular functions. In this study the intracellular distribution of Syk was examined. The Lysotracker red fluorophore was used to visualise the distribution of lysosomes within neurons and cells were monitored using confocal microscopy. The findings demonstrate that Syk resides in the cytosol, however, upon Aβ-treatment for 2 hr Syk translocates from the cytosol and localises to the lysosomal membrane. The role of Syk at the lysosomal membrane is unclear however, given the previous result I speculate that it may modulate the integrity of the lysosomal membrane and regulate release of cathepsin-L into the cytosol. Zhou and colleagues recently reported that Syk is distributed in cytosolic and nuclear regions in B cells (Zhou *et al.*, 2006), however, this is the first report to suggest that Syk associates with lysosomes. Changes in the location of Syk upon inducement of a stimulus has been noticed in a previous study (Ma *et al.*, 2001). Alterations in cellular location was found to modulate the responses of cells to oxidative stress, such that cells with Syk in the nucleus were resistant to stress-induced activation of caspase-3, while cells with Syk in the cytoplasm were more susceptible (Zhou *et al.*, 2006), highlighting the importance of cellular location to Syk function. Thus, association of Syk at lysosomes found in this study may be pertinent to its role in modulating Aβ-mediated apoptosis in cortical neurons.

The role of the tumour suppressor protein, p53, in Aβ-induced association of Syk at lysosomes was investigated. Use of the p53 inhibitor, pifithrin-α, demonstrated that p53 is not involved in mediating Syk association at the lysosome. There is some evidence that identifies Syk among the genes

whose expression is down-regulated by p53 (Okamura *et al.*, 1999). In human colon carinoma cells, Syk gene expresssion is repressed in a p53-dependent manner, suggesting that loss of p53 function during tumorigenesis can lead to reduced Syk activity. This result indicates no involvement of p53 in Aβ-mediated association of Syk at lysosomes. In chapter 3, the results demonstrated an association between phospho-p53 and lysosomes, induced by exposing cells to Aβ for 6 hr. To determine whether Syk is involved in mediating phospho-p53 association with lysosomes, the Syk inhibitor was used. The findings indicate that following 6 hr of Aβ exposure, co-localisation of phospho-p53 at lysosomes is Syk dependent, suggestive of a role for Syk in the transport of intracellular molecules. In B cells, evidence indicates that Syk is necessary for the transport of BCR-endosomes to lysosomes, that is, movement of BCR from the plasma membrane, its internalisation and vesicular transport to lysosomes (He et al., 2005). Syk was also required for phagocytosis in macrophages (Bonnerot *et al.*, 1998). However, the results of that study do not exclude the possibility that a downstream effector activated by Syk and not Syk itself is the actual direct effector controlling lysosomal transport.

Whether Syk is directly influencing the transport of p53 to lysosomes remains to be clarified. Interestingly, the findings presented in chapter 3 also demonstrated a role for p53 in loss of lysosomal membrane integrity. Thus, lysosomal instability by p53 could be regulated by Syk.

Destabilisation of the lysosomal membrane by Aβ, as evidenced by the acridine orange relocation technique, was demonstrated in chapter 3. To examine the role of Syk in this process, cells were pretreated with the Syk inhibitor prior to Aβ treatment. The results provide evidence that Aβ-mediated loss of lysosomal membrane integrity at 6 hr, 24 hr and 48 hr is regulated by Syk. As previously mentioned, He and colleagues (2005) reported that after BCR crosslinking (antigen binding), lysosomal permeability was enhanced with the release of cathepsin-B, correlated with early apoptotic hallmarks. Syk appears essential for this BCR-induced apoptosis as lysosomes remained intact in Syk-deficient cells. It has been suggested that lysosomal membrane permeabilisation occurs upstream of mitochondrial permeabilisation in

apoptosis. As I have reported that Syk is also involved in Aβ-induced apoptosis in cortical cells, this result suggests that Syk is critical in the induction of the lysosomal branch of the cell death pathway. The ability of Syk to induce destabilisation of the lysosomal membrane is not fully understood, however, it may promote the association of certain proteins to the lysosome, such as the pro-apoptotic protein, Bax.

Results in chapter 4 demonstrated Bax association at lysosomes induced by 6 hr of Aβ treatment and in mitochondria following Aβ treatment for 30 min and 24 hr. To investigate whether Syk is involved in regulating colocalisation of Bax at lysosomes and mitochondria, Bax distribution was assessed using the Syk inhibitor in conjuction with Lysotracker red and Mitotracker red, respectively. Bax association at lysosomes and mitochondria was prevented by the Syk inhibitor, suggesting that Syk mediates the translocation of Bax from the cytosol to the intracellular organelles, the lysosome and the mitochondria. The significance of this finding is unclear. Initially, Syk was believed to control only the immune response, however, recent findings have reported that Syk plays a central role in multiple biological functions that are unrelated to the adaptive immune response. Bax is a member of the Bcl-2 family of proteins that can either induce (Bax) or inhibit (Bcl-2 and Bcl-XL) apoptosis by virtue of their ability to associate with the mitochondrial membrane and induce or prevent cytochrome *c* release, respectively. Although the mechanism of the interaction between Syk and Bax is at present unknown it may involve calcineurin signalling. Following apoptotic stimuli in hippocampal neurons, increases in intracellular calcium promotes calcineurin-induced dephosphorylation of Bad (Wang *et al.*, 1999), resulting in the activation and subsequent dimerisation of Bad with the antiapoptotic protein, Bcl-XL. Bax is then displaced from being bound by Bcl-XL (Yang *et al.*, 1995) and translocates to the mitochondria, where it promotes release of cytochrome *c* and activates the caspase cascade (Yamada *et al.*, 1993). Activation of Syk also induces an increase in intracellular calcium (Takata *et al.*, 1994) and can subsuquently induce calcineurin activation in immune cells (Hao et al., 2003). Our findings indicate that Syk mediates translocation of Bax from the cytosol to subcellular

organelles, whether this translocation could induce cell death in cortical neurons is unknown at present. Additional studies are required to investigate whether this signalling cascade involves calcineurin, whether the lysosome is an alternative target for Bax translocation, and if this signalling pathway is pertinent to $A\beta_{1-40}$-induced neurodegeneration.

In conclusion, the results presented here demonstrate the diverse roles of Syk in neuronal signalling. Although the exact nature of the Aβ-induced activation of Syk remains unknown, the evidence suggests that Syk modulates apoptosis through alterations in lysosomal stability and this may be highly pertinent in Aβ-mediated neurodegeneration. Recently, models of Syk-negative mice have been developed and studying these will be of great benefit to clarify the mechanism of Syk activation and functions in the brain.

*Chapter 6*

## 6.1 Introduction

The MAPK represent a group of enzymes that are activated by environmental stresses (Ip & Davis, 1998). The function of these kinases is to convert extracellular stimuli to intracellular signals, that in turn control the expression of genes that are essential for many cellular responses, including cell growth and death (Marshall, 1995). Three structurally related MAPK subfamilies have been identified in mammalian cells; the p42 and p44 kinases ERKs, JNKs SAPKs and the p38 MAPK family. These widely distributed kinases are activated by dual phosphorylation on threonine and tyrosine residues by upstream kinases as part of the cellular response to extracellular stimuli (Derkinderen *et al.*, 1999). Activation of MAP kinases is closely associated with synaptic plasticity (especially ERK1/2) and cell stress (JNK).

The stress-activated protein kinase, JNK, has been proposed as a mediator of cell death in response to a variety of stimuli such as growth factor deprivation (Logan *et al.*, 1997; Eilers *et al.*, 2001), excitotoxicity (Yang *et al.*, 1997), oxidative stress (Yoshizumi *et al.*, 2002), irradiation (Timokhina *et al.*, 1998), heat shock (Kyriakis *et al.*, 1994) and the cytokines IL-1β (Vereker *et al.*, 2000b) and TNF-α (De Cesaris *et al.*, 1999; Avdi *et al.*, 2001). Several pathways leading to JNK activation have been described, which although stimulus-dependent, display common features. These include the small G-proteins, Cdc42 and Rac1(Coso *et al.*, 1995; Minden *et al.*, 1995) and PI3K (Timokhina *et al.*, 1998; Ishizuka *et al.*, 1999). Three JNK isoforms have been identified, JNK1, JNK2 and JNK3, and these are encoded by independent genes, *jnk1, jnk2* and *jnk3*. The product of each gene reveal isoforms with approximate molecular weights of 46 (JNK1), 54 (JNK2) and 57 (JNK3), all of which are found in the mammalian brain (Gupta *et al.*, 1996). Since each of these isoforms is expressed in the brain (Gupta *et al.*, 1996) Aβ has the potential to couple to JNK1, JNK2 or JNK3. Indeed, studies from this and other laboratories have implicated JNK in Aβ-mediated effects (Troy *et al.*, 2001; Fogarty *et al.*, 2003)

JNK has the proclivity to phosphorylate a variety of nuclear and cytoplasmic substrates, some of which are vital for the apoptotic action of

JNK. It has been reported that JNK promotes cell death by promoting cytochrome *c* release from the mitochondria (Tournier *et al.*, 2000). In the nervous system, the proapoptotic mitochondrial-associated protein, Bax, acts downstream of JNK in regulating the translocation of mitochondrial cytochrome *c* into the cytosol (Kang *et al.*, 1998), and several studies have demonstrated an interaction between JNK and Bax in the cell death cascade (Lei *et al.*, 2002). Furthermore, increases in JNK are found in association with apoptotic neurons that are detected in the AD brain (Anderson *et al.*, 1994; de la Monte *et al.*, 1997), suggesting that activation of the JNK signalling cascade may mediate Aβ-induced neuronal cell death.

ERK, is a family of protein serine/threonine kinases of which the best characterised members are ERK1 (p44) and ERK2 (p42). ERK activation is typically associated with neuronal survival, proliferation, and differentiation given their activation by mitogens and some cell survival factors (Xia *et al.*, 1995). The ERK2 MAPK cascade is known to play a critical role in hippocampus synaptic plasticity and learning (English & Sweatt, 1997). Activation of ERK2 is required for contextual and spatial memory formation in mammals (Atkins *et al.*, 1998). In the CA1 area of the rodent hippocampus ERK2 is necessary for the expression of a late phase of LTP and is an important pathway through which neurotransmitters modulate LTP induction (Watabe *et al.*, 2000). Activation of ERK occurs after phosphorylation at threonine and tyrosine residues (Robbins *et al.*, 1993). ERKs are activated by MEKs which, in turn, are activated by MEKKs. Once activated, ERK phosphorylates and activates other protein kinases, among the substrates of ERK is the family of p90 ribosomal S6 kinases (p90rsk), and CREB protein (Wiggin *et al.*, 2002).

ERK activation can lead to contrasting physiological responses in the same cellular type, either transient stimulation of the ERK cascade leading to proliferation in PC12 cells, or sustained stimulation leads to differentiation (Marshall, 1995). Studies using a variety of cell cultures point to a possible linkage between Aβ and ERK activation (McDonald *et al.*, 1998; Combs *et al.*, 1999). $A\beta_{1\text{-}40}$ was also linked to the biphasic modulation of protein kinase C in neuronal cell cultures after anoxic stress (Kuperstein *et al.*, 2001).

It has been well established that extracellular stimuli promoting cellular activation induce the activation of nonreceptor PTK, including Syk, leading to the activation of Ras-Raf-Mek ERK signalling cascade (Macdonald *et al.*, 1993) in hematopoietic cells. Furthermore, Syk has been described as an upstream activator of JNK, in adherent neutrophils after TNF-$\alpha$ stimulation (Avdi *et al.*, 2001) and in B cells where JNK activity has been induced by oxidative stress (Qin *et al.*, 1997a). Promoted by the involvement of Syk in JNK and ERK activation in hematopoietic cells and the fact that A$\beta$ can couple to the JNK and ERK pathway in the nervous system, I set out to determine the role of Syk in the A$\beta_{1\text{-}40}$-mediated activation of JNK and ERK in cultured neurons.

## Chapter 6 RESULTS

### 6.1 $A\beta_{1-40}$ activates JNK1, JNK2 and JNK3 isoforms within a differential timeframe

In this study, the time course of $A\beta_{1-40}$ -induced activation of JNK, and the nature of the JNK isoform activated by $A\beta_{1-40}$, in cultured cortical neurons was assessed. Cytosolic expression levels of the phosphorylated (active) form of JNK1, JNK2 and JNK3 were measured by western immunoblot using an anti-active JNK antibody, which recognises JNK1, JNK2 and JNK3, phosphorylated on amino acid residues Thr-183 and Tyr-185. Expression of total JNK was analysed by western immunoblot with a polyclonal antibody, which recognises total JNK. Bandwidths were quantified using densitometry. The data presented is % of phosphorylated JNK expression over total JNK expression.

Exposure of cultured cortical neurons to $A\beta_{1-40}$ (2$\mu$M) resulted in the activation of the JNK protein within the cytosol in a time-dependent manner (Figure 6.1). Interestingly, there was a differential timeframe of activation for JNK1, JNK2 and JNK3. JNK1 activity at 1 hr was not expressed at sufficiently high levels for densitometric analysis, see Figure 6.1A. There was no effect on JNK1 activity following treatment of cells with $A\beta_{1-40}$ (2$\mu$M) for 24 hr or 48 hr (Figure 6.1A). In terms of the JNK 2 time course of activation (Figure 6.1B), in control cells % JNK2 expression was 1.45 ± 0.14 (arbitrary units; mean band width ± SEM) and this was significantly increased to 2.01 ± 0.07 following treatment with $A\beta_{1-40}$ for 24 hr ($p<0.01$, ANOVA, n=6) and 1.96 ± 0.05 following treatment with$_{1-40}$ A$\beta$ for 48 hr ($p<0.01$, ANOVA, n=6). At the earlier time point of 1 hr, treatment with $A\beta_{1-40}$ had no effect on JNK2 expression (1.35 ± 0.08 ).

In contrast, Figure 6.1C demonstrates that activation of JNK3 occured within 1 hr. Thus, expression of active JNK3 was 0.55 ± 0.09 (arbitrary units; mean bandwidth ± SEM) in control cells and this was significantly increased to 1.70 ± 0.44 when neurons were cultured in media containing $A\beta_{1-40}$ (2$\mu$M) for 1 hr ($P<0.001$, ANOVA, n=6). However, no change in JNK3 activity was

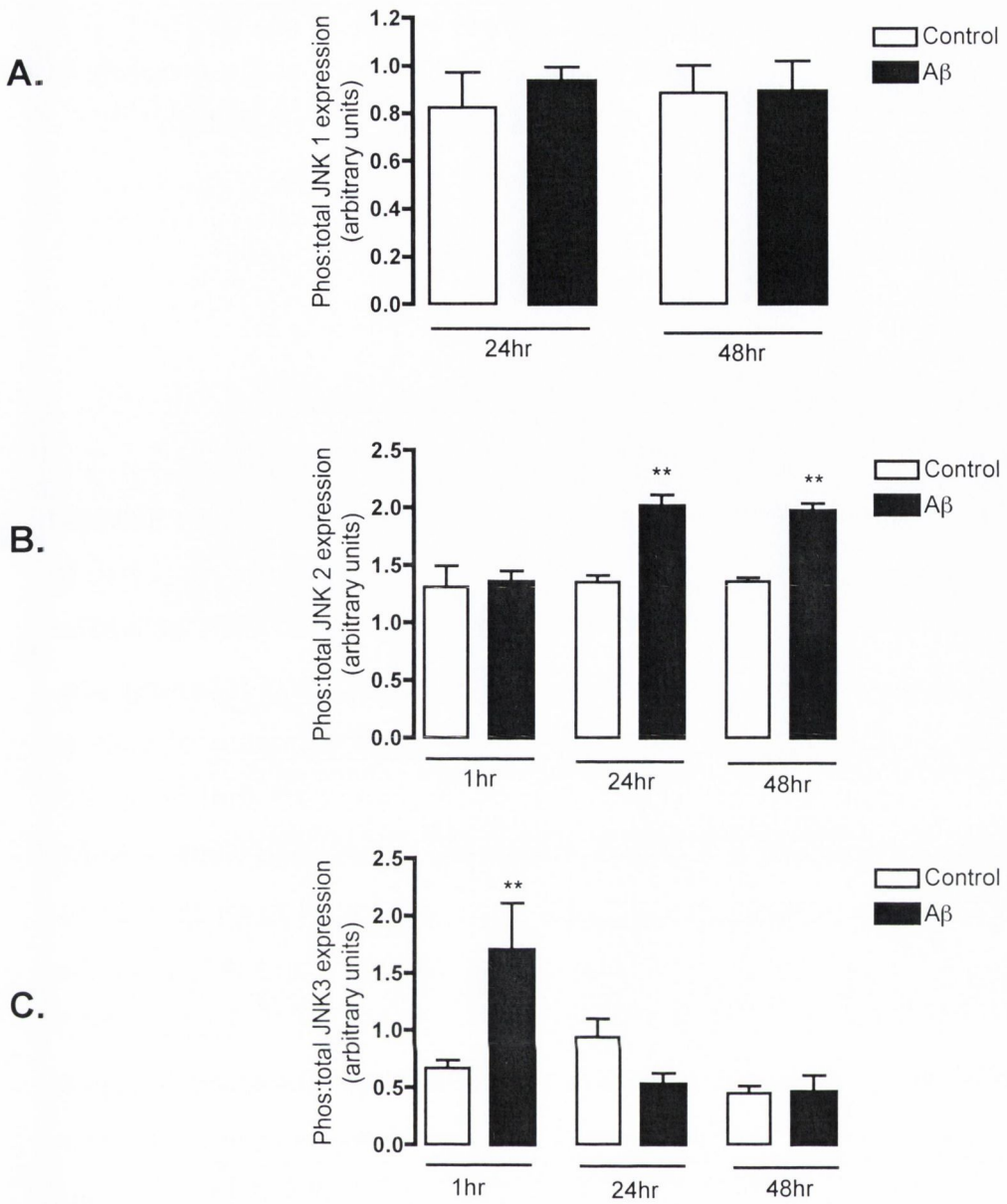


**Figure 6.1 Timecourse of $A\beta_{1-40}$-induced activation of JNK**

Cortical neurons were exposed with $A\beta_{1-40}$ (2μM) for 1-48 hr, cells were harvested and fractions analysed for the expression levels of the phosphorylated and total forms of JNK1, JNK2 and JNK3 using western immunoblot. Results are expressed as mean ± SEM for 6 independent observations.

**A.** No significant changes in levels of JNK1 activiation were found at 24 hr or 48 hr.

**B.** A significant increase in JNK2 activity was found following treatment with $A\beta_{1-40}$ for 24 hr and 48 hr (ANOVA**$p<0.01$).

**C.** JNK3 activity was significantly increased when neurons were treated with $A\beta_{1-40}$ for 1 hr (ANOVA***$p<0.001$).

observed at subsequent timepoints. This result indicates that the proclivity of $A\beta_{1-40}$ to regulate JNK1/2/3 isoforms follows a distinct temporal pattern.

## 6.2 Effect of $A\beta_{1-40}$ on JNK1 activity at 24 hr and 48 hr

JNK protein kinases are activated by dual phosphorylation on threoine and tyrosine residues by upstream kinases as part of the cellular response to stress. In order to determine whether the effect of $A\beta_{1-40}$ on JNK activation was dependent on the Syk, activity of JNK1 was measured following pre-treatment with the Syk inhibitor (50nM) for 60 min and exposure of cells to $A\beta_{1-40}$ (2$\mu$M) for 24 hr and 48 hr. Figure 6.2A demonstrates that in control cells JNK1 activity was 8.22 ± 1.47 (arbitrary units; mean band width ± SEM) and this did not alter following $A\beta_{1-40}$ (2$\mu$M) treatment for 24 hr (9.35 ± 0.68). Neurons treated with Syk inhibitor alone (6.26 ± 1.21) and $A\beta_{1-40}$ in the presence of Syk inhibitor (5.75 ± 1.63) for 24 hr displayed a level of JNK1 activity comparable to control cells. Similarly, exposure of cells to $A\beta_{1-40}$ (2$\mu$M) for 48 hr had no effect on levels of JNK1 activity, where control expression was (0.344 ± 0.09) and following treatment with $A\beta_{1-40}$ (0.38 ± 0.11). Neurons treated to Syk inhibitor alone (0.38 ± 0.10) and $A\beta_{1-40}$ in the presence of Syk inhibitor (0.311 ± 0.10) for 48 hr displayed a level of JNK1 activity comparable to control cells. This demonstrates that $A\beta_{1-40}$ does not modulate the activity of JNK1 at the time points measured. A sample immunoblot demonstrating the effects of $A\beta_{1-40}$ on JNK1 is shown in Figure 6.2B.

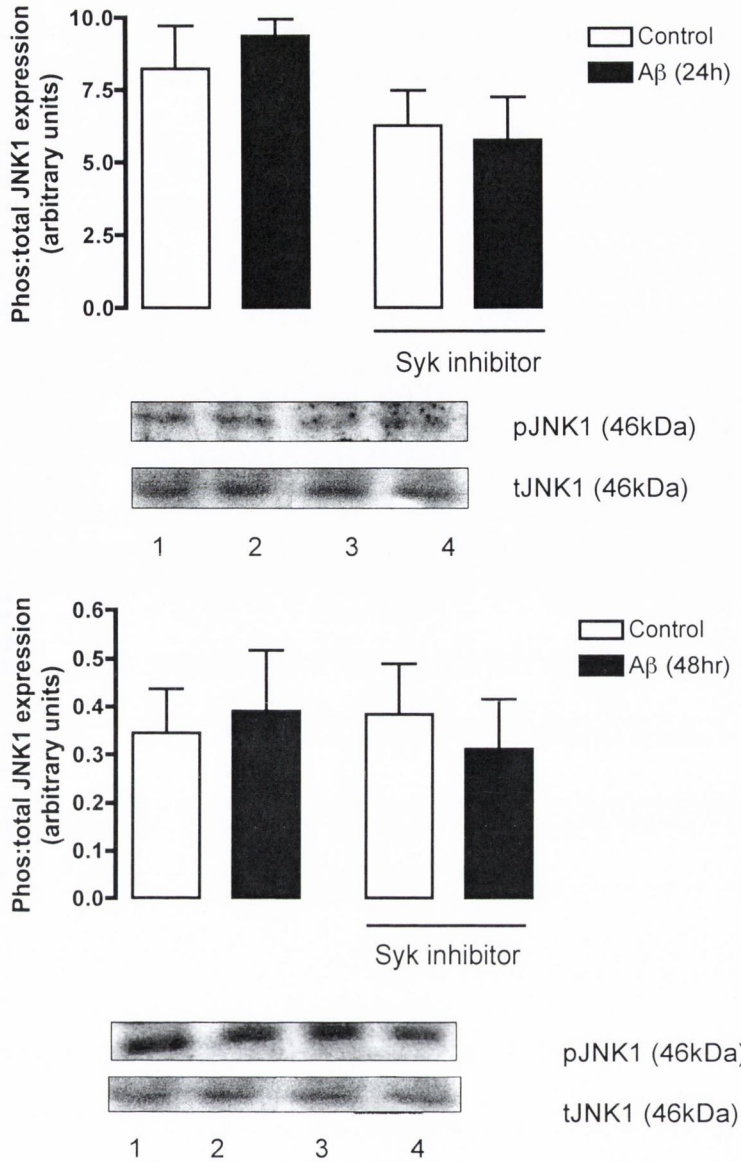


**Figure 6.2 Effect of $A\beta_{1-40}$ on JNK 1 activation at 24 hr and 48 hr**

Cortical neurons were treated with $A\beta_{1-40}$ (2μM) in the presence or absence of Syk inhibitor (50nM) for 24 hr and 48 hr and the levels of JNK1 activation assessed by western immunoblot.

**A** $A\beta_{1-40}$ had no effect on JNK1 activity at 24 hr. Results are expressed as mean ± SEM for 6 independent observations. Inset: Sample western immunoblot demonstrating pJNK and tJNK expression in control (lane1), $A\beta_{1-40}$-treated (lane 2), Syk inhibitor (lane 3) and $A\beta_{1-40}$+ Syk inhibitor (lane 4).

**B** Incubation of cells for 48 hr with $A\beta_{1-40}$ did not effect JNK1 activity. Results are expressed as mean ± SEM for 6 independent observations. Inset: Sample western immunoblot demonstrating pJNK and tJNK expression in control (lane1), $A\beta_{1-40}$-treated (lane 2), Syk inhibitor (lane 3) and $A\beta_{1-40}$ + Syk inhibitor (lane 4).

## 6.3 Effect of $A\beta_{1-40}$ on JNK2 activity at 1 hr

In this study, expression levels of JNK2 were measured by western immunoblot using a polyclonal anti-phospho-specific JNK2 antibody and bandwidths were quantified using densitometry (Figure 6.3). No change in JNK2 activity was observed following exposure of neurons to $A\beta_{1-40}$ (2μM) for 1 hr, where controls values were 1.56 ± 0.21 and 1.35 ± 0.08 in cells treated with $A\beta_{1-40}$. Neurons treated to Syk inhibitor (50nM) alone (1.40 ± 0.12) and $A\beta_{1-40}$ in the presence of Syk inhibitor (1.37 ± 0.19) for 1 hr displayed a level of JNK2 activity comparable to control cells. This demonstrates that $A\beta_{1-40}$ does not modulate the activity of JNK2 at 1 hr. A sample immunoblot demonstrating the effects of $A\beta_{1-40}$ on JNK2 is shown in Figure 6.3B.

## 6.4 $A\beta_{1-40}$-induced increase in JNK2 activity is dependent on Syk

To determine whether the $A\beta_{1-40}$-induced JNK2 activation at 24 hr was dependent on Syk, we employed the use of the selective Syk inhibitor (50nM). Figure 6.4 demonstrates that in neurons treated with NBM alone (control) for 24 hr, JNK2 activity was 30.17 ± 1.96 (arbitrary units; mean band width ± SEM) and this was significantly increased following $A\beta_{1-40}$ (2μM; 24 hr) treatment to 40.69 ± 1.92 ($p<0.05$, ANOVA, n=6). Pretreatment with Syk inhibitor alone has no effect on JNK2 activity in control cells (36.67 ± 1.63 ), and in the presence of the Syk inhibitor $A\beta_{1-40}$ has no influence on JNK2 activation (37.33 ± 2.70). This suggests that $A\beta_{1-40}$-mediates an increase in JNK2 activity at 24 hr and this is prevented by Syk inhibition. A sample immunoblot demonstrating the effects of $A\beta_{1-40}$ on JNK2 is shown in Figure 6.4B.

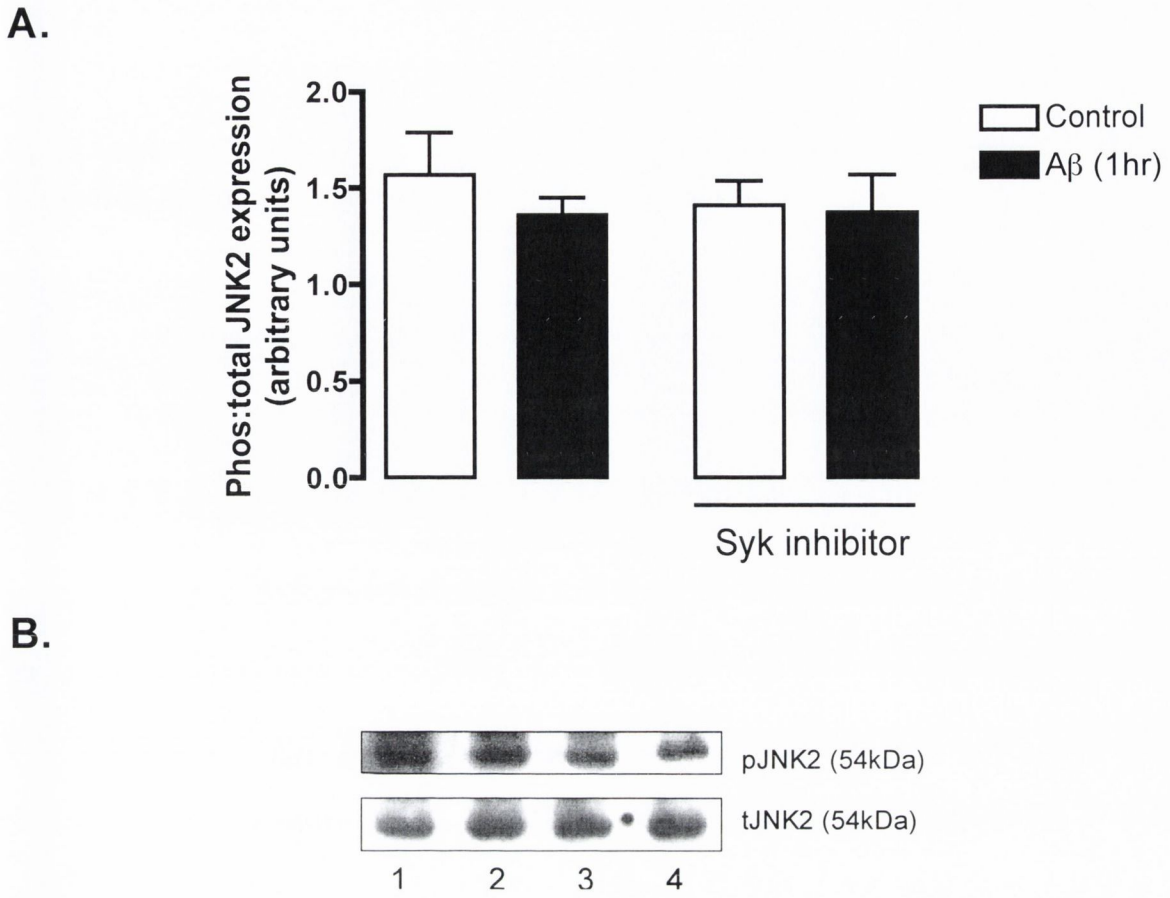


**Figure 6.3 Effect of $A\beta_{1-40}$ on JNK2 activity at 1 hr**

**A** Cortical neurons were treated with $A\beta_{1-40}$ (2μM) in the presence or absence of Syk inhibitor (50nM) for 1 hr and the levels of JNK2 activation assessed by western immunoblot. $A\beta_{1-40}$ had no effect on JNK2 activity at 1 hr. Results are expressed as mean ± SEM for 6 independent observations, ANOVA $p>0.05$.

**B** A sample western immunoblot showing equal expression levels of tJNK2 in vehicle-treated controls (lane 1), $A\beta_{1-40}$-treated neuons (lane 2), Syk inhibitor (lane 3) and Syk inhibitor + $A\beta_{1-40}$-treated (lane 4) cortical neurons.

A.

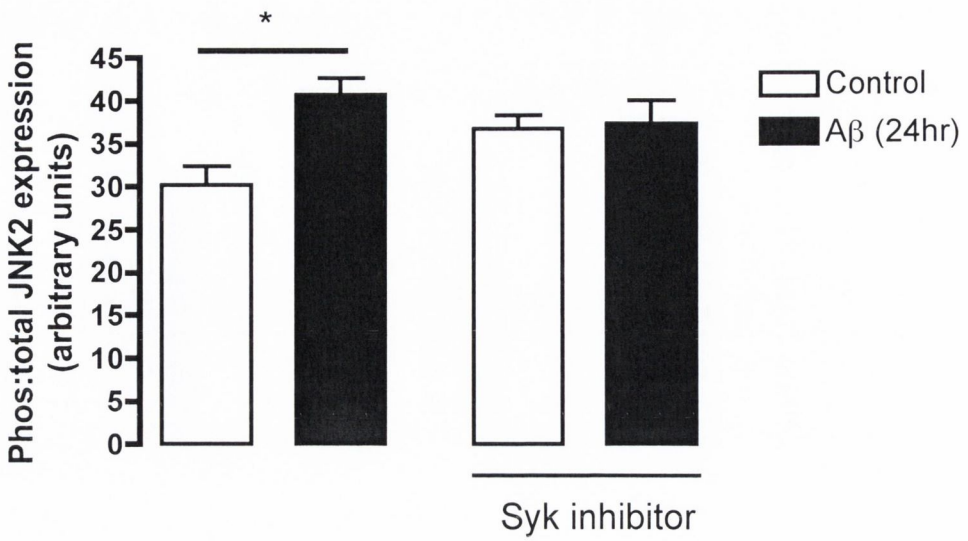


B.

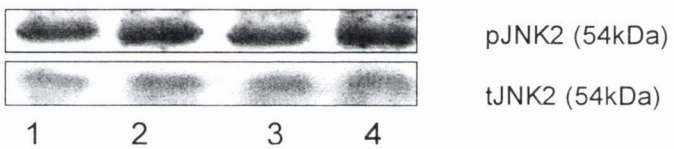


**Figure 6.4 $A\beta_{1-40}$ increases JNK2 activity at 24 hr**

Cultured cortical neurons were pre-incubated with Syk inhibitor (50nM) for 60 min prior to $A\beta_{1-40}$ (2μM) treatment for 24 hr. Following treatments cell protein was harvested and analysed for JNK2 activity using western immunoblot.

**A** Pre-incubation of cells with the Syk inhibitor prior to $A\beta_{1-40}$ exposure prevented the $A\beta_{1-40}$-induced increase in JNK2 activity observed at 24 hr. Results are expressed as mean ± SEM for 6 independent observations, ANOVA *$p<0.05$

**B** A sample western immunoblot showing equal expression levels of tJNK2 in vehicle-treated controls (lane 1), $A\beta_{1-40}$-treated neuons (lane 2), Syk inhibitor (lane 3) and Syk inhibitor + $A\beta_{1-40}$-treated (lane 4) cortical neurons.

A.

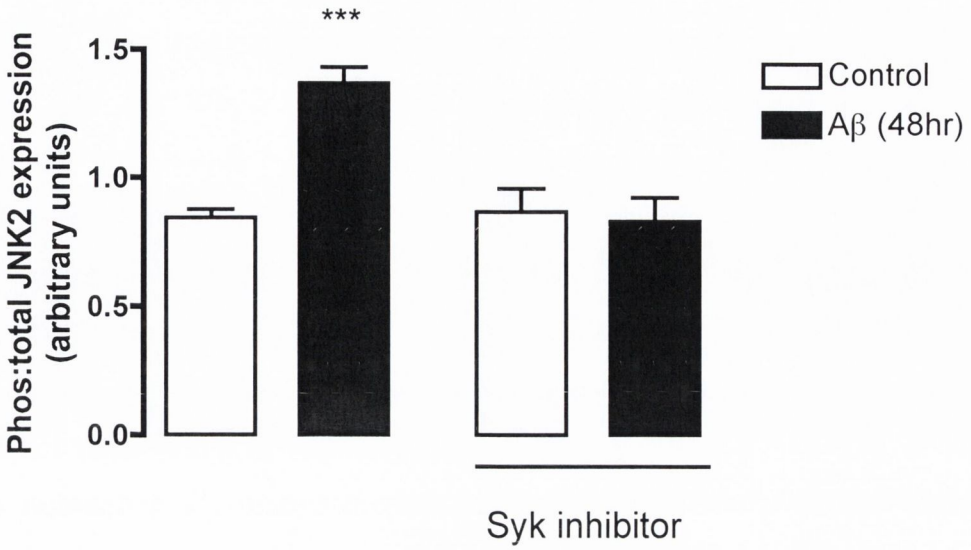


B.

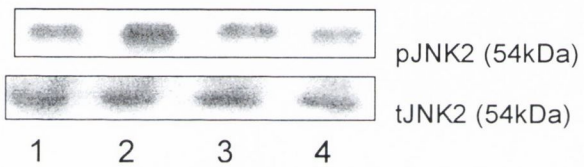


**Figure 6.5 Syk is required for JNK2 activation in $A\beta_{1-40}$-treated cells**

**A** Treatment of primary cortical neurons with $A\beta_{1-40}$ (2μM; 48 hr) significantly increased activity of JNK2 as assessed by western immunoblot. The stimulatory effect of $A\beta_{1-40}$ on JNK2 activity was prevented by Syk inhibitor (50nM). Exposure of cells to Syk inhibitor alone had no effect on JNK2 activity. Results are expressed as mean ± SEM for 6 independent observations, ANOVA ***$p<0.001$

**B** A sample western immunoblot showing equal expression levels of tJNK2 in vehicle-treated controls (lane 1), $A\beta_{1-40}$-treated neuons (lane 2), Syk inhibitor (lane 3) and Syk inhibitor + $A\beta_{1-40}$-treated (lane 4) cortical neurons.

## 6.5 Syk inhibitor pretreatment prevents $A\beta_{1-40}$-induced JNK activation

To determine whether Syk is involved in $A\beta_{1-40}$-induced JNK2 activation at 48 hr, cortical neuronal cells were pre-treated with Syk inhibitor (50nM) for 60 min and exposure of cells to $A\beta_{1-40}$ (2μM) for 48 hr. Figure 6.5 demonstrates that Syk inhibitor prevented the Aβ-induced activation of JNK2. Thus, in neurons treated with vehicle for 48 hr, JNK2 activity was 0.84 ± 0.03 (arbitrary units; mean band width ± SEM) and this was significantly increased following $A\beta_{1-40}$ (2μM) treatment (48hr) to 1.36 ± 0.06 ($p<0.001$, ANOVA, n=6). While pretreatment with Syk inhibitor alone has no effect on JNK2 activity (0.86 ± 0.10), it prevented the $A\beta_{1-40}$-induced increase in JNK2 activity (0.82 ± 0.10). Sample immunoblots demonstrating the activation of JNK2 following $A\beta_{1-40}$-treatment and the abolition of these effects in Syk inhibitor-treated cells are shown in figure 6.5B. This result provides evidence of a role for Syk in $A\beta_{1-40}$-induced activation of JNK2.

## 6.6 $A\beta_{1-40}$ activates JNK3 at 1 hr via Syk

The involvement of Syk in $A\beta_{1-40}$-induced activation of JNK3 was assessed using western immunoblot analysis. Cortical neuronal cells were pre-treated with Syk inhibitor (50nM) for 60 min and exposure of cells to $A\beta_{1-40}$ (2μM) for 1 hr. Figure 6.6 demonstrates that in neurons treated with vehicle for 1 hr, JNK3 activity was 0.67 ± 0.08 (arbitrary units; mean band width ± SEM) and this was significantly increased following $A\beta_{1-40}$ (2μM) treatment (1hr) to 1.70 ± 0.17 ($p<0.01$, ANOVA, n=6). While pretreatment with Syk inhibitor alone has no effect on JNK3 activity (0.26 ± 0.10), it prevented the $A\beta_{1-40}$-induced increase in JNK3 activity (0.48 ± 0.17). Sample immunoblots demonstrating the activation of JNK3 following $A\beta_{1-40}$-treatment and the abolition of these effects in Syk inhibitor-treated cells are shown in figure 6.6B. This result provides evidence of a role for Syk in $A\beta_{1-40}$-induced activation of JNK3.

A.

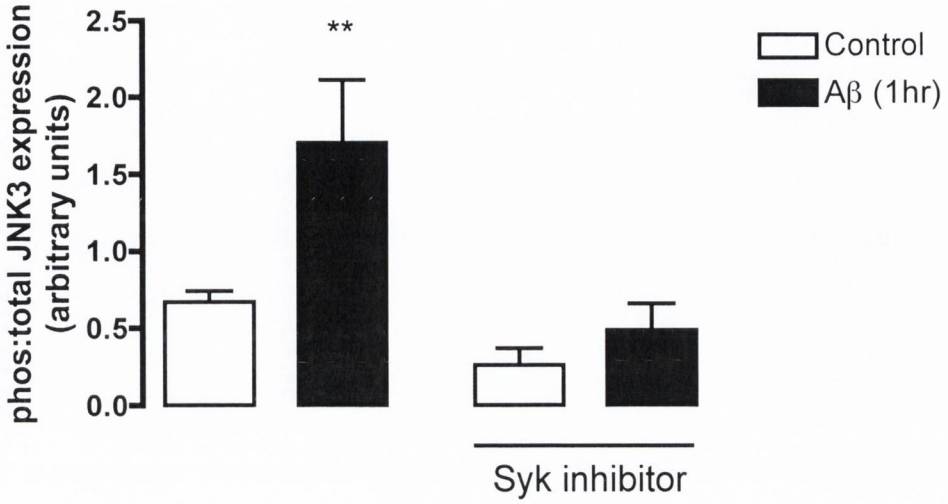


B.

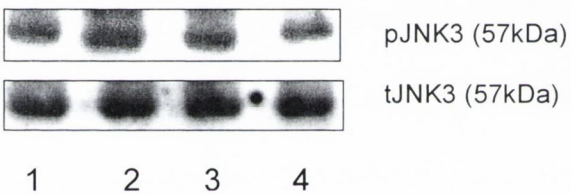


**Figure 6.6 $A\beta_{1-40}$ induces an increase in JNK3 activity at 1 hr via Syk**

**A** Cortical neurons were treated with $A\beta_{1-40}$ (2μM) in the presence or absence of Syk inhibitor (50nM) for 1 hr and the levels of JNK3 activation assessed by western immunoblot. $A\beta_{1-40}$ significantly increased JNK3 activity at 1 hr. Exposure to Syk inhibitor abolished the $A\beta_{1-40}$-induced increse in JNK3 activation. Results are expressed as mean ± SEM for 6 independent observations, ANOVA **$p<0.01$

**B** A sample western immunoblot showing equal expression levels of tJNK3 in vehicle-treated controls (lane 1), $A\beta_{1-40}$-treated neuons (lane 2), Syk inhibitor (lane 3) and Syk inhibitor + $A\beta_{1-40}$-treated (lane 4) cortical neurons.

## 6.7 $A\beta_{1-40}$ does not effect JNK3 activity at 24 hr

In this study, activity levels of JNK3 were measured by western immunoblot and the role of Syk was investigated using the Syk inhibitor (50nM). Bandwidths were quantified using densitometry (Figure 6.7). No change in JNK3 activity was observed following exposure of neurons to $A\beta_{1-40}$ (2μM) for 24 hr, where controls values were 11.10 ± 2.38 and 5.26 ± 1.07 in cells treated with $A\beta_{1-40}$. Neurons treated with Syk inhibitor alone (11.55 ± 4.34) and $A\beta_{1-40}$ in the presence of Syk inhibitor (7.48 ± 2.59) for 1 hr displayed a level of JNK3 activity comparable to control cells. This demonstrates that $A\beta_{1-40}$ does not modulate the activity of JNK3 at 24 hr. A sample immunoblot demonstrating the effects of $A\beta_{1-40}$ on JNK3 is shown in Figure 6.7B.

## 6.8 Effect of $A\beta_{1-40}$ on JNK3 activity at 48 hr

In this experiment, activity of JNK3 was measured following pre-treatment with the Syk inhibitor (50nM) for 60 min and exposure of cultures to $A\beta_{1-40}$ (2μM) for 48 hr. Figure 6.8 demonstrates that in control cells JNK3 activity was 0.44 ± 0.05 (arbitrary units; mean band width ± SEM) and this did not alter following $A\beta_{1-40}$ treatment for 48 hr (0.46 ± 0.10). Neurons treated to Syk inhibitor alone (0.50 ± 0.04) and $A\beta_{1-40}$ in the presence of Syk inhibitor (0.44 ± 0.03) for 48 hr displayed a level of JNK3 activity comparable to control cells. This demonstrates that $A\beta_{1-40}$ does not modulate the activity of JNK3 at 48 hr. A sample immunoblot demonstrating the effects of $A\beta_{1-40}$ on JNK3 is shown in Figure 6.8B.

A.

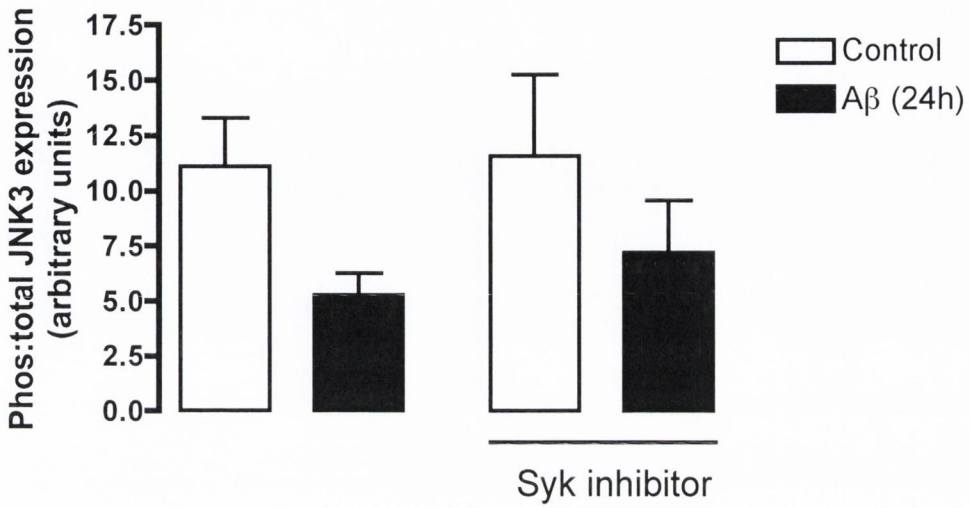


B.

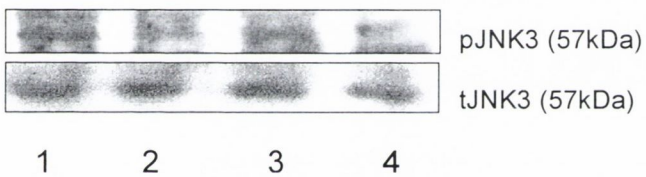


**Figure 6.7 Effect of $A\beta_{1-40}$ on JNK3 activity at 24 hr**

Cultured cortical neurons were pre-incubated with Syk inhibitor (50nM) for 60 min prior to $A\beta_{1-40}$ (2$\mu$M) treatment for 24 hr. Following treatments cell protein was harvested and analysed for JNK3 activity using western immunoblot.

**A** Exposure of cells to $A\beta_{1-40}$ (2$\mu$M) for 24 hr did not effect activity of JNK3. Results are expressed as mean ± SEM for 6 independent observations, ANOVA *$p<0.05$

**B** A sample western immunoblot showing equal expression levels of tJNK3 in vehicle-treated controls (lane 1), $A\beta_{1-40}$-treated neuons (lane 2), Syk inhibitor (lane 3) and Syk inhibitor + $A\beta_{1-40}$-treated (lane 4) cortical neurons.

A.

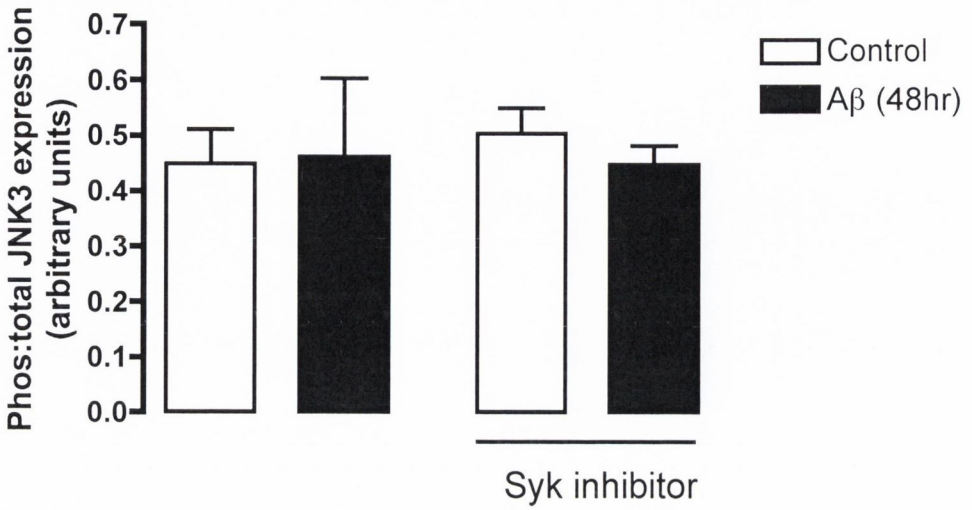


B.

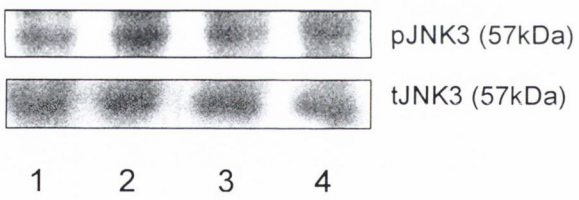


**Figure 6.8 Effect of $A\beta_{1-40}$ on JNK3 activity at 48 hr**

**A** Cortical neurons were treated with $A\beta_{1-40}$ (2μM) for 48 hr in the presence or absence of Syk inhibitor (50nM) and the levels of JNK3 activation assessed by western immunoblot. $A\beta_{1-40}$ had no effect on JNK3 activity at 1 hr. Results are expressed as mean ± SEM for 6 independent observations, ANOVA $p>0.05$

**B** A sample western immunoblot showing equal expression levels of tJNK3 in vehicle-treated controls (lane 1), $A\beta_{1-40}$-treated neuons (lane 2), Syk inhibitor (lane 3) and Syk inhibitor + $A\beta_{1-40}$-treated (lane 4) cortical neurons.

## 6.9 $A\beta_{1-40}$ activates ERK2 in a time-dependent manner

To delineate the time course of $A\beta_{1-40}$-induced ERK2 activation and to furthermore characterise the role of ERK2 in Aβ-mediated neuronal signalling, cultured cortical neurons were exposed to $A\beta_{1-40}$ (2μM) for various time points (1-48 hr). Expression levels of phosphorylated ERK2 and total ERK were measured by western immunoblotting and band widths were quantified using densitometry (Figure 6.9). Exposure of cells to $A\beta_{1-40}$ (2μM) for 1 hr resulted in no change in ERK2 activity (0.64 ± 0.07) compared to control ( 0.72 ± 0.17; ANOVA, $p>0.05$, n=6). However, at the later time points of 24 hr and 48 hr, there was a significant increase in ERK2 activity, (1.87 ± 0.31, $p<0.01$, ANOVA, n=6) at 24 hr and (3.18 ± 0.61, $p<0.001$, ANOVA, n=6) at 48 hr. This result indicates that the proclivity of $A\beta_{1-40}$ to regulate ERK2 activity follows a distinct temporal pattern.

## 6.10 $A\beta_{1-40}$ does not modulate ERK2 activity at 1 hr

To investigate whether Syk is involved in $A\beta_{1-40}$-mediated neuronal signalling, cortical cultured neuronal cells were treated with $A\beta_{1-40}$ (2μM) for 1 hr in the presence or absence of Syk inhibitor (50nM) and the levels of ERK2 activation assessed by western immunoblot. Figure 6.10 demonstrates that in control cells ERK2 activity was 0.51 ± 0.11 (arbitrary units; mean band width ± SEM) and this did not alter following $A\beta_{1-40}$ treatment for 1 hr (0.60 ± 0.05). Neurons treated with Syk inhibitor alone (0.63 ± 0.02) or $A\beta_{1-40}$ in the presence of Syk inhibitor (0.60 ± 0.13) for 1 hr displayed a level of ERK2 activity comparable to control cells. This demonstrates that $A\beta_{1-40}$ does not modulate the activity of ERK2 at 1 hr. A sample immunoblot demonstrating the effects of $A\beta_{1-40}$ on ERK2 is shown in Figure 6.10B.

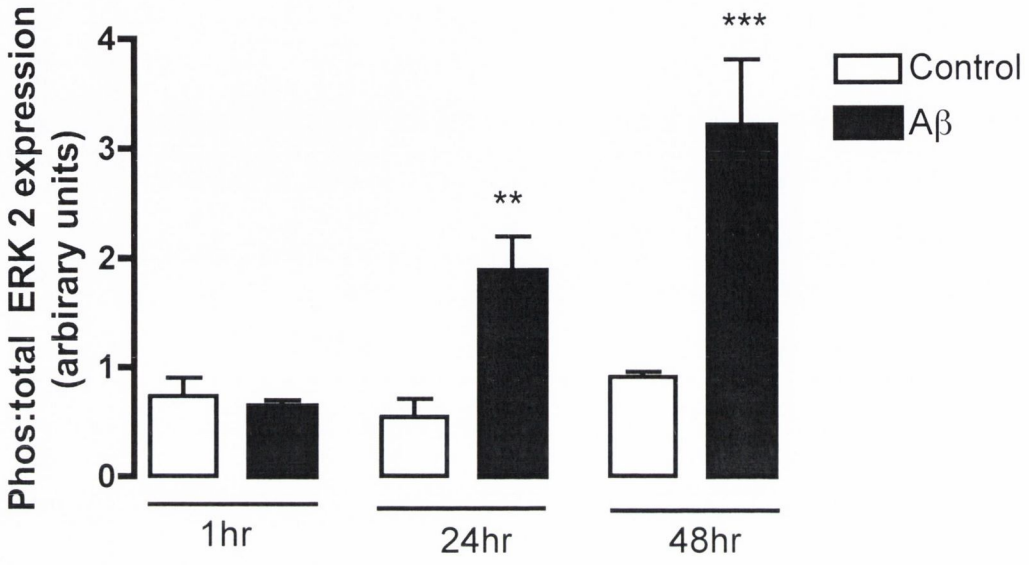


**Figure 6.9 Timecourse of $A\beta_{1-40}$-induced activation of ERK 2**

Cortical neurons were exposed with $A\beta_{1-40}$ (2μM) for 1-48 hr, cells were harvested and fractions analysed for the expression levels of the phosphorylated and total forms of ERK2 using western immunoblot. Results are expressed as mean ± SEM for 6 independent observations. A significant increase in ERK2 activity was found following treatment with $A\beta_{1-40}$ for 24 hr and 48 hr (ANOVA**$p<0.0$, ***$p<0.001$).

A.

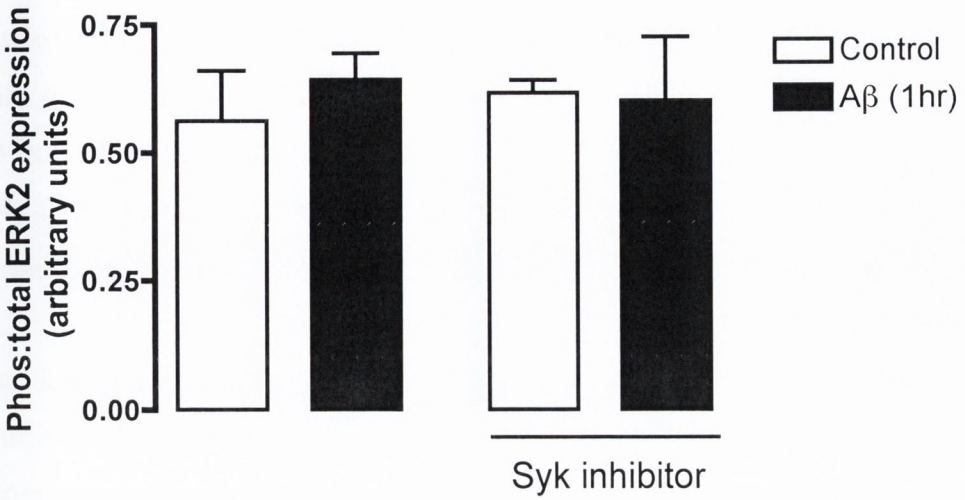


B.

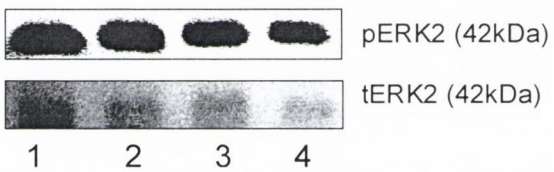


**Figure 6.10 Effect of $A\beta_{1-40}$ on ERK2 activity at 1 hr**

**A** Cortical neurons were treated with $A\beta_{1-40}$ (2μM) for 1 hr in the presence or absence of Syk inhibitor (50nM) and the levels of ERK2 activation assessed by western immunoblot. $A\beta_{1-40}$ had no effect on ERK2 activity at 1 hr. Results are expressed as mean ± SEM for 6 independent observations, ANOVA $p>0.05$

**B** A sample western immunoblot showing equal expression levels of tERK2 in vehicle-treated controls (lane 1), $A\beta_{1-40}$-treated neuons (lane 2), Syk inhibitor (lane 3) and Syk inhibitor + $A\beta_{1-40}$-treated (lane 4) cortical neurons.

## 6.11 $A\beta_{1-40}$-induced modulation of ERK2 at 24 hr and 48 hr is Syk dependent

To determine whether $A\beta_{1-40}$-induced ERK2 activation was reliant on signalling through Syk, cultured cortical neurons were pre-treated with the Syk inhibitor (50nM) for 60 min prior to $A\beta_{1-40}$ (2μM) exposure for 24 hr and 48 hr. Since $A\beta_{1-40}$ was found to activate ERK2 activation at 24hr and 48 hr (Figure 6.10), the effects of Syk inhibitor (50nM) on ERK2 activation at these time points was evaluated.

Figure 6.11 shows that in control neurons the level of ERK2 activity was 0.94 ± 0.02 and this was significantly increased following $A\beta_{1-40}$ (2μM; 24 hr) treatment to 1.87 ± 0.28 ($p<0.05$, ANOVA, n=6). While pre-treatment with Syk inhibitor alone had no effect on ERK2 activation (1.35 ± 0.25), it prevented the $A\beta_{1-40}$-induced increase in ERK2 activity (1.58 ± 0.35). This result provides evidence of a role for Syk in the $A\beta_{1-40}$-induced activation of ERK2. A sample immunoblot demonstrating the activation of ERK2 following $A\beta_{1-40}$ treatment for 24 hr and the abolition of this effect in Syk inhibitor-treated cells is shown in Figure 6.11B.

Figure 6.12 demonstrates that ERK2 activation in control neurons was significantly increased from 2.33 ± 0.23 to 4.69 ± 0.55 following treatment with $A\beta_{1-40}$ (2μM) for 48 hr ($p<0.05$, ANOVA, n=6). Exposure to Syk inhibitor alone had no effect on ERK2 activity (1.96 ± 0.50) and it prevented the $A\beta_{1-40}$-induced increase in ERK2 activity (2.40 ± 0.47), indicating that $A\beta_{1-40}$-induces ERK2 activity via Syk. A sample immunoblot demonstrating the Syk-dependent activation of ERK2 following $A\beta_{1-40}$ treatment is shown in Figure 6.12B.

A.

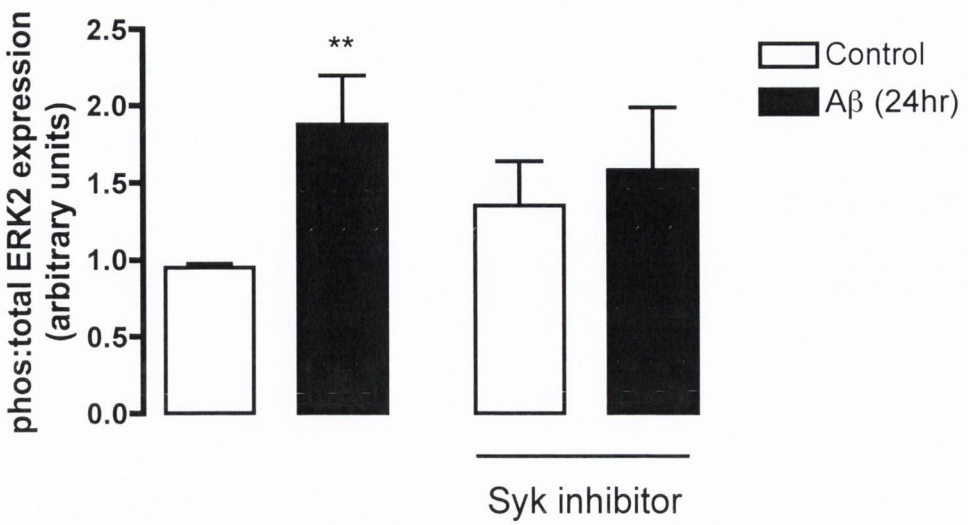


B.

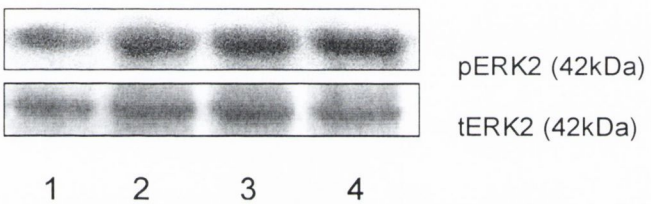


**Figure 6.11 $A\beta_{1-40}$ induces an increase in ERK2 activity at 24 hr**

**A** Cortical neurons were treated with $A\beta_{1-40}$ (2μM) in the presence or absence of Syk inhibitor (50nM) for 24 hr and the levels of ERK2 activation assessed by western immunoblot. $A\beta_{1-40}$ significantly increased ERK2 activity at 24 hr. Exposure to Syk inhibitor abolished the $A\beta_{1-40}$-induced increse in ERK2 activation.Results are expressed as mean ± SEM for 6 independent observations, ANOVA **$p<0.01$

**B** A sample western immunoblot showing equal expression levels of tERK2 in vehicle-treated controls (lane 1), $A\beta_{1-40}$-treated neuons (lane 2), Syk inhibitor (lane 3) and Syk inhibitor + $A\beta_{1-40}$-treated (lane 4) cortical neurons.

A.

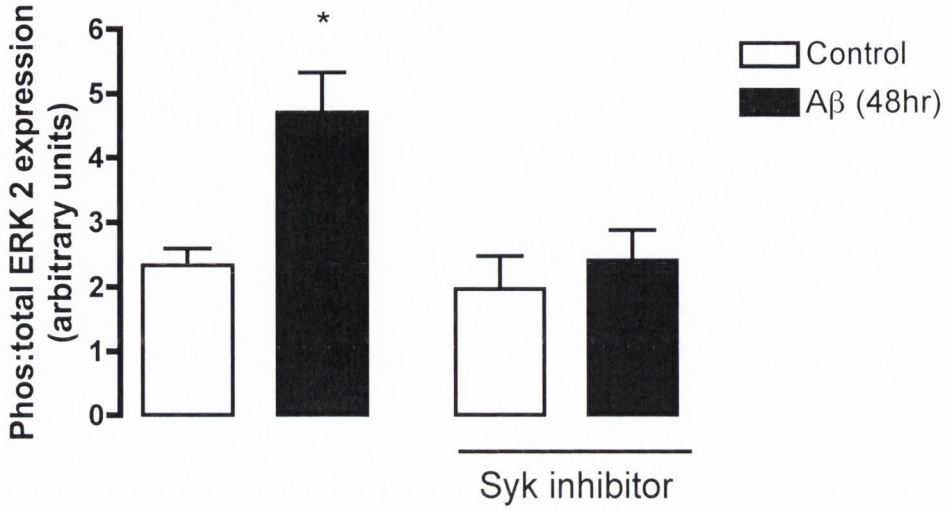


B.

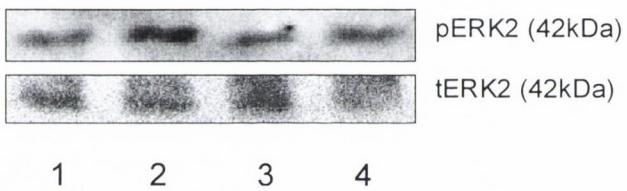


**Figure 6.12 $A\beta_{1-40}$ induces an increase in ERK2 activity at 48 hr**

**A** Cortical neurons were treated with $A\beta_{1-40}$ (2μM) in the presence or absence of Syk inhibitor (50nM) for 48 hr and the levels of ERK2 activation assessed by western immunoblot. $A\beta_{1-40}$ significantly increased ERK2 activity at 48 hr. Exposure to Syk inhibitor abolished the $A\beta_{1-40}$-induced increse in ERK2 activation.Results are expressed as mean ± SEM for 6 independent observations, ANOVA **$p<0.01$

**B** A sample western immunoblot showing equal expression levels of tERK2 in vehicle-treated controls (lane 1), $A\beta_{1-40}$-treated neuons (lane 2), Syk inhibitor (lane 3) and Syk inhibitor + $A\beta_{1-40}$-treated (lane 4) cortical neurons.

## 6.3 Discussion

The aim of this study was to examine the role of Syk in $A\beta_{1-40}$-mediated induction of JNK and ERK in cultured cortical neurons. The findings demonstrate a differential timeframe of JNK2 and JNK3 activation by $A\beta_{1-40}$ in this system, with JNK1 not being activated by $A\beta_{1-40}$. While JNK2 activation was apparent after a 24 hr exposure to $A\beta_{1-40}$ and continued up to 48 hr, JNK3 activation was rapidly induced by $A\beta_{1-40}$ (within 1 hr) and then returned to basal levels at 24 hr and 48 hr. The early activation of JNK3 suggests it may be involved in the $A\beta_{1-40}$-induced activation of apoptosis. To determine if Syk plays a role in JNK2 and JNK3 activation, the Syk inhibitor was used. The findings demonstrated that the regulation of JNK2 by $A\beta_{1-40}$ was mediated via Syk at 24 hr and 48 hr and the $A\beta_{1-40}$-induced activation of JNK3 at 1 hr was also Syk-dependent. In addition, $A\beta_{1-40}$ induced activation of ERK2, at the relatively late timepoint of 24 hr and 48 hr respectively in cultured cortical cells. Again, the ability of Syk to regulate $A\beta_{1-40}$-induced ERK activation was blocked by the Syk inhibitor implicating a role for Syk in modulating ERK activation in cultured cortical neurons. These results demonstrate that $A\beta_{1-40}$ has a differential pattern of signalling through the JNK pathway and provide evidence that $A\beta_{1-40}$-meditates activation of ERK2, suggesting an interaction between the MAP kinases, JNK and ERK, and Syk in this system.

Generally, JNK signalling functions in stress responses, such as DNA damage and apoptosis, while activation of ERK is associated with regulation of growth and differentiation. However, since cells are simultaneously exposed to multiple extracellular stimuli, each cell must intergrate these signals and instigate the appropriate response. Consequently, the biological context of a signal plays an important role in how the cell will respond to MAPK activation. JNK1 protein expression was moderate in my cell culture model, hence the role of Syk in mediating $A\beta_{1-40}$-induced activation of the JNK2 and JNK3 isoforms was investigated. JNK2 activation was significantly increased at 24 hr and 48 hr following treatment with $A\beta_{1-40}$, while the activation of JNK3 occurred at the earlier timepoint of 1 hr and returned to basal levels at 24 hr and 48 hr. This finding that $A\beta_{1-40}$ activates JNK2 and

JNK3 within dissimilar timeframes suggests that the JNK isoforms may mediate different signals in cultured cortical neurons. In support of this, JNK activation has been shown to occur early (Xia *et al.*, 1995) or late (Virdee, 1997) in apoptosis. A potential function of JNK may be to initiate programmed cell death (Johnson *et al.*, 1996) and the data demonstrate the early activation (within 1hr) of JNK3, may reflect a role for JNK3 in regulating downstream apoptotic effectors. However, the finding that $A\beta_{1-40}$ activates JNK2 at 24 hr of treatment is consistent with the time point at which we found caspase-3 activation induced by $A\beta_{1-40}$, in Chapter 5. Therefore, JNK2 activation may have occurred in response to DNA fragmentation, which is consistent with other studies (Ghahremani *et al.*, 2002). Furthermore, considering that JNK activity may be regulated by caspase-3 (Ozaki *et al.*, 1999; Hatai *et al.*, 2000), it is possible that JNK2 activity is also modulated by caspase-3 in this system. It is of note that although JNK2 activity was increased at 24hr and 48hr, a concomitant decline in JNK3 activity was observed at these timepoints. This suggests a functional interaction between JNK2 and JNK3 isoforms and warrants further investigation. Previous results from this laboratory have demonstrated that $A\beta_{1-40}$ increases JNK expression within cortical neurons (Fogarty *et al.*, 2003), while JNK2 activation was delayed by 24 hr, similar to my results, no JNK3 activity was detected. JNK1 was activated within minutes of $A\beta_{1-40}$, whereas I found no activation of JNK1. It is suprising that although the same model and stimulus was used, there seems to be a discrepancy between these findings. It has been determined that *JNK1* and *JNK2* genes are ubiquitously expressed, while *JNK3* gene is selectively expressed in the brain (Gupta *et al.*, 1996), consistent with my data and implying a significant role for JNK3 in the brain. Indeed, in support of my findings Morishima and colleagues (2001) report activation of JNK3 following Aβ treatment in cultured cortical neurons. However, JNK3 expression has been reported to vary in the cortex depending on developmental age (Carboni *et al.*, 1998) and even the difference of a day could alter gene expression.

There has been much interest in the signalling events that underly Aβ-mediated induction of the apoptotic cascade. Although I did not investigate the downstream consequences of Syk-dependent JNK activation induced by

$A\beta_{1-40}$ in this study, previous work from this laboratory has indicated a role for JNK1 but not JNK2 in $A\beta_{1-40}$-induced cell death (Fogarty *et al.*, 2003). Depletion of JNK1 following exposure to antisense oligonucleotides prevented the apoptotic effects of $A\beta_{1-40}$ in cultured cortical neurons. Induction of the apoptotic cascade has been attributed to activation of JNK in several systems (Mielke & Herdegen, 2000). In sympathetic neurons and PC12 cells the 1-42 fragment of Aβ activated JNK and the synthetic JNK inhibitor, CEP-1347, blocks Aβ-mediated neurotoxicity (Troy *et al.*, 2001). Increased activation of JNK has been reported in the hippocampi of aged rats (O'Donnell *et al.*, 2000; Lynch & Lynch, 2002), rats exposed to whole body irradiation (Lonergan *et al.*, 2002), and rats injected with the pro-inflammatory cytokine, interleukin-1-beta (Anderson *et al.*, 1995; Vereker *et al.*, 2000a; Vereker *et al.*, 2000b) or LPS (Vereker *et al.*, 2000a). The JNK pathway is activated by oxidative stress, raising the possibility that Aβ might also activate the JNK cascade in response to oxidative stress. In addition, activation of the JNK pathway triggers the induction of gene transcription, thus the protein synthesis dependence of Aβ-induced apoptosis might reflect a requirement for JNK-dependent transcription. Activated JNK phosphorylates several transcription factors, c-Jun, activating transcription factor 2 (ATF2), and ELK-1 (Ip & Davis, 1998). The precise mechanism by which activation of the JNK cascade leads to apoptosis is not known. However, it was demonstrated recently that Fas ligand transcription is activated in neuronal cells by a JNK-dependent mechanism (Le-Niculescu *et al.*, 1999). Several recent observations also provide initial support for the possibility that JNK-Fas ligand pathway may mediate cell death in AD. First, in AD brains, JNK3 immunoreactivity is co-localised with ALZ-50 antigen, a marker for early neurofibrillary degeneration (Mohit *et al.*, 1995), suggesting that JNK-expressing neurons are highly vulnerable in AD brains. Second, JNK activation is detected in degenerating neurons in AD brains (Shoji *et al.*, 2000; Zhu *et al.*, 2001). Third, c-Jun is expressed at high levels specifically in apoptotic neurons that are detected in the AD brain (Anderson *et al.*, 1994). Finally, Fas expression is upregulated in the neurons of AD brains (de la Monte *et al.*, 1997). Taken together, this correlative evidence suggests a role for the JNK signalling cascade in AD,

although additional experimentation will be required to confirm this. It will be of interest to establish the mechanism by which extracellular Aβ induces intracellular JNK activation. The fibrillar form of Aβ appears to bind to the surface of neurons through multiple receptors. Aβ has been shown to bind to a variety of proteins, including the APP, an endoplasmic reticulum Aβ peptide binding protein/L-3-hydroxyacyl-coenzyme A dehydrogenase (Yan *et al.*, 1997; Yan *et al.*, 1999) and RAGE, which mediates oxidative stress (Yan *et al.*, 1996). Whether one or several of these Aβ-binding proteins mediates Aβ induction of JNK activation is not known.

The work presented here provides evidence for Syk impacting on the JNK signalling pathway, following $A\beta_{1-40}$-treatment. JNK2 activation at 24 hr and 48 hr was increased by $A\beta_{1-40}$ in a Syk-dependent manner. Similarly, activation of JNK3 by $A\beta_{1-40}$ at 1 hr was dependent on Syk, suggesting that Syk is upstream of JNK activation in cortical cells. Although this is the first report, that we know of, implicating a role for Syk in JNK signalling in neuronal populations, numerous reports have found JNK activity downstream of Syk signalling in hematopoietic cells. Syk has been described as an upstream activator of JNK in adherent neutrophils after TNF-α stimulation (Avdi *et al.*, 2001) and Syk associates with TLR4 in neutrophils after LPS exposure (Arndt *et al.*, 2004) with subsequent JNK activation. In addition, a study showed that BCR-mediated JNK activation required a calcium signal (Jiang *et al.*, 1998) which was dependent on Syk-mediated PLC-γ2 and in Jurkat T cells it was determined that Syk in cooperation with Rac led to enhanced JNK activation (Jacinto *et al.*, 1998). Interestingly, oxidative stress-induced activation of JNK was compromised in DT40/Syk(-) cells, indicating that Syk was required for oxidative stress-induced activation of JNK (Qin *et al.*, 1997b). Syk alone was not sufficient to induce activation of JNK, as a calcium signal was also required. The precise mechanism by which Syk activates JNK in B cells at least, appears to rely on a Syk-induced PLC-γ2 phosphorylation which leads to calcium mobilisation and PKC activation and subsequent JNK activation. Evidence from studies of Jurkat cells also supports this model (Werlen *et al.*, 1998). Although the mechanism of JNK activation by Syk is unknown in cortical cells, previous work from our laboratory has shown that $A\beta_{1-40}$-

mediates increases in calcium (MacManus *et al.*, 2000), therefore this may modulate the Syk-JNK pathway.

The role of Syk in regulating JNK in cortical cells is not yet clear, but there is evidence of an essential role for Syk in the activation of apoptosis in B cells (Takata *et al.*, 1995) and the activation of JNK correlates with induction of death in a B cell line (Graves *et al.*, 1996). Given that the previous chapter demonstrated caspase-3 activation at 24 hr and DNA fragmentation at 48 hr both mediated by Syk it is possible that Syk regulates JNK3 to induce apoptosis, as JNK3 is activated before these timepoints. However, more experimentation is required to ascertain the validity of this hypothesis.

Previous reports have demonstrated concurrent activation of parallel MAPK cascades in response to the same stimuli (Westwick *et al.*, 1994; Pyo *et al.*, 1998). To establish whether the JNK and ERK signalling cascades were simultaneously activated by $A\beta_{1-40}$ treatment, levels of ERK activity were examined over the same time frame at which JNK activity had been assessed, ranging from 1 hr to 48 hr. To determine whether ERK signalling cascades were regulated by $A\beta_{1-40}$ and to ascertain if Syk had a role in modulating ERK activation, cells were exposed to $A\beta_{1-40}$ and ERK expression was examined in the presence and absence of the Syk inhibitor. The data demonstrate that activation of ERK2 was increased in $A\beta_{1-40}$-treated cells at the relatively late timepoint of 24 hr and 48 hr and that the Syk inhibitor blocked this increase, suggesting that the $A\beta_{1-40}$-induced increase in ERK activity was dependent on Syk.

ERK is generally proposed to have an anti-apoptotic pro-survival role in neurons, with reports that ERK activation can protect certain populations of neurons against specific insults (Hetman & Xia, 2000). Xia and colleagues (1995) were the first to provide definite evidence for a neuroprotective role of ERK using growth factor withdrawal from differentiated PC12 cells as a model of apoptosis. Although numerous studies in other neuronal cells have likewise implicated ERK in neuronal survival (Yujiri *et al.*, 1998), ERK does not appear to act universally to promote cell survival in all models of neurodegeneration. Sustained activation of ERKs brought about by protein phosphatase inhibition induced neuronal cell death in hippocampal slice cultures. Furthermore, the

specific MEK-1/2 inhibitor, PD098059, reduced neuronal injury in a cell culture model of seizure (Murray et al., 1998). The protective effect of MEK1/2 inhibitors has also been observed in non-neuronal cells (Chen & Cooper, 1995). However, it is interesting to note that in cases where ERK activation was detrimental to cell survival, cell death was brought about by oxidative stress. Oxidative stress also activates other members of the MAPK famiy (Guyton *et al.*, 1996; Luo *et al.*, 1998), which in some cell types may be required for the induction of programmed cell death. Thus, where the inhibition of ERK activation is protective, it will be instructive to examine whether other MAPK family members are likewise activated. Perhaps activated ERKs will be detrimental to cell survival if other MAPKs are insensitive to cell death-inducing stimuli. While this work adds to the accumulating evidence pointing to ERK as a component in the cell death cascade (Grewal *et al.*, 1999; Satoh *et al.*, 2000; Stanciu *et al.*, 2000), the detailed mechanisms remain unclear. Clearly the view that JNK/SAPK and p38 MAPK promote apoptotis whereas ERKs oppose apoptosis in neuronal cells is overly simplistic, and detailed analysis of these pathways is warranted in any model of neurotoxicity or neurodegeneration.

The finding that $A\beta_{1\text{-}40}$ mediated induction of ERK activation in cultured neurons is consistent with other reports demonstrating ERK activation in response to Aβ treatment in a variety of cell cultures (McDonald *et al.*, 1998; Pyo *et al.*, 1998; Combs *et al.*, 1999; Abe & Saito, 2000; Rapoport & Ferreira, 2000). In addition, a combined presence of Aβ1-40 and $fe^{2+}$ in cultured cortical neurons resulted in rapid (5 min) ERK activation followed by a decline by 30 min and a second activation that continued up to 24 hr (Kuperstein & Yavin, 2002). Previous studies have reported the Aβ activates calcium channels via ERK dependent phosphorylation, resulting in sustained accumulation of calcium, reactive oxygen species and induction of apoptosis (Ekinci *et al.*, 1999). It was recently reported that ERK activation induced by Aβ, when followed by nuclear translocation, renders neuronal cells susceptible to death (Kuperstein *et al.*, 2001). Aβ induced an increase in both ERK isoforms after 30 min and nuclear translocation was evident after 30 min in the presence of the Aβ peptide. Nuclear translocation has been indicated

as a mode of conveying information from the cytoplasm to the nucleus (Chen *et al.*, 1992). Furthermore, active ERK within damaged areas of the AD brain has been reported (Perry *et al.*, 1999). However the results remain conflicted on the exact mechanism by which ERK may lead to neurotoxicity. Other reports dispute the above results, finding no link between Aβ-mediated neurotoxicy and the ERK cascade (Abe & Saito, 2000).

The data presented here demonstrates that ERK2 activation is increased following a relatively protracted treatment (24 hr) with $A\beta_{1\text{-}40}$, consistent with other reports. Maximal ERK activation by Aβ occurred at 24 hr in cultured neurons (Rapoport & Ferreira, 2000). Thus, if indeed ERK is involved in regulating the apoptotic cascade this finding suggests that ERK is not involved in the execution phase of the cell death program initiated by Aβ. In support of this finding there is evidence that ERK activation occurs in HT22 cells and primary cortical neurons following treatment with glutamate for a minimum of 6-9 hr (Stanciu *et al.*, 2000) Interestingly, they demonstrated that ERK activation required 12-LOX metabolites, indicating that it may be downstream of elevated ROS, suggesting that while ERK may be involved in the cell death cascade its not an inducer of apoptosis. In contrast to these results, Dineley and colleagues suggest a mechanism linking Aβ overproduction to memory dysfunction; specifically, their data suggest that memory deficits occur in part via Aβ42 eliciting downstream derangements (downregulation) in ERK signalling (Dineley *et al.*, 2001). They hypothesise that Aβ42 impinges on the ERK cascade suggesting a molecular basis for the disruptions in memory formation accompanying AD, because the proper functioning of the ERK cascade is critical for certain types of memory formation. In light of the above findings, it appears that the regulation of ERK in cell death is probably dependent on the type of signal that triggers cell death.

The data presented here provide evidence that Syk plays a role in ERK signalling in cortical neurons. This is the first time this interaction has been implicated in this paradigm. However, Syk has been found to be upstream of ERK in other cell types. Syk is essential for BCR-mediated activation of ERK2 (Jiang *et al.*, 1998) in B cells. They have elucidated that Syk is imperative for

both Ras-dependent activation of ERK2 and the PCγ2- and PKC-dependent pathways. In microglia, amyloid stimulation leads to Syk activation followed by elevated levels of intracellular calcium, due to its release from intracellular stores, followed by phospholipase-dependent PKC activation with subsequent downstream activation of ERK (Combs *et al.*, 1999). It was unclear whether PYK2 activation was required for ERK activation, however, PYK2 activation was clearly linked to ras/raf-dependent ERK activation via binding to the small adapter protein, shc (Lev *et al.*, 1995). ERK involvement in FcγR signalling has been suggested in various cell types (Trotta *et al.*, 1996; Garcia-Garcia *et al.*, 2001). Recently, evidence from microglia indicate that events downstream of FcγR signalling include Syk activation, followed by phospholipase C activation, phosphatidylinositol 3-kinase, Ras induction and ERK activation, leading to chemokine expression (Song *et al.*, 2004). It is well established that the activation of ERK involves a linear cascade comprising p21ras, Raf-1,guanidine nucleotide exchange factors and MAP/ERK kinases (MEK). However, the above findings also indicate signalling pathways involving phosphatidylinositol 3-kinase and protein kinase C that can also phosphorylate MEK. Although the precise mechanism underlying ERK activation via Syk in neurons is unknown it is likely these pathways could be involved.

Interestingly, the results presented here demonstrated that ERK2 activation exhibits the same profile as JNK2 activation and in most circumstances, these kinases are activated through different pathways (Kyriakis *et al.*, 1994). The consequence of ERK2 and JNK2 activation in this system is not clear, nevertheless, simultaneous activation of these contrasting kinases is intriguing, however it has been shown in other models. In B cells, activation of ERK and JNK by BCR cross-linking has been reported (Healy *et al.*, 1997). A long standing question has been how the same signal from a single BCR can lead to the activation of different transcription factors that ultimately lead to different cell fates. Ongoing experimentation is attempting to answer this question. The simultaneous activation of these kinases and the fact that both are known to induce cell death in certain situations, suggests that both ERK and JNK may be working in collaboration to induce cell death in

neurons. In addition to exhibiting a similar timeframe of activation, both ERK and JNK are regulated via Syk. As mentioned previously, following BCR cross-linking both JNK and ERK are activated, upon further analysis the authors determined that Syk was required for the activation of both these MAP kinases. Although the kinase cascade leading to activation of JNK is distinct from the kinase cascade leading to ERK, there is potential for crosstalk between these signalling cascades at each level of the signal transduction cascade, due to the fact that MAPK members share a common phosphorylation sequence (Minden & Karin, 1997). Generally, MEKK1/2 preferentially regulates JNK whereas MEKK3 shows a preference for the activation of ERK (Blank *et al.*, 1996). However, MEKKs are capable of activating both JNK and ERK. The ability of MEKKs to regulate multiple sequential protein kinase pathways within cells suggests that Syk may be upstream of MEKK, thus Syk activation allows the activation of both JNK and ERK simultaneously.

In summary, the results from this study demonstrate that treatment of cortical cultures with $A\beta_{1-40}$ activates the JNK2, JNK3 and ERK2 pathways via the protein tyrosine kinase, Syk. There was a temporal pattern of activation of JNK2 and JNK3. In addition, the profiles of JNK2 and ERK2 activation was similar, and both were modulated by Syk, suggesting a functional interaction between these MAP kinases. Overall, these findings demonstrate that $A\beta_{1-40}$ activates JNK and ERK in neonatal cortical cells and that Syk is upstream of these signalling pathways, implicating an important role for Syk in regulating the signalling pathways that underlie the control of neuronal fate in cortical cells.

*Chapter 7*

# Discussion

## 7.1 General Discussion

AD is a form of senile dementia that is characterised by a progressive and irreversible deterioration of cognitive functions. Pathological changes in the AD brain can go unnoticed for up to 20 years prior to clinical recognition (Braak & Braak, 1991). AD is the leading cause of senile dementia worldwide and as the world population continues to age and lifespan increases in developed countries, AD will be a huge burden on families and governments. Therefore, we need to understand and hopefully prevent this insidious disease. There is currently no effective treatment for preventing this progressive dementia, however medical and social management of the disease can ease the burdens on the patient, and his or her caregiver and family. A number of pharmacological drugs for AD have been demonstrated to have some beneficial effects on cognitive, functional, and behavioural symptoms of AD. The majority of these drugs are inhibitors that prevent the break down of acetylcholine and prolong cholinergic transmission at synapses. None of these drugs is expected to postpone or slow the process of degeneration, they simply compensate somewhat for the lact of acetyl choline caused by the degeneration of cholinergic neurons.

One of the defining features of AD is the accumulation of extracellular plaques. These plaques are mainly composed of aggregates of the Aβ peptide, which is cleaved from the APP a ubiquitous protein found in all cells (Selkoe *et al.,* 1988). These senile plaques have been observed throughout the cerebral cortex and hippocampus of the brain (Braak & Braak, 1997), areas which are involved in memory. Experiments on patients with the inherited form of AD have demonstrated a central role for this peptide in the pathogenesis of AD, as all AD mutations increase the production of Aβ (Selkoe, 2001). Therefore research into the prevention of Aβ production or increasing its clearance are currently under investigation. Inhibitors of β- and γ-secretases currently under development are intendent to lower both intracellular and cell surface Aβ production and they should be able to decrease the levels of intramembranous Aβ dimers. Immunotherapy is aimed at preventing fibrillisation of Aβ, as this is believe to cause the toxicity

associated with Aβ. Establishing the detailed mechanism of Aβ aggregation, including non-fibril aggregates is also under examination. What this study is attempting to do is to identify the biochemical events inside neurons through which $A\beta_{1-40}$ (directly or indirectly), induces altered neuronal structure and function, resulting in apoptosis. As we further define the biochemical pathways through which $A\beta_{1-40}$ signals we can then sceen for inhibitors and attempt to prevent the neurotoxicity associated with Aβ.

Dowstream of Aβ production, the characterisation of toxic mechanisms produced by Aβ on neurons is a major goal of AD research today, as was the focus for this study. The primary objective of this study therefore was to investigate the downstream cellular and molecular signalling events associated with the neurodegeneration observed in $A\beta_{1-40}$-treated neurons, with particular emphasis on the role of the lysosomal system. Treatment of cortical cultured neurons with $A\beta_{1-40}$ represents an *in vitro* model for Aβ deposition in the brain. Previous work from this laboratory has demonstrated that the aggregated $A\beta_{1-40}$ and not the reverse sequence $A\beta_{40-1}$ increased the number of cells displaying morphological hallmarks of cell degeneration and DNA fragmentation (Boland & Campbell, 2003) Hence, this studied focused on the effects mediated by $A\beta_{1-40}$ on cortical neurons, as this peptide is the dominant species of Aβ produced (Kanai et al., 1998) and previous work in our laboratory on $A\beta_{1-40}$-mediated disruption in $Ca^{2+}$ homeostasis had used this form of the Aβ peptide (MacManus *et al.*, 2000).

*In vitro,* Aβ-induced neurotoxicity has been well characterised since Yankner et al (1989) concluded 'a peptide from the amyloid procursor may be neurotoxic'. Controversy still surrounds the nature of cell death induced by Aβ, be it apoptotic or necrotic. For a long time, apoptosis and necrosis were considered as fundamentally different. Only recently it has been pointed out that a dying cell can exhibit simultaneously and upon the same stimulus features characteristic of different death programmes (Jaattela *et al.,* 2004). Apoptosis related proteins, such as Bax, Bcl-2, Bak, Bad, p53, Par-4, caspase-2, -3 and Fas have been observed in AD brains (Kitamura et al., 1998), so although Aβ may stimulate necrotic changes (Sutton et al., 1997; Tan et al., 1999), Aβ-mediated induction of apoptosis predominates (Forloni et

al., 1993; Loo et al., 1993; Morimoto et al., 1998). The findings in this study implicate $A\beta_{1-40}$ as a stimulus that promotes DNA fragmentation in cortical neurons. In addition, $A\beta_{1-40}$ mediated increases in Bax protein, p53 activity and caspase-3 activity, all apoptotic related proteins.

Disruption of the lysosomal system has been implicated in AD (Cataldo *et al.*, 1996). The lysosomal system is one of the main pathways that degrades molecules into their consitituent parts or degrades old organelles that are worn out. To accomplish this degradation, lysosomes contain a variety of enzymes, including the cathepsins (Turk *et al.*, 2000). Most of these enzymes require an acidic pH to function efficiently, so the lysosomal membrane has developed a thick glycocalix to prevent release of these acidic components into the cytosol (Eskelinen *et al.*, 2003). However, there are compounds which can induce destabilisation of this membrane followed by enzyme leakage and the induction of cell death (Kagedal *et al.*, 2001, Antunes *et al.*, 2001). A key factor in determining the type fo cell death (necrosis versus apoptosis) mediated by the lysosomal pathway seems to be the magnitude of lysosomal permeabilisation and, consequently, the amount of proteolytic enzymes relased into the cytosol (Li *et al.*, 2000). A complete breakdown of the organelle with release of high concentrations of lysosomal enzymes into the cytosol results in unregulated necrosis, whereas partial, selective permeabilisation triggers apoptosis (Guicciardi *et al.*, 2004). It was therefore appropriate to examine whether Aβ impacted on the lysosomal system in cultured cortical neurons. One of the factors implicated in mediating lysosomal membrane permeabilisation is the tumor supressor protein, p53 (Yuan *et al.*, 2002), so the involvement of p53 in this pathway was also examined.

Analysis of p53 expression in $A\beta_{1-40}$-treated cells revealed a $A\beta_{1-40}$-mediated increase within 5 min and continuing for 1 hr after $A\beta_{1-40}$-treatment. Evidence for an interaction between Aβ and p53 is supported by other studies (LaFerla *et al.*, 1996; Culmsee *et al.*, 2001). Expression of p53 at the lysosome was also evident. Since p53 has been previously reported to induce destabilisation of the lysosomal membrane, the effect of $A\beta_{1-40}$ on lysosomal integrity was assessed. At the early timepoint of 1 hr no change in lysosomal

integrity was observed, however at 6 hr and 24 hr, destabilisation of the lysosomal membrane was evident as assesssed by AO relocation. Treatment with the p53 inhibitor, pifithrin-$\alpha$, abolished the $A\beta_{1-40}$-mediated increase in lysosomal membrane permeabilisation, indicating that destabilisation of the lysosomal membrane by $A\beta_{1-40}$ is p53 dependent. The exact mechanism underlying this loss of lysosomal membrane integrity has yet to be elucidated. The lysosomal membrane is composed of many membrane proteins and some reports speculate that these highly glycosylated proteins function to protect the membrane from digestion by the highly acidic lumenal contents. The data presented here indicate that $A\beta_{1-40}$-mediates a reduction in LAMP expression at 2 hr, 6 hr and 24 hr, which appears to be independent of p53. This reduction in LAMP expression could potentially lead to a loss of the protective coverage, which the membrane proteins confer to the lumenal portion of the lysosomal membrane. Thus allowing acidic enzymes to penetrate the lysosomal membrane and hence translocate into the cytosol. However, further experiments are required to fully elucidate this process.

Similarly, Bax is known to translocate to the mitochondria where it facilitates the release of cytochrome *c* through the formation of pores in the outer mitochondrial membrane (Gao & Dou, 2000). Analysis of the effects of $A\beta_{1-40}$ on Bax expression and use of pifithrin-$\alpha$ revealed that Bax is upregulated by $A\beta_{1-40}$ in a p53-manner in cortical neurons. To ascertain whether Bax can likewise associate at the lysosomal membrane, expression of Bax with the Mitotracker and Lysotracker marker, Mitotracker red and Lysotracker red respectively, was investigated. The results revealed increased association of Bax with both mitochondria and lysosomes. These findings indicate a possible mechanism whereby p53 and Bax contribute to a lysosomal branch of the apoptotic pathway in $A\beta_{1-40}$-treated cultured cortical neurons. Since alterations in neuronal lysosomal systems is an early event in AD and lysosomal leakage is thought to be one of the earliest detectable events during apoptosis (Cataldo *et al.*, 1996), the finding that p53 is involved in destabilisation of the lysosomal membrane offers a therapeutic intervention at an early stage. A recent study has implicated the protein tyrosin kinase, Syk in mediating lysosomal membrane instability in B cells (He *et al.*, 2005),

although the mechanism is as yet unknown. I therefore felt it was appropriate to investigate whether Syk is expressed in cortical neurons and if so, to determine the effect of Syk on lysosomal integrity. Furthermore, I examined the role of $A\beta_{1-40}$ on Syk expression in primary neurons. The findings indicate that $A\beta_{1-40}$ increased Syk expression in a time-dependent from 30 min to 6 hr. In addition, Aβ increased Syk expression at the lysosome at 2 hr. The role of Syk in mediating the $A\beta_{1-40}$-induced loss of lysosomal integrity was assessed by pretreating cells with the Syk inhibitor. The results reveal that destabilisation of the lysosomal membrane by $A\beta_{1-40}$ was Syk dependent at 6 hr, 24 hr and 48 hr. In support of this, previous findings in hematopoietic cells have implicated a role for Syk in permeabilisation of the lysosomal membrane (Bonnerot *et al.*, 1998; He *et al.*, 2005). In light of this, I examined the effect of Syk on $A\beta_{1-40}$-mediated increase in cytosolic cathepsin-L and the data demonstrate that the increase in cytosolic cathepsin-L induced by $A\beta_{1-40}$ was also Syk dependent. In addition, activation of the cell death protease, caspase-3, by $A\beta_{1-40}$ was also found to be reliant on Syk. These findings suggest a role for Syk in mediating $A\beta_{1-40}$-induced apoptosis in cortical neurons. In the literature there is conflicting evidence as to the involvement of Syk in cell death (Combs *et al.*, 2001) (Moroni *et al.*, 2004; Takada & Aggarwal, 2004). Similar to JNK, the role of Syk in cell death appears to be stimulus and cell type dependent. However, DNA fragmentation was also assessed in our cell culture model and the $A\beta_{1-40}$-mediated increase in DNA fragmenation was dependent on Syk signalling. Thus, the data presented here strongly support a role for Syk in mediating the apoptotic process induced by $A\beta_{1-40}$. This is a very exciting result as it unveils potential therapeutic opportunities and the possibility to halt the induction of cell death in neurodegeneration in cultured cortical neurons.

Moreover, confocal microscopy revealed that the proclivity of Bax to associate at the mitochondria was dependent on Syk, and Bax association at the lysosome was also Syk-dependent. Furthermore, the $A\beta_{1-40}$-induced association of p53 at the lysosome was also reliant on Syk signalling. These results suggest that Syk in involved in a wide variety of signalling events induced by $A\beta_{1-40}$ in cortical neurons and in particular, indicate that Syk may

be pertinent in mediating the neurotoxic properties of Aβ. Therefore, Syk may be a potential target in the neurodegeneration process.

Finally, the last set of experiments carried out were aimed at establishing a role for Syk in $A\beta_{1-40}$-induced activation of JNK and ERK signalling events. In the previous chapter the findings indicated that Syk played a crucial role in regulating $A\beta_{1-40}$-mediated destabilisation of the lysosomal membrane and induction of cell death. To further clarify the functions of Syk in cortical neurons and to elucidate whether or not it is involved in other signalling events, I decided to examine the effect of Syk on JNK and ERK activation, both MAP kinases shown previously to be downstream of Aβ signalling (Fogarty et al., 2004; McDonald *et al.*, 1998; Pyo *et al.*, 1998; Combs *et al.*, 1999; Abe & Saito, 2000). Furthermore, JNK activation has been demonstrated to play a significant role in induction of apoptosis in a number of cells (Logan *et al.*, 1997; Avdi *et al.*, 2001; Yoshizumi *et al.*, 2002). Although ERK activation has classically been depicted to be anti-apoptotic (Xia *et al.*, 1995), numerous studies have demonstrated ERK involvement in cell death (Murray *et al.*, 1998; Chen *et al.*, 1995). The work presented here provides evidence for Syk impacting on the JNK signalling pathway, following $A\beta_{1-40}$-treatment. JNK2 activation at 24 hr and 48 hr was increased by $A\beta_{1-40}$ in a Syk-dependent manner. Similarly, activation of JNK3 by $A\beta_{1-40}$ at 1 hr was dependent on Syk, suggesting that Syk is upstream of JNK activation in cortical cells. The precise mechanism by which Syk activates JNK in B cells appears to rely on a Syk-induced PLC-γ2 phosphorylation which leads to calcium mobilisation and PKC activation with subsequent JNK activation. Evidence from studies of Jurkat cells also supports this model (Werlen *et al.*, 1998). Although the exact mechanism of JNK activation by Syk is unknown in cortical cells, previous work from our laboratory has shown that $A\beta_{1-40}$-mediates increases in calcium (MacManus *et al.*, 2000).

The data demonstrate that activation of ERK2 was increased in $A\beta_{1-40}$-treated cells at the relatively late timepoint of 24 hr and 48 hr and that the Syk inhibitor blocked this increase, suggesting that the $A\beta_{1-40}$-induced increase in ERK activity was dependent on Syk. This is the first time this interaction has

been implicated in this paradigm. However, Syk has been found to be upstream of ERK in other cell types. Syk is essential for BCR-mediated activation of ERK2 (Jiang *et al.*, 1998) in B cells. They have elucidated that Syk is imperative for both Ras-dependent activation of ERK2 and the PC$\gamma$2- and PKC-dependent pathways. In microglia, amyloid stimulation leads to Syk activation followed by elevated levels of intracellular calcium, followed by phospholipase-dependent PKC activation with subsequent downstream ERK activation (Combs *et al.*, 1999). In conclusion, Syk appears to modulate multiple signalling events downstream of A$\beta_{1\text{-}40}$, suggestive of an important role for this kinase in A$\beta_{1\text{-}40}$ signaling in cortical neurons.

It is obvious that AD research is ultimately oriented toward one major goal: a therapy for this tragic disease. So are investigations into the role of the lysosomal system warranted in this regard? Certainly, seeking drugs that may prevent leakage of lysosomal constituents, thereby preventing the induction of cell death and neurodegeneration is a major goal. An understanding of the multiple signalling pathways involved in A$\beta$-induced cell death will allow design of compounds which will interfere with the cell death process in a specific manner and will prove to be beneficial in slowing or preventing the progression of AD. In summary, this study characterised cellular and molecular mechanisms leading to cell death in A$\beta_{1\text{-}40}$-treated cultured cortical neurons.

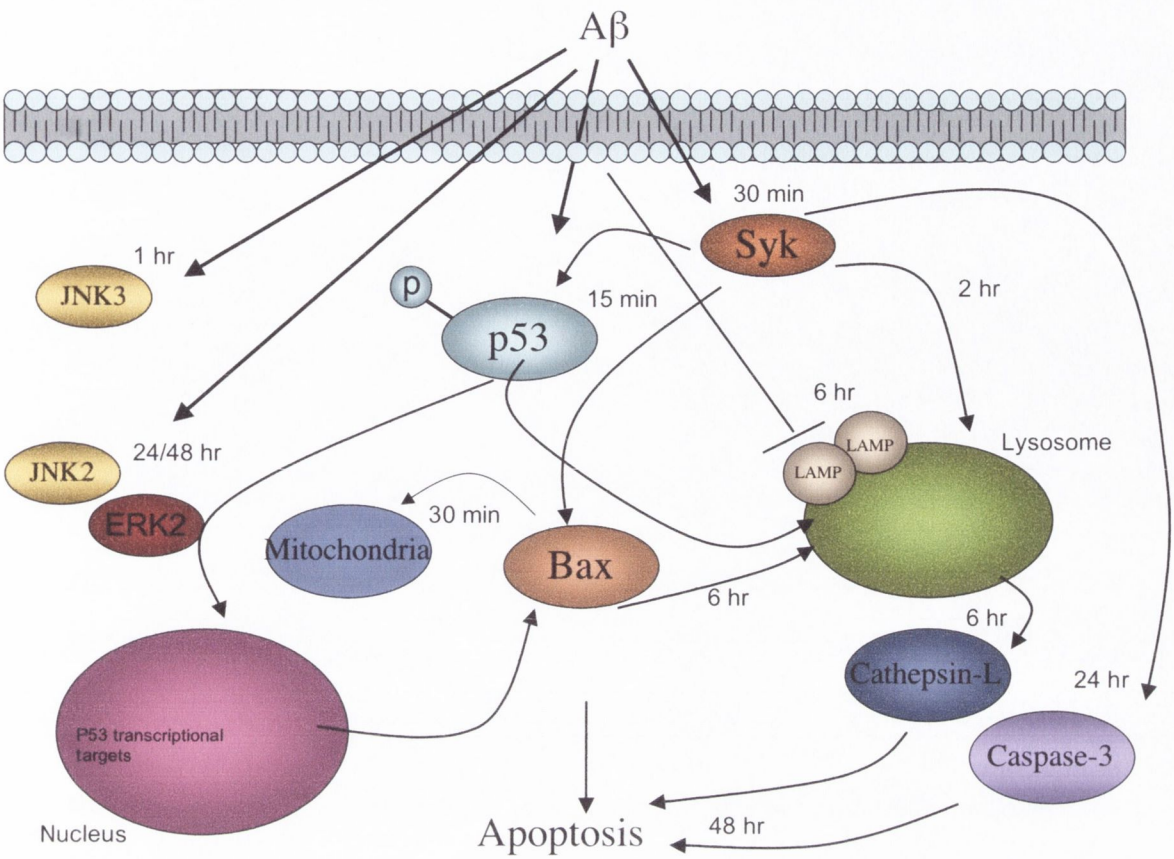


**Figure 8.1** Proposed model contributing to the $A\beta_{1-40}$-induced neuronal apoptosis is rat cultured cortical neurons.

## 7.2 Proposed work

Although this study elucidated some of the downstream pathways of $A\beta_{1-40}$, particularly those involved in altering the integrity of the lysosomal membrane, several important questions remain to be answered. While it was determined that p53 associated at the lysosomal membrane and the $A\beta_{1-40}$-induced destabilisation of the lysosome was p53 dependent, the data suggested that p53 did not modulate expression of the lysosomal membrane protein, LAMP. It would be interesting to examine the role of p53 on other types of lysosomal membrane proteins, such as LIMP or LAP, as reports suggest that these proteins could protect the lysosomal membrane (Eskelinen *et al.,* 2003). In addition to using the p53 inhibitor, pifithrin-$\alpha$, it would be beneficial to repeat the above studies in a p53 knockout model and also to utilise SiRNA for p53. Furthermore, Bax was also found to associate at lysosomes. To clarify whether the effect of Bax at the lysosome is similar to the documented role of Bax in regulating mitochondrial instability (Zornig *et al.,* 2001), experiments examining the pore forming ability of Bax at the lysosome will also be necessary.

Although it was determined that $A\beta_{1-40}$-mediated Syk activation was JNK2/3 and ERK 2 dependent, the downstream consequences of this event was not determined. Using JNK antisense oligonucleotides, the role of JNK1/2 in Syk-dependent cell death could be investigated. Syk could be an important molecule in transducing apoptotic signalling cascades in cortical neurons.

In this study, $A\beta_{1-40}$-induced apoptosis and regulation of the lysosomal system was investigated using the 1-40 species of the A$\beta$ peptide. However, it is known that the 1-42 species is the more toxic form of the peptide. It would be interesting to examine the effect of the 1-42 peptide on the lysosomal system. Moreover, the precise mechanism whereby A$\beta$ interacts with the plasma membrane was beyond the scope of this study. Future experiments examining the nature of this interaction warrants investigation.

In conclusion, the data presented in this study demonstrates the involvement of the lysosomal system and associated proteins in $A\beta_{1-40}$-

induced neurodegeneration, inhibition of this pathway may aid prevention of the neuronal degeneration characteristic of AD.

## VIII Bibliography


Abe K & Saito H. (2000). Amyloid beta neurotoxicity not mediated by the mitogen-activated protein kinase cascade in cultured rat hippocampal and cortical neurons. *Neurosci Lett* **292,** 1-4.

Achkar C, Gong QM, Frankfater A & Bajkowski AS. (1990). Differences in targeting and secretion of cathepsins B and L by BALB/3T3 fibroblasts and Moloney murine sarcoma virus-transformed BALB/3T3 fibroblasts. *J Biol Chem* **265,** 13650-13654.

Adams JM & Cory S. (1998). The Bcl-2 protein family: arbiters of cell survival. *Science* **281,** 1322-1326.

Adler AJ. (1989). Selective presence of acid hydrolases in the interphotoreceptor matrix. *Exp Eye Res* **49,** 1067-1077.

Adler V, Pincus MR, Minamoto T, Fuchs SY, Bluth MJ, Brandt-Rauf PW, Friedman FK, Robinson RC, Chen JM, Wang XW, Harris CC & Ronai Z. (1997). Conformation-dependent phosphorylation of p53. *Proc Natl Acad Sci U S A* **94,** 1686-1691.

Adrain C & Martin SJ. (2001). The mitochondrial apoptosome: a killer unleashed by the cytochrome seas. *Trends Biochem Sci* **26,** 390-397.

Agarwal A, Salem P & Robbins KC. (1993). Involvement of p72syk, a protein-tyrosine kinase, in Fc gamma receptor signaling. *J Biol Chem* **268,** 15900-15905.

Anderson AJ, Cummings BJ & Cotman CW. (1994). Increased immunoreactivity for Jun- and Fos-related proteins in Alzheimer's disease: association with pathology. *Exp Neurol* **125,** 286-295.

Anderson DM, Kumaki S, Ahdieh M, Bertles J, Tometsko M, Loomis A, Giri J, Copeland NG, Gilbert DJ, Jenkins NA & et al. (1995). Functional characterization of the human interleukin-15 receptor alpha chain and close linkage of IL15RA and IL2RA genes. *J Biol Chem* **270,** 29862-29869.

Anderton BH, Betts J, Blackstock WP, Brion JP, Chapman S, Connell J, Dayanandan R, Gallo JM, Gibb G, Hanger DP, Hutton M, Kardalinou E, Leroy K, Lovestone S, Mack T, Reynolds CH & Van Slegtenhorst M. (2001). Sites of phosphorylation in tau and factors affecting their regulation. *Biochem Soc Symp*, 73-80.

Andrejewski N, Punnonen EL, Guhde G, Tanaka Y, Lullmann-Rauch R, Hartmann D, von Figura K & Saftig P. (1999). Normal lysosomal

morphology and function in LAMP-1-deficient mice. *J Biol Chem* **274,** 12692-12701.

Antunes F, Cadenas E & Brunk UT. (2001). Apoptosis induced by exposure to a low steady-state concentration of H2O2 is a consequence of lysosomal rupture. *Biochem J* **356,** 549-555.

Appella E & Anderson CW. (2001). Post-translational modifications and activation of p53 by genotoxic stresses. *Eur J Biochem* **268,** 2764-2772.

Armstrong RA. (1994). Differences in beta-amyloid (beta/A4) deposition in human patients with Down's syndrome and sporadic Alzheimer's disease. *Neurosci Lett* **169,** 133-136.

Arndt PG, Suzuki N, Avdi NJ, Malcolm KC & Worthen GS. (2004). Lipopolysaccharide-induced c-Jun NH2-terminal kinase activation in human neutrophils: role of phosphatidylinositol 3-Kinase and Syk-mediated pathways. *J Biol Chem* **279,** 10883-10891.

Atkins CM, Selcher JC, Petraitis JJ, Trzaskos JM & Sweatt JD. (1998). The MAPK cascade is required for mammalian associative learning. *Nat Neurosci* **1,** 602-609.

Attardi LD, Lowe SW, Brugarolas J & Jacks T. (1996). Transcriptional activation by p53, but not induction of the p21 gene, is essential for oncogene-mediated apoptosis. *Embo J* **15,** 3693-3701.

Avdi NJ, Nick JA, Whitlock BB, Billstrom MA, Henson PM, Johnson GL & Worthen GS. (2001). Tumor necrosis factor-alpha activation of the c-Jun N-terminal kinase pathway in human neutrophils. Integrin involvement in a pathway leading from cytoplasmic tyrosine kinases apoptosis. *J Biol Chem* **276,** 2189-2199.

Baron R. (1989). Polarity and membrane transport in osteoclasts. *Connect Tissue Res* **20,** 109-120.

Barrett AJ & Kirschke H. (1981). Cathepsin B, Cathepsin H, and cathepsin L. *Methods Enzymol* **80 Pt C,** 535-561.

Behl C. (2000). Apoptosis and Alzheimer's disease. *J Neural Transm* **107,** 1325-1344.

Behl C, Davis JB, Lesley R & Schubert D. (1994). Hydrogen peroxide mediates amyloid beta protein toxicity. *Cell* **77,** 817-827.

Benetti R, Del Sal G, Monte M, Paroni G, Brancolini C & Schneider C. (2001). The death substrate Gas2 binds m-calpain and increases susceptibility

to p53-dependent apoptosis. *Embo J* **20,** 2702-2714.

Benhamou M, Ryba NJ, Kihara H, Nishikata H & Siraganian RP. (1993). Protein-tyrosine kinase p72syk in high affinity IgE receptor signaling. Identification as a component of pp72 and association with the receptor gamma chain after receptor aggregation. *J Biol Chem* **268,** 23318-23324.

Bennett M, Macdonald K, Chan SW, Luzio JP, Simari R & Weissberg P. (1998a). Cell surface trafficking of Fas: a rapid mechanism of p53-mediated apoptosis. *Science* **282,** 290-293.

Bennett MW, O'Connell J, O'Sullivan GC, Brady C, Roche D, Collins JK & Shanahan F. (1998b). The Fas counterattack in vivo: apoptotic depletion of tumor-infiltrating lymphocytes associated with Fas ligand expression by human esophageal carcinoma. *J Immunol* **160,** 5669-5675.

Bi X, Gall CM, Zhou J & Lynch G. (2002). Uptake and pathogenic effects of amyloid beta peptide 1-42 are enhanced by integrin antagonists and blocked by NMDA receptor antagonists. *Neuroscience* **112,** 827-840.

Bi X, Yong AP, Zhou J, Gall CM & Lynch G. (2000). Regionally selective changes in brain lysosomes occur in the transition from young adulthood to middle age in rats. *Neuroscience* **97,** 395-404.

Bidere N, Lorenzo HK, Carmona S, Laforge M, Harper F, Dumont C & Senik A. (2003). Cathepsin D triggers Bax activation, resulting in selective apoptosis-inducing factor (AIF) relocation in T lymphocytes entering the early commitment phase to apoptosis. *J Biol Chem* **278,** 31401-31411.

Blacker D. (1997). The genetics of Alzheimer's disease: progress, possibilities, and pitfalls. *Harv Rev Psychiatry* **5,** 234-237.

Blank JL, Gerwins P, Elliott EM, Sather S & Johnson GL. (1996). Molecular cloning of mitogen-activated protein/ERK kinase kinases (MEKK) 2 and 3. Regulation of sequential phosphorylation pathways involving mitogen-activated protein kinase and c-Jun kinase. *J Biol Chem* **271,** 5361-5368.

Blass JP. (2001). Brain metabolism and brain disease: is metabolic deficiency the proximate cause of Alzheimer dementia? *J Neurosci Res* **66,** 851-856.

Blatt NB & Glick GD. (2001). Signaling pathways and effector mechanisms pre-programmed cell death. *Bioorg Med Chem* **9,** 1371-1384.

Boland B & Campbell V. (2003). beta-Amyloid (1-40)-induced apoptosis of cultured cortical neurones involves calpain-mediated cleavage of poly-ADP-ribose polymerase. *Neurobiol Aging* **24,** 179-186.

Boland B & Campbell V. (2004). Abeta-mediated activation of the apoptotic cascade in cultured cortical neurones: a role for cathepsin-L. *Neurobiol Aging* **25,** 83-91.

Boland K, Behrens M, Choi D, Manias K & Perlmutter DH. (1996). The serpin-enzyme complex receptor recognizes soluble, nontoxic amyloid-beta peptide but not aggregated, cytotoxic amyloid-beta peptide. *J Biol Chem* **271,** 18032-18044.

Bonini P, Cicconi S, Cardinale A, Vitale C, Serafino AL, Ciotti MT & Marlier LN. (2004). Oxidative stress induces p53-mediated apoptosis in glia: p53 transcription-independent way to die. *J Neurosci Res* **75,** 83-95.

Bonnerot C, Briken V, Brachet V, Lankar D, Cassard S, Jabri B & Amigorena S. (1998). syk protein tyrosine kinase regulates Fc receptor gamma-chain-mediated transport to lysosomes. *Embo J* **17,** 4606-4616.

Bounhar Y, Zhang Y, Goodyer CG & LeBlanc A. (2001). Prion protein protects human neurons against Bax-mediated apoptosis. *J Biol Chem* **276,** 39145-39149.

Bowen DM, Smith CB & Davison AN. (1973). Molecular changes in senile dementia. *Brain* **96,** 849-856.

Boya P, Andreau K, Poncet D, Zamzami N, Perfettini JL, Metivier D, Ojcius DM, Jaattela M & Kroemer G. (2003a). Lysosomal membrane permeabilization induces cell death in a mitochondrion-dependent fashion. *J Exp Med* **197,** 1323-1334.

Boya P, Gonzalez-Polo RA, Poncet D, Andreau K, Vieira HL, Roumier T, Perfettini JL & Kroemer G. (2003b). Mitochondrial membrane permeabilization is a critical step of lysosome-initiated apoptosis induced by hydroxychloroquine. *Oncogene* **22,** 3927-3936.

Braak H & Braak E. (1991a). Alzheimer's disease affects limbic nuclei of the thalamus. *Acta Neuropathol (Berl)* **81,** 261-268.

Braak H & Braak E. (1991b). Neuropathological stageing of Alzheimer-related changes. *Acta Neuropathol (Berl)* **82,** 239-259.

Braak H & Braak E. (1997). Staging of Alzheimer-related cortical destruction. *Int Psychogeriatr* **9 Suppl 1,** 257-261; discussion 269-272.

Brachfeld N. (1969). Bioenergetics of the normal and anoxic myocardium. *Adv Cardiopulm Dis* **4,** 66-90.

Bradford M. (1976). A rapid and sensitive method for the quantification of microgram quantities of proteins utilizing the principle of protein-dye binding. *Analytical Biochemistry*, 248-254.

Brasseur R, Pillot T, Lins L, Vandekerckhove J & Rosseneu M. (1997). Peptides in membranes: tipping the balance of membrane stability. *Trends Biochem Sci* **22,** 167-171.

Brumell JH, Burkhardt AL, Bolen JB & Grinstein S. (1996). Endogenous reactive oxygen intermediates activate tyrosine kinases in human neutrophils. *J Biol Chem* **271,** 1455-1461.

Brunk U & Brun A. (1972). The effect of aging on lysosomal permeability in nerve cells of the central nervous system. An enzyme histochemical study in rat. *Histochemie* **30,** 315-324.

Brunk UT. (2000). Lysosomotropic detergents induce time- and dose-dependent apoptosis/necrosis in cultured cells. *Redox Rep* **5,** 87-88.

Brunk UT, Neuzil J & Eaton JW. (2001). Lysosomal involvement in apoptosis. *Redox Rep* **6,** 91-97.

Buck MR, Karustis DG, Day NA, Honn KV & Sloane BF. (1992). Degradation of extracellular-matrix proteins by human cathepsin B from normal and tumour tissues. *Biochem J* **282 ( Pt 1),** 273-278.

Bursch W. (2001). The autophagosomal-lysosomal compartment in programmed cell death. *Cell Death Differ* **8,** 569-581.

Canbay A, Guicciardi ME, Higuchi H, Feldstein A, Bronk SF, Rydzewski R, Taniai M & Gores GJ. (2003). Cathepsin B inactivation attenuates hepatic injury and fibrosis during cholestasis. *J Clin Invest* **112,** 152-159.

Cantor AB & Kornfeld S. (1992). Phosphorylation of Asn-linked oligosaccharides located at novel sites on the lysosomal enzyme cathepsin D. *J Biol Chem* **267,** 23357-23363.

Carboni L, Carletti R, Tacconi S, Corti C & Ferraguti F. (1998). Differential expression of SAPK isoforms in the rat brain. An in situ hybridisation study in the adult rat brain and during post-natal development. *Brain Res Mol Brain Res* **60,** 57-68.

Cataldo AM, Barnett JL, Berman SA, Li J, Quarless S, Bursztajn S, Lippa C & Nixon RA. (1995). Gene expression and cellular content of cathepsin D in Alzheimer's disease brain: evidence for early up-regulation of the endosomal-lysosomal system. *Neuron* **14,** 671-680.

Cataldo AM, Barnett JL, Mann DM & Nixon RA. (1996). Colocalization of lysosomal hydrolase and beta-amyloid in diffuse plaques of the cerebellum and striatum in Alzheimer's disease and Down's syndrome. *J Neuropathol Exp Neurol* **55,** 704-715.

Cataldo AM & Nixon RA. (1990). Enzymatically active lysosomal proteases are associated with amyloid deposits in Alzheimer brain. *Proc Natl Acad Sci U S A* **87,** 3861-3865.

Chalmers K, Wilcock GK & Love S. (2003). APOE epsilon 4 influences the pathological phenotype of Alzheimer's disease by favouring cerebrovascular over parenchymal accumulation of A beta protein. *Neuropathol Appl Neurobiol* **29,** 231-238.

Chan AC, van Oers NS, Tran A, Turka L, Law CL, Ryan JC, Clark EA & Weiss A. (1994). Differential expression of ZAP-70 and Syk protein tyrosine kinases, and the role of this family of protein tyrosine kinases in TCR signaling. *J Immunol* **152,** 4758-4766.

Chapman HA, Riese RJ & Shi GP. (1997). Emerging roles for cysteine proteases in human biology. *Annu Rev Physiol* **59,** 63-88.

Chard PS, Bleakman, D., Savidge, J. R. and Miller, R. J. (1995). Capsaicin-induced neurotoxicity in cultured dorsal root ganglion neurons: involvement of calcium-activated proteses. *Neuroscience*, 1099-1108.

Chen D, Van Horn DJ, White MF & Backer JM. (1995). Insulin receptor substrate 1 rescues insulin action in CHO cells expressing mutant insulin receptors that lack a juxtamembrane NPXY motif. *Mol Cell Biol* **15,** 4711-4717.

Chen JW, Madamanchi N, Madamanchi NR, Trier TT & Keherly MJ. (2001). Lamp-1 is upregulated in human glioblastoma cell lines induced to undergo apoptosis. *J Biomed Sci* **8,** 365-374.

Chen M & Cooper JA. (1995). Ser-3 is important for regulating Mos interaction with and stimulation of mitogen-activated protein kinase kinase. *Mol Cell Biol* **15,** 4727-4734.

Chen RH, Sarnecki C & Blenis J. (1992). Nuclear localization and regulation of erk- and rsk-encoded protein kinases. *Mol Cell Biol* **12,** 915-927.

Cheng AG, Huang T, Stracher A, Kim A, Liu W, Malgrange B, Lefebvre PP, Schulman A & Van de Water TR. (1999). Calpain inhibitors protect auditory sensory cells from hypoxia and neurotrophin-withdrawal induced apoptosis. *Brain Res* **850,** 234-243.

Cheng AM, Rowley B, Pao W, Hayday A, Bolen JB & Pawson T. (1995). Syk tyrosine kinase required for mouse viability and B-cell development. *Nature* **378,** 303-306.

Choi WS, Lee EH, Chung CW, Jung YK, Jin BK, Kim SU, Oh TH, Saido TC & Oh YJ. (2001). Cleavage of Bax is mediated by caspase-dependent or -independent calpain activation in dopaminergic neuronal cells: protective role of Bcl-2. *J Neurochem* **77,** 1531-1541.

Chu DH, Morita CT & Weiss A. (1998). The Syk family of protein tyrosine kinases in T-cell activation and development. *Immunol Rev* **165,** 167-180.

Chua CC, Liu X, Gao J, Hamdy RC & Chua BH. (2006). Multiple actions of pifithrin-alpha on doxorubicin-induced apoptosis in rat myoblastic H9c2 cells. *Am J Physiol Heart Circ Physiol* **290,** H2606-2613.

Chwieralski CE, Welte T & Buhling F. (2006). Cathepsin-regulated apoptosis. *Apoptosis* **11,** 143-149.

Cifone MG, Roncaioli P, De Maria R, Camarda G, Santoni A, Ruberti G & Testi R. (1995). Multiple pathways originate at the Fas/APO-1 (CD95) receptor: sequential involvement of phosphatidylcholine-specific phospholipase C and acidic sphingomyelinase in the propagation of the apoptotic signal. *Embo J* **14,** 5859-5868.

Clarke PG. (1990). Developmental cell death: morphological diversity and multiple mechanisms. *Anat Embryol (Berl)* **181,** 195-213.

Combs CK, Johnson DE, Cannady SB, Lehman TM & Landreth GE. (1999). Identification of microglial signal transduction pathways mediating a neurotoxic response to amyloidogenic fragments of beta-amyloid and prion proteins. *J Neurosci* **19,** 928-939.

Combs CK, Karlo JC, Kao SC & Landreth GE. (2001). beta-Amyloid stimulation of microglia and monocytes results in TNFalpha-dependent expression of inducible nitric oxide synthase and neuronal apoptosis. *J Neurosci* **21,** 1179-1188.

Coopman PJ, Do MT, Barth M, Bowden ET, Hayes AJ, Basyuk E, Blancato JK, Vezza PR, McLeskey SW, Mangeat PH & Mueller SC. (2000). The Syk tyrosine kinase suppresses malignant growth of human breast

cancer cells. *Nature* **406,** 742-747.

Coopman PJ & Mueller SC. (2006). The Syk tyrosine kinase: a new negative regulator in tumor growth and progression. *Cancer Lett* **241,** 159-173.

Coraci IS, Husemann J, Berman JW, Hulette C, Dufour JH, Campanella GK, Luster AD, Silverstein SC & El-Khoury JB. (2002). CD36, a class B scavenger receptor, is expressed on microglia in Alzheimer's disease brains and can mediate production of reactive oxygen species in response to beta-amyloid fibrils. *Am J Pathol* **160,** 101-112.

Coso OA, Chiariello M, Yu JC, Teramoto H, Crespo P, Xu N, Miki T & Gutkind JS. (1995). The small GTP-binding proteins Rac1 and Cdc42 regulate the activity of the JNK/SAPK signaling pathway. *Cell* **81,** 1137-1146.

Cotman CW & Anderson AJ. (2000). The brain's microenvironment, early functional loss, and the conversion to Alzheimer's disease. *Ann N Y Acad Sci* **924,** 112-116.

Cuervo AM & Dice JF. (1996). A receptor for the selective uptake and degradation of proteins by lysosomes. *Science* **273,** 501-503.

Cuervo AM & Dice JF. (2000). Regulation of lamp2a levels in the lysosomal membrane. *Traffic* **1,** 570-583.

Culmsee C, Zhu X, Yu QS, Chan SL, Camandola S, Guo Z, Greig NH & Mattson MP. (2001). A synthetic inhibitor of p53 protects neurons against death induced by ischemic and excitotoxic insults, and amyloid beta-peptide. *J Neurochem* **77,** 220-228.

Davies P & Maloney AJ. (1976). Selective loss of central cholinergic neurons in Alzheimer's disease. *Lancet* **2,** 1403.

De Cesaris P, Starace D, Starace G, Filippini A, Stefanini M & Ziparo E. (1999). Activation of Jun N-terminal kinase/stress-activated protein kinase pathway by tumor necrosis factor alpha leads to intercellular adhesion molecule-1 expression. *J Biol Chem* **274,** 28978-28982.

De Duve C. (1976). [Cellular pathology]. *Verh K Acad Geneeskd Belg* **38,** 161-184.

de la Monte SM, Sohn YK & Wands JR. (1997). Correlates of p53- and Fas (CD95)-mediated apoptosis in Alzheimer's disease. *J Neurol Sci* **152,** 73-83.

Dekroom RM & Armati PJ. (2001). Synthesis and processing of apolipoprotein E in human brain cultures. *Glia,* 298-305.

Demoz M, Castino R, Cesaro P, Baccino FM, Bonelli G & Isidoro C. (2002). Endosomal-lysosomal proteolysis mediates death signalling by TNFalpha, not by etoposide, in L929 fibrosarcoma cells: evidence for an active role of cathepsin D. *Biol Chem* **383,** 1237-1248.

Derkinderen P, Enslen H & Girault JA. (1999). The ERK/MAP-kinases cascade in the nervous system. *Neuroreport* **10,** R24-34.

Desagher S, Osen-Sand A, Nichols A, Eskes R, Montessuit S, Lauper S, Maundrell K, Antonsson B & Martinou JC. (1999). Bid-induced conformational change of Bax is responsible for mitochondrial cytochrome c release during apoptosis. *J Cell Biol* **144,** 891-901.

Dineley KT, Westerman M, Bui D, Bell K, Ashe KH & Sweatt JD. (2001). Beta-amyloid activates the mitogen-activated protein kinase cascade via hippocampal alpha7 nicotinic acetylcholine receptors: In vitro and in vivo mechanisms related to Alzheimer's disease. *J Neurosci* **21,** 4125-4133.

Ding J, Takano T, Gao S, Han W, Noda C, Yanagi S & Yamamura H. (2000a). Syk is required for the activation of Akt survival pathway in B cells exposed to oxidative stress. *J Biol Chem* **275,** 30873-30877.

Ding J, Takano T, Hermann P, Gao S, Han W, Noda C, Yanagi S & Yamamura H. (2000b). Distinctive functions of Syk N-terminal and C-terminal SH2 domains in the signaling cascade elicited by oxidative stress in B cells. *J Biochem (Tokyo)* **127,** 791-796.

Ditaranto-Desimone K, Saito, M., Tekirian, T. L., Saito, M., Berg, M., Dubowchik, G. M., Soreghan, B., Thomas, S., Marks, N. and Yang, A. J,. (2003). Neuronal endosomal/lysosomal membrane destabilisation activates caspases and induces abnormal accumulation of the lipid secondary messenger ceramide. *Brain Research*, 523-531.

Dowjat WK, Wisniewski T, Efthimiopoulos S & Wisniewski HM. (1999). Inhibition of neurite outgrowth by familial Alzheimer's disease-linked presenilin-1 mutations. *Neurosci Lett* **267,** 141-144.

Duprez V, Blank U, Chretien S, Gisselbrecht S & Mayeux P. (1998). Physical and functional interaction between p72(syk) and erythropoietin receptor. *J Biol Chem* **273,** 33985-33990.

Dypbukt JM, Ankarcrona M, Burkitt M, Sjoholm A, Strom K, Orrenius S & Nicotera P. (1994). Different prooxidant levels stimulate growth, trigger apoptosis, or produce necrosis of insulin-secreting RINm5F cells. The role of intracellular polyamines. *J Biol Chem* **269,** 30553-30560.

Eikelenboom P, Bate, C., Van Gool, W A., Hoozemans, J. J., Rozemuller, J. M., Veerhuis, R. and Williams, A. (2002). Neuroinflammation in Alzheimer's disease and prion disease. *Glia*, 232-239.

Eilers A, Whitfield J, Shah B, Spadoni C, Desmond H & Ham J. (2001). Direct inhibition of c-Jun N-terminal kinase in sympathetic neurones prevents c-jun promoter activation and NGF withdrawal-induced death. *J Neurochem* **76,** 1439-1454.

Ekinci FJ, Malik KU & Shea TB. (1999). Activation of the L voltage-sensitive calcium channel by mitogen-activated protein (MAP) kinase following exposure of neuronal cells to beta-amyloid. MAP kinase mediates beta-amyloid-induced neurodegeneration. *J Biol Chem* **274,** 30322-30327.

Elkeles A, Juven-Gershon T, Israeli D, Wilder S, Zalcenstein A & Oren M. (1999). The c-fos proto-oncogene is a target for transactivation by the p53 tumor suppressor. *Mol Cell Biol* **19,** 2594-2600.

Ellis HM & Horvitz HR. (1986). Genetic control of programmed cell death in the nematode C. elegans. *Cell* **44,** 817-829.

Ellis RE, Yuan JY & Horvitz HR. (1991). Mechanisms and functions of cell death. *Annu Rev Cell Biol* **7,** 663-698.

Ely CM, Oddie KM, Litz JS, Rossomando AJ, Kanner SB, Sturgill TW & Parsons SJ. (1990). A 42-kD tyrosine kinase substrate linked to chromaffin cell secretion exhibits an associated MAP kinase activity and is highly related to a 42-kD mitogen-stimulated protein in fibroblasts. *J Cell Biol* **110,** 731-742.

English JD & Sweatt JD. (1997). A requirement for the mitogen-activated protein kinase cascade in hippocampal long term potentiation. *J Biol Chem* **272,** 19103-19106.

Enokido Y, Araki T, Aizawa S & Hatanaka H. (1996). p53 involves cytosine arabinoside-induced apoptosis in cultured cerebellar granule neurons. *Neurosci Lett* **203,** 1-4.

Epand RF, Martinou JC, Fornallaz-Mulhauser M, Hughes DW & Epand RM. (2002). The apoptotic protein tBid promotes leakage by altering membrane curvature. *J Biol Chem* **277,** 32632-32639.

Erdal H, Berndtsson M, Castro J, Brunk U, Shoshan MC & Linder S. (2005). Induction of lysosomal membrane permeabilization by compounds that activate p53-independent apoptosis. *Proc Natl Acad Sci U S A* **102,** 192-197.

Eriksen JL, Przedborski S & Petrucelli L. (2005). Gene dosage and pathogenesis of Parkinson's disease. *Trends Mol Med* **11,** 91-96.

Eskelinen EL, Tanaka Y & Saftig P. (2003). At the acidic edge: emerging functions for lysosomal membrane proteins. *Trends Cell Biol* **13,** 137-145.

Eskes R, Antonsson B, Osen-Sand A, Montessuit S, Richter C, Sadoul R, Mazzei G, Nichols A & Martinou JC. (1998). Bax-induced cytochrome C release from mitochondria is independent of the permeability transition pore but highly dependent on Mg2+ ions. *J Cell Biol* **143,** 217-224.

Estus S, Golde TE & Younkin SG. (1992). Normal processing of the Alzheimer's disease amyloid beta protein precursor generates potentially amyloidogenic carboxyl-terminal derivatives. *Ann N Y Acad Sci* **674,** 138-148.

Evan G & Littlewood T. (1998). A matter of life and cell death. *Science* **281,** 1317-1322.

Evan GI, Brown L, Whyte M & Harrington E. (1995). Apoptosis and the cell cycle. *Curr Opin Cell Biol* **7,** 825-834.

Fagan AM & Holtzman DM. (2000). Astrocyte lipoproteins, effects of apoE on neuronal function, and role of apoE in amyloid-beta deposition in vivo. *Microsc Res Tech* **50,** 297-304.

Felbor U, Kessler B, Mothes W, Goebel HH, Ploegh HL, Bronson RT & Olsen BR. (2002). Neuronal loss and brain atrophy in mice lacking cathepsins B and L. *Proc Natl Acad Sci U S A* **99,** 7883-7888.

Firestone RA, Pisano JM & Bonney RJ. (1979). Lysosomotropic agents. 1. Synthesis and cytotoxic action of lysosomotropic detergents. *J Med Chem* **22,** 1130-1133.

Fluck M, Zurcher G, Andres AC & Ziemiecki A. (1995). Molecular characterization of the murine syk protein tyrosine kinase cDNA, transcripts and protein. *Biochem Biophys Res Commun* **213,** 273-281.

Fogarty MP, Downer EJ & Campbell V. (2003). A role for c-Jun N-terminal kinase 1 (JNK1), but not JNK2, in the beta-amyloid-mediated stabilization of protein p53 and induction of the apoptotic cascade in cultured cortical neurons. *Biochem J* **371,** 789-798.

Foghsgaard L, Wissing D, Mauch D, Lademann U, Bastholm L, Boes M,

Elling F, Leist M & Jaattela M. (2001). Cathepsin B acts as a dominant execution protease in tumor cell apoptosis induced by tumor necrosis factor. *J Cell Biol* **153,** 999-1010.

Forloni G, Chiesa, R., Smiroldo, S., Verga, L., Salmona, M., Tagliavini, F. and Angeretti, N. (1993). Apoptosis mediated neurotoxicity induced by chronic application of beta amyloid fragment 25-35. *Neuroreport*, 523-526.

Forloni G, Demicheli F, Giorgi S, Bendotti C & Angeretti N. (1992). Expression of amyloid precursor protein mRNAs in endothelial, neuronal and glial cells: modulation by interleukin-1. *Brain Res Mol Brain Res* **16,** 128-134.

Fukuda M. (1991). Lysosomal membrane glycoproteins. Structure, biosynthesis, and intracellular trafficking. *J Biol Chem* **266,** 21327-21330.

Gandy S & Petanceska S. (2000). Regulation of Alzheimer beta-amyloid precursor trafficking and metabolism. *Biochim Biophys Acta* **1502,** 44-52.

Gao G & Dou QP. (2000). N-terminal cleavage of bax by calpain generates a potent proapoptotic 18-kDa fragment that promotes bcl-2-independent cytochrome C release and apoptotic cell death. *J Cell Biochem* **80,** 53-72.

Gao J, Zoller KE, Ginsberg MH, Brugge JS & Shattil SJ. (1997). Regulation of the pp72syk protein tyrosine kinase by platelet integrin alpha IIb beta 3. *Embo J* **16,** 6414-6425.

Garcia-Garcia E, Sanchez-Mejorada G & Rosales C. (2001). Phosphatidylinositol 3-kinase and ERK are required for NF-kappaB activation but not for phagocytosis. *J Leukoc Biol* **70,** 649-658.

Gardella S, Andrei C, Lotti LV, Poggi A, Torrisi MR, Zocchi MR & Rubartelli A. (2001). CD8(+) T lymphocytes induce polarized exocytosis of secretory lysosomes by dendritic cells with release of interleukin-1beta and cathepsin D. *Blood* **98,** 2152-2159.

Geinisman Y, deToledo-Morrell, L. and Morrell, F. (1991). Induction of long-term potentiation is associated with an increase in he number of axospinous synapses with egmented postsynaptic densities. *Brain Res*, 77-88.

Geisow M. (1982). Lysosome proton pump identified. *Nature* **298,** 515-516.

Gerschenson LE & Rotello RJ. (1992). Apoptosis: a different type of cell death. *Faseb J* **6,** 2450-2455.

Ghahremani MH, Keramaris E, Shree T, Xia Z, Davis RJ, Flavell R, Slack RS & Park DS. (2002). Interaction of the c-Jun/JNK pathway and cyclin-dependent kinases in death of embryonic cortical neurons evoked by DNA damage. *J Biol Chem* **277,** 35586-35596.

Giulian D, Haverkamp LJ, Yu J, Karshin W, Tom D, Li J, Kazanskaia A, Kirkpatrick J & Roher AE. (1998). The HHQK domain of beta-amyloid provides a structural basis for the immunopathology of Alzheimer's disease. *J Biol Chem* **273,** 29719-29726.

Goldman SA. (1991). Concerns and issues of the diagnostic category of organic mental disorders in the DSM-IV. *Psychosomatics* **32,** 112.

Goodman Y & Mattson MP. (1994). Secreted forms of beta-amyloid precursor protein protect hippocampal neurons against amyloid beta-peptide-induced oxidative injury. *Exp Neurol* **128,** 1-12.

Graeber MB & Moran LB. (2002). Mechanisms of cell death in neurodegenerative diseases: fashion, fiction, and facts. *Brain Pathol* **12,** 385-390.

Graves JD, Draves KE, Craxton A, Saklatvala J, Krebs EG & Clark EA. (1996). Involvement of stress-activated protein kinase and p38 mitogen-activated protein kinase in mIgM-induced apoptosis of human B lymphocytes. *Proc Natl Acad Sci U S A* **93,** 13814-13818.

Green DR. (1998). Apoptotic pathways: the roads to ruin. *Cell* **94,** 695-698.

Grewal SS, York RD & Stork PJ. (1999). Extracellular-signal-regulated kinase signalling in neurons. *Curr Opin Neurobiol* **9,** 544-553.

Griffin WS, Stanley LC, Ling C, White L, MacLeod V, Perrot LJ, White CL, 3rd & Araoz C. (1989). Brain interleukin 1 and S-100 immunoreactivity are elevated in Down syndrome and Alzheimer disease. *Proc Natl Acad Sci U S A* **86,** 7611-7615.

Gross A, Jockel J, Wei MC & Korsmeyer SJ. (1998). Enforced dimerization of BAX results in its translocation, mitochondrial dysfunction and apoptosis. *Embo J* **17,** 3878-3885.

Gudkov AV & Komarova EA. (2005). Prospective therapeutic applications of p53 inhibitors. *Biochem Biophys Res Commun* **331,** 726-736.

Guicciardi ME, Bronk SF, Werneburg NW, Yin XM & Gores GJ. (2005). Bid is

upstream of lysosome-mediated caspase 2 activation in tumor necrosis factor alpha-induced hepatocyte apoptosis. *Gastroenterology* **129,** 269-284.

Guicciardi ME, Deussing J, Miyoshi H, Bronk SF, Svingen PA, Peters C, Kaufmann SH & Gores GJ. (2000). Cathepsin B contributes to TNF-alpha-mediated hepatocyte apoptosis by promoting mitochondrial release of cytochrome c. *J Clin Invest* **106,** 1127-1137.

Guicciardi ME, Leist M & Gores GJ. (2004). Lysosomes in cell death. *Oncogene* **23,** 2881-2890.

Gupta S, Campbell, D., Derijard, B. and Davis, R. (1995). Transcriptional factor ATF2 regulation by the JNK signal transduction pathway. *Science*, 389-393.

Gupta S, Barrett T, Whitmarsh AJ, Cavanagh J, Sluss HK, Derijard B & Davis RJ. (1996). Selective interaction of JNK protein kinase isoforms with transcription factors. *Embo J* **15,** 2760-2770.

Guyton KZ, Liu Y, Gorospe M, Xu Q & Holbrook NJ. (1996). Activation of mitogen-activated protein kinase by H2O2. Role in cell survival following oxidant injury. *J Biol Chem* **271,** 4138-4142.

Haass C, Hung AY, Schlossmacher MG, Teplow DB & Selkoe DJ. (1993). beta-Amyloid peptide and a 3-kDa fragment are derived by distinct cellular mechanisms. *J Biol Chem* **268,** 3021-3024.

Haass C, Lemere CA, Capell A, Citron M, Seubert P, Schenk D, Lannfelt L & Selkoe DJ. (1995). The Swedish mutation causes early-onset Alzheimer's disease by beta-secretase cleavage within the secretory pathway. *Nat Med* **1,** 1291-1296.

Haddad JJ. (2004). Mitogen-activated protein kinases and the evolution of Alzheimer's: a revolutionary neurogenetic axis for therapeutic intervention? *Prog Neurobiol* **73,** 359-377.

Haimovitz-Friedman A, Cordon-Cardo C, Bayoumy S, Garzotto M, McLoughlin M, Gallily R, Edwards CK, 3rd, Schuchman EH, Fuks Z & Kolesnick R. (1997). Lipopolysaccharide induces disseminated endothelial apoptosis requiring ceramide generation. *J Exp Med* **186,** 1831-1841.

Halestrap AP, Doran E, Gillespie JP & O'Toole A. (2000). Mitochondria and cell death. *Biochem Soc Trans* **28,** 170-177.

Hamakubo T, Kannagi, R., Murachi, T. and Matus, A. (1986). Disruption of

calpains I and II in rat brain. *Journal of Neuroscience*, 3103-3111.

Hao S, Kurosaki T & August A. (2003). Differential regulation of NFAT and SRF by the B cell receptor via a PLCgamma-Ca(2+)-dependent pathway. *Embo J* **22,** 4166-4177.

Hardwick JS & Sefton BM. (1995). Activation of the Lck tyrosine protein kinase by hydrogen peroxide requires the phosphorylation of Tyr-394. *Proc Natl Acad Sci U S A* **92,** 4527-4531.

Hardy J, Duff K, Hardy KG, Perez-Tur J & Hutton M. (1998). Genetic dissection of Alzheimer's disease and related dementias: amyloid and its relationship to tau. *Nat Neurosci* **1,** 355-358.

Hardy J & Selkoe DJ. (2002). The amyloid hypothesis of Alzheimer's disease: progress and problems on the road to therapeutics. *Science* **297,** 353-356.

Hashiguchi M, Sobue K & Paudel HK. (2000). 14-3-3zeta is an effector of tau protein phosphorylation. *J Biol Chem* **275,** 25247-25254.

Hatai T, Matsuzawa A, Inoshita S, Mochida Y, Kuroda T, Sakamaki K, Kuida K, Yonehara S, Ichijo H & Takeda K. (2000). Execution of apoptosis signal-regulating kinase 1 (ASK1)-induced apoptosis by the mitochondria-dependent caspase activation. *J Biol Chem* **275,** 26576-26581.

He J, Tohyama Y, Yamamoto K, Kobayashi M, Shi Y, Takano T, Noda C, Tohyama K & Yamamura H. (2005). Lysosome is a primary organelle in B cell receptor-mediated apoptosis: an indispensable role of Syk in lysosomal function. *Genes Cells* **10,** 23-35.

He LM, Chen, L. Y., Lou, X. L., Qu. L., Zhou, Z. and Xu, T. (2002). Evaluation of beta-amyloid peptide 25-35 on calcium homeostasis in cultured rat dorsal root ganglion neurons. *Brain Research*, 65-75.

Healy JI, Dolmetsch RE, Timmerman LA, Cyster JG, Thomas ML, Crabtree GR, Lewis RS & Goodnow CC. (1997). Different nuclear signals are activated by the B cell receptor during positive versus negative signaling. *Immunity* **6,** 419-428.

Hecht D & Zick Y. (1992). Selective inhibition of protein tyrosine phosphatase activities by H2O2 and vanadate in vitro. *Biochem Biophys Res Commun* **188,** 773-779.

Hellsten E, Vesa J, Olkkonen VM, Jalanko A & Peltonen L. (1996). Human palmitoyl protein thioesterase: evidence for lysosomal targeting of the

enzyme and disturbed cellular routing in infantile neuronal ceroid lipofuscinosis. *Embo J* **15,** 5240-5245.

Hengartner MO. (2000). The biochemistry of apoptosis. *Nature* **407,** 770-776.

Herdegen T, Skene, P. and Bahr, M. (1997). The c-Jun transcriptional factor-bipotential mediator of neuronal cell death, survival and regeneration. *Trends in Neuroscience*, 227-231.

Herr I & Debatin KM. (2001). Cellular stress response and apoptosis in cancer therapy. *Blood* **98,** 2603-2614.

Hetman M, Filipkowski RK, Domagala W & Kaczmarek L. (1995). Elevated cathepsin D expression in kainate-evoked rat brain neurodegeneration. *Exp Neurol* **136,** 53-63.

Hetman M & Xia Z. (2000). Signaling pathways mediating anti-apoptotic action of neurotrophins. *Acta Neurobiol Exp (Wars)* **60,** 531-545.

Himeno M, Noguchi Y, Sasaki H, Tanaka Y, Furuno K, Kono A, Sakaki Y & Kato K. (1989). Isolation and sequencing of a cDNA clone encoding 107 kDa sialoglycoprotein in rat liver lysosomal membranes. *FEBS Lett* **244,** 351-356.

Hirai S. (2000). Alzheimer disease: current therapy and future therapeutic strategies. *Alzheimer Dis Assoc Disord* **14 Suppl 1,** S11-17.

Hirai S, Kawasaki H, Yaniv M & Suzuki K. (1991). Degradation of transcription factors, c-Jun and c-Fos, by calpain. *FEBS Lett* **287,** 57-61.

Hirose M, Kitano J, Nakajima Y, Moriyoshi K, Yanagi S, Yamamura H, Muto T, Jingami H & Nakanishi S. (2004). Phosphorylation and recruitment of Syk by immunoreceptor tyrosine-based activation motif-based phosphorylation of tamalin. *J Biol Chem* **279,** 32308-32315.

Hoffman K. (1999). The modular nature of apoptotic signaling proteins. *Cellular and Molecular Life Sciences*, 1113-1128.

Honn KV, Tang DG, Grossi IM, Renaud C, Duniec ZM, Johnson CR & Diglio CA. (1994). Enhanced endothelial cell retraction mediated by 12(S)-HETE: a proposed mechanism for the role of platelets in tumor cell metastasis. *Exp Cell Res* **210,** 1-9.

Hung WC, Chang HC & Chuang LY. (1999). Activation of caspase-3-like proteases in apoptosis induced by sphingosine and other long-chain bases in Hep3B hepatoma cells. *Biochem J* **338 ( Pt 1),** 161-166.

Ichihara K, Haneda T, Onodera S & Abiko Y. (1987). Inhibition of ischemia-induced subcellular redistribution of lysosomal enzymes in the perfused rat heart by the calcium entry blocker, diltiazem. *J Pharmacol Exp Ther* **242,** 1109-1113.

Ip YT & Davis RJ. (1998). Signal transduction by the c-Jun N-terminal kinase (JNK)--from inflammation to development. *Curr Opin Cell Biol* **10,** 205-219.

Isahara K, Ohsawa Y, Kanamori S, Shibata M, Waguri S, Sato N, Gotow T, Watanabe T, Momoi T, Urase K, Kominami E & Uchiyama Y. (1999). Regulation of a novel pathway for cell death by lysosomal aspartic and cysteine proteinases. *Neuroscience* **91,** 233-249.

Ishidoh K & Kominami E. (2002). Processing and activation of lysosomal proteinases. *Biol Chem* **383,** 1827-1831.

Ishisaka R, Utsumi T, Kanno T, Arita K, Katunuma N, Akiyama J & Utsumi K. (1999). Participation of a cathepsin L-type protease in the activation of caspase-3. *Cell Struct Funct* **24,** 465-470.

Ishiura S, Murofushi H, Suzuki K & Imahori K. (1978). Studies of a calcium-activated neutral protease from chicken skeletal muscle. I. Purification and characterization. *J Biochem (Tokyo)* **84,** 225-230.

Ishizuka S, Yano T, Hagiwara K, Sone M, Nihei H, Ozasa H & Horikawa S. (1999a). Extracellular signal-regulated kinase mediates renal regeneration in rats with myoglobinuric acute renal injury. *Biochem Biophys Res Commun* **254,** 88-92.

Ishizuka T, Chayama K, Takeda K, Hamelmann E, Terada N, Keller GM, Johnson GL & Gelfand EW. (1999b). Mitogen-activated protein kinase activation through Fc epsilon receptor I and stem cell factor receptor is differentially regulated by phosphatidylinositol 3-kinase and calcineurin in mouse bone marrow-derived mast cells. *J Immunol* **162,** 2087-2094.

Itagaki S, McGeer PL, Akiyama H, Zhu S & Selkoe D. (1989). Relationship of microglia and astrocytes to amyloid deposits of Alzheimer disease. *J Neuroimmunol* **24,** 173-182.

Jaattela M, Cande C & Kroemer G. (2004). Lysosomes and mitochondria in the commitment to apoptosis: a potential role for cathepsin D and AIF. *Cell Death Differ* **11,** 135-136.

Jacinto E, Werlen G & Karin M. (1998). Cooperation between Syk and Rac1 leads to synergistic JNK activation in T lymphocytes. *Immunity* **8,** 31-

41.

Ji ZS, Miranda RD, Newhouse YM, Weisgraber KH, Huang Y & Mahley RW. (2002). Apolipoprotein E4 potentiates amyloid beta peptide-induced lysosomal leakage and apoptosis in neuronal cells. *J Biol Chem* **277,** 21821-21828.

Jiang A, Craxton A, Kurosaki T & Clark EA. (1998). Different protein tyrosine kinases are required for B cell antigen receptor-mediated activation of extracellular signal-regulated kinase, c-Jun NH2-terminal kinase 1, and p38 mitogen-activated protein kinase. *J Exp Med* **188,** 1297-1306.

Jiang X & Wang X. (2000). Cytochrome c promotes caspase-9 activation by inducing nucleotide binding to Apaf-1. *J Biol Chem* **275,** 31199-31203.

Johnson NL, Gardner AM, Diener KM, Lange-Carter CA, Gleavy J, Jarpe MB, Minden A, Karin M, Zon LI & Johnson GL. (1996). Signal transduction pathways regulated by mitogen-activated/extracellular response kinase kinase kinase induce cell death. *J Biol Chem* **271,** 3229-3237.

Jordan J, Galindo MF, Prehn JH, Weichselbaum RR, Beckett M, Ghadge GD, Roos RP, Leiden JM & Miller RJ. (1997). p53 expression induces apoptosis in hippocampal pyramidal neuron cultures. *J Neurosci* **17,** 1397-1405.

Jurgensmeier JM, Xie Z, Deveraux Q, Ellerby L, Bredesen D & Reed JC. (1998). Bax directly induces release of cytochrome c from isolated mitochondria. *Proc Natl Acad Sci U S A* **95,** 4997-5002.

Kagedal K, Johansson AC, Johansson U, Heimlich G, Roberg K, Wang NS, Jurgensmeier JM & Ollinger K. (2005). Lysosomal membrane permeabilization during apoptosis--involvement of Bax? *Int J Exp Pathol* **86,** 309-321.

Kagedal K, Johansson U & Ollinger K. (2001a). The lysosomal protease cathepsin D mediates apoptosis induced by oxidative stress. *Faseb J* **15,** 1592-1594.

Kagedal K, Zhao M, Svensson I & Brunk UT. (2001b). Sphingosine-induced apoptosis is dependent on lysosomal proteases. *Biochem J* **359,** 335-343.

Kakio A, Nishimoto S, Yanagisawa K, Kozutsumi Y & Matsuzaki K. (2002). Interactions of amyloid beta-protein with various gangliosides in raft-like membranes: importance of GM1 ganglioside-bound form as an endogenous seed for Alzheimer amyloid. *Biochemistry* **41,** 7385-7390.

Kalra J, Lautner D, Massey KL & Prasad K. (1988). Oxygen free radicals induced release of lysosomal enzymes in vitro. *Mol Cell Biochem* **84,** 233-238.

Kanai M, Matsubara, E., Isoe, K., Urakami, K., Nakashima, K., Arai, H., Sasaki, H., Abe, K., Iwatsubo, T., Kosaka, T., Watanabe, M., Tomidokoro, Y., Shizuka, M., Mizushima, K., Nakamura, T., Igeta, Y., Iketa, Y., Amari, M., Kawarabayahi, T., Ishiguro, K., Harigaya, Y., Wakabayashi, K., Okamoto, K., Hirai, S. and Shoji, M. . (1998). Longitudinal study of cerebrospinal fluid levels of tau, A beta 1-40, and A beta 1-42 (43) in Alzheimer's disease: a study in Japan. *Annals of Neurology*, 17-26.

Kang CD, Jang JH, Kim KW, Lee HJ, Jeong CS, Kim CM, Kim SH & Chung BS. (1998). Activation of c-jun N-terminal kinase/stress-activated protein kinase and the decreased ratio of Bcl-2 to Bax are associated with the auto-oxidized dopamine-induced apoptosis in PC12 cells. *Neurosci Lett* **256,** 37-40.

Kang J, Lemaire HG, Unterbeck A, Salbaum JM, Masters CL, Grzeschik KH, Multhaup G, Beyreuther K & Muller-Hill B. (1987). The precursor of Alzheimer's disease amyloid A4 protein resembles a cell-surface receptor. *Nature* **325,** 733-736.

Karpinich NO, Tafani M, Rothman RJ, Russo MA & Farber JL. (2002). The course of etoposide-induced apoptosis from damage to DNA and p53 activation to mitochondrial release of cytochrome c. *J Biol Chem* **277,** 16547-16552.

Katunuma N, Matsui A, Le QT, Utsumi K, Salvesen G & Ohashi A. (2001). Novel procaspase-3 activating cascade mediated by lysoapoptases and its biological significances in apoptosis. *Adv Enzyme Regul* **41,** 237-250.

Katz E, Lord C, Ford CA, Gauld SB, Carter NA & Harnett MM. (2004). Bcl-(xL) antagonism of BCR-coupled mitochondrial phospholipase A(2) signaling correlates with protection from apoptosis in WEHI-231 B cells. *Blood* **103,** 168-176.

Katz SA, Opsahl JA & Forbis LM. (2001). Myocardial enzymatic activity of renin and cathepsin D before and after bilateral nephrectomy. *Basic Res Cardiol* **96,** 659-668.

Katzman R. (1986). Alzheimer's disease. *N Engl J Med* **314,** 964-973.

Kaufmann SH, Desnoyers S, Ottaviano Y, Davidson NE & Poirier GG. (1993). Specific proteolytic cleavage of poly(ADP-ribose) polymerase: an early

marker of chemotherapy-induced apoptosis. *Cancer Res* **53,** 3976-3985.

Kerr JF, Wyllie AH & Currie AR. (1972). Apoptosis: a basic biological phenomenon with wide-ranging implications in tissue kinetics. *Br J Cancer* **26,** 239-257.

Kerr JFR & Harmon BV. (1991). *Definition and incidence of apoptosis: An historical perspective*. Cold Spring Harbour Laboratory Press.

Kharbanda S, Yuan ZM, Rubin E, Weichselbaum R & Kufe D. (1994). Activation of Src-like p56/p53lyn tyrosine kinase by ionizing radiation. *J Biol Chem* **269,** 20739-20743.

Kiener PA, Rankin BM, Burkhardt AL, Schieven GL, Gilliland LK, Rowley RB, Bolen JB & Ledbetter JA. (1993). Cross-linking of Fc gamma receptor I (Fc gamma RI) and receptor II (Fc gamma RII) on monocytic cells activates a signal transduction pathway common to both Fc receptors that involves the stimulation of p72 Syk protein tyrosine kinase. *J Biol Chem* **268,** 24442-24448.

Kim YJ, Sapp E, Cuiffo BG, Sobin L, Yoder J, Kegel KB, Qin ZH, Detloff P, Aronin N & DiFiglia M. (2006). Lysosomal proteases are involved in generation of N-terminal huntingtin fragments. *Neurobiol Dis* **22,** 346-356.

Kingham PJ & Pocock JM. (2001). Microglial secreted cathepsin B induces neuronal apoptosis. *J Neurochem* **76,** 1475-1484.

Kitamura Y, Shimohama, S., Kamoshima, W., Ota, T., Matsuoka, Y., Nomura, Y., Smith, M. A., Perry, G., Whitehouse, P.J. and Taniguchi, T. (1998). Altheration of proteins regulating apoptosis, Bcl-2, Bcl-x, Bax, Bak, ICH-1 and CPP32, in Alzheimer's disease. *Brain Research*, 260-269.

Kitamura Y, Shimohama S, Kamoshima W, Matsuoka Y, Nomura Y & Taniguchi T. (1997). Changes of p53 in the brains of patients with Alzheimer's disease. *Biochem Biophys Res Commun* **232,** 418-421.

Kitano J, Kimura K, Yamazaki Y, Soda T, Shigemoto R, Nakajima Y & Nakanishi S. (2002). Tamalin, a PDZ domain-containing protein, links a protein complex formation of group 1 metabotropic glutamate receptors and the guanine nucleotide exchange factor cytohesins. *J Neurosci* **22,** 1280-1289.

Klein WL, Krafft GA & Finch CE. (2001). Targeting small Abeta oligomers: the solution to an Alzheimer's disease conundrum? *Trends Neurosci* **24,** 219-224.

Knudson CM, Tung KS, Tourtellotte WG, Brown GA & Korsmeyer SJ. (1995). Bax-deficient mice with lymphoid hyperplasia and male germ cell death. *Science* **270,** 96-99.

Koblinski JE, Ahram M & Sloane BF. (2000). Unraveling the role of proteases in cancer. *Clin Chim Acta* **291,** 113-135.

Komarov PG, Komarova EA, Kondratov RV, Christov-Tselkov K, Coon JS, Chernov MV & Gudkov AV. (1999). A chemical inhibitor of p53 that protects mice from the side effects of cancer therapy. *Science* **285,** 1733-1737.

Komatsu M, Takahashi T, Abe T, Takahashi I, Ida H & Takada G. (2001). Evidence for the association of ultraviolet-C and H(2)O(2)-induced apoptosis with acid sphingomyelinase activation. *Biochim Biophys Acta* **1533,** 47-54.

Kontush A. (2001). Amyloid-beta: An antioxidant that becomes a pro-oxidant and critically contributes to Alzheimer's disease. *Free Radic Biol Med,* 1120-1131.

Kornfeld S & Mellman I. (1989). The biogenesis of lysosomes. *Annu Rev Cell Biol* **5,** 483-525.

Korsmeyer SJ. (1995). Regulators of cell death. *Trends Genet* **11,** 101-105.

Koudinov ARaK, N. V. (2001). Essential role for cholesterol in synaptic plasticity and neuronal degeneration. *Faseb J,* 1858-1860.

Krajewski S, Krajewska M, Ehrmann J, Sikorska M, Lach B, Chatten J & Reed JC. (1997). Immunohistochemical analysis of Bcl-2, Bcl-X, Mcl-1, and Bax in tumors of central and peripheral nervous system origin. *Am J Pathol* **150,** 805-814.

Krajewski S, Krajewska M, Shabaik A, Miyashita T, Wang HG & Reed JC. (1994). Immunohistochemical determination of in vivo distribution of Bax, a dominant inhibitor of Bcl-2. *Am J Pathol* **145,** 1323-1336.

Kroemer G & Jaattela M. (2005). Lysosomes and autophagy in cell death control. *Nat Rev Cancer* **5,** 886-897.

Kroemer G, Zamzami N & Susin SA. (1997). Mitochondrial control of apoptosis. *Immunol Today* **18,** 44-51.

Kuan CY, Yang, D. D., Samanta Roy, D. R., Davis, R. J., Rakic, P. and Flavell, R. A. (1999). The Jnk1 and Jnk2 protein kinases are required

for regional specific apoptosis during early brain development. *Neuron*, 667-676.

Kubbutat MH & Vousden KH. (1997). Proteolytic cleavage of human p53 by calpain: a potential regulator of protein stability. *Mol Cell Biol* **17,** 460-468.

Kundra R & Kornfeld S. (1999). Asparagine-linked oligosaccharides protect Lamp-1 and Lamp-2 from intracellular proteolysis. *J Biol Chem* **274,** 31039-31046.

Kuo YM, Emmerling MR, Bisgaier CL, Essenburg AD, Lampert HC, Drumm D & Roher AE. (1998). Elevated low-density lipoprotein in Alzheimer's disease correlates with brain abeta 1-42 levels. *Biochem Biophys Res Commun* **252,** 711-715.

Kuperstein F, Reiss N, Koudinova N & Yavin E. (2001). Biphasic modulation of protein kinase C and enhanced cell toxicity by amyloid beta peptide and anoxia in neuronal cultures. *J Neurochem* **76,** 758-767.

Kuperstein F & Yavin E. (2002). ERK activation and nuclear translocation in amyloid-beta peptide- and iron-stressed neuronal cell cultures. *Eur J Neurosci* **16,** 44-54.

Kurosaki T, Takata M, Yamanashi Y, Inazu T, Taniguchi T, Yamamoto T & Yamamura H. (1994). Syk activation by the Src-family tyrosine kinase in the B cell receptor signaling. *J Exp Med* **179,** 1725-1729.

Kyriakis JM, Banerjee P, Nikolakaki E, Dai T, Rubie EA, Ahmad MF, Avruch J & Woodgett JR. (1994). The stress-activated protein kinase subfamily of c-Jun kinases. *Nature* **369,** 156-160.

LaFerla FM, Hall CK, Ngo L & Jay G. (1996). Extracellular deposition of beta-amyloid upon p53-dependent neuronal cell death in transgenic mice. *J Clin Invest* **98,** 1626-1632.

Lai JY, Cox PJ, Patel R, Sadiq S, Aldous DJ, Thurairatnam S, Smith K, Wheeler D, Jagpal S, Parveen S, Fenton G, Harrison TK, McCarthy C & Bamborough P. (2003). Potent small molecule inhibitors of spleen tyrosine kinase (Syk). *Bioorg Med Chem Lett* **13,** 3111-3114.

Lane NJ, Balbo A, Fukuyama R, Rapoport SI & Galdzicki Z. (1998). The ultrastructural effects of beta-amyloid peptide on cultured PC12 cells: changes in cytoplasmic and intramembranous features. *J Neurocytol* **27,** 707-718.

Latour S & Veillette A. (2001). Proximal protein tyrosine kinases in

immunoreceptor signaling. *Curr Opin Immunol* **13,** 299-306.

Lazebnik YA, Kaufmann SH, Desnoyers S, Poirier GG & Earnshaw WC. (1994). Cleavage of poly(ADP-ribose) polymerase by a proteinase with properties like ICE. *Nature* **371,** 346-347.

Le-Niculescu H, Bonfoco E, Kasuya Y, Claret FX, Green DR & Karin M. (1999). Withdrawal of survival factors results in activation of the JNK pathway in neuronal cells leading to Fas ligand induction and cell death. *Mol Cell Biol* **19,** 751-763.

Lee S, Christokos, S. and Small, M. B. (1993). Apoptosis and signal transduction: clues to a molecular mechanism. *Current Opinion in Cell Biology*, 286-291.

Lees-Miller SP, Chen YR & Anderson CW. (1990). Human cells contain a DNA-activated protein kinase that phosphorylates simian virus 40 T antigen, mouse p53, and the human Ku autoantigen. *Mol Cell Biol* **10,** 6472-6481.

Lei K, Nimnual A, Zong WX, Kennedy NJ, Flavell RA, Thompson CB, Bar-Sagi D & Davis RJ. (2002). The Bax subfamily of Bcl2-related proteins is essential for apoptotic signal transduction by c-Jun NH(2)-terminal kinase. *Mol Cell Biol* **22,** 4929-4942.

Leist M & Jaattela M. (2001a). Four deaths and a funeral: from caspases to alternative mechanisms. *Nat Rev Mol Cell Biol* **2,** 589-598.

Leist M & Jaattela M. (2001b). Triggering of apoptosis by cathepsins. *Cell Death Differ* **8,** 324-326.

Leong SK & Ling EA. (1992). Amoeboid and ramified microglia: their interrelationship and response to brain injury. *Glia* **6,** 39-47.

Lerner TJ, D'Arigo KL, Haines JL, Doggett NA, Taschner PE, de Vos N & Buckler AJ. (1995). Isolation of genes from the Batten candidate region using exon amplification. Batten Disease Consortium. *Am J Med Genet* **57,** 320-323.

Lev S, Moreno H, Martinez R, Canoll P, Peles E, Musacchio JM, Plowman GD, Rudy B & Schlessinger J. (1995). Protein tyrosine kinase PYK2 involved in Ca(2+)-induced regulation of ion channel and MAP kinase functions. *Nature* **376,** 737-745.

Levine AJ. (1997). p53, the cellular gatekeeper for growth and division. *Cell* **88,** 323-331.

Lewis J, Dickson DW, Lin WL, Chisholm L, Corral A, Jones G, Yen SH, Sahara N, Skipper L, Yager D, Eckman C, Hardy J, Hutton M & McGowan E. (2001). Enhanced neurofibrillary degeneration in transgenic mice expressing mutant tau and APP. *Science* **293,** 1487-1491.

Li H, Zhu H, Xu CJ & Yuan J. (1998). Cleavage of BID by caspase 8 mediates the mitochondrial damage in the Fas pathway of apoptosis. *Cell* **94,** 491-501.

Li W, Yuan X, Nordgren G, Dalen H, Dubowchik GM, Firestone RA & Brunk UT. (2000). Induction of cell death by the lysosomotropic detergent MSDH. *FEBS Lett* **470,** 35-39.

Li Y, Chopp M, Zhang ZG, Zaloga C, Niewenhuis L & Gautam S. (1994). p53-immunoreactive protein and p53 mRNA expression after transient middle cerebral artery occlusion in rats. *Stroke* **25,** 849-855; discussion 855-846.

Liu Q, Kawai H & Berg DK. (2001). beta -Amyloid peptide blocks the response of alpha 7-containing nicotinic receptors on hippocampal neurons. *Proc Natl Acad Sci U S A* **98,** 4734-4739.

Liu X, Kim CN, Yang J, Jemmerson R & Wang X. (1996). Induction of apoptotic program in cell-free extracts: requirement for dATP and cytochrome c. *Cell* **86,** 147-157.

Logan SK, Falasca M, Hu P & Schlessinger J. (1997). Phosphatidylinositol 3-kinase mediates epidermal growth factor-induced activation of the c-Jun N-terminal kinase signaling pathway. *Mol Cell Biol* **17,** 5784-5790.

Lohi O & Lehto VP. (1998). ITAM motif in an apoptosis-receptor. *Apoptosis* **3,** 335-336.

Lonergan PE, Martin DS, Horrobin DF & Lynch MA. (2002). Neuroprotective effect of eicosapentaenoic acid in hippocampus of rats exposed to gamma-irradiation. *J Biol Chem* **277,** 20804-20811.

Loo DT, Copani, A. P., Pike,C. J., Whittemore, E. R., Walencewicz, A. J. and Cotman, C. W. . (1993). Apoptosis is induced by beta-amyloid in cutured central nervous system neurons. *Proc Natl Acad Sci U S A,* 7951-7955.

Lorenzo A, Yuan M, Zhang Z, Paganetti PA, Sturchler-Pierrat C, Staufenbiel M, Mautino J, Vigo FS, Sommer B & Yankner BA. (2000). Amyloid beta interacts with the amyloid precursor protein: a potential toxic mechanism in Alzheimer's disease. *Nat Neurosci* **3,** 460-464.

Lu H, Taya Y, Ikeda M & Levine AJ. (1998). Ultraviolet radiation, but not gamma radiation or etoposide-induced DNA damage, results in the phosphorylation of the murine p53 protein at serine-389. *Proc Natl Acad Sci U S A* **95,** 6399-6402.

Luo Y, Umegaki H, Wang X, Abe R & Roth GS. (1998). Dopamine induces apoptosis through an oxidation-involved SAPK/JNK activation pathway. *J Biol Chem* **273,** 3756-3764.

Lynch AM & Lynch MA. (2002). The age-related increase in IL-1 type I receptor in rat hippocampus is coupled with an increase in caspase-3 activation. *Eur J Neurosci* **15,** 1779-1788.

Lynch AM, Walsh C, Delaney A, Nolan Y, Campbell VA & Lynch MA. (2004). Lipopolysaccharide-induced increase in signalling in hippocampus is abrogated by IL-10--a role for IL-1 beta? *J Neurochem* **88,** 635-646.

Ma H, Yankee TM, Hu J, Asai DJ, Harrison ML & Geahlen RL. (2001). Visualization of Syk-antigen receptor interactions using green fluorescent protein: differential roles for Syk and Lyn in the regulation of receptor capping and internalization. *J Immunol* **166,** 1507-1516.

Macdonald SG, Crews CM, Wu L, Driller J, Clark R, Erikson RL & McCormick F. (1993). Reconstitution of the Raf-1-MEK-ERK signal transduction pathway in vitro. *Mol Cell Biol* **13,** 6615-6620.

MacGibbon GA, Lawlor PA, Sirimanne ES, Walton MR, Connor B, Young D, Williams C, Gluckman P, Faull RL, Hughes P & Dragunow M. (1997). Bax expression in mammalian neurons undergoing apoptosis, and in Alzheimer's disease hippocampus. *Brain Res* **750,** 223-234.

MacManus A, Ramsden M, Murray M, Henderson Z, Pearson HA & Campbell VA. (2000). Enhancement of (45)Ca(2+) influx and voltage-dependent Ca(2+) channel activity by beta-amyloid-(1-40) in rat cortical synaptosomes and cultured cortical neurons. Modulation by the proinflammatory cytokine interleukin-1beta. *J Biol Chem* **275,** 4713-4718.

Maeda K, Hata R, Gillardon F & Hossmann KA. (2001). Aggravation of brain injury after transient focal ischemia in p53-deficient mice. *Brain Res Mol Brain Res* **88,** 54-61.

Manna SK & Aggarwal BB. (1998a). Alpha-melanocyte-stimulating hormone inhibits the nuclear transcription factor NF-kappa B activation induced by various inflammatory agents. *J Immunol* **161,** 2873-2880.

Manna SK, Zhang HJ, Yan T, Oberley LW & Aggarwal BB. (1998b). Overexpression of manganese superoxide dismutase suppresses tumor necrosis factor-induced apoptosis and activation of nuclear transcription factor-kappaB and activated protein-1. *J Biol Chem* **273,** 13245-13254.

Marchenko ND, Zaika A & Moll UM. (2000). Death signal-induced localization of p53 protein to mitochondria. A potential role in apoptotic signaling. *J Biol Chem* **275,** 16202-16212.

Marsh D. (1987). Selectivity of lipid-protein interactions. *J Bioenerg Biomembr* **19,** 677-689.

Marshall CJ. (1995). Specificity of receptor tyrosine kinase signaling: transient versus sustained extracellular signal-regulated kinase activation. *Cell* **80,** 179-185.

Martin JH, Mohit, A. A. and Miller C. A. (1996). Developmental expression in the mouse nervous system of the $p493^{F12}$ SAP kinase. *Molecular Brain Research*, 47-57.

Martin SJ, and Green, D. R. (1995). Protease activation during apoptosis: Death by a thousand cuts? *Cell*, 349-352.

Mathiasen IS & Jaattela M. (2002). Triggering caspase-independent cell death to combat cancer. *Trends Mol Med* **8,** 212-220.

Mattson MP, Cheng B, Culwell AR, Esch FS, Lieberburg I & Rydel RE. (1993a). Evidence for excitoprotective and intraneuronal calcium-regulating roles for secreted forms of the beta-amyloid precursor protein. *Neuron* **10,** 243-254.

Mattson MP, Tomaselli KJ & Rydel RE. (1993b). Calcium-destabilizing and neurodegenerative effects of aggregated beta-amyloid peptide are attenuated by basic FGF. *Brain Res* **621,** 35-49.

McCormack RM, Fogarty, M. P. and Campbell, V. A. (2006). Bea-Amyloid regulaes the lysosomal system in rat cultured cortical nerons in a p53-dependent manner. *Neurobiology of Ageing* **Submitted 2006**.

McDonald DR, Bamberger ME, Combs CK & Landreth GE. (1998). beta-Amyloid fibrils activate parallel mitogen-activated protein kinase pathways in microglia and THP1 monocytes. *J Neurosci* **18,** 4451-4460.

McDonald DR, Brunden KR & Landreth GE. (1997). Amyloid fibrils activate tyrosine kinase-dependent signaling and superoxide production in microglia. *J Neurosci* **17,** 2284-2294.

McGeer EG & McGeer PL. (2003). Inflammatory processes in Alzheimer's disease. *Prog Neuropsychopharmacol Biol Psychiatry* **27,** 741-749.

McGeer PL, Akiyama H, Itagaki S & McGeer EG. (1989). Activation of the classical complement pathway in brain tissue of Alzheimer patients. *Neurosci Lett* **107,** 341-346.

McGeer PL, Kawamata T, Walker DG, Akiyama H, Tooyama I & McGeer EG. (1993). Microglia in degenerative neurological disease. *Glia* **7,** 84-92.

McHugh K, Olsen EO & Vellodi A. (2004). Gaucher disease in children: radiology of non-central nervous system manifestations. *Clin Radiol* **59,** 117-123.

Mielke K & Herdegen T. (2000). JNK and p38 stresskinases--degenerative effectors of signal-transduction-cascades in the nervous system. *Prog Neurobiol* **61,** 45-60.

Mihara M, Erster S, Zaika A, Petrenko O, Chittenden T, Pancoska P & Moll UM. (2003). p53 has a direct apoptogenic role at the mitochondria. *Mol Cell* **11,** 577-590.

Miller FD, Pozniak CD & Walsh GS. (2000). Neuronal life and death: an essential role for the p53 family. *Cell Death Differ* **7,** 880-888.

Minden A & Karin M. (1997). Regulation and function of the JNK subgroup of MAP kinases. *Biochim Biophys Acta* **1333,** F85-104.

Minden A, Lin A, Claret FX, Abo A & Karin M. (1995). Selective activation of the JNK signaling cascade and c-Jun transcriptional activity by the small GTPases Rac and Cdc42Hs. *Cell* **81,** 1147-1157.

Minn AJ, Velez P, Schendel SL, Liang H, Muchmore SW, Fesik SW, Fill M & Thompson CB. (1997). Bcl-x(L) forms an ion channel in synthetic lipid membranes. *Nature* **385,** 353-357.

Minogue AM, Schmid AW, Fogarty MP, Moore AC, Campbell VA, Herron CE & Lynch MA. (2003). Activation of the c-Jun N-terminal kinase signaling cascade mediates the effect of amyloid-beta on long term potentiation and cell death in hippocampus: a role for interleukin-1beta? *J Biol Chem* **278,** 27971-27980.

Miyashita T & Reed JC. (1995). Tumor suppressor p53 is a direct transcriptional activator of the human bax gene. *Cell* **80,** 293-299.

Mohit AA, Martin JH & Miller CA. (1995). p493F12 kinase: a novel MAP

kinase expressed in a subset of neurons in the human nervous system. *Neuron* **14,** 67-78.

Morimoto K, Yoshimi, K., Tonohiro, T., Yamada, N. and Oda, T.K.I. (1998). Co-injection of beta-amyloid with ibotenic acid induces synergistic loss of rat hippocampal neurons. *Neuroscience*, 479-487.

Morishma Y, Gotoh, Y., Zieg, J., Barrett, T., Takano, H., Flavell, R., Davis, R. J., Shiraski, Y. and Greenberg, M. E. (2001). Beta-amyloid induced neuronal apoptosis via a mechanism that involves the c-Jun N-terminal kinase pathway and the induction of Fas Ligand. *Journal of Neuroscience*, 7551-7560.

Moroni M, Soldatenkov V, Zhang L, Zhang Y, Stoica G, Gehan E, Rashidi B, Singh B, Ozdemirli M & Mueller SC. (2004). Progressive loss of Syk and abnormal proliferation in breast cancer cells. *Cancer Res* **64,** 7346-7354.

Morrison RS, Wenzel HJ, Kinoshita Y, Robbins CA, Donehower LA & Schwartzkroin PA. (1996). Loss of the p53 tumor suppressor gene protects neurons from kainate-induced cell death. *J Neurosci* **16,** 1337-1345.

Muchmore SW, Sattler M, Liang H, Meadows RP, Harlan JE, Yoon HS, Nettesheim D, Chang BS, Thompson CB, Wong SL, Ng SL & Fesik SW. (1996). X-ray and NMR structure of human Bcl-xL, an inhibitor of programmed cell death. *Nature* **381,** 335-341.

Murray B, Alessandrini A, Cole AJ, Yee AG & Furshpan EJ. (1998). Inhibition of the p44/42 MAP kinase pathway protects hippocampal neurons in a cell-culture model of seizure activity. *Proc Natl Acad Sci U S A* **95,** 11975-11980.

Nagata E, Sawa A, Ross CA & Snyder SH. (2004). Autophagosome-like vacuole formation in Huntington's disease lymphoblasts. *Neuroreport* **15,** 1325-1328.

Nakamura Y, Takeda M, Suzuki H, Hattori H, Tada K, Hariguchi S, Hashimoto S & Nishimura T. (1991). Abnormal distribution of cathepsins in the brain of patients with Alzheimer's disease. *Neurosci Lett* **130,** 195-198.

Nakamura Y, Takeda M, Suzuki H, Morita H, Tada K, Hariguchi S & Nishimura T. (1989). Age-dependent change in activities of lysosomal enzymes in rat brain. *Mech Ageing Dev* **50,** 215-225.

Nakanishi H. (2003). Microglial functions and proteases. *Mol Neurobiol* **27,**

163-176.

Namura S, Zhu J, Fink K, Endres M, Srinivasan A, Tomaselli KJ, Yuan J & Moskowitz MA. (1998). Activation and cleavage of caspase-3 in apoptosis induced by experimental cerebral ischemia. *J Neurosci* **18,** 3659-3668.

Napieralski JA, Raghupathi R & McIntosh TK. (1999). The tumor-suppressor gene, p53, is induced in injured brain regions following experimental traumatic brain injury. *Brain Res Mol Brain Res* **71,** 78-86.

Narita M, Shimizu S, Ito T, Chittenden T, Lutz RJ, Matsuda H & Tsujimoto Y. (1998). Bax interacts with the permeability transition pore to induce permeability transition and cytochrome c release in isolated mitochondria. *Proc Natl Acad Sci U S A* **95,** 14681-14686.

Nechushtan A, Smith CL, Hsu YT & Youle RJ. (1999). Conformation of the Bax C-terminus regulates subcellular location and cell death. *Embo J* **18,** 2330-2341.

Nicotera P, Leist M & Manzo L. (1999). Neuronal cell death: a demise with different shapes. *Trends Pharmacol Sci* **20,** 46-51.

Nixon RA. (2003). The calpains in aging and aging-related diseases. *Ageing Res Rev* **2,** 407-418.

Nixon RA & Cataldo AM. (1995). The endosomal-lysosomal system of neurons: new roles. *Trends Neurosci* **18,** 489-496.

Nixon RA, Cataldo AM & Mathews PM. (2000). The endosomal-lysosomal system of neurons in Alzheimer's disease pathogenesis: a review. *Neurochem Res* **25,** 1161-1172.

Nourhashemi F, Ousset PJ, Guyonnet S, Andrieu S, Rolland Y, Adoue D, Vellas B & Albarede JL. (2000). Alzheimer's disease: from pathology to preventive methods. *Rev Med Interne* **21,** 524-532.

Nykjaer A, Christensen EI, Vorum H, Hager H, Petersen CM, Roigaard H, Min HY, Vilhardt F, Moller LB, Kornfeld S & Gliemann J. (1998). Mannose 6-phosphate/insulin-like growth factor-II receptor targets the urokinase receptor to lysosomes via a novel binding interaction. *J Cell Biol* **141,** 815-828.

Nylandsted J, Wick W, Hirt UA, Brand K, Rohde M, Leist M, Weller M & Jaattela M. (2002). Eradication of glioblastoma, and breast and colon carcinoma xenografts by Hsp70 depletion. *Cancer Res* **62,** 7139-7142.

O'Donnell E, Vereker E & Lynch MA. (2000). Age-related impairment in LTP is accompanied by enhanced activity of stress-activated protein kinases: analysis of underlying mechanisms. *Eur J Neurosci* **12,** 345-352.

Ohyagi Y, Asahara H, Chui DH, Tsuruta Y, Sakae N, Miyoshi K, Yamada T, Kikuchi H, Taniwaki T, Murai H, Ikezoe K, Furuya H, Kawarabayashi T, Shoji M, Checler F, Iwaki T, Makifuchi T, Takeda K, Kira J & Tabira T. (2005). Intracellular Abeta42 activates p53 promoter: a pathway to neurodegeneration in Alzheimer's disease. *Faseb J* **19,** 255-257.

Okamura S, Ng CC, Koyama K, Takei Y, Arakawa H, Monden M & Nakamura Y. (1999). Identification of seven genes regulated by wild-type p53 in a colon cancer cell line carrying a well-controlled wild-type p53 expression system. *Oncol Res* **11,** 281-285.

Ollinger K & Brunk UT. (1995). Cellular injury induced by oxidative stress is mediated through lysosomal damage. *Free Radic Biol Med* **19,** 565-574.

Oltvai ZN, Milliman CL & Korsmeyer SJ. (1993). Bcl-2 heterodimerizes in vivo with a conserved homolog, Bax, that accelerates programmed cell death. *Cell* **74,** 609-619.

Ozaki I, Tani E, Ikemoto H, Kitagawa H & Fujikawa H. (1999). Activation of stress-activated protein kinase/c-Jun NH2-terminal kinase and p38 kinase in calphostin C-induced apoptosis requires caspase-3-like proteases but is dispensable for cell death. *J Biol Chem* **274,** 5310-5317.

Pagano M, Capony F & Rochefort H. (1989). [Pro-cathepsin D can activate in vitro pro-cathepsin B secreted by ovarian cancers]. *C R Acad Sci III* **309,** 7-12.

Panegyres PK. (2001). The functions of the amyloid precursor protein gene. *Rev Neurosci* **12,** 1-39.

Paradis E, Douillard H, Koutroumanis M, Goodyer C & LeBlanc A. (1996). Amyloid beta peptide of Alzheimer's disease downregulates Bcl-2 and upregulates bax expression in human neurons. *J Neurosci* **16,** 7533-7539.

Perez RG, Zheng H, Van der Ploeg LH & Koo EH. (1997). The beta-amyloid precursor protein of Alzheimer's disease enhances neuron viability and modulates neuronal polarity. *J Neurosci* **17,** 9407-9414.

Perry G, Roder H, Nunomura A, Takeda A, Friedlich AL, Zhu X, Raina AK, Holbrook N, Siedlak SL, Harris PL & Smith MA. (1999). Activation of neuronal extracellular receptor kinase (ERK) in Alzheimer disease

links oxidative stress to abnormal phosphorylation. *Neuroreport* **10,** 2411-2415.

Petanceska S, Canoll P & Devi LA. (1996). Expression of rat cathepsin S in phagocytic cells. *J Biol Chem* **271,** 4403-4409.

Pieper AA, Verma A, Zhang J & Snyder SH. (1999). Poly (ADP-ribose) polymerase, nitric oxide and cell death. *Trends Pharmacol Sci* **20,** 171-181.

Polyak K, Xia Y, Zweier JL, Kinzler KW & Vogelstein B. (1997). A model for p53-induced apoptosis. *Nature* **389,** 300-305.

Puranam KL, Guo WX, Qian WH, Nikbakht K & Boustany RM. (1999). CLN3 defines a novel antiapoptotic pathway operative in neurodegeneration and mediated by ceramide. *Mol Genet Metab* **66,** 294-308.

Pyo H, Jou I, Jung S, Hong S & Joe EH. (1998). Mitogen-activated protein kinases activated by lipopolysaccharide and beta-amyloid in cultured rat microglia. *Neuroreport* **9,** 871-874.

Qin S, Ding J, Kurosaki T & Yamamura H. (1998). A deficiency in Syk enhances ceramide-induced apoptosis in DT40 lymphoma B cells. *FEBS Lett* **427,** 139-143.

Qin S, Minami Y, Hibi M, Kurosaki T & Yamamura H. (1997a). Syk-dependent and -independent signaling cascades in B cells elicited by osmotic and oxidative stress. *J Biol Chem* **272,** 2098-2103.

Qin S, Minami Y, Kurosaki T & Yamamura H. (1997b). Distinctive functions of Syk and Lyn in mediating osmotic stress- and ultraviolet C irradiation-induced apoptosis in chicken B cells. *J Biol Chem* **272,** 17994-17999.

Raber J, Wong, D., Buttini, M., Bellosta, S., Pitas, R. E. Mahley, R. W. and Mucke, L. (1998). Isoform-specific effects of human apolipoprotein E on brain function revealed in ApoE knockout mice: Increased susceptibility of females. *Proc Natl Acad Sci U S A*, 9480-9484.

Raff M. (1998). Cell suicide for beginners. *Nature* **396,** 119-122.

Raffray M & Cohen GM. (1997). Apoptosis and necrosis in toxicology: a continuum or distinct modes of cell death? *Pharmacol Ther* **75,** 153-177.

Raina AK, Hochman A, Zhu X, Rottkamp CA, Nunomura A, Siedlak SL, Boux H, Castellani RJ, Perry G & Smith MA. (2001). Abortive apoptosis in Alzheimer's disease. *Acta Neuropathol (Berl)* **101,** 305-310.

Rapoport M & Ferreira A. (2000). PD98059 prevents neurite degeneration induced by fibrillar beta-amyloid in mature hippocampal neurons. *J Neurochem* **74,** 125-133.

Raynaud F & Marcilhac A. (2006). Implication of calpain in neuronal apoptosis. A possible regulation of Alzheimer's disease. *Febs J* **273,** 3437-3443.

Reed JC. (1997). Cytochrome c: can't live with it--can't live without it. *Cell* **91,** 559-562.

Reiners JJ, Jr., Caruso JA, Mathieu P, Chelladurai B, Yin XM & Kessel D. (2002). Release of cytochrome c and activation of pro-caspase-9 following lysosomal photodamage involves Bid cleavage. *Cell Death Differ* **9,** 934-944.

Reinheckel T, Deussing J, Roth W & Peters C. (2001). Towards specific functions of lysosomal cysteine peptidases: phenotypes of mice deficient for cathepsin B or cathepsin L. *Biol Chem* **382,** 735-741.

Reitman ML & Kornfeld S. (1981). Lysosomal enzyme targeting. N-Acetylglucosaminylphosphotransferase selectively phosphorylates native lysosomal enzymes. *J Biol Chem* **256,** 11977-11980.

Richard F & Amouyel P. (2001). Genetic susceptibility factors for Alzheimer's disease. *Eur J Pharmacol* **412,** 1-12.

Riikonen R, Vanhanen SL, Tyynela J, Santavuori P & Turpeinen U. (2000). CSF insulin-like growth factor-1 in infantile neuronal ceroid lipofuscinosis. *Neurology* **54,** 1828-1832.

Robbins DJ, Zhen E, Owaki H, Vanderbilt CA, Ebert D, Geppert TD & Cobb MH. (1993). Regulation and properties of extracellular signal-regulated protein kinases 1 and 2 in vitro. *J Biol Chem* **268,** 5097-5106.

Roberg K, Johansson U & Ollinger K. (1999). Lysosomal release of cathepsin D precedes relocation of cytochrome c and loss of mitochondrial transmembrane potential during apoptosis induced by oxidative stress. *Free Radic Biol Med* **27,** 1228-1237.

Roberg K & Ollinger K. (1998). Oxidative stress causes relocation of the lysosomal enzyme cathepsin D with ensuing apoptosis in neonatal rat cardiomyocytes. *Am J Pathol* **152,** 1151-1156.

Roberts LR, Kurosawa H, Bronk SF, Fesmier PJ, Agellon LB, Leung WY, Mao F & Gores GJ. (1997). Cathepsin B contributes to bile salt-

induced apoptosis of rat hepatocytes. *Gastroenterology* **113,** 1714-1726.

Rodriguez A, Webster P, Ortego J & Andrews NW. (1997). Lysosomes behave as Ca2+-regulated exocytic vesicles in fibroblasts and epithelial cells. *J Cell Biol* **137,** 93-104.

Rosenberg RN. (2003). Metal chelation therapy for Alzheimer disease. *Arch Neurol* **60,** 1678-1679.

Roth KA. (2001). Caspases, apoptosis, and Alzheimer disease: causation, correlation, and confusion. *J Neuropathol Exp Neurol* **60,** 829-838.

Rowley RB, Burkhardt AL, Chao HG, Matsueda GR & Bolen JB. (1995). Syk protein-tyrosine kinase is regulated by tyrosine-phosphorylated Ig alpha/Ig beta immunoreceptor tyrosine activation motif binding and autophosphorylation. *J Biol Chem* **270,** 11590-11594.

Ryan RE, Sloane BF, Sameni M & Wood PL. (1995). Microglial cathepsin B: an immunological examination of cellular and secreted species. *J Neurochem* **65,** 1035-1045.

Sada K, Takano T, Yanagi S & Yamamura H. (2001). Structure and function of Syk protein-tyrosine kinase. *J Biochem (Tokyo)* **130,** 177-186.

Sadik G, Kaji H, Takeda K, Yamagata F, Kameoka Y, Hashimoto K, Miyanaga K & Shinoda T. (1999). In vitro processing of amyloid precursor protein by cathepsin D. *Int J Biochem Cell Biol* **31,** 1327-1337.

Saftig P, Hetman M, Schmahl W, Weber K, Heine L, Mossmann H, Koster A, Hess B, Evers M, von Figura K & et al. (1995). Mice deficient for the lysosomal proteinase cathepsin D exhibit progressive atrophy of the intestinal mucosa and profound destruction of lymphoid cells. *Embo J* **14,** 3599-3608.

Santana P, Pena LA, Haimovitz-Friedman A, Martin S, Green D, McLoughlin M, Cordon-Cardo C, Schuchman EH, Fuks Z & Kolesnick R. (1996). Acid sphingomyelinase-deficient human lymphoblasts and mice are defective in radiation-induced apoptosis. *Cell* **86,** 189-199.

Satoh T, Nakatsuka D, Watanabe Y, Nagata I, Kikuchi H & Namura S. (2000). Neuroprotection by MAPK/ERK kinase inhibition with U0126 against oxidative stress in a mouse neuronal cell line and rat primary cultured cortical neurons. *Neurosci Lett* **288,** 163-166.

Schenk D, Games D & Seubert P. (2001). Potential treatment opportunities for Alzheimer's disease through inhibition of secretases and Abeta

immunization. *J Mol Neurosci* **17,** 259-267.

Schieven GL, Kirihara JM, Burg DL, Geahlen RL & Ledbetter JA. (1993). p72syk tyrosine kinase is activated by oxidizing conditions that induce lymphocyte tyrosine phosphorylation and Ca2+ signals. *J Biol Chem* **268,** 16688-16692.

Schlesinger PH, Gross A, Yin XM, Yamamoto K, Saito M, Waksman G & Korsmeyer SJ. (1997). Comparison of the ion channel characteristics of proapoptotic BAX and antiapoptotic BCL-2. *Proc Natl Acad Sci U S A* **94,** 11357-11362.

Schmechel DE, Saunders AM, Strittmatter WJ, Crain BJ, Hulette CM, Joo SH, Pericak-Vance MA, Goldgaber D & Roses AD. (1993). Increased amyloid beta-peptide deposition in cerebral cortex as a consequence of apolipoprotein E genotype in late-onset Alzheimer disease. *Proc Natl Acad Sci U S A* **90,** 9649-9653.

Schotte P, Van Criekinge, W., Van de Craen, M., Van Loo, G., Desedt, M., Grooten, J., Cornelissen, M., De Ridder, L., Vandekerckhove, J., Fiers, W., Vandenabeele, P. and Beyaert, R. . (1998). Cathepsin B-mediated activation of the proinflammatory caspase-11. *Biochem Biophys Res Commun*, 379-387.

Schubert D & Behl C. (1993). The expression of amyloid beta protein precursor protects nerve cells from beta-amyloid and glutamate toxicity and alters their interaction with the extracellular matrix. *Brain Res* **629,** 275-282.

Schutze S, Machleidt T, Adam D, Schwandner R, Wiegmann K, Kruse ML, Heinrich M, Wickel M & Kronke M. (1999). Inhibition of receptor internalization by monodansylcadaverine selectively blocks p55 tumor necrosis factor receptor death domain signaling. *J Biol Chem* **274,** 10203-10212.

Schweichel JU & Merker HJ. (1973). The morphology of various types of cell death in prenatal tissues. *Teratology* **7,** 253-266.

Sedarous M, Keramaris E, O'Hare M, Melloni E, Slack RS, Elce JS, Greer PA & Park DS. (2003). Calpains mediate p53 activation and neuronal death evoked by DNA damage. *J Biol Chem* **278,** 26031-26038.

Seidl R, Fang-Kircher S, Bidmon B, Cairns N & Lubec G. (1999). Apoptosis-associated proteins p53 and APO-1/Fas (CD95) in brains of adult patients with Down syndrome. *Neurosci Lett* **260,** 9-12.

Selkoe DJ. (1991). The molecular pathology of Alzheimer's disease. *Neuron*

**6,** 487-498.

Selkoe DJ. (1994). Alzheimer's disease beyond 1994: the path to therapeutics. *Neurobiol Aging* **15 Suppl 2,** S131-133.

Selkoe DJ. (1995). Alzheimer's disease. Missense on the membrane. *Nature* **375,** 734-735.

Selkoe DJ. (2001). Alzheimer's disease: genes, proteins, and therapy. *Physiol Rev* **81,** 741-766.

Selkoe DJ, Podlisny MB, Joachim CL, Vickers EA, Lee G, Fritz LC & Oltersdorf T. (1988). Beta-amyloid precursor protein of Alzheimer disease occurs as 110- to 135-kilodalton membrane-associated proteins in neural and nonneural tissues. *Proc Natl Acad Sci U S A* **85,** 7341-7345.

Selznick LA, Holtzman DM, Han BH, Gokden M, Srinivasan AN, Johnson EM, Jr. & Roth KA. (1999). In situ immunodetection of neuronal caspase-3 activation in Alzheimer disease. *J Neuropathol Exp Neurol* **58,** 1020-1026.

Shaulsky G, Goldfinger N, Ben-Ze'ev A & Rotter V. (1990). Nuclear accumulation of p53 protein is mediated by several nuclear localization signals and plays a role in tumorigenesis. *Mol Cell Biol* **10,** 6565-6577.

Shieh SY, Ikeda M, Taya Y & Prives C. (1997). DNA damage-induced phosphorylation of p53 alleviates inhibition by MDM2. *Cell* **91,** 325-334.

Shoji M, Iwakami N, Takeuchi S, Waragai M, Suzuki M, Kanazawa I, Lippa CF, Ono S & Okazawa H. (2000). JNK activation is associated with intracellular beta-amyloid accumulation. *Brain Res Mol Brain Res* **85,** 221-233.

Shumway SD, Maki M & Miyamoto S. (1999). The PEST domain of IkappaBalpha is necessary and sufficient for in vitro degradation by mu-calpain. *J Biol Chem* **274,** 30874-30881.

Sidorenko SP, Law CL, Chandran KA & Clark EA. (1995). Human spleen tyrosine kinase p72Syk associates with the Src-family kinase p53/56Lyn and a 120-kDa phosphoprotein. *Proc Natl Acad Sci U S A* **92,** 359-363.

Siman RaN, J. C. (1988). Excitatory amino acids actiate calpain I and induce structural protein breakdown in vivo. *Neuron*, 279-287.

Simmons LK, May, P. C., Tomaseli, K. J,m Rydel, R. E., Fuson, K.S., Brigham, E. F., Wright, S., Lieberburg, I., Becker, G. W. and Brems, D. N. (1994). Secondary structure of amyloid beta peptide correlates with neurotoxic activity in vitro. *Molecular Pharmacology*, 373-379.

Simons M, Schwarzler F, Lutjohann D, von Bergmann K, Beyreuther K, Dichgans J, Wormstall H, Hartmann T & Schulz JB. (2002). Treatment with simvastatin in normocholesterolemic patients with Alzheimer's disease: A 26-week randomized, placebo-controlled, double-blind trial. *Ann Neurol* **52,** 346-350.

Singer SJ & Dewji NN. (2006). Evidence that Perutz's double-beta-stranded subunit structure for beta-amyloids also applies to their channel-forming structures in membranes. *Proc Natl Acad Sci U S A* **103,** 1546-1550.

Slee EA, Adrain C & Martin SJ. (1999a). Serial killers: ordering caspase activation events in apoptosis. *Cell Death Differ* **6,** 1067-1074.

Slee EA, Harte MT, Kluck RM, Wolf BB, Casiano CA, Newmeyer DD, Wang HG, Reed JC, Nicholson DW, Alnemri ES, Green DR & Martin SJ. (1999b). Ordering the cytochrome c-initiated caspase cascade: hierarchical activation of caspases-2, -3, -6, -7, -8, and -10 in a caspase-9-dependent manner. *J Cell Biol* **144,** 281-292.

Smith-Swintosky VL, Pettigrew LC, Craddock SD, Culwell AR, Rydel RE & Mattson MP. (1994). Secreted forms of beta-amyloid precursor protein protect against ischemic brain injury. *J Neurochem* **63,** 781-784.

Smolen JE, Stoehr SJ & Boxer LA. (1986). Human neutrophils permeabilized with digitonin respond with lysosomal enzyme release when exposed to micromolar levels of free calcium. *Biochim Biophys Acta* **886,** 1-17.

Song X, Tanaka S, Cox D & Lee SC. (2004). Fcgamma receptor signaling in primary human microglia: differential roles of PI-3K and Ras/ERK MAPK pathways in phagocytosis and chemokine induction. *J Leukoc Biol* **75,** 1147-1155.

Songyang Z, Shoelson SE, McGlade J, Olivier P, Pawson T, Bustelo XR, Barbacid M, Sabe H, Hanafusa H, Yi T & et al. (1994). Specific motifs recognized by the SH2 domains of Csk, 3BP2, fps/fes, GRB-2, HCP, SHC, Syk, and Vav. *Mol Cell Biol* **14,** 2777-2785.

Sperandio S, de Belle I & Bredesen DE. (2000). An alternative, nonapoptotic form of programmed cell death. *Proc Natl Acad Sci U S A* **97,** 14376-14381.

St George-Hyslop PH. (2000a). Genetic factors in the genesis of Alzheimer's disease. *Ann N Y Acad Sci* **924,** 1-7.

St George-Hyslop PH. (2000b). Piecing together Alzheimer's. *Sci Am* **283,** 76-83.

St George-Hyslop PH, McLaurin J & Fraser PE. (2000c). Neuropathological, biochemical and genetic alterations in AD. *Drug News Perspect* **13,** 281-288.

Stanciu M, Wang Y, Kentor R, Burke N, Watkins S, Kress G, Reynolds I, Klann E, Angiolieri MR, Johnson JW & DeFranco DB. (2000). Persistent activation of ERK contributes to glutamate-induced oxidative toxicity in a neuronal cell line and primary cortical neuron cultures. *J Biol Chem* **275,** 12200-12206.

Stoka V, Turk B, Schendel SL, Kim TH, Cirman T, Snipas SJ, Ellerby LM, Bredesen D, Freeze H, Abrahamson M, Bromme D, Krajewski S, Reed JC, Yin XM, Turk V & Salvesen GS. (2001). Lysosomal protease pathways to apoptosis. Cleavage of bid, not pro-caspases, is the most likely route. *J Biol Chem* **276,** 3149-3157.

Strosznajder RP, Jesko H, Banasik M & Tanaka S. (2005). Effects of p53 inhibitor on survival and death of cells subjected to oxidative stress. *J Physiol Pharmacol* **56 Suppl 4,** 215-221.

Su JH, Cummings BJ & Cotman CW. (1994). Subpopulations of dystrophic neurites [correction of neuritis] in Alzheimer's brain with distinct immunocytochemical and argentophilic characteristics. *Brain Res* **637,** 37-44.

Sugden PH & Clerk A. (1997). Regulation of the ERK subgroup of MAP kinases cascades through G protein-coulped receptors. *Cell Signalling*, 337-351.

Sutton ET, Hellerman, G. R. and Thomas, T. (1997). beta-amyloid-induced endothelial necrosis and inhibition of nitric oxide production. *Exp Cell Res*, 368-376.

Suzuki A. (1997). Amyloid beta-protein induces necrotic cell death mediated by ICE cascade in PC12 cells. *Exp Cell Res* **234,** 507-511.

Takada Y & Aggarwal BB. (2004). TNF activates Syk protein tyrosine kinase leading to TNF-induced MAPK activation, NF-kappaB activation, and apoptosis. *J Immunol* **173,** 1066-1077.

Takano T, Sada K & Yamamura H. (2002). Role of protein-tyrosine kinase

syk in oxidative stress signaling in B cells. *Antioxid Redox Signal* **4,** 533-541.

Takata M, Homma Y & Kurosaki T. (1995). Requirement of phospholipase C-gamma 2 activation in surface immunoglobulin M-induced B cell apoptosis. *J Exp Med* **182,** 907-914.

Takata M, Sabe H, Hata A, Inazu T, Homma Y, Nukada T, Yamamura H & Kurosaki T. (1994). Tyrosine kinases Lyn and Syk regulate B cell receptor-coupled Ca2+ mobilization through distinct pathways. *Embo J* **13,** 1341-1349.

Talaga P & Quere L. (2002). The plasma membrane: a target and hurdle for the development of anti-Abeta drugs? *Curr Drug Targets CNS Neurol Disord* **1,** 567-574.

Tan J, Town, T., Placzek, A., Kundtz, A., Yu, H. and Mullan, M. (1999). Bcl-X(L) inhibits apoptosis and necrosis produced by Alzheimer's beta-amyloid 1-40 peptide in PC12 cells. *Neurosci Lett*, 5-8.

Tanaka Y, Guhde G, Suter A, Eskelinen EL, Hartmann D, Lullmann-Rauch R, Janssen PM, Blanz J, von Figura K & Saftig P. (2000). Accumulation of autophagic vacuoles and cardiomyopathy in LAMP-2-deficient mice. *Nature* **406,** 902-906.

Taniguchi T. (1995). Cytokine signaling through nonreceptor protein tyrosine kinases. *Science* **268,** 251-255.

Taniguchi T, Kobayashi T, Kondo J, Takahashi K, Nakamura H, Suzuki J, Nagai K, Yamada T, Nakamura S & Yamamura H. (1991). Molecular cloning of a porcine gene syk that encodes a 72-kDa protein-tyrosine kinase showing high susceptibility to proteolysis. *J Biol Chem* **266,** 15790-15796.

Tanzi RE & Bertram L. (2001). New frontiers in Alzheimer's disease genetics. *Neuron* **32,** 181-184.

Tardy C, Andrieu-Abadie N, Salvayre R & Levade T. (2004). Lysosomal storage diseases: is impaired apoptosis a pathogenic mechanism? *Neurochem Res* **29,** 871-880.

Terzi E, Holzemann G & Seelig J. (1997). Interaction of Alzheimer beta-amyloid peptide(1-40) with lipid membranes. *Biochemistry* **36,** 14845-14852.

Timokhina I, Kissel H, Stella G & Besmer P. (1998). Kit signaling through PI 3-kinase and Src kinase pathways: an essential role for Rac1 and JNK

activation in mast cell proliferation. *Embo J* **17,** 6250-6262.

Tischer E & Cordell B. (1996). Beta-amyloid precursor protein. Location of transmembrane domain and specificity of gamma-secretase cleavage. *J Biol Chem* **271,** 21914-21919.

Tobin DJ, Foitzik K, Reinheckel T, Mecklenburg L, Botchkarev VA, Peters C & Paus R. (2002). The lysosomal protease cathepsin L is an important regulator of keratinocyte and melanocyte differentiation during hair follicle morphogenesis and cycling. *Am J Pathol* **160,** 1807-1821.

Tolnai SaK, B. (1986). Calcium-dependent proteolysis and its inhibition in the ischemic rat myocardium. *Canadian journal of Cardiology*, 42-47.

Tournier C, Hess P, Yang DD, Xu J, Turner TK, Nimnual A, Bar-Sagi D, Jones SN, Flavell RA & Davis RJ. (2000). Requirement of JNK for stress-induced activation of the cytochrome c-mediated death pathway. *Science* **288,** 870-874.

Trotta R, Kanakaraj P & Perussia B. (1996). Fc gamma R-dependent mitogen-activated protein kinase activation in leukocytes: a common signal transduction event necessary for expression of TNF-alpha and early activation genes. *J Exp Med* **184,** 1027-1035.

Troy CM, Rabacchi SA, Friedman WJ, Frappier TF, Brown K & Shelanski ML. (2000). Caspase-2 mediates neuronal cell death induced by beta-amyloid. *J Neurosci* **20,** 1386-1392.

Troy CM, Rabacchi SA, Xu Z, Maroney AC, Connors TJ, Shelanski ML & Greene LA. (2001). beta-Amyloid-induced neuronal apoptosis requires c-Jun N-terminal kinase activation. *J Neurochem* **77,** 157-164.

Tsubata T, Wu J & Honjo T. (1993). B-cell apoptosis induced by antigen receptor crosslinking is blocked by a T-cell signal through CD40. *Nature* **364,** 645-648.

Tsuchida S, Yanagi S, Inatome R, Ding J, Hermann P, Tsujimura T, Matsui N & Yamamura H. (2000). Purification of a 72-kDa protein-tyrosine kinase from rat liver and its identification as Syk: involvement of Syk in signaling events of hepatocytes. *J Biochem (Tokyo)* **127,** 321-327.

Turk B, Dolenc I, Turk V & Bieth JG. (1993). Kinetics of the pH-induced inactivation of human cathepsin L. *Biochemistry* **32,** 375-380.

Turk B, Stoka V, Rozman-Pungercar J, Cirman T, Droga-Mazovec G, Oresic K & Turk V. (2002). Apoptotic pathways: involvement of lysosomal proteases. *Biol Chem* **383,** 1035-1044.

Turk B, Turk D & Turk V. (2000). Lysosomal cysteine proteases: more than scavengers. *Biochim Biophys Acta* **1477,** 98-111.

Turner M, Mee PJ, Costello PS, Williams O, Price AA, Duddy LP, Furlong MT, Geahlen RL & Tybulewicz VL. (1995). Perinatal lethality and blocked B-cell development in mice lacking the tyrosine kinase Syk. *Nature* **378,** 298-302.

Turner M, Schweighoffer E, Colucci F, Di Santo JP & Tybulewicz VL. (2000). Tyrosine kinase SYK: essential functions for immunoreceptor signalling. *Immunol Today* **21,** 148-154.

Urzainqui A, Serrador JM, Viedma F, Yanez-Mo M, Rodriguez A, Corbi AL, Alonso-Lebrero JL, Luque A, Deckert M, Vazquez J & Sanchez-Madrid F. (2002). ITAM-based interaction of ERM proteins with Syk mediates signaling by the leukocyte adhesion receptor PSGL-1. *Immunity* **17,** 401-412.

Vancompernolle K, Van Herreweghe F, Pynaert G, Van de Craen M, De Vos K, Totty N, Sterling A, Fiers W, Vandenabeele P & Grooten J. (1998). Atractyloside-induced release of cathepsin B, a protease with caspase-processing activity. *FEBS Lett* **438,** 150-158.

Varki A & Kornfeld S. (1981). Purification and characterization of rat liver alpha-N-acetylglucosaminyl phosphodiesterase. *J Biol Chem* **256,** 9937-9943.

Velez-Pardo C, Ospina GG & Jimenez del Rio M. (2002). Abeta[25-35] peptide and iron promote apoptosis in lymphocytes by an oxidative stress mechanism: involvement of H2O2, caspase-3, NF-kappaB, p53 and c-Jun. *Neurotoxicology* **23,** 351-365.

Vellodi A. (2005). Lysosomal storage disorders. *Br J Haematol* **128,** 413-431.

Vereker E, Campbell V, Roche E, McEntee E & Lynch MA. (2000). Lipopolysaccharide inhibits long term potentiation in the rat dentate gyrus by activating caspase-1. *J Biol Chem* **275,** 26252-26258.

Vereker E, O'Donnell E & Lynch MA. (2000). The inhibitory effect of interleukin-1beta on long-term potentiation is coupled with increased activity of stress-activated protein kinases. *J Neurosci* **20,** 6811-6819.

Virdee K, Bannister, A. J., Hunt, S. P. and Tolkovsky, A. M. (1997). Comparison between the timing of JNK activation, c-Jun phosphorylation, and onset of death comitment in sympathetic neurons. **69**.

Waheed A, Pohlmann R, Hasilik A & von Figura K. (1981). Subcellular location of two enzymes involved in the synthesis of phosphorylated recognition markers in lysosomal enzymes. *J Biol Chem* **256,** 4150-4152.

Walsh DM, Hartley DM, Kusumoto Y, Fezoui Y, Condron MM, Lomakin A, Benedek GB, Selkoe DJ & Teplow DB. (1999). Amyloid beta-protein fibrillogenesis. Structure and biological activity of protofibrillar intermediates. *J Biol Chem* **274,** 25945-25952.

Walter J, Capell A, Grunberg J, Pesold B, Schindzielorz A, Prior R, Podlisny MB, Fraser P, Hyslop PS, Selkoe DJ & Haass C. (1996). The Alzheimer's disease-associated presenilins are differentially phosphorylated proteins located predominantly within the endoplasmic reticulum. *Mol Med* **2,** 673-691.

Wang H & Malbon CC. (1999). G(s)alpha repression of adipogenesis via Syk. *J Biol Chem* **274,** 32159-32166.

Wang HG, Pathan N, Ethell IM, Krajewski S, Yamaguchi Y, Shibasaki F, McKeon F, Bobo T, Franke TF & Reed JC. (1999). Ca2+-induced apoptosis through calcineurin dephosphorylation of BAD. *Science* **284,** 339-343.

Wang J & Lenardo MJ. (2000). Roles of caspases in apoptosis, development, and cytokine maturation revealed by homozygous gene deficiencies. *J Cell Sci* **113 ( Pt 5),** 753-757.

Wang JH, Redmond HP, Watson RW & Bouchier-Hayes D. (1997). Induction of human endothelial cell apoptosis requires both heat shock and oxidative stress responses. *Am J Physiol* **272,** C1543-1551.

Wang KK. (2000). Calpain and caspase: can you tell the difference? *Trends Neurosci* **23,** 20-26.

Wang L, Duke L, Zhang PS, Arlinghaus RB, Symmans WF, Sahin A, Mendez R & Dai JL. (2003). Alternative splicing disrupts a nuclear localization signal in spleen tyrosine kinase that is required for invasion suppression in breast cancer. *Cancer Res* **63,** 4724-4730.

Watabe AM, Zaki PA & O'Dell TJ. (2000). Coactivation of beta-adrenergic and cholinergic receptors enhances the induction of long-term potentiation and synergistically activates mitogen-activated protein kinase in the hippocampal CA1 region. *J Neurosci* **20,** 5924-5931.

Werlen G, Jacinto E, Xia Y & Karin M. (1998). Calcineurin preferentially synergizes with PKC-theta to activate JNK and IL-2 promoter in T

lymphocytes. *Embo J* **17,** 3101-3111.

Werneburg NW, Guicciardi ME, Bronk SF & Gores GJ. (2002). Tumor necrosis factor-alpha-associated lysosomal permeabilization is cathepsin B dependent. *Am J Physiol Gastrointest Liver Physiol* **283,** G947-956.

Westwick JK, Cox AD, Der CJ, Cobb MH, Hibi M, Karin M & Brenner DA. (1994). Oncogenic Ras activates c-Jun via a separate pathway from the activation of extracellular signal-regulated kinases. *Proc Natl Acad Sci U S A* **91,** 6030-6034.

Wherrett JR & Huterer S. (1972). Enrichment of bis-(monoacylglyceryl) phosphate in lysosomes from rat liver. *J Biol Chem* **247,** 4114-4120.

White BC, Daya A, DeGracia DJ, O'Neil BJ, Skjaerlund JM, Trumble S, Krause GS & Rafols JA. (1993). Fluorescent histochemical localization of lipid peroxidation during brain reperfusion following cardiac arrest. *Acta Neuropathol (Berl)* **86,** 1-9.

Wiggin GR, Soloaga A, Foster JM, Murray-Tait V, Cohen P & Arthur JS. (2002). MSK1 and MSK2 are required for the mitogen- and stress-induced phosphorylation of CREB and ATF1 in fibroblasts. *Mol Cell Biol* **22,** 2871-2881.

Winchester BG. (2001). Lysosomal membrane proteins. *Eur J Paediatr Neurol* **5 Suppl A,** 11-19.

Wolter KG, Hsu YT, Smith CL, Nechushtan A, Xi XG & Youle RJ. (1997). Movement of Bax from the cytosol to mitochondria during apoptosis. *J Cell Biol* **139,** 1281-1292.

Wood JG & Zinsmeister P. (1991). Tyrosine phosphorylation systems in Alzheimer's disease pathology. *Neurosci Lett* **121,** 12-16.

Wu MP, Jay D & Stracher A. (1994). Existence of multiple phosphorylated forms of human platelet actin binding protein. *Cell Mol Biol Res* **40,** 351-357.

Xia Z, Dickens M, Raingeaud J, Davis RJ & Greenberg ME. (1995). Opposing effects of ERK and JNK-p38 MAP kinases on apoptosis. *Science* **270,** 1326-1331.

Xiang H, Hochman DW, Saya H, Fujiwara T, Schwartzkroin PA & Morrison RS. (1996). Evidence for p53-mediated modulation of neuronal viability. *J Neurosci* **16,** 6753-6765.

Xie L, Helmerhorst E, Taddei K, Plewright B, Van Bronswijk W & Martins R. (2002). Alzheimer's beta-amyloid peptides compete for insulin binding to the insulin receptor. *J Neurosci* **22,** RC221.

Yaar M, Zhai S, Fine RE, Eisenhauer PB, Arble BL, Stewart KB & Gilchrest BA. (2002). Amyloid beta binds trimers as well as monomers of the 75-kDa neurotrophin receptor and activates receptor signaling. *J Biol Chem* **277,** 7720-7725.

Yaar M, Zhai S, Pilch PF, Doyle SM, Eisenhauer PB, Fine RE & Gilchrest BA. (1997). Binding of beta-amyloid to the p75 neurotrophin receptor induces apoptosis. A possible mechanism for Alzheimer's disease. *J Clin Invest* **100,** 2333-2340.

Yamada T, Taniguchi T, Yang C, Yasue S, Saito H & Yamamura H. (1993). Association with B-cell-antigen receptor with protein-tyrosine kinase p72syk and activation by engagement of membrane IgM. *Eur J Biochem* **213,** 455-459.

Yamashima T, Kohda Y, Tsuchiya K, Ueno T, Yamashita J, Yoshioka T & Kominami E. (1998). Inhibition of ischaemic hippocampal neuronal death in primates with cathepsin B inhibitor CA-074: a novel strategy for neuroprotection based on 'calpain-cathepsin hypothesis'. *Eur J Neurosci* **10,** 1723-1733.

Yan SD, Chen X, Fu J, Chen M, Zhu H, Roher A, Slattery T, Zhao L, Nagashima M, Morser J, Migheli A, Nawroth P, Stern D & Schmidt AM. (1996). RAGE and amyloid-beta peptide neurotoxicity in Alzheimer's disease. *Nature* **382,** 685-691.

Yan SD, Fu J, Soto C, Chen X, Zhu H, Al-Mohanna F, Collison K, Zhu A, Stern E, Saido T, Tohyama M, Ogawa S, Roher A & Stern D. (1997). An intracellular protein that binds amyloid-beta peptide and mediates neurotoxicity in Alzheimer's disease. *Nature* **389,** 689-695.

Yan SD, Shi Y, Zhu A, Fu J, Zhu H, Zhu Y, Gibson L, Stern E, Collison K, Al-Mohanna F, Ogawa S, Roher A, Clarke SG & Stern DM. (1999). Role of ERAB/L-3-hydroxyacyl-coenzyme A dehydrogenase type II activity in Abeta-induced cytotoxicity. *J Biol Chem* **274,** 2145-2156.

Yang AJ, Chandswangbhuvana D, Margol L & Glabe CG. (1998). Loss of endosomal/lysosomal membrane impermeability is an early event in amyloid Abeta1-42 pathogenesis. *J Neurosci Res* **52,** 691-698.

Yang AJ, Knauer M, Burdick DA & Glabe C. (1995a). Intracellular A beta 1-42 aggregates stimulate the accumulation of stable, insoluble amyloidogenic fragments of the amyloid precursor protein in

transfected cells. *J Biol Chem* **270,** 14786-14792.

Yang DD, Kuan CY, Whitmarsh AJ, Rincon M, Zheng TS, Davis RJ, Rakic P & Flavell RA. (1997). Absence of excitotoxicity-induced apoptosis in the hippocampus of mice lacking the Jnk3 gene. *Nature* **389,** 865-870.

Yang E, Zha J, Jockel J, Boise LH, Thompson CB & Korsmeyer SJ. (1995b). Bad, a heterodimeric partner for Bcl-XL and Bcl-2, displaces Bax and promotes cell death. *Cell* **80,** 285-291.

Yankner BA, Dawes, L. R., Fisher, S., Villa-Komaroff, L., Oster-Granite, M. L. and Neve, R. L. (1989). Neurotoxicity of a fragment of the amyloid precursor associated with Alzheimer's disease. *Science*, 417-420.

Yankner BA. (1996). Mechanisms of neuronal degeneration in Alzheimer's disease. *Neuron* **16,** 921-932.

York RD, Yao H, Dillon T, Ellig CL, Eckert SP, McCleskey EW & Stork PJ. (1998). Rap1 mediates sustained MAP kinase activation induced by nerve growth factor. *Nature* **392,** 622-626.

Yoshiyama Y, Arai K, Oki T & Hattori T. (2000). Expression of invariant chain and pro-cathepsin L in Alzheimer's brain. *Neurosci Lett* **290,** 125-128.

Yoshizumi M, Kogame T, Suzaki Y, Fujita Y, Kyaw M, Kirima K, Ishizawa K, Tsuchiya K, Kagami S & Tamaki T. (2002). Ebselen attenuates oxidative stress-induced apoptosis via the inhibition of the c-Jun N-terminal kinase and activator protein-1 signalling pathway in PC12 cells. *Br J Pharmacol* **136,** 1023-1032.

Yousefi S, Hoessli DC, Blaser K, Mills GB & Simon HU. (1996). Requirement of Lyn and Syk tyrosine kinases for the prevention of apoptosis by cytokines in human eosinophils. *J Exp Med* **183,** 1407-1414.

Yuan J, Shaham S, Ledoux S, Ellis HM & Horvitz HR. (1993). The C. elegans cell death gene ced-3 encodes a protein similar to mammalian interleukin-1 beta-converting enzyme. *Cell* **75,** 641-652.

Yuan J & Yankner BA. (2000). Apoptosis in the nervous system. *Nature* **407,** 802-809.

Yuan XM, Li W, Brunk UT, Dalen H, Chang YH & Sevanian A. (2000). Lysosomal destabilization during macrophage damage induced by cholesterol oxidation products. *Free Radic Biol Med* **28,** 208-218.

Yuan XM, Li W, Dalen H, Lotem J, Kama R, Sachs L & Brunk UT. (2002). Lysosomal destabilization in p53-induced apoptosis. *Proc Natl Acad Sci*

*U S A* **99,** 6286-6291.

Yujiri T, Sather S, Fanger GR & Johnson GL. (1998). Role of MEKK1 in cell survival and activation of JNK and ERK pathways defined by targeted gene disruption. *Science* **282,** 1911-1914.

Zang Y, Beard RL, Chandraratna RA & Kang JX. (2001). Evidence of a lysosomal pathway for apoptosis induced by the synthetic retinoid CD437 in human leukemia HL-60 cells. *Cell Death Differ* **8,** 477-485.

Zha H, Fisk HA, Yaffe MP, Mahajan N, Herman B & Reed JC. (1996). Structure-function comparisons of the proapoptotic protein Bax in yeast and mammalian cells. *Mol Cell Biol* **16,** 6494-6508.

Zhang Y, Mattjus P, Schmid PC, Dong Z, Zhong S, Ma WY, Brown RE, Bode AM, Schmid HH & Dong Z. (2001). Involvement of the acid sphingomyelinase pathway in uva-induced apoptosis. *J Biol Chem* **276,** 11775-11782.

Zhang Y, McLaughlin R, Goodyer C & LeBlanc A. (2002). Selective cytotoxicity of intracellular amyloid beta peptide1-42 through p53 and Bax in cultured primary human neurons. *J Cell Biol* **156,** 519-529.

Zhao M, Eaton, J W. and Brunk, U. T. (2001a). Bcl-2 phosphorylation is required for inhibition of oxidative stress-induced lysosomal leak and ensuing apoptosis. *FEBS Lett*, 405-412.

Zhao ZQ, Budde JM, Morris C, Wang NP, Velez DA, Muraki S, Guyton RA & Vinten-Johansen J. (2001b). Adenosine attenuates reperfusion-induced apoptotic cell death by modulating expression of Bcl-2 and Bax proteins. *J Mol Cell Cardiol* **33,** 57-68.

Zhou F, Hu J, Ma H, Harrison ML & Geahlen RL. (2006). Nucleocytoplasmic trafficking of the Syk protein tyrosine kinase. *Mol Cell Biol* **26,** 3478-3491.

Zhu J & Chen X. (2000). MCG10, a novel p53 target gene that encodes a KH domain RNA-binding protein, is capable of inducing apoptosis and cell cycle arrest in G(2)-M. *Mol Cell Biol* **20,** 5602-5618.

Zhu X, Raina AK, Rottkamp CA, Aliev G, Perry G, Boux H & Smith MA. (2001). Activation and redistribution of c-jun N-terminal kinase/stress activated protein kinase in degenerating neurons in Alzheimer's disease. *J Neurochem* **76,** 435-441.

Zioncheck TF, Harrison ML, Isaacson CC & Geahlen RL. (1988). Generation of an active protein-tyrosine kinase from lymphocytes by proteolysis. *J*

*Biol Chem* **263,** 19195-19202.

Zornig M, Hueber A, Baum W & Evan G. (2001). Apoptosis regulators and their role in tumorigenesis. *Biochim Biophys Acta* **1551,** F1-37.

Zou H, Henzel WJ, Liu X, Lutschg A & Wang X. (1997). Apaf-1, a human protein homologous to C. elegans CED-4, participates in cytochrome c-dependent activation of caspase-3. *Cell* **90,** 405-413.

Zou L, Sato N & Kone BC. (2004). Alpha-melanocyte stimulating hormone protects against H2O2-induced inhibition of wound restitution in IEC-6 cells via a Syk kinase- and NF-kappabeta-dependent mechanism. *Shock* **22,** 453-459.

# IX Appendix-Solutions

*Cell Culture Solutions*

**70% EtOH (100ml)**

70ml EtOH

30ml $H_2O$

**PBS (cell culture)**

10mL Dublecco's Modified Phosphate Buffered Saline

100mL $H_2O$

**Trypsin Solution (cell culture)**

Soyabean trypsin inhibitor (0.02mg/mL)

Dnase (0.2mg/mL)

$MgSO_4$ (0.1M)

1mL PBS

**Supplemented Neurobasal Solution (day 1)**

Heat inactivated horse serum (10mL)

Penicillin/Strepomycin (100U/mL)

Glutamax (2mM)

B27 (1% 1mL)

100mL Neurobasal medium

**Supplemented Neurobasal Solution (day 4)**

Heat inactivated horse serum (10mL)

Penicillin/Strepomycin (100U/mL)

Glutamax (2mM)

ARA-C (5ng/mL)

100mL Neurobasal medium

**Supplemented Neurobasal Solution (day 5)**

Heat inactivated horse serum (10mL)

Penicillin/Strepomycin (100U/mL)

Glutamax (2mM)

100mL Neurobasal medium

*Cell Harvesting Solutions*

**Lysis Buffer, pH 7.4 (Harvesting total protein)**

HEPES (20mM)

KCL (10mM)

EGTA (1mM)

$MgCl_2$ (1.5mM)

DTT (1mM)

PMSF (0.1mM)

Leupeptin (2μg/mL)

Aprotinin (2μg/mL)

Sucrose(200mM)

**Permeabilisation Buffer pH7.2 (Harvesting cytosolic extracts)**

Sucrose(250mM)

KCL (70mM)

NaCl (137mM)

$Na_2HPO_4$ (4.5mM)

$KH_2PO_4$ (1.4mM)

PMSF(100μM)

Leupeptin (10μg/mL)

Aprotinin (2μg/mL)

Digitonin (200μg/mL)

*SDS-PAGE Solutions*

**Phosphate Buffered Saline-Tween 20 (PBS-Tween), ph 7.4**

$Na_2HPO_4$ (80mM)

$NaH_2PO_4$ (20mM)

NaCl (137mM)

Tween 20 (0.1%)

**Tris Buffered Saline-Tween (PBS-Tween), ph 7.4**

Tris-NaCl (20mM)

NaCl (150mM)

Tween 20 (0.1%)

**Sample Buffer (pH6.8)**

Tris-NaCl (0.5mM)

Glycerol 20% (v/v)

SDS 2% (w/v)

β-Mercaptoethanol 5% (v/v)

Bromophenol blue 0.05%(w/v)

**Stacking gel (4% pH 6.8)**

Acylamide/bis-acrylamide (30% stock, 13 % (v/v)

$dH_2O$ 60%

Tris-NaCl (0.5mM)

SDS 2% (w/v)

APS (10%w/v stock, 0.5%(v/v))

TEMED 0.5% (v/v)

**Separting gel (10%)**

Acylamide/bis-acrylamide (30% stock, 13 % (v/v)

$dH_2O$ 40%

Tris-NaCl (0.5mM) pH6.8

SDS 10% (w/v)

APS (10%w/v stock, 0.5%(v/v))

TEMED 0.5% (v/v)

**Separting gel (12%)**

Acylamide/bis-acrylamide (30% stock, 13 % (v/v)

$dH_2O$ 33%

Tris-NaCl (0.5mM) pH6.8

SDS 10% (w/v)

APS (10%w/v stock, 0.5%(v/v))

TEMED 0.5% (v/v)

**Electrode running gel**

Tris-Base (25mM)

Glycine (192mM)

SDS (0.1%)

**Transfer Buffer (pH8.3)**

Tris-Base (25mM)

Glycine (192mM)

MeOH (20%)

SDS (0.05%)

*Polymerase Chain Reaction Gel Electrode Solution*

**Tris borate EDTA (TBE) Buffer, pH8.3**

Tris-Base (0.08mM)

Boric Acid (0.04M)

EDTA (1mM)

**RNA Separating Agarose Gel (1%pH8.3)**

Agarose 1.5%(w/v)

100mL TBE Buffer

**PCR Products separating agarose gel (1.5%, pH8.3)**

Agarose 1.5%(w/v)

100mL TBE Buffer

*Fluorogenic Assay Solution*

**Lysis buffer (Cathepsin-L assay, pH5)**

NaOAc (20mM)

EDTA (4mM)

DTT (8mM)

Urea (4M)

**Incubation Buffer (Cathepsin-L assay, pH7.4)**

HEPES(100mM)

DTT (5mM)

# X Appendix- Suppliers

AGB Scientific Ltd., Dublin Industrial Estate, Dublin 11, Ireland

ALEXIS Corporation LTD., P.O. Box 6757, Bingham, Nottingham, NG13 8LS, UK.

Amersham plc, Amersham Place, Little Chalfont, Buckinghanshire, HP79NA, UK.

Astee-Microflow Systems, 2180 Andrea Lane, Fort Myers, Fl33912, U.S.A.

B.Braun Melsungen AG, Carl-Braun Srtaβe 1, D-34212 Melsungen, Germany.

Bachem Ltd., PO Box 260, 17 Westside Industrial Estate, Jackson Street, St. Helens, Meryerside WA9 3AJ, UK.

BD Bioscience Pharmingen, 10975 Torreyana Road, San Diago, CA 921121, U.S.A.

BDH Laboratory Supplies, Poole, Dorset, BH151TD, UK

Becton Dickinson Labware Europe, Becton Dickinson France S.A., 1 rue Aristide Bergees, BP4, 38800 Le Pont De Claix, France.

Bel-Art Products Inc., 6 Industrial Road, Pequannock, New Jersey 07440, U.S.A.

Bibby Sterilin Ltd., Tilling Drive, Straffordshire, ST15OSA, England.

Biognostik GmbH, Gerhard-Gerdes-Str. 19, 37079 Gottingen, Germany.

Biometra GmbH, Rudolpf-Wissell Strabe 30, D-37079 G\ttingen, Germany.

Bio-Rad Laboratories GmbH., Heidemannstrasse 164, D-80939 Munich, Germany.

Biosource International , 542 Flynn Road, Camarillo, California 93012, U.S.A.

Calbiochem International, Merck KGaA, Frankfurter Str. 250, D-64293 Darmstadt, Germany.

Cell Signalling Technology, INC, 166B Cummings Centre, Beverly, MA 01915

CN BIOSCIENCES Ltd., Boulevard Industrial Park, Padge Road, Beeston, Nottingham, NG9 2JR, UK.

Dako Corporation, 6392 Via Road, Carpenteria, C.A. 93013, U.S.A.

FUGIFILM Medical Systems USA, Inc. Headquarters, 419 West Avenue Stamford, CT 06902, U.S.A.

Greiner Bio-One GmbH, Bad Haller Strasse 32, 4550 Kremsmuenster, Austria.

Improvision Software, Viscount Centre II, University of Warwick Science Park, Millcurn Hill Road, Conventry, CV4 7HS, UK.

InVitrogen Ltd, Inchinnan Business Park, 3 Fountain Drive, Paisley PA49RF, UK.

Jencons Scientific Ltd., Cherrycourt Way Industraial Estate, Stanbridge Road, Lancashire, WN8 9SP, UK.

Leica Microsystems AG, Ernst-Leitz-Strasse 17-37, Wetzlar, 35578, Germany.

Medical Supply Company Ltd., Damastown, Mulhuddart, Dublin 15, Ireland.

Millipore Ireland B.V. Tullagreen Carrigtwohill, Co. Cork, Ireland.

Molecular Probes Europe BV, PoortGebouw, Rijnsburgerweg 10, 2333 AA Leiden, The Netherlands.

Nikon Instech Co., Ltd. Parale Mitsui Bldg., 8, Higashida-cho, Kawasaki-ku, Kawasaki, Kanagawa 210-0005, Japan.

Pall Corporation, 600 South Wagner Road, Ann Arbour, M148103-9019 U.S.A.

Pierce Biotechnology, 3747 N. Meridian Rd, P.O. Box 117, Rockford, IL61105, U.S.A.

Promega Sciences, 2800 Woods Hollow Road Madison WI 5371, U.S.A.

Roche Diagnostics Ltd., Bell Lane, Lewes, East Sussex, BN7 1LG, UK.

Sarstedt Ltd., Sinnottstown Lane, Drinagh, Wexford, Ireland.

Sartorius AG Ltd., 94-108 Weender Landstrabe, D-37075 Goettingen, Germany.

Scanalytics Inc. 8550 Lee Highway, Suite 400, Fairfax, VA 22031, U.S.A.

Sigma-Aldrich Company Ltd., The Old Brickyard, New Road, Gillingham, Dorset, SP84XT,UK.

Tocris Cookson Ltd., Northpoint Fourth Way, Avonmouth, Bristol BS11 8 TA,UK.

Vector Laboratories Inc., Burlingame, CA94010, USA.

Whatman International Ltd., Whatman House, St.Leonard's Road, 20/20 Maidstone, Kent ME160LS, UK.

## XI Publications

**McCormack, R.M.,** Fogarty, M.P., and Campbell, V.A. (2006) Beta-Amyloid regulates the lysosomal system in rat cultured cortical neurons in a p53 dependent manner. *Neurobiology of Ageing.* Submitted July 2006.

**McCormack, R.M.** and Campbell, V.A. (2006) The role of Syk in Aβ-mediated neuronal apoptosis in cultured neurons *Irish Journal of Medical Science.**175** (1) 4.*

**McCormack, R.M.,** Fogarty, M.P., and Campbell, V.A. (2005) Aβ regulates the lysosomal system via p53 in cultured cortical neurons. *Biochemical Society Transactions*. **33** (4). Abstracts P064.

**McCormack, R.M.,** Fogarty, M.P., and Campbell, V.A. (2004) β-amyloid modulates the lysosomal system in cultured cortical neurons in a p53-dependent manner. American Society for Neuroscience. Abstracts 908.4;YY1

**McCormack, R.M.,** Fogarty, M.P., and Campbell, V.A. (2004) β-amyloid modulates the lysosomal system in rat cortical neurons *in vitro* in a p53-dependent manner. *Proceedings of the Anatomical Society of Great Britain and Ireland.Journal of Anatomy* **205** (6), 519-545. PC13